

ACC.POSTER CONTRIBUTIONS

1018

General Echocardiography:TTE/ Echocardiography:3-D, TEE, and Intracardiac Echo

Sunday, March 29, 2009, 9:30 a.m.-12:30 p.m.
Orange County Convention Center, West Hall D

9:30 a.m.

1018-233

Left Ventricular Untwisting and Non-uniformity of Apex-to-Basal Lengthening in Patients With Hypertrophic Cardiomyopathy

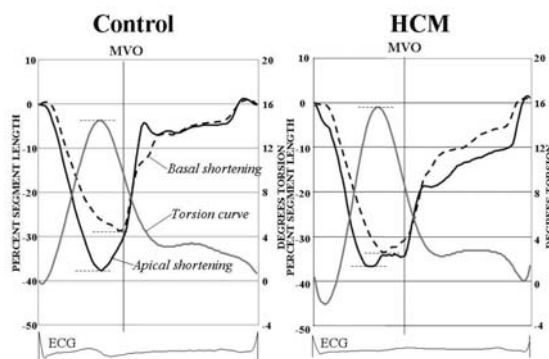
Takeo Tanaka, Kazuya Murata, Eizo Akagawa, Chikage Kihara, Hiroko Yoshino, Yoshio Nose, Yasuhiro Fukagawa, Takehisa Susa, Shinichi Okuda, Yasuaki Wada, Masunori Matsuzaki, Yamaguchi University Graduate School of Medicine, Ube, Japan

Background: Left ventricular (LV) untwisting proceeds diastolic LV filling in normal subjects. However, behavior of LV untwisting and apex-to-basal lengthening before LV filling in patients with hypertrophic cardiomyopathy (HCM) were unknown.

Method: We obtained basal and apical LV short-axis views in 25 patients with non-obstructive HCM and 25 healthy volunteers (N). Eight equiangular points on endo-myocardium at end-diastole were placed in each view, and the movements of these points were automatically tracked by 2D tissue tracking system (EUB-7500, Hitachi, Japan). The shortening ratios of four directions were calculated and averaged, and LV torsion was also calculated as net-difference between basal and apical rotation angles. Then, the time-shortening and the time-torsion curves were obtained. At the time of mitral valve opening (MVO), recovery rate from peak shortening (RRS) and peak torsion (RRT) were calculated.

Results: The onset of LV untwisting proceeded the onset of LV filling, and RRT were same in both N and HCM (32 ± 16 vs. $35 \pm 10\%$, ns). RRS of apex reduced in HCM (8 ± 4 vs. $22 \pm 8\%$, $p < 0.0001$), however, RRS of base were not different between N and HCM (7 ± 6 vs. $10 \pm 5\%$, ns).

Conclusion: Despite same grade of LV untwisting, apical lengthening was disturbed in HCM. LV impaired relaxation in HCM may attribute to non-uniformity of LV lengthening, not reduced untwisting.



9:30 a.m.

1018-234

Prognostic Value of Echocardiographic Estimation of Pulmonary Vascular Resistance in Patients With Acute Pulmonary Thromboembolism

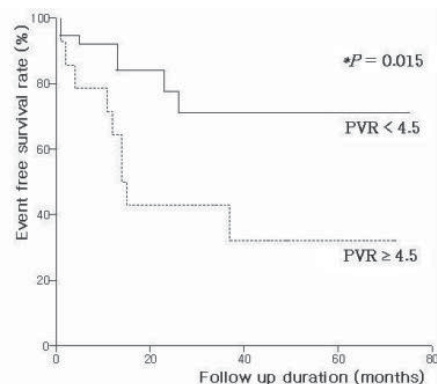
Myung-Zoon Yi, Sung-Hwan Kim, Sung Sik Kim, Sun Yang Min, Jeong-Sook Seo, Jong-Min Song, Duk-Hyun Kang, Jae-Kwan Song, Asan Medical Center, Seoul, South Korea

Background: Recently the feasibility of noninvasive calculation of pulmonary vascular resistance (PVR) has been reported. We sought to evaluate whether baseline PVR is useful to predict clinical outcomes in acute pulmonary thromboembolism (aPTE).

Methods: 58 patients (35 females, mean age 61 ± 16 years) with aPTE who underwent both pre-treatment and follow-up echocardiography were included. Doppler-derived PVR was calculated using the following equation: PVR (Woods unit) = (peak tricuspid regurgitant velocity [TRV_{max}]/time-velocity integral of right ventricular outflow tract [TVI_{RVOT}]) * 10 + 0.16. Adverse clinical events included death, recurrence of aPTE and persistent pulmonary hypertension defined as TRV_{max} > 3.5 m/s at follow-up echocardiography.

Results: Adverse clinical events developed in 17 patients (29%) and baseline clinical characteristics including age, sex, the prevalence of diabetes, hypertension, and smoking did not show any difference between groups. Baseline left ventricular ejection fraction and TRV_{max} were not different between groups. Patients with adverse events had significantly higher PVR than those without (4.3 ± 1.5 vs. 3.4 ± 1.1 ; $p = 0.029$). In ROC curve, cut-off value of 4.5 showed the sensitivity and specificity of 56% and 86%, respectively. The event-free survival rate was significantly worse in patients with PVR ≥ 4.5 Woods unit ($p = 0.015$).

Conclusions: Echocardiographic estimation of PVR provides important prognostic information in patients with aPTE.



9:30 a.m.

1018-235

Utility of End-Diastolic Strain Rate in the Estimation of Left Ventricular Passive Compliance

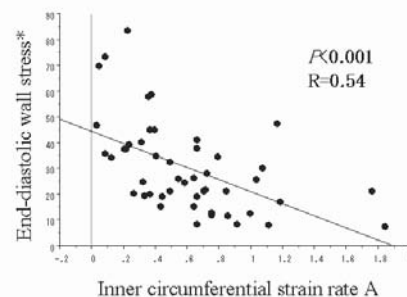
Tomoko Ishizu, Yoshihiro Seo, Masako Baba, Masayoshi Yamamoto, Tomoko Machino, Ryo Kawamura, Shigeyuki Watanabe, Kazutaka Aonuma, University of Tsukuba, Ibaraki, Japan

Background: Increased chamber stiffness and elevated left ventricular end diastolic pressure (LVEDP) are central hemodynamic property in the diastolic heart failure. The speckle tracking echo (STE) technique allows the non-invasive measurement of myocardial strain rate. We assessed the hypothesis that end-diastolic strain rate during atrial contraction may reflect left ventricular passive compliance.

Methods: We performed STE on 50 consecutive patients who underwent cardiac catheterization and measure inner-, mid- and outer- myocardial peak circumferential strains rate (CSR), radial strain rate (RSR), and inner longitudinal strain rate (LSR) during atrial contraction using newly developed STE software (Toshiba Medical Systems, Tokyo, Japan).

Results: Inner-CSR significantly correlated with the LVEDP ($r = 0.45$, $p = 0.001$), and wall stress ($r = 0.54$, $p < 0.001$) (Figure), and log-BNP ($r = 0.51$, $p = 0.002$). In multiple regression analysis, after adjusting for LVEF and E/A, Inner-CSR, LV mass, LV volume change by atrial contraction revealed to be significant determinants for LVEDP ($r = 0.69$, $p = 0.009$, $p = 0.022$, $p = 0.008$, respectively). The sensitivity to detect an abnormal LVEDP (> 15) by an inner-CSR ≥ 0.42 was 77% and the specificity was 67%.

Conclusion: Endocardial circumferential deformation rate during atrial contraction reflects end-diastolic wall stress and LVEDP. Strain rate analysis could be the non-invasive parameter assessing LV passive compliance.



$$\text{End-diastolic wall stress} = -0.334 \times \text{EDP} \times \text{LVd} / \text{WT} (1 + \text{WT} / \text{LVd})$$

9:30 a.m.

1018-236

Increased Left Atrial Size With Obstructive Sleep Apnea After Myocardial Infarction

Tomas Konecny, Marek Orban, Grace Lin, Fatima Sert Kuniyoshi, Rebecca Lindquist, Taro Adachi, Peter A. Brady, Apoor Gami, Tomas Kara, Gregg S. Pressman, Francisco Lopez-Jimenez, Virend K. Somers, Mayo Clinic, Rochester, MN

Background: Obstructive sleep apnea (OSA) is associated with increased risk of cardiac arrhythmias and worse cardiovascular outcomes in patients with coronary artery disease yet the mechanism (s) is unknown. OSA increases left atrial size, a known risk factor for cardiac arrhythmias and increased cardiovascular mortality. Therefore, we hypothesized that OSA may act via changes in left atrial volume index (LAVI) to increase risk of both cardiac arrhythmias and poorer outcomes in patients presenting with myocardial infarction.

Methods: Patients with recent ST elevation myocardial infarction (STEMI) treated with percutaneous revascularization were recruited to undergo comprehensive attended overnight polysomnography. Apnea hypopnea index (AHI) was determined using standard criteria. OSA was defined as AHI ≥ 5 events/hour, with higher AHI indicating more severe OSA. LAVI was calculated by transthoracic echo performed at baseline and after at least 3

months using the biplane area-length method, and indexed to body surface area. Results are reported as mean \pm SD or *SEM; a 2-sided t test† and linear regression were used; AHI was transformed by log due to skewness.

Results: A total of 57 patients (age 62 ± 12 years; 21% female) were included, of whom OSA (AHI = 15.5 ± 15.9) was present in 40 (70%). At baseline, mean LAVI was 30 ± 9 cc/m2. Increased LAVI was associated with more severe OSA ($r = 0.32$; $p = 0.015$) and remained so at follow up ($r = 0.35$; $p = 0.025$; after 25 ± 15 months). A divergent effect of OSA on LAVI was observed in that LAVI of OSA patients increased ($+4 \pm 1.7^*$) during the follow up while LAVI decreased in patients without OSA ($-0.7 \pm 2.6^*$), although this difference was not statistically significant ($p = 0.15$ †).

Conclusions: In patients presenting with myocardial infarction prevalence of OSA is high and the severity of OSA correlates with increased left atrial size. Untreated OSA is associated with less favorable left atrial remodeling and may be one mechanism whereby OSA is associated with increased risk of cardiac arrhythmias and worse CV outcomes.

9:30 a.m.

1018-237

Carotid Stiffness and Cardiac Function in Normal Subjects: A Correlation Between Tissue Doppler/Left Ventricular Structure and Echo-Tracking

Olga Vriz, Scipione Careri, Daniela Pavan, Gian Luigi Nicolosi, Arianna Ius, Manola Bettio, Eduardo Bossone, Concetta Zito, Francesco Antonini-Canterin, Cardiology, "S. Maria degli Angeli" Hospital, Pordenone, Italy, Department of Medicine and Pharmacology, University Hospital, Messina, Italy

Background: It is well known the role of arterial stiffness in cardiovascular diseases and other pathologies, less data are available about the relationship between arterial stiffness and cardiac function in normals. The purpose of this study was to assess the correlation between indices of local stiffness at carotid level and parameters of cardiac structure and function in normal subjects.

Methods: 74 normal subjects (48 men, 26 women; mean age: 47 ± 12 years) were studied. They underwent an echocardiographic study and systolic and diastolic left ventricular (LV) structure and function were assessed using standard 2D and tissue Doppler imaging techniques (LV ejection fraction, interventricular septum (IVSD), posterior wall thickness (PWT), E and A mitral wave velocities, E/A ratio, septal E' and S'-wave velocities, E'/E' ratio). Local stiffness have been obtained at the common carotid artery before the bifurcation (using an high definition echo-tracking system). Carotid measurements were: Beta (stiffness index), Ep (pressure-strain elasticity modulus), AC (arterial compliance), PWV (one-point pulse wave velocity).

Results: In univariate analyses, all the carotid stiffness indices were significantly correlated to E and E' wave velocities, E/A ratio and with wall thickness. Only Beta index was significantly related to A wave velocity.

Conclusions: Our study showed in normal subjects a significant correlation between carotid stiffness and parameters of diastolic function and wall thickness.

Correlation of carotid stiffness and cardiac function

(*p<0.01, §p<0.05).

	IVSD	PWSD	E	A	E/A	E'	S'	E'/E'
Beta	0.026§	0.28§	-0.34*	0.4*	-0.23§	-0.44*	0.11	-0.01
Ep	0.03*	0.30*	-0.43*	0.33*	-0.25§	-0.5*	0.06	-0.008
AC	-0.03	-0.03	0.33	-0.24§	0.18	0.35*	0.04	0.22
PWV	0.29§	0.29§	-0.45*	0.35*	-0.25§	-0.55*	0.03	0.05

9:30 a.m.

1018-238

Relationship of Age-Related Changes in Left Atrial Strain With Left Ventricular Untwisting: A Speckle-Tracking Echocardiography Study in Normal Subjects

Bogdan Alexandru Popescu, Denisa Muraru, Carmen C. Beladan, Andreea Teodorescu, Oana Savu, Monica Hirsu, Carmen Ginghina, "Carol Davila" University of Medicine and Pharmacy, Bucharest, Romania, Institute of Cardiovascular Diseases, Bucharest, Romania

Background: Left ventricular (LV) mechanics and left atrial (LA) function are both important for LV filling at normal pressures. Previous studies have emphasized the role of LV untwisting for effective diastolic suction, but its relation to atrial strain has not been studied so far.

Purpose: We aimed to assess by speckle-tracking echocardiography atrial strain (S) and strain-rate (Sr) and their relationship with LV untwisting and conventional indices of LV diastolic function. **Methods:** We studied prospectively 78 normal subjects (age 38 ± 14 , range 18-77, 27 men) who underwent a comprehensive echocardiogram. LV basal and apical short-axis loops were analysed offline with dedicated 2D strain software (EchoPAC). Longitudinal LA strain parameters were assessed with the same software from apical 4 chamber view by measuring peak values of average segmental S and Sr (SSr, ESr and ASr) and time intervals from R (ECG) wave to each peak (TS, TSSr, TESr, TASr). LV untwist was quantified as time from R wave to peak early diastolic velocity measured on the torsional velocity curve. Systolic intervals were normalized to peak R - aortic valve closure time and diastolic intervals to duration of diastole.

Results: Peak LA S was $36 \pm 10\%$, while SSr, ESr and ASr were: 1.6 ± 0.4 s⁻¹; -2 ± 0.6 s⁻¹; -1.7 ± 0.5 s⁻¹. Age was inversely related to LA S, SSr and directly with ESr ($r > 0.5$, $p < 0.001$ for all). There was a significant relation between ESr and EDT, E/A, septal and lateral E' ($p < 0.0001$ for all), E'/E'sep, E'/E'lat, pulmonary venous Ar wave amplitude and duration and indexed LA volume ($p < 0.01$ for all). LV untwisting correlated strongly with TESr and TASr ($r = 0.9$, $r = 0.53$ respectively, $p < 0.0001$ for both) and had a significant relation with ASr

($p < 0.001$), mitral A and lateral A' ($p < 0.03$ for both).

Conclusions: Speckle-tracking is feasible for assessment of both LV untwisting and LA strain. LA function components are significantly correlated with age and with LV diastolic function parameters. Delayed LV untwisting is compensated for by an augmented atrial contraction. These findings highlight the complementary role of LA strain and LV untwisting for effective LV filling and normal cardiac performance.

9:30 a.m.

1018-239

Influence of Body Mass on Left Atrial Size and Reservoir Function in Healthy Children

Walter P. Abhayaratna, Ramanujan Ganesalingam, Christine O'Reilly, Katrina Abhayaratna, Satoru Sakuragi, Richard D. Telford, Canberra Hospital, Canberra, Australia, Australian National University, Canberra, Australia

Background: In this study of healthy children, we evaluated the influence of body mass index (BMI) on i) left atrial (LA) size, a marker of left ventricular (LV) diastolic burden and cardiovascular risk in adults; and ii) total LA emptying fraction (LAEF), an index that characterizes the function of the left atrium as a reservoir during ventricular systole.

Methods: Four hundred and five community-based children (mean age 10.1 ± 0.3 years; 50% boys) underwent clinical examination and assessment of cardiac structure and function by echocardiography. Maximum and minimum LA volumes were quantitated and LAEF was calculated [(maximum-minimum LA volume)/maximum LA volume].

Results: In univariate analysis, maximum indexed LA volume (LAVi) was positively correlated with BMI ($p = 0.33$), LV mass ($p = 0.42$), LV end-diastolic volume ($p = 0.42$), LV end-systolic volume ($p = 0.30$) and early diastolic mitral annular velocity (e') ($p = 0.16$); and inversely related to heart rate ($p = -0.14$) (all $p < 0.01$). LAEF was inversely related to BMI ($p = -0.15$), LV mass ($p = -0.10$), LV end-systolic volume ($p = -0.14$); and positively correlated to LV ejection fraction ($p = 0.17$), e' ($p = 0.14$) and heart rate ($p = 0.14$) (all $p < 0.01$). In multivariable analysis, body mass index was independently associated with increased LAVi and reduced LAEF, independent of heart rate and LV size/function (Table).

Conclusion: Body mass is associated with increased LA size and reduced reservoir function in healthy prepubescent children.

Table: Associations between BMI and i) LA size and ii) total LA emptying fraction in multivariable analysis

Maximum LA volume (mL/m2.7)		Total LA emptying fraction (%)	
Beta	p-value	Beta	p-value
0.11	<0.001	-0.002	0.004

Adjusted for heart rate, LV mass, LV ejection fraction, LV chamber size and early diastolic mitral annular velocity

9:30 a.m.

1018-240

Cardiac Dimensions of Football Players Differ by Position

Geoffrey A. Day, Kent E. Morris, Adam Dawkins, Mark Smith, John R. Bates, The Care Group, Indianapolis, IN, St. Vincent Hospital, Indianapolis, IN

Background: Cardiac adaptation is unique to the type of athletic training. American football players represent a heterogeneous group with different body habitus, training regimens, and occupational demands. We hypothesize that cardiac dimensions measured by standard echocardiography differ according to player position.

Methods: Between 1997 and 2008, 3931 athletes participated in the NFL pre-draft combine. All were evaluated by physical examination and ECG. Players were referred for echocardiography at the discretion of the examining physician. Results were grouped according to player position: 1) lineman (LM), 2) linebackers and running backs (LBRB), and 3) wide receivers and defensive backs (WRDB). Left ventricular (LV) wall thickness and diameters were measured. LV mass was calculated. Measurements were indexed for body surface area (BSA).

Results: Data was obtained in 385 players. Compared to RBLB and WRDB, LM had larger chamber sizes, wall thickness, and LV mass. After correcting for BSA, chamber sizes and wall thickness were smaller in the lineman, while LV mass remained greater.

Conclusion: Football players demonstrate significant differences in cardiac dimensions when stratified by player position. Player position should be considered when evaluating heart size and hypertrophy in these athletes.

Echocardiographic Measurements of 385 American Football Players

	LM (N=143)	RBLB (N=103)	WRDB (N=139)	p-value
LVIDd (cm)	5.57	5.28	5.10	<0.001
LVIDd/BSA (cm/m2)	0.94	1.10	1.05	<0.001
LVIDs (cm)	3.71	3.54	3.44	<0.001
LVIDs/BSA (cm/m2)	0.33	0.36	0.38	<0.001
IVS (cm)	1.21	1.08	1.06	<0.01
IVS/BSA (cm/m2)	0.11	0.11	0.12	0.01
LV mass (grams)	501.12	411.47	377.03	<0.001
LV mass/BSA (grams/m2)	44.96	41.75	41.47	0.001

9:30 a.m.

1018-241

Determinants of Surgical Outcome in Patients With Isolated Tricuspid Regurgitation

Hyu Eun Park, Yong-Jin Kim, Hyung-Kwan Kim, Kyung-Hwan Kim, Ki-Bong Kim, Hyuk Ahn, Dae-Won Sohn, Byung-Hee Oh, Young-Bae Park, Yun-Shik Choi, Seoul National University Hospital, Seoul, South Korea

Background: Determining optimal time for corrective surgery remains a difficult clinical problem in patients with severe tricuspid regurgitation (TR). In the present study, we prospectively enrolled patients with severe TR to identify determinants of clinical outcome.

Methods: 59 consecutive patients with pure severe TR were enrolled. 21 patients (36 %) were in NYHA functional class 2, 38 (64 %) in class 3 and 4. Preoperative echocardiography revealed that pulmonary systolic pressure of 42 ± 9 mmHg, right ventricular (RV) end-diastolic area of 35 ± 9 cm² and RV fractional area change (FAC) of 42 ± 9 %.

Results: Mean follow-up duration after surgery was 33 ± 16 months. 6-month echocardiographic follow-up showed decrease in RV end-diastolic area by 26% (25 ± 7 cm²) with a corresponding reduction of RVFAC by 29% (31 ± 9 %). 32 patients (62%) showed improved functional capacity after surgery. In multivariate logistic regression analysis, NYHA functional class ($p=0.03$, fig 1) and RVFAC ($p=0.006$, fig 2) emerged as independent determinants for event-free survival. In ROC curve analysis, RVFAC ≥ 40 % predicted event-free survival with sensitivity of 61% and specificity of 80%.

Conclusions: Timely correction of severe TR improves functional capacity and RV remodeling. Preoperative functional status and RV systolic function are independent predictors for clinical outcome. Surgery should be considered in these patients when symptom develops or RV dysfunction ensues.

Figure 1

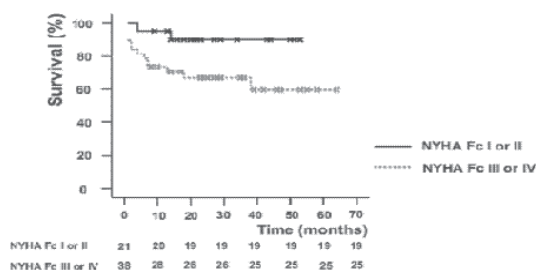
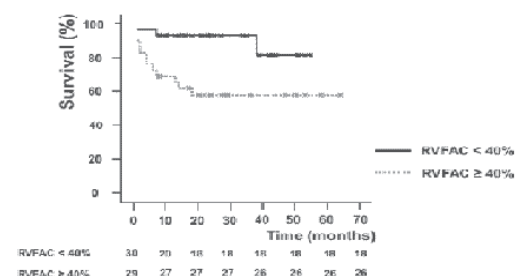


Figure 2



9:30 a.m.

1018-242

Preventive Effect of Renin-Angiotensin System Inhibitor on Left Atrial Remodeling in Patients With Chronic Atrial Fibrillation: Long-Term Echocardiographic Study

Yamato Fukuda, Nobuo Fukuda, Satofumi Morishita, Koichi Sakabe, Hisanori Shinohara, Yoshiyuki Tamura, National Hospital Organization Zentsuji Hospital, Zentsuji, Japan

Background: Dilatation of the left atrium (LA) is a strong predictor of cerebral infarction in patients with atrial fibrillation (AF). Renin-angiotensin system (RAS) inhibitor is reported to prevent a new onset of AF. The aim of this study is to examine whether RAS inhibitor could prevent LA remodeling in the patients with chronic AF.

Methods: In 1594 examples performed echocardiography during 16 months since October 2007, we picked out the patients with chronic non-valvular AF. Patients with left ventricular (LV) systolic dysfunction (ejection fraction (EF) < 45%) and pacemaker implantation were excluded. The 41 patients (mean age, 75 ± 8 years old) were finally enrolled and divided into following two group: RAS groups (23 patients) taking RAS inhibitors and C group (18 patients) without taking these drugs. We compared age, blood pressure (BP), and echocardiographic parameters at the beginning and the end of follow-up between the groups. The echocardiographic parameters were LA diameter (LAD), LA expansion fraction (LAEF = maximum / minimum LAD), LA volume index (LAVI), LV mass index (LVMI), E velocity of the LV inflow (E), e' velocity of the mitral annulus (e'), and the ratio of E to e' (E/e'). Percent change of each echocardiographic parameter was calculated from the value at the end of follow-up divided by the value at the beginning of follow-up. Associations with increasing LAVI and decreasing LAEF were sought using multivariate linear regression analysis.

Results: No significant differences were present in mean follow-up periods, systolic and diastolic BP, and percent change of LVMI, LVEF between the groups. However, RAS group

as compared to C group were showed significantly worse percent changes of E/e' (103 ± 34 vs. 140 ± 58 %, $p < 0.05$), LAEF (99 ± 6 vs. 93 ± 8 %, $p < 0.05$), and LAVI (119 ± 24 vs. 146 ± 33 %, $p < 0.05$). Long term administration of RAS inhibitors was associated with the prevention of increasing LAVI ($p = 0.04$) and decreasing LAEF ($p = 0.04$) in multivariate analysis.

Conclusions: The retrospective echocardiographic study suggests that the long term administration of RAS inhibitors prevent structural and functional degradation of the LA in patients with chronic non-valvular AF.

9:30 a.m.

1018-243

Detection of Post-systolic Shortening by Tissue Doppler Imaging for the Risk Stratification for Chest Pain in Emergency Department Settings

Nobuaki Tanaka, Masaaki Uematsu, Toshinari Onishi, Shinsuke Nanto, Takakazu Morozumi, Tetsuya Watanabe, Masaki Awata, Osamu Iida, Kenji Kawamoto, Fusako Sera, Hitoshi Minamiguchi, Masamichi Yano, Kuniyasu Ikeoka, Shin Okamoto, Haruyo Yasui, Takayuki Ishihara, Tomoharu Dohi, Seiki Nagata, Kansai Rosai Hospital, Amagasaki, Japan

Background: Risk stratification for chest pain in emergency department (ED) settings is an important issue in cardiology practice. Post-systolic shortening (PSS) is a sensitive marker of myocardial ischemia. We have developed a novel tissue Doppler imaging (TDI) technique that readily visualizes the presence of PSS on 2-dimensional echocardiograms, and investigated whether acute coronary syndrome (ACS) is detectable by combining this technique with routine echocardiography in ED settings.

Methods: Detection of diastolic abnormality by dyssynchrony Imaging (DADI): PSS was detected by using tissue Doppler displacement timing analysis. In this method, end-systole was automatically determined from tissue velocity, and delays of the displacement peaks from the end-systole were displayed from green (0 ms) to red (≥ 100 ms) on the left ventricular apical views. Consecutive 56 patients (male=38, age ranged 33-88 years) who visited ED complaining of chest pain were enrolled. DADI was additionally performed using Toshiba SSA-770A when the routine echocardiography was normal. ACS was considered present either when LV asynergy was detected by routine echocardiography or when the left ventricular segments were color coded red in accordance with the coronary anatomy by DADI. Diagnosis of ACS was confirmed by coronary angiography as having critical coronary artery diameter stenosis >90 %. Patients stratified as normal were followed up at least for a month.

Results: ACS was confirmed in 41 (73%) patients. Routine echocardiography (presence of asynergy) alone detected ACS with the sensitivity of 75% and with the specificity of 100%. When combined with DADI, the sensitivity improved to 97% with the specificity of 66%. The combination yielded accuracy of 89%, and negative predictive value of 91%.

Conclusion: DADI, when added to routine echocardiography, may provide robust risk stratification in patients presenting with chest pain in ED settings.

9:30 a.m.

1018-244

Validation of Intramural Strain With a Newly Developed Two-Dimensional Speckle Tracking System

Tomoko Ishizu, Yoshihiro Seo, Yoshiharu Enomoto, Haruhiko Sugimori, Shigeyuki Watanabe, Kazutaka Aonuma, University of Tsukuba, Ibaraki, Japan

Background: A newly developed speckle tracking imaging (STI) system (Toshiba Medical Systems, Japan) allows tracking the endo-, epi-cardial border and intra-mural speckle and thus offers potential to quantify the left ventricular (LV) intramural strain. The aim of this study was to validate the reliability of intramural strain measured by the STI system against strain measurements by sonomicrometry crystals.

Methods: In 10 anesthetized ovine, 3 sets of sonomicrometry crystals were placed at endo-, midwall-, and epimyocardium at anterior and lateral wall. Circumferential strain (CS) was calculated 3 layers at endo-, midwall, and epicardial speckle. Radial strain (RS) was assessed separating inner-, and outer half myocardium; inner half RS were measured as thickening between endo- and midwall speckle, and outer half RS as between midwall- and epicardial speckle. We compared ultrasound derived strain measurements against those by sonomicrometry at baseline and during various interventions: dobutamine and propranolol infusions and coronary occlusion.

Results: Statistically significant correlation was observed between STI and sonomicrometry for CS (endocardial CS: $r=0.84$, $p < 0.001$, 95% of limit of agreement 12.4%, midwall CS: $r=0.88$, $p < 0.001$, 8.9%, epicardial CS: $r=0.67$, $p < 0.001$, 11.8%) and RS (inner RS: $r=0.67$, $p < 0.001$, 14.2%, outer RS: $r=0.29$, $p=0.026$, 14.6%, total wall RS: $r=0.57$, $p < 0.001$, 16.6%). Changes in peak systolic strain in ischemic segments were significant in midwall CS ($p < 0.001$) and inner RS ($p < 0.001$), outer RS ($p=0.008$).

Conclusions: The newly developed STI system can accurately assess the intramural strain in normal segments at rest, and those alternations in normal segments at drug stress tests and those in abnormal segments with myocardial ischemia and has potential to become a clinical non-invasive bed-side tool for characterize myocardial strain gradient.

9:30 a.m.

1018-245

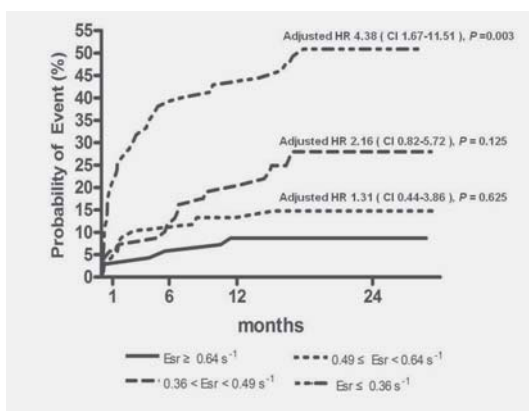
Influence of Diastolic Function on Outcome Following High Risk Myocardial Infarction

Sung-Hee Shin, Chung Lih Hung, Amira H. Hassanein, John J.V McMurray, Eric J. Velazquez, Lars Kober, Marc A. Pfeffer, Scott D. Solomon, Brigham and Women's Hospital, Boston, MA

Background Systolic function is a major determinant of prognosis after myocardial infarction (MI). However, the influence of diastolic function on outcomes following MI is less well established.

Methods We assessed the prognostic significance of diastolic strain rate in patients with

left ventricular (LV) dysfunction, heart failure (HF), or both following MI who were enrolled in the VALSartan In Acute myocardial infarction (VALIANT) echo study. B-mode speckle tracking (velocity vector Imaging, Siemens Inc) was used to obtain early diastolic strain rate (Esr) on 12 segments from apical views in 274 patients who had image quality sufficient for analysis. The relationship between average Esr and the risk of death or HF was assessed. **Results** Esr was significantly related to age, history of hypertension, eGFR, LV volumes, left atrial volume, LV mass index, LV ejection fraction, and wall motion score (all $P < 0.001$). In a multivariate Cox model, adjusting for 11 clinical variables and LV ejection fraction, Esr was an independent predictor of all cause mortality or HF ($P < 0.001$). Patients in the lowest Esr quartile had an increased risk of all cause mortality or HF hospitalization as compared with the highest Esr quartile (adjusted HR 4.38, 95% CI 1.67-11.51, Figure) **Conclusions** Diastolic strain rate is an independent predictor of death or hospitalization for HF after MI, suggesting that diastolic function may be an important determinant of outcome after myocardial infarction.

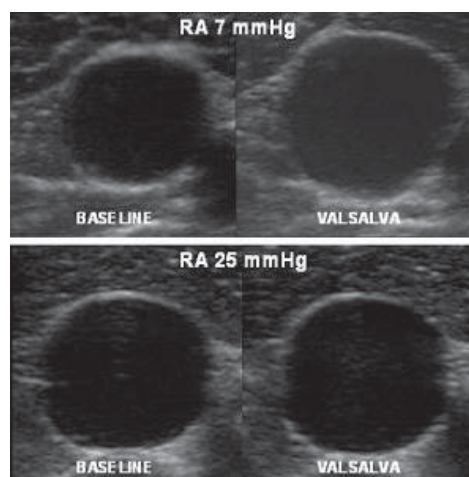


9:30 a.m.

1018-246 Detection of Elevated Right Atrial Pressure Using a Simple Bedside Ultrasound Measure

Dustin E. Kliner, John P. Girod, Marc A. Simon, Flordeliza S. Villanueva, John J. Pacella, University of Pittsburgh Medical Center, Pittsburgh, PA

Background: Measurement of right atrial pressure (RAP) via the height of the internal jugular (IJ) vein is a key component of the physical examination. In certain patients, or to the inexperienced observer, accurate assessment is often difficult, and invasive measurement is needed. In patients with normal RAP, Valsalva is associated with a 20-30% increase in IJ cross-sectional area (CSA). In patients with high RAP, who fall on the flatter portion of the venous compliance curve, we hypothesized that the increase in CSA would be blunted and could be detected non-invasively using bedside ultrasound. **Methods:** Ultrasound images of the IJ vein with and without Valsalva were obtained in 50 patients undergoing right heart catheterization. IJ CSA was measured and percent change in IJ CSA with Valsalva compared to baseline RAP. RAP of ≥ 12 mmHg was defined as high.



Results: With Valsalva, the percent change in IJ CSA at RAP < 12 mmHg was $38 \pm 30\%$ compared to a $12 \pm 11\%$ change ($p < 0.004$) at RAP ≥ 12 mmHg. ROC curve analysis showed that less than 17% increase in IJ CSA with Valsalva predicted high RA pressure with the following test characteristics: sensitivity 92%, specificity 81%, PPV 57% and NPV 96% (AUC 0.87, $p < 0.001$). A blunted increase in IJ CSA with Valsalva in a patient with high RAP is shown. **Conclusions:** An increase in IJ CSA $> 17\%$ with Valsalva effectively rules out high RA pressure. This simple bedside ultrasound technique may be useful to diagnose high RA pressure, guide therapy and reduce the need for invasive pressure measurement.

1018-247

A Comparison of Ventricular Torsion Between Cardiac Amyloidosis and Pressure Overload Left Ventricular Hypertrophy Caused by Aortic Valve Stenosis

Jun Koyama, Hirohiko Motoki, Kazunori Aizawa, Hiroki Kasai, Megumi Koshikawa, Atsushi Izawa, Takeshi Tomita, Setsuo Kumazaki, Hiroshi Tsutsui, Uichi Ikeda, Shinshu University School of Medicine, Matsumoto, Japan

Background: Left ventricular (LV) torsion is a key parameter of cardiac performance. Previous studies have demonstrated that LV hypertrophy shows abnormal LV torsion, but there is no data regarding the difference between infiltrative cardiomyopathy (cardiac amyloidosis) and pressure overload hypertrophy (aortic valve stenosis).

Methods: We examined 87 patients with cardiac amyloidosis (50 patients with primary amyloidosis (AL), and 37 with familial amyloid polyneuropathy (FAP)), and 33 patients with aortic valve stenosis (AS). Basal and apical short-axis LV images were acquired and LV torsion was calculated as the net difference of LV rotation at the basal and apical planes. Systolic torsion rate was also measured.

Results: There was no difference in mean LV wall thickness among 3 groups.

The LV torsion is smaller in FAP compared to AL and AS (FAP: 7.5 ± 4.1 , AL: 8.2 ± 4.6 , AS: 10.1 ± 5.7 , $p < 0.05$). The Torsion rate is significantly smaller in amyloidosis (AL and FAP) compared to AS (FAP: 64 ± 25 , AL: 71 ± 27 , AS: 93 ± 48 , $p < 0.001$ by ANOVA). There was no significant difference in global longitudinal/circumferential LV strains among 3 groups.

Conclusions: The LV torsion and torsion rate are deteriorated in patients with cardiac amyloidosis compared to pressure overload LV hypertrophy.

9:30 a.m.

1018-248

Tissue Doppler Imaging Including E/e' Is a Powerful Predictor of Major Adverse Cardio Cerebrovascular Events in Patients With a First Anterior ST-Elevation Acute Myocardial Infarction

Noriaki Iwahashi, Masami Kosuge, Jun Okuda, Kengo Tsukahara, Yoshio Tahara, Kiyoshi Hibi, Toshiaki Ebina, Shinichi Sumita, Toshiyuki Ishikawa, Kazuaki Uchino, Satoshi Umemura, Kazuo Kimura, Yokohama City University Medical Center, Yokohama, Japan

Background: It has been established restrictive mitral filling pattern (RFP: deceleration time < 140 ms) is an important independent predictor after AMI (Circulation.2008;117). Tissue Doppler (TDI) of mitral annulus is very useful while also being simple and easy. The aim of this study was to explore whether TDI is superior to RFP to predict the prognosis after a first anterior ST elevation AMI (STEMI) when we divided them by LV contraction.

Methods: 2D echo with TDI and blood sampling were obtained in 138 consecutive patients (age 64 yrs, male 110, peak CPK = 4426), 2 weeks after onset of a first anterior STEMI. All patients underwent PCI successfully within 12 hours and were followed for 24 months. Primary end point was major adverse cardio-cerebrovascular event (MACCE: death from cardiovascular disease, ACS, readmission because of heart failure, stroke). Exclusion criteria; non-STEMI, A-C bypass, atrial fibrillation, renal failure on dialysis.

Results: MACCE occurred in 22 patients (2 patients died, 3 had ACS, 13 with readmission because of heart failure, 1 with arrhythmia, 3 with stroke). Table shows Univariate and Multivariate analysis by Cox proportional-hazards model. TDI parameters were stronger predictors compared with RFP, regardless of systolic function. E/e' was extremely powerful predictor especially for preserved EF.

Conclusion: TDI is superior to RFP for predicting the prognosis of a first anterior STEMI within 24 months. It was useful especially for those with preserved LV contraction.

	Univariate analysis		Multivariate analysis	
	HR(95% CI)	p Value	HR(95% CI)	p Value
(A) EF $\geq 45\%$: n=98				
LAVI > 32 ml/m ²	5.37	0.09		
RFP (TMDct < 140 msec)	11.31	0.0009	1.92	0.73
PVDct < 150 msec	8.87	0.07		
e' < 5	17.22	0.008	0.93	0.83
E/e' > 15	49.74	0.0003	10.88	0.007
MR \geq moderate	1.29	0.7		
BNP > 180 pg/ml	8.51	0.009	4.73	0.06
Hb < 11 g/dl	2.84	0.15		
eGFR < 30 ml/min	3.29	0.28		
(B) EF $< 45\%$: n=40				
LAVI > 32 ml/m ²	2.19	0.31		
RFP (TMDct < 140 msec)	1.45	0.59		
PVDct < 150 msec	3.73	0.28		
e' < 5	3.28	0.09		
E/e' > 15	5.01	0.01	6.91	0.03
MR \geq moderate	1.29	0.7		
BNP > 180 pg/ml	2.55	0.08		
Hb < 11 g/dl	2.83	0.11		
eGFR < 30 ml/min	13.2	0.005	10.29	0.01

9:30 a.m.

9:30 a.m.

1018-249

Obesity as an Independent Risk for the Left Ventricular Diastolic Dysfunction in 814 Japanese Adult Patients

Kinuko Dote, Yoko Miyasaka, Mio Haiden, Satoshi Tsujimoto, Hirofumi Maeba, Toshiji Iwasaka, Kansai Medical University, Hirakata, Japan

Background: Abnormal left ventricular diastolic function has been shown to be risk factor for cardiovascular events. Obesity is associated with an increased risk of cardiovascular morbidity and mortality. We sought to determine if obesity is independently associated with left ventricular diastolic dysfunction.

Methods: To evaluate the risk for the left ventricular diastolic dysfunction, adult patients referred for a clinically indicated echocardiogram, who had no history of valvular or congenital heart disease, were prospectively included in this study. Diastolic function was classified by an algorithm incorporating data from mitral and pulmonary venous flow indices and tissue Doppler imaging (normal, impaired relaxation, pseudonormal, or restrictive). A body mass index value ≥ 30 kg/m² was defined as obese.

Results: Of a total number of 1,209 patients who performed echocardiography, 814 patients met all study criteria (mean age 59 ± 15 years; 52% men; 7% obese, 21% chronic kidney disease, 16% coronary artery disease, 48% hypertension, 19% diabetes, 68% dyslipidemia). Of these, 635 patients (78%) were abnormal diastolic function. Diastolic dysfunction was significantly associated with advancing age (Odds ratio 2.6, 95% confidential interval 1.2-5.6, $P=0.01$) and female sex (Odds ratio 1.6, 95% confidential interval 1.1-2.2, $P=0.01$). After adjusting for age, sex, history of coronary artery disease, hypertension, diabetes, chronic kidney disease, and dyslipidemia in a multivariate model, obesity was significantly associated with abnormal left ventricular diastolic function (Odds ratio 2.7, 95% confidential interval 1.2-7.3, $P=0.01$).

Conclusions: Obesity was independently associated with left ventricular diastolic dysfunction. Further studies are needed to determine whether effective treatment of obesity improves left ventricular diastolic function and cardiovascular outcome in these patients.

9:30 a.m.

1018-250

Incremental Value of Temporal Analysis of Transmitral Inflow and Mitral Annular Velocity for Estimating Elevated Left Ventricular Filling Pressure

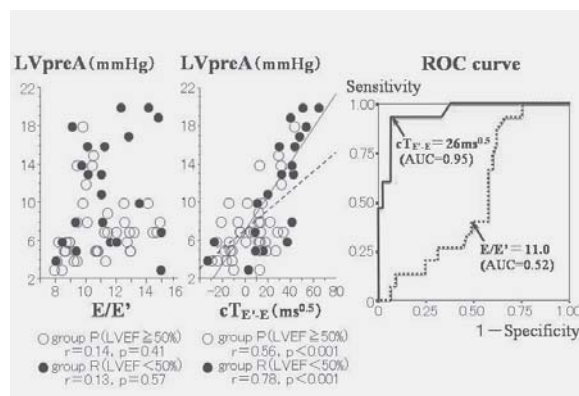
Yasuaki Wada, Kazuya Murata, Shinishi Okuda, Takeo Tanaka, Yoshio Nose, Chikage Kihara, Yasuhiro Fukagawa, Hiroko Yoshino, Takehisa Susa, Yukari Kishida, Ayako Yamaguchi, Masunori Matsuzaki, Yamaguchi University Graduate School of Medicine, Ube, Japan, Yamaguchi University Hospital, Ube, Japan

Background: A ratio of early transmitral flow velocity (E) to early diastolic mitral annular velocity (E') from 8 to 15 is classified as a "gray zone" for estimating left ventricular (LV) filling pressure (FP). However, the values of E/E' from 8 to 15 is recognized as "gray zone" for estimating LVFP.

Methods: To evaluate the feasibility for estimating LVFP by time interval between onsets of E and E' ($T_{E-E'}$), we analyzed 60 patients with heart disease whose E/E' ranged 8 to 15. Patients were subdivided into two groups according to their LV ejection fraction (group P: LVEF $\geq 50\%$, n=38 patients; group R: LVEF $< 50\%$, n=22). We measured $T_{E-E'}$ corrected by R-R interval ($cT_{E-E'}$) within 24 hours before invasively measuring a LV pre-atrial pressure (LVpreA).

Results: In both two groups, $cT_{E-E'}$ had significant correlations with LVpreA ($P: r=0.56$, $p<0.001$; $R: r=0.78$, $p<0.001$), whereas there were no correlations between E/E' and pre-A. Among all patients, sensitivity and specificity for predicting elevated LVpreA (>12 mmHg) by $cT_{E-E'}$ were superior to that by E/E' using receiver-operating characteristic (ROC) analysis. E/E' had a sensitivity of 40% and a specificity of 51% in predicting elevated LVpreA, while $cT_{E-E'}$ had a 93% sensitivity and a 93% specificity in predicting it.

Conclusions: In noninvasive assessment of LVFP in patients with indeterminate E/E', using temporal analysis of the time difference between onsets of E and E' may have an incremental value for estimating elevated LVFP.



1018-251

The Mitral L-Wave Predicts Adverse Response to Volume Overloading in Patients With Atrial Fibrillation

Hirotsugu Yamada, Kenya Kusunose, Susumu Nishio, Noriko Tomita, Toshiyuki Niki, Koji Yamaguchi, Kunihiro Koshiba, Shusuke Yagi, Takashi Iwase, Takeshi Soeki, Tetsuzo Wakatsuki, Masashi Akaike, Masataka Sata, The University of Tokushima Graduate School of Medicine, Tokushima, Japan

Backgrounds: Appearance of mid-diastolic transmitral flow velocity wave (L-wave) in patients with chronic atrial fibrillation (AF) has been reported to indicate elevated filling pressure and delayed LV relaxation. We hypothesized that this wave may become a predictor of cardiac response to volume overloading in patients with AF.

Methods: Subjects consisted of 35 patients with non-valvular chronic AF (mean age 71 ± 11 years old) who underwent transthoracic echocardiographic studies before and during lower body positive pressure (LBPP). A novel dual Doppler technique was used to record transmitral and LV outflow tract velocities simultaneously. Cardiac output was calculated from the LV outflow tract diameter and time-velocity integral of the flow velocity. Plasma BNP level was measured in all subjects.

Results: According to the presence of the L-wave, we divided the subjects into L-wave (+) and L-wave (-) groups. Age, LV end-diastolic dimension, left atrial dimension, LV ejection fraction and peak early diastolic transmitral flow velocity showed no significant differences between the both groups. The BNP level in the L-wave (+) group is greater than in the L-wave (-) group. The cardiac output increased by LBPP in 22 of 24 patients in the L-wave (-) group, while the cardiac output decreased by LBPP in 6 of 8 patients in the L-wave (+) group. Presence of the L-wave predicted adverse response to LBPP with sensitivity of 75.0% and specificity of 91.7%. The L-wave appeared during LBPP in 6 patients with normal response. In the L-wave (+) group, amplitude of the L-wave velocity increased by LBPP (19.7 to 22.3 cm/s, $p<0.05$).

Conclusions: Frank-Starling mechanism was preserved and working during volume overloading in AF patients without mitral L-wave, whereas the cardiac output was decreased by volume overloading in AF patients accompanied with the L-wave. Appearance of this wave is useful to identify the high-risk in patients with AF.

9:30 a.m.

1018-252

Left Atrial Size and Left Ventricular Mass Predict Heart Failure Hospitalization in Coronary Artery Disease Irrespective of Indexing Method: The Heart and Soul Study

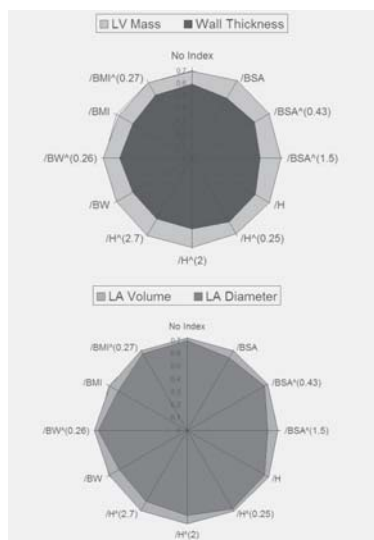
Bryan Ristow, Sadia Ali, Mary A. Whooley, Nelson B. Schiller, California Pacific Medical Center, San Francisco, CA, VA Medical Center, San Francisco, CA

Background: Echocardiographic measurements of left ventricular (LV) mass and left atrial (LA) size predict heart failure (HF) hospitalization. The American Society of Echocardiography recommends indexing by body surface area (BSA), but other indexing methods have been advocated.

Methods: Echocardiographic measurements were collected in 1024 ambulatory adults with coronary artery disease. C-statistics were calculated to compare various indexing methods.

Results: Mean LV posterior wall thickness was 1.2 ± 0.2 cm, mean LV mass was 192 ± 57 g, mean LA diameter was 4.3 ± 0.6 cm, and mean LA end systolic volume was 65 ± 24 ml. At average 4.9 year follow-up, there were 139 HF hospitalizations. C-statistics are shown (Figure) where a further distance from the center indicates a higher predictive ability, and a circular shape indicates equivalence among indexing methods. Mean c-statistics among indexing methods were higher for LV mass than posterior wall thickness (0.70 vs 0.57 , $p<0.0001$) and higher for LA volume than LA diameter (0.71 vs 0.66 , $p=0.0001$). Significant differences were not present among different indexing parameters.

Conclusion: The choice of indexing method by parameters of BSA, height (H), body weight (BW), or body mass index (BMI) does not affect the clinical usefulness of LV mass and LA volume in predicting HF hospitalization; continued use of BSA is acceptable. Volumetric methods maintain their superiority over linear dimensions in predicting HF hospitalization.



9:30 a.m.

1018-253 Change of Tricuspid Annular Velocity Profile by the Treatment of Left-sided Heart Failure With Secondary Pulmonary Hypertension Determined by Pulsed Tissue Doppler Imaging

Susumu Nishio, Hirotosugu Yamada, Kenya Kusunose, Noriko Tomita, Toshiyuki Niki, Koji Yamaguchi, Kunihiro Koshida, Shusuke Yagi, Takashi Iwase, Takeshi Soeki, Tetsuzo Wakatsuki, Masashi Akaike, Masataka Sata, The University of Tokushima Graduate School of Medicine, Tokushima, Japan, Tokushima University Hospital, Tokushima, Japan

Backgrounds: Tricuspid annular motion velocity profile derived from pulsed tissue Doppler imaging has been utilized for easy and quantitative evaluation of right ventricular function, however the effect of pulmonary hypertension (PH) on the annular velocity is unknown. We observed the serial changes of this velocity profile before and after treatment in patients with left-sided heart failure with secondary PH.

Methods: Subjects consisted of 34 patients (mean age: 72.3 ± 8.6 years old) with left-sided heart failure and secondary PH (15 with chronic myocardial infarction, 12 with dilated cardiomyopathy, 5 with hypertensive heart disease and 2 with hypertrophic cardiomyopathy). None of them had organic right-sided heart disease. Tricuspid annular motion at right ventricular free wall side was obtained from 4 chamber view by tissue Doppler imaging before treatment when they were presenting heart failure and after conventional treatment when they were about to discharge. The peak systolic (s'), early diastolic (e'), atrial systolic (a'), time from the onset of electrographic Q wave to the onset of s' (Q-s' onset) and peak s' (Q-s' peak) were measured from the velocity profile.

Results: Average left ventricular ejection fraction and end-diastolic volume at heart failure in all subjects were 45 ± 16% and 106 ± 152ml, respectively. Estimated systolic pulmonary artery pressure (PAP) decreased from 53.7 ± 9.8 to 31.4 ± 5.1 mmHg by the heart failure treatment. The s', e' and a' did not significantly change, while the Q-s' onset and the Q-s' peak significantly prolonged after the treatment (94.8 ± 27.5 to 118.0 ± 22.0 msec, p<0.0001, and 173.8 ± 29.4 to 188.5 ± 23.5 msec, p<0.005, respectively). There was a linear negative relationship between the Q-s' onset and PAP (r=-0.400, p<0.01) in all measurements.

Conclusions: Time interval index from tricuspid annular motion velocity significantly changed by the heart failure treatment as the secondary hypertension improved. These time indices are not affected by the Doppler angle. The tricuspid annular velocity profile obtained by tissue Doppler imaging is a valuable, noninvasive tool for evaluating secondary hypertension in patients with left-sided heart failure.

9:30 a.m.

1018-254 Systolic Peak Velocity of Mitral Annular Longitudinal Movement as an Index of Global Left Ventricular Contractility

Jeong-Sook Seo, Won-Jang Kim, Yun-Jeong Kim, Jee-Hye Kang, Yoo-Jin Jung, Jong-Min Song, Duk-Hyun Kang, Jae-Kwan Song, Asan Medical Center, University of Ulsan College of Medicine, Seoul, South Korea

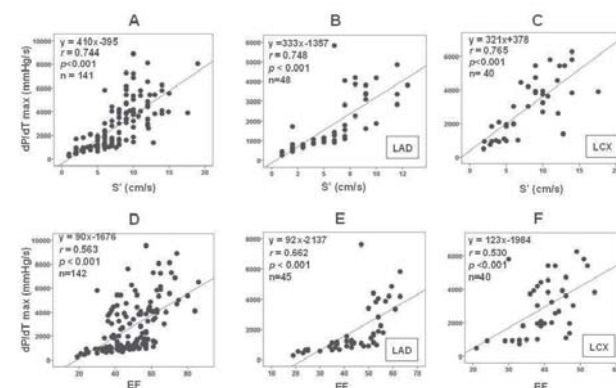
Background: Although mitral annular systolic velocity by tissue Doppler (S') has been reported to represent left ventricular (LV) contractility, the relative accuracy of S' against LV ejection fraction (EF) under a wide range of contractility conditions and the impact of regional wall motion abnormalities have not been seriously investigated.

Methods: We measured S' in 11 open chest anesthetized mongrel dogs under different inotropic stages using dobutamine and esmolol before and after coronary ligation (left anterior descending artery [LAD] in 6 and left circumflex artery [LCX] in 5). We measured LV pressure simultaneously with a high-fidelity pressure catheter and calculated LV EF with the biplane Simpson's method. Maximal positive dP/dt (dP/dt max) was used as the gold standard measurement of LV contractility. We compared S' and EF against dP/dt max

by linear regression.

Results: S' showed dose-dependent increases and decreases following dobutamine and esmolol infusion, respectively. There was a stronger association between dP/dt max and S' (r=0.744) than between dP/dt max and EF (r=0.563, p=0.003), and this trend was more apparent with coronary ligation (p<0.001). Before coronary ligation, the association did not show any significant difference (p=0.199). Coronary ligation site did not affect the association between S' and dP/dt max.

Conclusions: S' is an effective noninvasive index of global LV contractility irrespective of coronary ligation and has better accuracy than LV EF.



9:30 a.m.

1018-255 Left Atrial Function Index Predicts Heart Failure and Mortality in Patients With Stable Coronary Artery Disease: Findings From the Heart and Soul Study

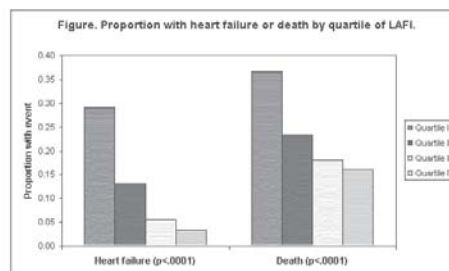
Damon M. Kwan, Ramin Farzaneh-Far, Sadia Ali, Mary A. Whooley, Nelson B. Schiller, University of California, San Francisco, San Francisco, CA

Background: The left atrial function index (LAFI) is a simple echocardiographic expression of atrial function that is indexed to atrial size and cardiac output. We sought to determine whether LAFI predicts heart failure (HF) or death in ambulatory patients with coronary artery disease (CAD).

Methods: We performed transthoracic echocardiography in 948 outpatients with stable CAD and no atrial fibrillation. Left ventricular outflow tract velocity time integral (LVOT_{VTI}) and biplane left atrial end systolic and diastolic volumes (LAESV, LAEDV) were measured. Left atrial ejection fraction (LAEF) was defined as (LAEDV-LAESV)/LAEDV. We calculated LAFI as [(LVOT_{VTI} × LAEF) / LAESV indexed to body surface area] × 10⁴. Cox proportional hazards models were used to investigate the association of LAFI with HF or death during 5.2 years of follow-up.

Results: LAFI ranged from 9 to 105. Lower LAFI was strongly predictive of HF and death (Figure). After adjustment for demographics, medical comorbidities, medication use, left ventricular ejection fraction, treadmill exercise capacity, inducible ischemia and NT-proBNP, participants with LAFI in the 4th quartile were twice as likely to develop HF or death as those in the 1st quartile (HR 2.0, 95% CI, 1.2 - 3.2; p=.006).

Conclusions: Low LAFI predicts HF and death in outpatients with stable coronary heart disease, independent of left ventricular ejection fraction and NT-proBNP levels.



9:30 a.m.

1018-256 Right Ventricular Septal Pacing Preserves Left Ventricular Synchrony and Torsional Behavior in Comparison With Conventional Apical Pacing

Katsuji Inoue, Hideki Okayama, Kazuhisa Nishimura, Takayuki Nagai, Jun Suzuki, Akiyoshi Ogimoto, Tomoaki Ohtsuka, Jitsuo Higaki, Makoto Saito, Go Hiasa, Toyofumi Yoshii, Tadakatsu Yamada, Takumi Sumimoto, Ehime University Graduate School of Medicine, Toon, Japan, Kitaishikai Hospital, Ozu, Japan

Background: Right ventricular apical pacing (RVA) is a conventional method of pacing therapy for patients with bradyarrhythmias, but creates left ventricular (LV) asynchronous

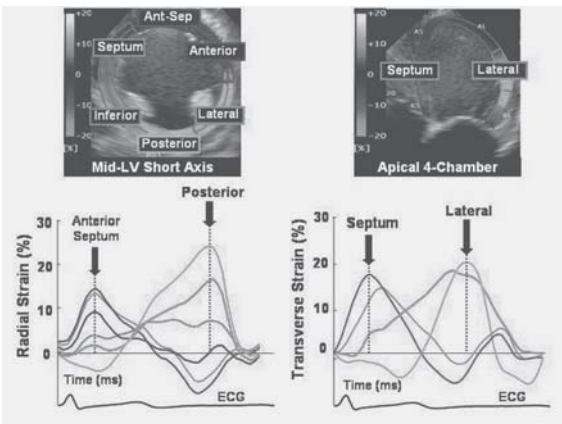
motion and thus occasionally LV dysfunction. RV septal pacing (RVS) is an alternative pacing to shorten LV electro-mechanical activation time especially in cases with that pacing leads ideally attached to RV septum. **Methods:** Forty consecutive patients (22 female, 74±6 years) with symptomatic sick sinus syndrome without organic heart disease were included. We assigned into two groups according to the RV pacing sites (RVA: n=20, RVS: n=20). The optimal RVS that was confirmed by fluoroscopic guidance was successfully performed in all patients. All patients underwent echocardiographic study with GE Vivid 7 during AAI- and DDD-mode after pacemaker implantation. The two indexes of LV dyssynchrony were estimated as follows: (1) Ts-Diff: max opposing wall delay in 4 LV models using tissue velocity imaging, (2) Te-SD: SD of longitudinal strain in 18 LV models using speckle tracking imaging. In addition, myocardial torsional properties were also evaluated using speckle tracking imaging as follows: (1) peak torsion, (2) peak untwisting rate. **Results:** The mean QRS width during DDD-mode was significantly longer in RVA compared to RVS (RVA: 161 ms, RVS: 138 ms, p<0.05). Ts-Diff and Te-SD during RV pacing were significantly greater in RVA compared to RVS (Ts-Diff: 68±41 ms vs 24±19 ms, Te-SD: 83±20 vs 53±11, p<0.01 for all). In addition, myocardial torsion and untwisting rate were significantly deteriorated in RVA compared to RVS (torsion: 9±3 deg vs 12±5 deg, untwisting rate: -78±29 deg/s vs -108±38 deg/s). Furthermore, the change of Te-SD from AAI- to DDD-mode was significantly associated with that of myocardial untwisting rate in this study population (r= -0.269, p<0.01). **Conclusions:** RV septal pacing is an effective method in comparison with RV apical pacing in terms of a less frequency of left ventricular dyssynchrony and torsional abnormalities.

9:30 a.m.

1018-257 A New Multiplane Speckle Tracking Imaging Approach to Quantify Dyssynchrony And Predict Response to Cardiac Resynchronization Therapy

Hidekazu Tanaka, Masaki Tanabe, Samir Saba, John Gorcsan, III, University of Pittsburgh, Pittsburgh, PA

Background: Our objective was to test the hypothesis that a new multiplane imaging approach using speckle tracking echocardiography could quantify dyssynchrony and predict response to cardiac resynchronization therapy (CRT). **Methods:** We studied 87 heart failure patients referred for CRT with ejection fraction (EF) 24±8% and QRS 153±28ms and 20 normal volunteers. Dyssynchrony was assessed for each patient by 4 different types of new speckle tracking strain (Toshiba Corp): radial and circumferential (using mid-short axis views) and transverse and longitudinal (using 3 apical views). A time to peak strain opposing wall delay of ≥ 130 ms was defined as significant dyssynchrony. Follow-up was available on 44 patients (7±4 mo), with CRT response defined as EF increase ≥ 15%. **Results:** Heart failure patients had significantly greater dyssynchrony, compared with normal controls who had reproducibly no dyssynchrony by speckle tracking strain (all p<0.0001). Radial strain was the best individual predictor of response to CRT with sensitivity 86%, specificity 73% and ROC area under curve (AUC)= 0.83. The combination of radial dyssynchrony from short axis views and transverse dyssynchrony from apical views best predicted response to CRT with AUC = 0.86. **Conclusions:** A new multiplane speckle tracking imaging approach successfully quantified dyssynchrony and predicted response to CRT. These observations may have clinical implications.



9:30 a.m.

1018-258 The Prevalence of Left Ventricular Hypertrophy (LVH) by New ASE-Guidelines in Koreans and Characteristics in Newly Diagnosed LVH Group

Hye-Sun Seo, Tae Soo Kang, Jon Suh, Yoon Haeng Cho, Nae-hee Lee, Soonchunhyang university hospital, Bucheon, South Korea

Background: Left ventricular hypertrophy (LVH) is an important marker of cardiovascular disease. The determination of cut off points to define LVH is frequently controversial, and ASE committee developed the new criteria of LVH at 2005 because traditional cut-off limits may ignore cardiovascular risk in the "normal" range. We sought to evaluate the prevalence of LVH after applying the new criteria in Koreans and characteristics in newly categorized LVH group compared with previously diagnosed LVH group.

Methods: We investigated 7640 subjects performed echocardiography in our center. Patients with significant heart problem, systemic disease and poor echo window were excluded. 2D linear measurements were used for chamber quantification and the patients with the criteria according to ASE guidelines (>115g/m² for men, >95g/m² for women) were categorized as LVH. **Results:** We analyzed 2489 patients (905 men, 1584 women) who are diagnosed as LVH. Among these patients, 331 men (8.8%) and 690 women (18%) who had LV mass below the limits traditionally employed for LVH definition are categorized as LVH by new criteria. The more proportion of non-hypertensive patients is included and the mean value of LV mass, LA volume and E/E' was lower. (Table) **Conclusions:** By new LVH classification criteria, the prevalence of LVH has increased about 9~18% in Korean. Further follow up evaluation whether these changes would predict major cardiovascular events better than previous criteria will be needed.

Table

Men	LVH By new criteria (n=905)	LVH by traditional criteria (n=574)	p value	Women	LVH By new criteria (n=1584)	LVH by traditional criteria (n=894)	p value
Age (years)	56.8 ± 13.8	57.1 ± 14.1	0.748		61.5 ± 13.5	63.2 ± 13.1	0.003
Hypertension (%)	592(67%)	405(72%)	0.040		993(65%)	518(71%)	0.001
LVEF (%)	63.5 ± 6.7	63.0 ± 7.2	0.130		65.6 ± 5.8	65.3 ± 6.0	0.328
LVEDD (mm)	49.7 ± 4.3	50.3 ± 4.5	0.013		46.0 ± 3.9	47.0 ± 4.0	<0.001
LVMI (g/m ²)	138.3 ± 26.9	149 ± 28.4	<0.001		117.8 ± 21.2	130.1 ± 20.9	<0.001
LAVI (ml/m ²)	29.1 ± 10.8	31.0 ± 11.7	0.001		28.2 ± 11.0	31.1 ± 12.4	<0.001
E/E'	11.4 ± 4.2	12.1 ± 4.5	0.004		12.6 ± 4.6	13.6 ± 4.9	<0.001

9:30 a.m.

1018-259 Clinical Categories of Pulmonary Artery Systolic Pressure by Echocardiography Versus Right Heart Catheterization in 619 Clinically-Performed Studies

Jeffrey Testani, Bonnie Ky, Julio A. Chirinos, Amit Khara, Martin G. Keane, Victor A. Ferrari, Martin St. John Sutton, James N. Kirkpatrick, University of Pennsylvania, Philadelphia, PA

Background: Pulmonary artery systolic pressure (PASP) by echo is used increasingly in clinical practice on the basis of relatively small studies. We evaluated agreement between echo and right heart cath (RHC) in a large sample of clinical studies. **Methods:** We studied 619 echo-RHC pairs performed <48 hours (287 same day, 513 <24 hours). PASP by echo was calculated as tricuspid regurgitant gradient (TRG) + right atrial pressure (RAP) estimated from inferior vena caval (IVC) collapse. In 190 cases the IVC was not visualized, and RAP was assumed to be 14mmHg. PASP was graded as normal (<30mmHg), mildly (31-45mmHg), moderately (46-60mmHg), or severely (60mmHg) elevated. **Results:** Mean difference between echo and RHC PASP was 9.9±7.9, TRG was 7.7±6.8, and RAP was 5.6±4.2 mmHg (p<0.0001 for each). Confining analysis to same day studies in which IVC was visualized (n=209), PASP difference was 8.9±7.5, TRG was 7.7±6.6, and RAP was 4.3±3.2 mmHg. Misclassifications of clinical categories were noted in 55% of normal and 29% of mildly, 70% of moderately, and 75% of severely elevated PASP. Only 8 studies were misclassified by 2 grades. **Conclusions:** In a large clinical series, differences in PASP by echo vs. RHC were substantial. Ongoing prospective studies may identify ranges of PASP in which echo PASP is more accurate, as well as sources of discrepancy. Clinicians making decisions based on PASP by echo should be aware of potential limitations of PASP by echo especially in patients with moderate and severe pulmonary hypertension.

Categorization of PASP by Echo vs. RHC in same day studies

PASP (mmHg)	Echo PASP <30	Echo PASP =30-44	Echo PASP =45-60	Echo PASP ≥60
RHC PASP<30	32	38	1	0
RHC PASP=30-44	12	60	11	1
RHC PASP=45-60	3	15	11	8
RHC PASP ≥60	0	3	9	4

9:30 a.m.

1018-260 Predictors of Outcome in an Elderly Population Presenting With Acute Decompensated Heart Failure

Thomas Km Cudjoe, Alfredo L. Clavell, Lyle J. Olson, Raquel M. Shears, Hector R. Villarraga, Mayo Clinic, Rochester, MN

Background: Heart failure (HF) is highly prevalent in the elderly. Our aim was to evaluate the relationship of clinical and echocardiographic parameters and biomarkers to mortality in an elderly population presenting to the emergency department (ED) with acute decompensated HF **Methods:** 50 consecutive patients over age 65 who presented to the Mayo Clinic

ED for evaluation of dyspnea were enrolled. Biomarkers included BNP and troponin (Trop I). Inclusion required meeting Framingham criteria for HF and a Transthoracic Echocardiogram (TTE) during subsequent hospitalization. Clinical characteristics were reviewed and recorded for analysis. Endpoints were mortality related to cardiovascular disease and all cause mortality. Analysis included estimation of likelihood ratios, uni and multivariate analysis with regard to total mortality and cardiac related mortality (CRM).

Results: Mean age was 79.7 years [7.04] (46% were women). Mean LVEF (%) in men was 40% [16] and women 53% [15]. Mean follow-up was 748 days [549]; 30 patients (60%) died during follow-up. Hypertension (HTN) was present in 68%, CAD in 64%, hyperlipidemia (HL) in 53%, chronic renal failure (CRF) in 34%, diabetes mellitus 2 (DM) in 28% and COPD in 24%. In a univariate model that evaluated all-cause mortality hazard ratios (HR) were: age (1.03), HTN (0.94), CAD (0.58), HL (0.91), CVA (0.97), DM (1.67) (p NS) and CRF (2.07) (p 0.055). For cardiac mortality only CRF was significant (2.88) p<0.03. Laboratory and echo parameters HRs for CRM were Trop I (2.33), Log BNP (1.33), BUN (1.02), RV dysfunction (1.51), LVEF less or equal to 50% (2.32), greater than mild MR (1.7), DT (0.99), medial E/e' (1.01) (all values with a p NS) and LA volume index (LAVI) (1.89) (p < 0.003). for all-cause mortality LAVI (1.07) (p < 0.0001), log BNP (1.42) (p = 0.07). A multivariate model including age, CRF, log BNP, LVEF, and LAVI demonstrated that LAVI was significantly associated with CRM with HR 1.06 [CI 1.02 - 1.12] p < 0.01

Conclusions: In elderly patients presenting with HF, only LAVI was significantly associated with all cause and CRM, suggesting that this is an important parameter to be included in the evaluation.

9:30 a.m.

1018-261 Change in Global Longitudinal Left Ventricular Strain Is a Strong Independent Predictor of Change in Plasma BNP Levels in Patients With Heart Failure

Jun Koyama, Hirokiko Motoki, Kazunori Aizawa, Hiroki Kasai, Megumi Koshikawa, Atsushi Izawa, Takeshi Tomita, Setsuo Kumazaki, Hiroshi Tsutsui, Uichi Ikeda, Shinshu University School of Medicine, Matsumoto, Japan

Background: Recent studies have indicated that longitudinal left ventricular (LV) dysfunction is strongly related to elevated plasma BNP levels in patients with heart failure. The purpose of this study was to clarify which echo parameters' change of standard echo/Doppler, and speckle-tracking echocardiography determined LV strain could predict changes in plasma BNP levels, a biomarker of clinical status of congestive heart failure (CHF).

Methods: Sixty-five patients with CHF were followed-up by echocardiography. The BNP levels were examined on the day of echocardiography. In addition to routine echocardiographic assessment, LV global longitudinal strain from apical 4 chamber view and LV global circumferential strain from short axis view of papillary muscle level were measured in each examination.

Results: The mean plasma BNP levels were 183±306 pg/ml at first time examination and 156±274 pg/ml at follow-up. Stepwise logistic regression analysis showed that the changes in LV global longitudinal strain (r=-0.52, F value to enter=22.8) and the changes in LV dimension at end-systole (r=0.49, F value to enter=20.3) were the only independent predictors of % changes in log plasma BNP levels.

Conclusions: The % changes in LV global longitudinal strain and the % changes in LV end-systolic dimension were strong independent predictors of plasma log BNP levels in patients with CHF.

Univariate analysis to predict changes in log BNP during follow up

Parameters (% changes)	R	F value to enter
LVDd	0.443	15.4
LVDs	0.494	20.3
FS	-0.50	21.3
TMF-E/A	0.27	4.97
TMF-DT	-0.34	8.23
PVF-D/S	0.27	4.96
LVOT VTI	-0.35	8.86
Global Circ Strain	-0.41	12.6
Global longitudinal Strain	-0.52	22.8

9:30 a.m.

1018-262 Increased Pulsatile Systolic Load in Hypertension Is Associated With Delayed Left Ventricular Untwisting

Julio Chirinos, Patrick Segers, Amit Gupta, Abigail Swillens, James Kirkpatrick, Martin Keane, Susan Wieggers, Victor Ferrari, Martin St. John Sutton, University of Pennsylvania, Philadelphia, PA, University of Ghent, Ghent, Belgium

Background: Epidemiologic data suggest a close link between increased pulsatile left ventricular (LV) systolic load and the risk of heart failure with preserved ejection fraction. LV twist/untwist are closely related phenomena by which stored potential energy during systolic contraction is subsequently released (elastic recoil) during diastole to promote diastolic filling. Therefore, twist mechanics represents a logical link between LV systolic load and diastolic dysfunction. We aimed to assess the relationship between specific components of systolic load and diastolic untwist.

Methods: We studied 27 hypertensive adults. We performed simultaneous carotid applanation tonometry and Doppler echocardiography. Speckle tracking echocardiography (echoPAC; GE Health Care) was used to determine rotation of the LV at the mitral annular and apical levels. Using custom designed software, we assessed: (1) Aortic pressure-flow relations (LV afterload) in the time and frequency domains; (2) LV twist mechanics,

including peak untwist rate and the timing of the onset of untwist (negative zero-crossing of the first time derivative of the twist curve). Timing of the onset of untwist was expressed as a percentage of the cardiac cycle.

Results: Both characteristic impedance (Z_c) of the proximal aorta ($\beta=94.9$; $P=0.0001$) and wave reflection magnitude ($\beta=36.0$; $P=0.03$) were independent predictors of a delayed onset of LV untwist after adjustment for resistive load, ejection duration and body height. These relationships were not affected by adjustment for age and gender. In contrast, systemic vascular resistance was associated with an earlier onset of untwist in multivariate models ($\beta=-19.03$; $P=0.0001$). None of the indices of systolic load predicted the peak rate of untwist.

Conclusions: Specific components of pulsatile (but not resistive) hemodynamic load are independently associated with a delayed onset of LV untwist in hypertension. Late untwist represents a plausible mechanistic link between LV pulsatile systolic load and diastolic dysfunction. Further studies are required to assess whether therapeutic reduction of systolic load may improve twist mechanics and diastolic function.

9:30 a.m.

1018-263 Intra and Interatrial Dyssynchrony Determined by Tissue Doppler Imaging Predict the New Onset Atrial Fibrillation in Patients With Acute Myocardial Infarction

Koichi Sakabe, Nobuo Fukuda, Yamato Fukuda, Satofumi Morishita, Hisanori Shinohara, Yoshiyuki Tamura, Zentsuji National Hospital, Kagawa, Japan

Background: New-onset atrial fibrillation (AF) often occurs following the acute myocardial infarction (AMI). We assessed the validity of the intra- and interatrial dyssynchrony, measured by tissue Doppler imaging (TDI), in determining patients at risk of new-onset AF after AMI.

Methods: One hundred sixty consecutive patients with AMI in sinus rhythm were prospectively followed after percutaneous coronary intervention (PCI) and transthoracic echocardiography with TDI performed within 2 hr after PCI. We measured the interval of time from initiation of the P wave on the electrocardiogram until the beginning of the atrial systolic TDI signal at the lateral border of the mitral annulus (P-A'(M)), the interatrial septum (P-A'(S)), and the tricuspid annulus (P-A'(T)). Intra- and interatrial dyssynchrony was defined as the difference between the P-A'(M) and P-A'(S) intervals (A'(M)-A'(S)), and the P-A'(M) and P-A'(T) intervals (A'(M)-A'(T)).

Results: Twenty patients had new-onset AF within 26 ± 43 hours after PCI during their hospital stay. Compared to those without AF, the patients who developed AF had longer A'(M)-A'(S) (38 ± 12 vs 12 ± 8 msec, p<0.001) and A'(M)-A'(T) (49 ± 6 vs 19 ± 9 msec, p<0.001) interval, as well as lower atrial systolic mitral (A'(M)) (9.1 ± 3.6 vs 11.7 ± 3.1 cm/sec, p<0.05), septal (A'(S)) (8.2 ± 2.7 vs 11.1 ± 2.6 cm/sec, p<0.01), and tricuspid (A'(T)) (12.6 ± 3.6 vs 16.8 ± 4.9 cm/sec, p<0.05) annular tissue Doppler velocity. Multivariate analysis showed that A'(M)-A'(S) (p<0.01) and A'(M)-A'(T) (p<0.001) interval was significant independent risk factor for the new-onset AF after AMI. We defined a cutoff point using ROC curve analysis, and chose 28 msec for A'(M)-A'(S) and 40 msec for A'(M)-A'(T) interval, which yielded 88.9, 100% sensitivity, 96.4, 98.2% specificity, 80, 90% positive predictive value, and 98.2, 100% negative predictive value for the prediction of new-onset AF after AMI, respectively.

Conclusions: Patients at risk of new-onset AF after AMI have intra- and interatrial dyssynchrony, and atrial systolic dysfunction on atrial TDI. Intra- and interatrial dyssynchrony detected by TDI could be a valuable method for identifying patients vulnerable to new-onset AF after AMI.

9:30 a.m.

1018-264 Impact of Left Atrial Volume Index and Left Ventricular Geometry on Mortality in Obese Versus Nonobese Elderly Patients With Preserved Ejection Fraction

Dharmendrakumar A. Patel, Carl J. Lavie, Jr., Richard V. Milani, Hector O. Ventura, Ochsner Clinic Foundation, New Orleans, LA

Background: Left atrial volume index (LAVi) and left ventricular (LV) geometry predicts CV events. Although obesity is a risk factor for CV diseases, studies have noted a paradox regarding obesity and prognosis. To our knowledge no studies have determined the impact of LAVi and LV geometry on mortality by obesity status in elderly with preserved ejection fraction (EF).

Methods: We evaluated 16,901 patients aged ≥ 70 years with preserved EF, including 4,529 obese as well as 12,372 non-obese patients to determine the impact of LAVi and LV geometry on mortality during an average follow-up of 1.7±1.0 yrs.

Results: Obese patients had higher LAVi than non-obese patients (35.6±12.4 vs 33.7±10.6, p<0.0001). Abnormal LV geometry occurred more commonly in obese than non-obese patients (61% vs 52%, p<0.0001). In obese patients, Concentric remodeling was the most prevalent abnormal pattern (40%), with eccentric and concentric LV hypertrophy occurring in 11% and 15%, respectively, compared with non-obese patients (32%, 9%, and 11%, respectively). Moreover, significant upward trend (p<0.0001) was observed in LAVi, LV mass index (LVMI), and relative wall thickness (RWT) with increasing age-, gender-adjusted quartiles of BMI. Overall mortality was considerably lower in obese than non-obese (3.4% vs. 10.8%, p<0.0001). Although, age-, gender-adjusted top vs. bottom quartiles of LAVi, LVMI, and RWT showed significant higher mortality (p<0.0001) in both obese and non-obese patients, the difference was far greater in obese patients. In both groups, higher age, RWT, and LAVi were independent predictor of mortality. Of note, increasing BMI was associated with lower mortality [OR:0.94(0.93-0.96), p<0.0001] in non-obese compared to obese patients where mortality increased with BMI [OR:1.05(1.03-1.07), p<0.0001]. Other mortality predictors were male gender and low EF (non-obese).

Conclusion: Although an obesity paradox exists, in that obesity is associated with higher prevalence of structural abnormalities but lower mortality than non-obese patients, LAVi and LV geometric abnormalities are more prevalent in obese vs. non-obese elderly patients with preserved EF and are associated with increase in mortality.

9:30 a.m.

1018-265

Prognostic Importance of Strain and Strain Rate After Acute Myocardial Infarction

M. Louisa Antoni, Sjoerd A. Mollema, Victoria Delgado, Jael Z. Atary, Eric Boersma, Eduard R. Holman, Ernst E. Van der Wall, Martin J. Schalij, Jeroen J. Bax, Leiden University Medical Center, Leiden, The Netherlands

Background: Recently, strain (S) and strain rate (SR) assessed with speckle tracking imaging have been introduced as novel parameters reflecting left ventricular (LV) function. No data are available about the prognostic importance of these parameters on outcome after acute myocardial infarction (AMI). The objective of this study was to evaluate the relation between S and SR and clinical outcome after AMI.

Methods: Patients admitted with AMI treated with primary percutaneous coronary intervention were evaluated. Baseline echocardiography (< 48 hours after AMI) was performed to assess systolic and diastolic LV function. Longitudinal peak systolic S and SR were assessed with speckle-tracking imaging. Global S and SR were calculated as mean values of all LV segments. Regional S and SR were calculated as mean values of segments supplied by the culprit vessel. Multivariate models were used to identify the individual prognostic importance of S and SR for the primary end point (all-cause mortality) and secondary end points (revascularization and/or reinfarction, and hospitalization for heart failure).

Results: A total of 659 patients (mean age: 60 ± 12 years, 78% men) were followed for 21 ± 13 months. During follow-up 51 patients died, 123 patients had a reinfarction and/or revascularization and 29 patients were hospitalized for heart failure. Mean global S and SR were -15.3 ± 4.5% and -1.08 ± 0.31/s. After adjustment for a broad range of clinical and echocardiographic parameters, global SR (HR 17, CI 1.3 - 215, p < 0.05) and regional SR (HR 53, CI 2.5 - 1132, p < 0.05) independently predicted all-cause mortality. Global SR (HR 32, CI 13 - 82, p < 0.0001) and regional SR (HR 15, CI 6.4 - 37, p < 0.0001) independently predicted revascularization and/or reinfarction. Global SR (HR 456, CI 19 - 10782, p < 0.0001), regional SR (HR 29, CI 2.0 - 412, p < 0.05) and global S (HR 1.4, CI 1.1 - 1.6, p < 0.0001) independently predicted hospitalization for heart failure.

Conclusions: Strain and strain rate are early independent predictors of clinical outcome after acute myocardial infarction.

9:30 a.m.

1018-266

Circumferential Strain Is Superior to Longitudinal Strain to Separate Subendocardial From Transmural Necrosis

Benthe Sjøli, Stein Orn, Bjørn Grenne, Halvdan Ihlen, Thor Edvardsen, Harald Brunvand, Sorlandet Hospital, Arendal, Arendal, Norway, Rikshospitalet University Hospital, Oslo, Norway

Background: Differentiation of transmural from subendocardial necrosis in myocardial segments is important for clinical risk stratification in patients with acute myocardial infarction. The aim of the present study was to determine accuracy of myocardial strain by speckle tracking in the diagnosis of segmental infarct size.

Materials and methods: Myocardial function was assessed in 36 patients (61 ± 11 years) with acute myocardial infarction treated with thrombolysis. In a 16 segments model of the left ventricle, peak systolic circumferential and longitudinal strain was measured. Strain measurements were validated against segmental infarct size in the corresponding segments as measured by contrast enhanced magnetic resonance imaging (ce-MRI).

Results: LV segmental infarct size by ce-MRI

	None	1-50 %	51-100 %
Circ strain	-20.5 ± 9.6	-15.0 ± 9.9*	-4.7 ± 8.7*#
Long strain	-18.5 ± 8.0	-13.1 ± 9.4*	-8.0 ± 10.3*#

* p < 0.05 vs none, # p < 0.05 vs 1-50 %.

Circumferential strain had a 80 % sensitivity and 74 % specificity to diagnose infarct size > 50 %. Longitudinal strain had a 82 % sensitivity and a 53 % specificity to diagnose infarct size > 50 %.

Conclusion: Circumferential strain could separate subendocardial from transmural necrosis with better sensitivity and specificity compared to longitudinal strain in patients with acute myocardial infarction.

9:30 a.m.

1018-267

Transnasal Transesophageal Echocardiography in the Detection of Intracardiac Embolic Source

Toshihiro Kawasaki, Shota Fukuda, Kenei Shimada, Kumiko Maeda, Hiromi Fujimoto, Hitoshi Inanami, Ken Yoshida, Satoshi Jisso, Haruyuki Taguchi, Junichi Yoshikawa, Minoru Yoshiyama, Osaka Ekisai Hospital, Osaka, Japan

Background: The advantages of transesophageal echocardiography (TEE) in the detection of the possible embolic sources has been described, particularly in the investigation of the left atrium (LA) and its appendage. The widespread use of TEE is however limited by its methodological disadvantages, including increased medical costs and patient intolerance. Safe and cost-effective TEE techniques is therefore needed.

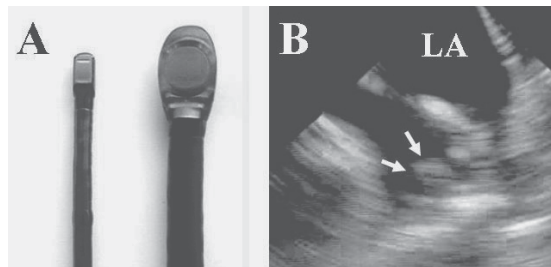
Purpose: To investigate the feasibility and safety of transnasal TEE without conscious sedation in the detection of the possible embolic sources in patients with atrial fibrillation (AF) and/or stroke, by using ultrathin TEE probe.

Methods: Fifty-two patients with AF and/or stroke had transnasal TEE without conscious sedation. The presence or absence of the following parameters was evaluated; LA thrombus, LA spontaneous echocardiographic contrast, intraatrial shunts, and aortic plaque. The

ultrathin and conventional TEE probes were shown for comparison (Figure A).

Results: The insertion of TEE probe was succeeded in 44 (85%) patients. TEE found LA thrombus in 9 (20%) patients (Figure B) and other embolic sources in 3 (7%) patients. Two (5%) patients had mild epistaxis, but other significant hemodynamic or mechanical complications were not noted during procedure or follow-up.

Conclusions: This study demonstrated that transnasal TEE without conscious sedation was feasible and safe in the detection of LA thrombus and other possible embolic sources in patients with AF and/or stroke.



9:30 a.m.

1018-268

Systolic Wringing of the Left Ventricular Myocardium: Characterization of Myocardial Rotation and Twist in Endocardial and Midmyocardial Layers in Normal Humans Employing Three-Dimensional Speckle Tracking Study

Antonietta Evangelista, Joachim Nesser, Stefano De Castro, Francesco Faletta, Jeffrey Kuvin, Ayan Patel, Alawi A. Alsheikh-Ali, Natesa Pandian, Tufts Medical Center, Boston, MA

Background: Myocardial design, geared to optimize LV performance, requires rotational and twisting motion. Studying this facet of myocardial mechanics has been limited to 2D methods and tissue Doppler with their inherent drawbacks (through plane motion, and angle dependency). 3D speckle tracking (3DST) provides a novel approach not hindered by the deficits of 2D and tissue Doppler methods.

Methods: To quantify the pattern of normal LV rotation and twist, we employed 3DST echocardiography (Artida, Toshiba) in 20 normal adults (15 males, age 34 ± 10). 3DST allows following of target regions through space and time based on the speckle signature. We derived systolic rotation and twist parameters (degrees) at multiple LV levels for both endocardial (ENDO) and midmyocardial (MID) layers.

Results: Globally, both myocardial layers exhibited counter-clockwise rotation, with a trend for more ENDO vs MID rotation (3.8 vs 2.9, p=0.09). This inter-layer distinction was evident at all levels of the LV (Table). The corresponding global twist values were similar in the two layers (4.5 vs 3.9, respectively). In both myocardial layers, inter-regional differences were also observed, with the apex exhibiting significantly more rotation and twist than the base (P<0.01).

Conclusion: 3DST echocardiography allows detailed study of myocardial rotation and twist. Understanding such patterns in normal hearts could provide insights into myocardial disorders and may have implications in planning interventional therapies.

	Endocardial	Midmyocardial	P (Endo vs Mid)
ROTATION			
Global	3.8 ± 1.6	2.9 ± 1.5	0.09
Basal LV	3.7 ± 1.7	0.26 ± 1.6	< 0.001
Mid LV	5.6 ± 1.7	4.8 ± 1.3	0.096
Apical LV	7.2 ± 2.2	4.9 ± 2.7	0.005
TWIST			
Global	4.5 ± 2.2	3.9 ± 2.4	0.4
Basal LV	2.0 ± 1.1	2.1 ± 1.0	0.7
Mid LV	6.7 ± 2.2	6.1 ± 2.7	0.5
Apical LV	8.6 ± 2.9	6.6 ± 3.6	0.07

9:30 a.m.

1018-269

Left Ventricular Mechanical Systole Is Shortened in Highly Trained Athletes

Stefano Caselli, Stefano De Castro, Fernando M. Di Paolo, Cataldo Piscicchio, Filippo M. Quattrini, Barbara Di Giacinto, Elvira De Biasiis, Roberto Ciardo, Antonio Pelliccia, Institute of Sports Medicine and Science, Rome, Italy, "Sapienza" University, Roma, Italy

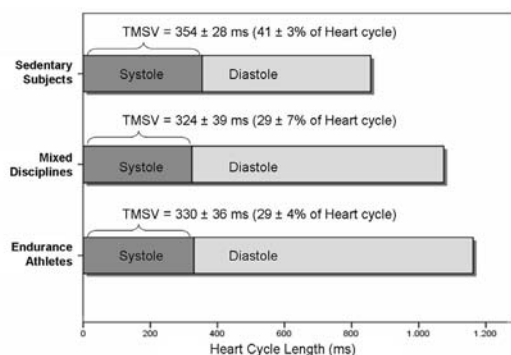
Background: We sought to evaluate mechanical systole duration comparatively in elite athletes and sedentary controls by 3-dimensional echocardiography (3DE).

Methods: 150 athletes, involved in endurance (n=96) and mixed disciplines (n=54) and 46 sedentary controls, matched for age, underwent 3DE examination. By off-line analysis, left ventricular volume-time curve was generated; time from the beginning of the QRS complex to the minimum systolic volume (TMSV) was considered to be the mechanical systole and was also expressed as percent of the heart cycle (TMSV%).

Results: Heart rate was lower in endurance (52 ± 7 bpm; p<0.001) and mixed disciplines athletes (55 ± 7 bpm; p<0.001) as compared to controls (71 ± 4 bpm). End-diastolic volume was significantly higher in endurance (90.2 ± 12.3 ml/m²; p<0.001)

and mixed athletes (75.4 ± 11.6 ml/m²; $p < 0.001$) as opposed to controls (56.9 ± 10.7 ml/m²). Mild but significant shortening of TMSV was identified both in endurance athletes (330 ± 36 ms; $p < 0.01$) and mixed disciplines (324 ± 39 ms; $p < 0.01$) than in controls (354 ± 28 ms). Lower TMSV% was observed both in endurance (29 ± 4 %; $p < 0.001$) and mixed athletes (29 ± 7 %; $p < 0.001$) as opposed to sedentary subjects (41 ± 3 %).

Conclusion: Elite athletes show a mild but significant shortening of mechanical systole time in comparison to sedentary controls, despite substantially increased volume. This adaptation, in addition to lengthening of diastolic time, may contribute to enhance systolic function in athletes.



9:30 a.m.

1018-270 Validation of a New Developed Three-Dimensional Speckle Tracking Imaging to Quantify Regional Myocardial Strain

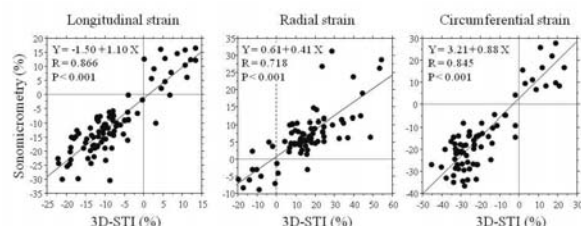
Yoshihiro Seo, Tomoko Ishizu, Yoshiharu Enomoto, Haruhiko Sugimori, Hiroyuki Ohuchi, Yasuhiro Abe, Shigeyuki Watanabe, Kazutaka Aonuma, Cardiovascular Division, University of Tsukuba, Ibaraki, Japan, Department of Cardiovascular Surgery, University of Tsukuba

Background: Three-dimensional speckle tracking imaging (3D-STI) using cubic pattern matching for 3D myocardial data set has been introduced to assess left ventricular (LV) myocardial function with a new developed ultrasound system (Artida, Toshiba medical systems, Tochigi, Japan). This study was designed to validate LV strain measurements using 3-D STI against segment shortening measurements with sonomicrometry.

Methods: In 10 anesthetized ovine, 12 sonomicrometry crystals were placed at the basal, mid and apical anterior and lateral end- and epicardial wall. LV 3D myocardial data was obtained from apical B-mode images. The both 3D endocardial and epicardial surfaces were tracked with 3D-STI technique. We compared segmental longitudinal, radial and circumferential strain measurements by 3D-STI with those by sonomicrometry at baseline and during dobutamine infusions, propranolol infusions and coronary occlusion.

Results: Good correlations were observed between strain measurements by 3D-STI and those by sonomicrometry (longitudinal strain: $r = 0.866$, $p < 0.001$; radial strain: $r = 0.718$, $p < 0.001$; circumferential strain: $r = 0.845$, $p < 0.001$).

Conclusions: The novel developed 3D-STI can accurately assess regional LV myocardial strain in normal and alternative segments by pharmacological and ischemic interventions.



9:30 a.m.

1018-271 Localization of Mitral Valve Prolapse Affects the Geometry of the Mitral Annulus

Koji Kurosawa, Hiroyuki Watanabe, Masaru Aikawa, Hirotugu Mihara, Rieko Takahashi, Kanki Inoue, Itaru Takamisawa, Atsushi Seki, Kouhei Tanizaki, Tetsuya Tobaru, Nobuo Iguchi, Masatoshi Nagayama, Ryuta Asano, Morimasa Takayama, Jun Umemura, Toshihiro Fukui, Tomoki Shimokawa, Hitoshi Kasegawa, Shuichi Takanashi, Tetsuya Sumiyoshi, Sakakibara Heart Institute, Tokyo, Japan, Hanzomon Cardiovascular Clinic, Tokyo

Backgrounds: It is unknown how localization of mitral valve prolapse (MVP) affects the mitral annular geometry. The purpose of this study was to examine geometrical differences of the mitral annulus of MVP using three-dimensional data-set obtained by real-time three dimensional transesophageal echocardiography (R3DTEE).

Methods: We studied 129 patients with MVP and divided them into three groups; anterior mitral leaflet prolapse (GroupA, n=33), posterior mitral leaflet prolapse (GroupP, n=68) and bileaflet prolapse group (GroupB, n=28). We recorded three-dimensional data-set by R3DTEE

for subsequent off-line analysis; heights, length, width and area of the mitral annulus.

Results: Table shows the results.

Conclusion: In patients with bileaflet prolapse, annulus area is larger and the shape is more planarized compared with other type of prolapse. This difference should be taken into account in surgical treatment of MVP.

Table

	Group A (n=33)	Group B (n=68)	Group P (n=28)	p value
ERO (cm ²)	0.40	0.45	0.40	0.28
AA (cm ²)	10.0	10.1	12.2	<0.01
AH (mm)	4.2	4.1	3.6	0.27
APL (mm)	31	30	34	0.019
LML (mm)	39	40	43	0.013
APL/LML	0.80	0.77	0.78	0.33
AH/AA	0.43	0.44	0.32	<0.01

ERO: effective regurgitant orifice

AA: annulus area

AH: annulus height

APL: antero-posterior length

LML: lateral-medial length

9:30 a.m.

1018-272 Importance of Performing Transesophageal Echocardiography in Acute Stroke Patients Older Than Fifty

Nishant Gupta, Anthony Al-Dehneh, Joseph Daoko, Chris Lau, Will B. Newton, Isha Gupta, Wishwdeep Dhillon, Padmaja Akkineni, Anuj Aggarwal, Bassem Barsoum, Rupen Parikh, Aman Vazir, Donna Konlian, Mahesh Bikkina, St. Joseph Regional Medical Center, Paterson, NJ

Background: The role of Transesophageal echocardiography (TEE) in changing the management of patients older than 65 years presenting with acute stroke was reported to be unwarranted. This is because of the poorly defined treatment based on finding of atrial septal aneurysm (ASA) with or without patent foramen ovale (PFO), as well as complex atheroma, which is defined as atherosclerotic plaque with protrusion of the atheroma of more than 4 mm in thickness, mobile debris or plaque ulceration. Recently, the treatment for such findings has been more defined. Therefore, we conducted a retrospective study to determine the incidence of cardiac findings that would require anticoagulation for patients presenting with acute stroke older than 50 years.

Methods: We consecutively selected 163 patients with suspected embolic stroke who were admitted to St. Joseph's Regional Medical Center between January 2005 and June 2008. We excluded 27 patients who had a history of atrial fibrillation and 10 patients who were on anticoagulation prior to admission. The remaining 126 patients were divided into subcategories according to age. TEE results were analyzed for cardiac findings of complex atheromas, PFO, ASA, and intracavitary thrombi. Comparisons were analyzed using Fisher's Exact Test.

Results: Out of 126 patients, 61% (77/126) were older than 50 years as compared to 39% (49/126) who were younger than 50 years. The incidence of complex atheroma was 15.6% (12/77) in patients older than 50 years as compared to 0% (0/49) in patients who were younger than 50 years ($P = 0.003$). In patients older than 50 years, findings indicating a need for anticoagulation based on TEE results were found in 28.6% (22/77) (atheroma = 12, PFO = 10, ASA = 3, thrombus = 2, PFO + ASA = 1) compared to 16.3% (8/49) (atheroma = 0, PFO = 5, ASA = 2, thrombus = 1, PFO + ASA = 1) in patients younger than 50 years.

Conclusions: We have demonstrated that TEE has identified higher incidence of atheroma and PFO in patients older than 50 years. It has therefore changed the management by adding anticoagulation in 22 patients presenting with acute stroke older than 50 as compared to 8 who were younger than 50.

9:30 a.m.

1018-273 High Intensity Focused Ultrasound Can Perforate Calcified Aortic Valves: An Ex Vivo Study

Kohei Fujimoto, Rebecca Hahn, Yasuyoshi Takei, Kotaro Arai, Takuya Hasegawa, Yukiko Sashida, Marco R. Di Tullio, Robert Muratore, Andrew Kalisz, Minoru Tabata, Hiroo Takayama, Yoshifumi Naka, Shunichi Homma, Columbia University Medical Center, New York, NY, Riverside Research Institute, New York, NY

Background: High-intensity focused ultrasound (HIFU) has been used clinically to treat a variety of tumors by producing limited and predictable tissue destruction of deep-seated targets while sparing overlying tissues. The potential application of HIFU in calcific cardiac valves has never been studied.

Methods: Excised aortic valves (AV) from 6 pts were collected at the time of AV surgery. Valves were placed in a degassed saline bath at 37°C. HIFU was generated using an ultrasound therapy transducer (Sonic Concepts, Bothell, Washington USA) with a diameter of 33 mm, focal length of 35mm, frequency of 5.25 MHz and acoustic power of 57W. HIFU discharge was delivered continuously until AV perforation or up to a maximum of 300 seconds. Thirty sites were randomly chosen in 6 valves. Based on visually qualitative acoustic characteristics on high frequency ultrasound images (Visualsonics Inc, Toronto,

Ontario, Canada), the sites were divided into 3 groups (10 sites/group) according to the severity of calcification: none or mild (group 1), moderate (group 2) and severe (group 3). The thickness and width of the 30 perforation lesions and time required to perforate (PT) were recorded.

Results: All sites in groups 1 and 2 were successfully perforated. In group 3 the average thickness of the 10 sites was 1.82 ± 0.52 mm and the success rate was 60%. The mean thickness of perforated lesion was significantly different between groups 1 and 2 (0.94 ± 0.16 vs 1.45 ± 0.28 mm), and between groups 1 and 3 (0.94 ± 0.16 vs 1.54 ± 0.46 mm) ($P < 0.01$). The mean PT was significantly different between groups 1 and 2 (31 ± 17 vs 95 ± 37 sec) ($P < 0.001$), groups 1 and 3 (31 ± 17 vs 181 ± 109 sec) ($P < 0.001$) and groups 2 and 3 (95 ± 37 vs 181 ± 109 sec) ($P < 0.05$). PT was significantly correlated with the thickness of the lesion ($r = 0.77$).

Conclusions: Predictable HIFU performance is required for reliable clinical use in calcified valvular heart disease. The current study shows that HIFU can perforate calcified ex vivo aortic valves with the thickness of perforation directly related to the duration of high frequency energy delivery.

9:30 a.m.

1018-274 Left Atrial Pressure Attenuates Mitral Annulus Behavior in Dilated Cardiomyopathy

Robin Chung, Avin Calcutt, Brunilda Pura, Alison M. Duncan, Wei Li, John R. Pepper, Michael Y. Henein, Royal Brompton Hospital, London, United Kingdom, Umea Heart Centre, Umea, Sweden

Background: Dilated cardiomyopathy (DCM) is commonly associated with functional mitral regurgitation and often raised left atrial (LA) pressure.

Methods: We studied 35 DCM patients (17 with normal LA pressure and 18 with raised LA pressure (LVEDV 168 ± 23 ml) and compared them with 15 normals (LVEDV 130 ± 28 ml). Mitral annulus (MA) antero-posterior (AP), commissure (CC) diameters, sphericity index (SI), annulus area (MVA), and non-planar angle (NPA) between leaflet projections were measured using real-time 3D transthoracic echocardiography.

Results: In all DCM patients, all mitral annulus measurements except SI were greater than normal ($p < 0.005$). Despite changes in LV cavity size, DCM with normal LA pressure behaved normally showing enlargement of AP ($p < 0.05$) and SI ($p < 0.01$) at end-systole vs end-diastole. In DCM with raised LA pressure, only SI was greater at end-systole vs end-diastole ($p = 0.05$). In them, MA AP ($p < 0.005$), SI ($p < 0.01$), and MVA ($p < 0.05$) were larger than in DCM with normal LA pressure.

Conclusion: MVA and subvalvar apparatus are uniformly dilated in DCM. In the absence of raised LA pressure the MA behaves normally, becoming more spherical at end-systole, a shape change that is attenuated by high LA pressure. This and the further increase in AP diameter, SI and MVA may partially contribute to the development of mitral regurgitation, frequently seen in DCM with raised LA pressure.

	Normals		DCM (LAP+)		DCM (normal LA pressure)	
	ES	ED	ES	ED	ES	ED
AP	$3.12 \pm 0.42^{\wedge}$	2.7 ± 0.43	$4.11 \pm 0.46^{***}$	$4.0 \pm 0.48^{***}$	$3.6 \pm 0.49^{\wedge}$	3.4 ± 0.47
CC	3.28 ± 0.39	3.3 ± 0.39	4.2 ± 0.51	4.3 ± 0.68	4.0 ± 0.63	4.1 ± 0.83
Sphericity Index (SI)	$0.91 \pm 0.07^{\wedge\wedge}$	0.82 ± 0.08	$0.94 \pm 0.08^{**}$	$0.91 \pm 0.07^{***}$	$0.88 \pm 0.12^{\wedge\wedge}$	0.82 ± 0.08
non-planar angle (deg)	130 ± 17	130 ± 16	146 ± 12	149 ± 17	140 ± 15	146 ± 17
MV area (cm ²)	9.0 ± 1.9	7.8 ± 1.8	$14.7 \pm 3.1^*$	$14.4 \pm 3.6^*$	12.3 ± 2.5	11.7 ± 3.6

ES v ED $^{\wedge}p < 0.05$, $^{\wedge\wedge}p < 0.01$, $^{\wedge\wedge\wedge}p < 0.005$;
LAP+ v normal LAP $^*p < 0.05$, $^{**}p < 0.01$, $^{***}p < 0.005$;
Normal v DCM sub-groups AP, CC, NPA, MVA all $p < 0.005$

9:30 a.m.

1018-275 Staphylococcal Aureus Bacteraemia: A Prospective Study of the Role of Transesophageal Echocardiography in Identifying Clinically Unsuspected Endocarditis

Alexander Incani, Chris Hair, Peter Purnell, Daniel O'Brien, Allen Cheng, Alan Appelbe, Eugene Athan, Geelong Hospital, Geelong, Australia

Background: Endocarditis is a serious complication of staphylococcal bacteremia (SAB) and mandates early detection to guide intensive therapy. Mortality often exceeds 50%. Although clinical diagnostic criteria are important, low case-rate identification results in poor sensitivity. Transesophageal echocardiogram (TEE) is gaining increasing recognition as the gold standard for aiding diagnosis.

Methods: We aimed to assess the introduction of routine TEE in all suitable adult patients with SAB between December 1998 and September 2006 to determine the incidence of endocarditis and to assess the percentage of cases not evident clinically. 144 consecutive patients with SAB were prospectively enrolled. Baseline patient data including demographics, clinical features and predisposing factors were recorded. Clinical suspicion of endocarditis was recorded prior to cardiac investigation on the basis of echocardiography naive Duke's Criteria (Duke minus). All patients proceeded to transthoracic echocardiography (TTE) within 7 days of presentation followed by TEE if TTE was normal or prosthetic valves were present.

Results: The median age was 68 years (IQR 53 to 76) with 111 (77%) being male. 20 (13.9%) were diabetic. 80 (55.6%) of staphylococcal infections were nosocomial with 29 (20.1%) methicillin-resistant staphylococcus aureus (MRSA). MRSA was more common in nosocomial infections than in community acquired cases 31% versus 7.8% $p = 0.001$. 28 (19.4%) had a pre-existing valve lesion. TEE was performed in 143 patients (99%). 41 patients (28%) of the 144 enrolled were diagnosed with endocarditis defined as either

definite or possible endocarditis by Duke's criteria. Of the 41 patients with the diagnosis of endocarditis, 37 (90.2%) had echocardiographically confirmed vegetations. Of the 41 cases of endocarditis, 22 (53.7%) were not suspected clinically by Duke minus. The clinical diagnosis of endocarditis had a sensitivity of 46% and specificity of 97%.

Conclusion: There is a high incidence of endocarditis in SAB and a large percentage of cases are not evident on clinical grounds. TEE evaluation is indicated for all medically suitable adult patients with SAB to improve detection of endocarditis.

9:30 a.m.

1018-276 Evaluation of In-stent Plaque Vulnerability After Drug Eluting Stent Implantation: Observation by IVUS, Angioscopy and OCT

Tadateru Takayama, Atushi Hirayama, Taro Kawano, Yasuko Watanabe, Satoshi Saito, Nihon University School of Medicine, Tokyo, Japan

Background: Drug-eluting stent (DES) are susceptible to late thrombosis due to delayed re-endothelialization over the stent struts, which may result in the fatal situation. Angioscopy can confirm the presence of neointima and thrombus, but the modality cannot quantify them. OCT, however, has high resolution and allows for the evaluation of neointima in the entire vessel circumference. Therein, we performed a comparative investigation of Cypher (SES) and Taxus (PES) with concurrent IVUS, angioscopy and optical coherence tomography (OCT) analysis in DES implantation cases of 8 to 12 months.

Methods: For 8 to 12 month (10.3 month average) follow up, observation of 50 lesions (SES 24, PES 26) in 50 DES patients was performed with IVUS, Angioscopy and OCT and comparatively examined. Stent malapposition, presence or absence of thrombus and neointimal proliferation (grade 0 to 3) were observed on each modality.

Results: Using IVUS, malapposition was identified in 4 cases for SES and 1 case for PES. Thrombus was not observed in either stent. Neointima was not confirmed in 3 SES cases but was confirmed in 15 PES cases. Angioscopy showed grade 1 to be most frequent in SES, and the average grade was 0.73. Grade 2 was most frequent in PES, and the average grade was 2.1. Thrombus was identified in 6 Cypher cases and was not observed in any PES cases. Yellow plaque was observed in 12 SES cases (50%), and all PES cases presented white plaque. OCT images revealed 8 cases of malapposition in SES and none in PES. Thrombus was identified in 3 SES case. Neointima was identified as fully circumferential in both stents, over 95% of struts were covered, and the average of thickness of the neointima was $74 \mu\text{m}$ for SES and $156 \mu\text{m}$ for PES.

Conclusions: OCT excels in the chronic phase evaluation of DES, and allows for evaluations equal or superior to those possible with angioscopy. Neointima was confirmed by OCT to exist in the majority of the stent, but the lining was thinner in SES compared to PES. Furthermore, asymptomatic thrombus and yellow plaque were identified in SES by angioscopy and OCT, suggesting vulnerability of the in-stent plaque as compared to PES and a possible cause for very late stent thrombosis.

9:30 a.m.

1018-277 Three-Dimensional Strain Is Useful to Find Regional Function of Myocardial Damage: An In Vitro Study

Zhiwen Zhou, Muhammad Ashraf, Weihui Shentu, Dayi Hu, David J. Sahn, Oregon Health & Science University, Portland, OR, Tongji University, Shanghai, People's Republic of China

Background: In this study, we assessed the accuracy of a new 3D/4D strain method for detecting modeled segmental myocardial scar using sonomicrometry as a reference standard.

Methods: Five freshly harvested pig hearts were studied on a model in a water bath designed to simulate heart motion - twisting, filling and emptying. Three sonomicrometry crystals were inserted in the middle of the left ventricular (LV) anterior wall in a triangle with 4 cm spacing. Four stroke volumes (20, 30, 40, 50 ml) were studied at a constant heart rate of 50 beats/min before and after myocardial damage induced by injecting 2 ml of glutaraldehyde solution into a 2×2 cm zone in the middle of the LV anterior wall. Cardiac motion was scanned with full volume sweeps using a 3.5 MHz sector probe on a Toshiba Aplio Arida system at > 24 volumes/sec. Images were analyzed on the system with WMT software for 3D strain analysis. Sonomicrometry data was analyzed in SonoView.

Results: As compared to normal heart, longitudinal and circumferential strain of the damaged segment were reduced significantly as detected by both 3D echocardiography and sonomicrometry. Although the strain measured by 3D echocardiography was larger than the strain measured by sonomicrometry, significant correlation was noted between the 2 methods for longitudinal strain ($r^2 = 0.78$, $p < 0.01$) and circumferential strain ($r^2 = 0.68$, $p < 0.05$).

Conclusions: 3D strain has the potential to detect discrete zones of myocardial damage from 4D images.

(24%) vs 21/143 (15%), $p=0.049$). The prevalence of complex atheroma was similar in pts with CS/TIA and control group pts, irrespective of the pts age (in pts <55 yrs: 11/114 (9.6%) vs 12/171 (7.0%), $p=0.424$; in pts >55 yrs: 29/115 (25%) vs 35/143 (24%), $p=0.891$, respectively). Multivariate analysis adjusted for age, sex, race, presence of hypertension, diabetes mellitus, hypercholesterolemia and smoking showed that PFO continued to be independently associated with CS/TIA, irrespective of the pts age (in pts <55 yrs: odds ratio, 2.4, 95% CI, 1.3 to 4.5, $p=0.007$; in pts >55 yrs: odds ratio, 1.9, 95% CI, 1.2 to 3.2, $p=0.033$, respectively). **Conclusion:** We found a significant association of PFO with CS or TIA, both in younger (<55 yrs) and older (>55 yrs) pts. Complex atheromas in the ascending aorta and aortic arch were relatively common in both age groups, but do not appear to be associated with CS /TIA.

9:30 a.m.

1018-283

Three-Dimensional Speckle Tracking Strain: A Novel Echocardiographic Technique to Quantify Dyssynchrony and the Site of the Latest Mechanical Activation

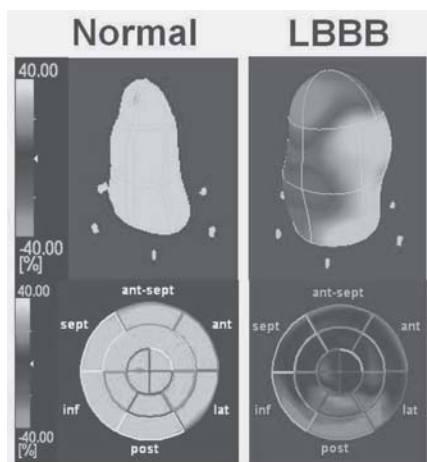
Hidekazu Tanaka, Hideyuki Hara, Samir Saba, John Gorcsan, III, University of Pittsburgh, Pittsburgh, PA

Background: Previous 3-dimensional (3D) echo methods to quantify dyssynchrony for resynchronization therapy (CRT); could not determine regional 3D strain. Our objective was to test the hypothesis that a newly developed 3-D speckle tracking system can quantify 3-D strain and the site of the latest mechanical activation in patients referred for CRT.

Methods: We studied 40 subjects; 30 patients for CRT with ejection fraction $24\pm7\%$ and QRS 150 ± 39 ms often with left bundle branch block (LBBB) and 10 normal controls. A new 3-dimensional speckle tracking system (Artida, Toshiba Corp.) determined strain simultaneously from 16 standard segments from pyramidal 3-D data sets acquired in a single beat. Dyssynchrony was quantified from mechanical activation mapped from all 16 sites as maximal opposing wall delay and standard deviation.

Results: 3-D speckle tracking radial strain analysis was possible in 94% of all segments. Dyssynchrony in heart failure patients was significantly greater than normal controls (maximal opposing wall delay 312 ± 108 ms vs. 59 ± 22 ms and standard deviation 126 ± 52 ms vs. 28 ± 11 ms, $p<0.001$ vs. normal). The prevalence of the site of the latest mechanical activation was as follows: mid-posterior 37%, basal-posterior 30%, mid-lateral 27% and basal-lateral 20%.

Conclusion: 3-D speckle tracing strain successfully quantified dyssynchrony and determined the site of the latest mechanical activation in the same cardiac cycle. These observations may have clinical implications for CRT.



9:30 a.m.

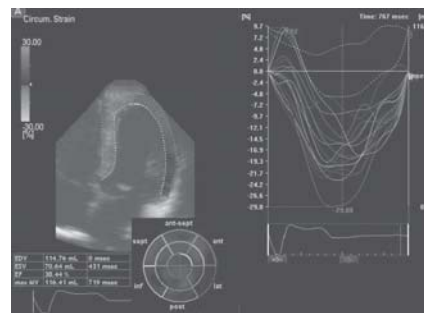
1018-284

Demonstration of Time Sequence of Left Ventricular Mechanical Activation Using Novel Three Dimensional Speckle Tracking Analysis

Mio Ebato, Hiroyoshi Mori, Hideyuki Maezawa, Daisuke Wakatsuki, Keisuke Kawachi, Hisa Shimojima, Yukei Higashi, Hiroshi Suzuki, Yoichi Takeyama, Showa University Fujigaoka Hospital Division of Cardiology, Yokohama, Japan

Background: Three dimensional (3D) analysis is ideal to evaluate wall motion and dyssynchrony in the left ventricle. Time sequence of left ventricular mechanical activation was studied using novel 3D speckle tracking analysis. **Method:** 3D strain images (Toshiba Medical Systems : Nasu, Japan) were recorded in 10 patients with cardiac resynchronization therapy (CRT) without ischemic heart disease (76 ± 8 years old, mean ejection fraction: $45\pm8\%$ on CRT). The images were recorded during right ventricular apical (RVP), left ventricular (LVP) and biventricular pacing (BVP) at a pacing rate of 70 bpm. Circumferential strain in 16 segments and left ventricular torsion were calculated. Maximum difference of time to peak strain (TPS) was also measured. **Results:** The initiation of increase in strain was observed first in the segments near the pacing site and extended to the remote segments. During univentricular pacing, the ratio of strain in the segments near the pacing site and the remote site was almost twice (ratio: 2.2 ± 0.5). BVP produced the more homogenous distribution of strain and less dyssynchrony (

TPS during RVP: 109 ± 21 ms LVP: 93 ± 32 ms, BIV: 44 ± 23 ms, $p<0.01$ RVP vs. BIV, LVP vs. BIV). The lowest amount of torsion was observed during RVP (BIV: $13\pm7\%$, LVP: $12\pm6\%$, RVP: $8\pm6\%$, $p<0.01$ BIV vs. RVP). **Conclusion:** The time sequence of mechanical activation of the left ventricle was able to demonstrate using novel 3D speckle tracking analysis. This technique may have clinical applications.



9:30 a.m.

1018-285

Aortic Annular Assessment for Transcatheter Aortic Valve Implantation: 2-D or 3-D Transesophageal Echocardiography?

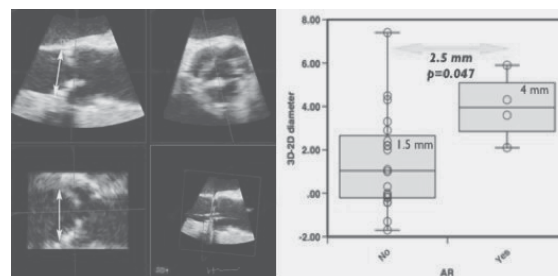
Amit Bhan, Stamatis Kapetanakis, Karen Wilson, Peter Pearson, Ahmed El-Gamel, Philip MacCarthy, Olaf Wendler, Martyn R. Thomas, Mark J. Monaghan, King's College Hospital, London, United Kingdom

Background: Transcatheter aortic valve implantation is a relatively new procedure for those deemed too high risk for conventional surgery. Accurate imaging is necessary throughout, not least in the assessment of aortic annular diameter (AAD) for valve sizing. We set out to see if 3D transesophageal echo (TEE) offers a more accurate measure of AAD than 2D TEE.

Methods: 2 independent observers measured AAD on 24 patients who underwent successful valve implantation. The distance between leaflet insertion points was taken in the "anteroposterior" (AP) dimension. A mid-esophageal long axis view was used for 2D AAD, while 3D AADs were taken from a volumetric dataset, using a 3D viewer (figure). An AP diameter was taken and rotation around the annulus was performed to get a maximal diameter (3D max).

Results: AADs were possible in all patients. Interobserver agreement (r) was 0.86 for 2D and 0.85 for 3D. Intraobserver correlation was 0.86 and 0.87 respectively. Mean AADs were 20.9mm for 2D AP, 22.1 for 3D AP and 22.9 for 3D max. The difference between 2D and 3D AP was 1.2 mm ($p=0.001$), while the difference between 2D AP and 3D max was 2 mm ($p<0.0001$). In those patients that had significant paraprothetic leak at one month the difference, when compared to those that did not, was 2.5 mm ($p=0.047$) (figure).

Conclusion: 2D TEE underestimates AAD when compared to 3D, particularly when obtaining a maximal diameter. This discrepancy may be implicated in paraprothetic leaks and is potentially important for valve sizing in the future.



9:30 a.m.

1018-286

Combined Use of Two- and Three-Dimensional Transesophageal Echocardiography Provides Accurate Diagnosis for Localization of Mitral Valve Prolapse

Masaru Aikawa, Hiroyuki Watanabe, Toshihiro Fukui, Tomoki Shimokawa, Hirotugu Mihara, Koji Kurosawa, Kanki Inoue, Itaru Takamisawa, Atsushi Seki, Kohei Tanizaki, Tetsuya Tobaru, Nobuo Iguchi, Masatoshi Nagayama, Ryuta Asano, Morimasa Takayama, Jun Umemura, Shuichi Takanashi, Tetsuya Sumiyoshi, Sakakibara Heart Institute, Tokyo, Japan

Background: Precise segmental analysis in mitral valve prolapse is important to decide the chances of valvular repair. Recently, real-time three-dimensional transesophageal echocardiography (RT3DTEE) has been developed that allows surgical view of mitral valve. The purpose of this study was to examine the accuracy of this three-dimensional system for diagnosing location of mitral valve prolapse.

Methods: In 53 consecutive patients with undergoing mitral valve surgery for mitral valve prolapse, RT3DTEE and two-dimensional transesophageal echocardiography (2DTEE) were performed before surgery (IE33, Philips Medical System). RT3DTEE and 2DTEE images were digitally stored for offline analysis. The mitral valve leaflets were divided into

six segments based on the recommendation of American Society of Echocardiography. Prolapsed sites were validated intraoperatively with surgical inspection.

Results: As shown in the table, accuracy of diagnosis using RT3DTEE was higher than that using 2DTEE. Highest accuracy was achieved by combined use of RT3DTEE and 2DTEE.

Conclusions: Surgical view of mitral valve by RT3DTEE is a new and powerful imaging in segmental analysis of mitral valve prolapse.

Methods	Sensitivity	Specificity	Positive predictive value	Negative predictive value	Accuracy
2D	87%	75%	61%	93%	79%
3D	91%	96%	92%	95%	94%
2D and 3D	98%	98%	97%	99%	98%

9:30 a.m.

1018-287

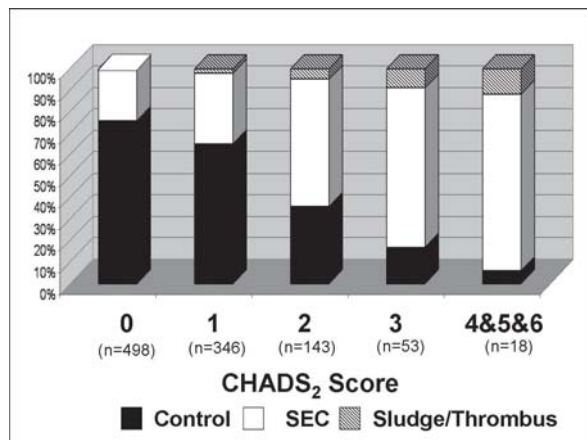
Selective Transesophageal Echocardiography Approach in Evaluation of Thromboembolic Risk in Patients With Atrial Fibrillation Undergoing Pulmonary Vein Isolation Stratified by CHADS₂ Score

Sarinya Puwanant, Brandon Varr, Kevin Shrestha, Sarah Hussain, Ruvin Gabriel, Sheldon Freeburg, Oussama Wazni, W.H. Wilson Tang, James D. Thomas, Bruce D. Lindsay, Allan L. Klein, Cleveland Clinic, Cleveland, OH

Background: There is no clear consensus of whether a screening transesophageal echocardiogram (TEE) prior to catheter ablation of atrial fibrillation (AF) should be performed in every patient.

Methods and results: 1,058 consecutive patients (pts) (age 57 ± 11 , 80% male) with AF undergoing initial TEEs for pre-pulmonary vein isolation (PVI) screening with a complete CHADS₂ score (congestive heart failure (CHF), hypertension, age > 75, diabetes, stroke [double]) were studied. A CHADS₂ score of 0, 1, 2, 3, 4, 5 and 6 were present in 47%, 33%, 14%, 5%, 1%, 0.3%, and 0%, respectively. The prevalence of left atrial appendage (LAA) thrombus, sludge (defined as a dynamic gelatinous, precipitous echodensity, without a discrete mass), and spontaneous echo contrast (SEC) were present in 0.6%, 1.5%, and 35%. The prevalence of LAA thrombus/sludge increased with ascending CHADS₂ score (Fig1). No pts with a CHADS₂ score of 0 had LAA sludge/thrombus while LAA thrombus & sludge were present in 1% (2/207) of pts with PAF with normal sinus rhythm at the time of PVI. In multivariate model, a history of persistent/permanent AF, CHF, and LVEF < 35% significantly associated with LAA sludge/thrombus.

Conclusions: The prevalence of LAA sludge/thrombus in pts with AF undergoing a pre-PVI screening TEE is very low, and significantly increases in patients with higher CHADS₂ scores. A screening TEE prior to PVI procedure is not necessary to assess stroke risk in pts with a CHADS₂ score of 0; however should be definitely done for a CHADS₂ score of ≥ 1



9:30 a.m.

1018-288

Quantitative Assessment of Left Ventricular Size and Function in Patient With Arrhythmia: Comparison of One Heart Beat, Quantitative Full B-Mode Volume Real-Time Transthoracic Three-Dimensional Echocardiography (RT-3DE) With Cardiac Magnetic Resonance Imaging/Computed Tomography

Jung-Hyun Choi, Snyder Michael, Shizhen Liu, David Orsinelli, Barbara Conwel, Thomas Ryan, Mani A. Vannan, the Ohio State University, Columbus, OH

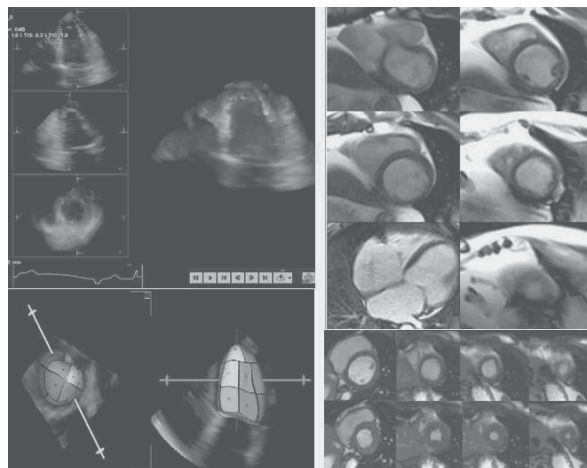
Background: RT-3DE has reported accurate for LV assessment, but it is limited in arrhythmic patient. Because arrhythmia can cause movement of the heart between cycles and result in artifacts in the images when the entire LV is reconstructed from multiple subvolumes. This new system is capable of broad beam transmission and receives up to 64 beams simultaneously. We assessed the clinical feasibility of a single heart-beat RT-3DE in LV assessment with arrhythmia patient.

Methods: 22 patients were prospectively enrolled in this study. Single heart-beat, full volume images were obtained using a 421c matrix array transducer (SC2000™, Siemens).

CMR images were obtained with a 1.5-T scanner (Tesla, Siemens) using a standard 12-channel cardiac coil. Volumetric CT images were acquired using 64-Slice CT (Avanto, Siemens). EDV, ESV and EF were measured automatically (RT-3DE) using LVA package software (Siemens), or semiautomatically (CMR, CT) using standard segmentation software (Argus, Siemens).

Results: Single heart-beat RT-3DE resulted in significant correlation compared with CMR/CT (EDV: $r=0.976$, $p=0.012$, ESV: $r=0.967$, $p=0.017$, EF: $r=0.995$, $p=0.002$). RT-3DE underestimated EDV and ESV with significant biases (EDV -32ml, ESV -11ml, EF -4%). Figures show representative examples of single heart-beat RT-3DE and CMR in patient with atrial fibrillation.

Conclusion: Non-stitched, single heart beat RT-3DE is feasible and may provide more accurate LV functional information in arrhythmic patient.



ACC.POSTER CONTRIBUTIONS

1027

Echocardiography: 3-D, TEE, and Intracardiac Echo; Stress Echocardiography; Contrast Echocardiography; Tissue Imaging

Sunday, March 29, 2009, 1:30 p.m.-4:30 p.m.

Orange County Convention Center, West Hall D

3:30 p.m.

1027-233

Is It Necessary for All The Patients With Atrial Fibrillation and Low CHADS₂ Score to Receive Transesophageal Echocardiography Before Left Atrial Catheter Ablation?

Eiji Yamashita, Hiroto Takamatsu, Hiroyuki Toide, Kouki Nakamura, Rie Tsuru, Chiduru Sato, Yasuhiko Hori, Yasuaki Tanaka, Joutaro Iwamoto, Koji Goto, Miki Yokokawa, Koji Kumagai, Shigeto Naito, Takuji Toyama, Hiroshi Hoshizaki, Shigeru Oshima, Gunma Prefectural Cardiovascular Center, Maebashi, Japan, Fujioka General Hospital, Fujioka, Japan

Background: Percutaneous left atrial catheter ablation (LACA) is used for the treatment of atrial fibrillation (AF). LA thrombus occasionally seen in AF patients could cause the thromboembolic event as one of complications of LACA. CHADS₂ score is useful for risk stratification of the thromboembolisms in AF patients. The purpose of this study is to observe the relationships between the patients with LA thrombus before LACA and CHADS₂ score.

Methods: The subjects consisted of 433 patients with drug resistant AF who were scheduled to undergo LACA (58 ± 11 years, 312 males). They all received transesophageal echocardiography (TEE) before LACA, and LA thrombus was detected in 13 cases (3.0%). In these cases, we evaluated the patient characteristics, CHADS₂ score, and echocardiographic parameters.

Results: Among the patients with LA thrombus, 12 cases (92%) had structural heart diseases (non-ischemic cardiomyopathy: 6 cases, hypertrophic cardiomyopathy: 3 cases, hypertensive heart disease: 1 case, old myocardial infarction (OMI): 1 case, moderate aortic stenosis: 1 case). 8 cases (62%) had a history of congestive heart failure, 4 (31%) had hypertension, 3 (23%) had an age of 75 years or older, 1 (8%) had Diabetes Mellitus, and 3 cases (23%) had a history of cerebral infarction or transient ischemic attack. Eleven patients (85%) were prescribed warfarin, and PT-INR were >1.5 in 9 patients. CHADS₂ score was 1.7 ± 1.7 , and there were 2 patients with CHADS₂ score of 0. One of them was 74 year-old male, who had persistent AF with posterior OMI and almost normal ejection fraction (EF: 58%). The other patient was 63 year old male, who had paroxysmal AF with no structural heart diseases, normal EF (70%), normal diastolic function (E/E' = 6.4) and mildly dilated LA (42mm).

Conclusions: Even in nonvalvular AF patients with low CHADS₂ score, the LA thrombus cases exist. Therefore, TEE screening prior to LACA should be mandatory.

3:30 p.m.

3:30 p.m.

1027-234

Incremental Value of hsCRP to Predict Transesophageal Markers of Thrombo Embolism in Nonvalvular Atrial Fibrillation Patients

Stephane Ederhy, Emanuele Di Angelantonio, Ghislaine Dufaitre, Louise Boyer-Chatenet, Catherine Meuleman, Fanny Douna, Emmanuelle Berthelot-Garcia, Joelle Masliah, Franck Boccara, Ariel Cohen, hopital saint antoine, Paris, France

Background: We sought to determine whether C-reactive protein (CRP) can refine stroke risk stratification by identifying transesophageal echocardiography (TEE) markers of thromboembolism such as left atrial (LA) thrombus and LA spontaneous echocardiographic contrast (LASEC)

Methods: TEE and CRP concentration measurement were performed among 178 patients (mean age 65.6±14.4; men 56.2%) with nonvalvular atrial fibrillation. Using all available stroke risk stratification schemes (AFI, SPAF, Framingham, ACCP 2001, ACCP 2004, Birmingham / Nice and ACC/AHA/ESC) patients were classified into three strata (Low, moderate and high risk).

Results: Median CRP concentration for the whole studied population was 3.40 mg/l (IQR 1.48-9). Moderate to severe LASEC was found in 41 patients (23 %) and thrombus in 12 patients (6.7 %). The best diagnostic performance is obtained with SPAF III classification and brimingham/NICE with respectively an AUC of 0.74 and 0.71. Discrimination of LA SEC or thrombus increased significantly when CRP was added to all schemes except SPAF III. A CRP cut-off concentration of 4.8 mg/l ensured the highest negative predictive value in ruling out the presence of LA/LAA SEC or thrombus (negative predictive value = 86 %).

Conclusion: A combination of CRP measurement and stroke risk stratification may help to identify TEE markers of thromboembolism among untreated patients with nonvalvular atrial fibrillation

Area under curve according to each classifications			
classification	AUC Classification	AUC Classification and CRP	p value
AFI 1997	0.63(0.56-0.79)	0.71(0.63-0.79)	0.02
SPAF III	0.74(0.66-0.81)	0.77(0.7-0.85)	0.053
AFI	0.66(0.6-0.72)	0.75(0.67-0.82)	0.01
CHADS2	0.67(0.6-0.74)	0.74(0.66-0.82)	0.036
ACCP 2001	0.67(0.61-0.73)	0.75(0.67-0.83)	0.01
Framingham	0.63(0.54-0.72)	0.72(0.64-0.84)	0.021
ACCP 2004	0.66(0.6-0.71)	0.74(0.66-0.82)	0.0089
Birmingham	0.71(0.63-0.79)	0.75(0.67-0.83)	0.097
ACC/AHA/ESC 2006	0.7 (0.63-0.78)	0.75 (0.67-0.83)	0.0399

3:30 p.m.

1027-235

Echocardiographic Characteristics of Patent Foramen Ovale Associated With Recurrence of Cryptogenic Stroke

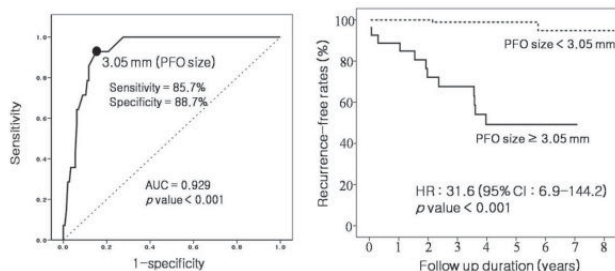
Jong-Young Lee, Jong Pil Park, Sun Yang Min, Sung Sik Kim, Sung-Hwan Kim, Myung-Zoon Yi, Duk-Hyun Kang, Jong-Min Song, Jae-Kwan Song, Asan Medical Center, Seoul, South Korea

Background: Although the potential association of patent foramen ovale (PFO) and cryptogenic stroke has been investigated, the frequency and risk factors associated with recurrent stroke are not known. Moreover, controversial data are available for an optimal management strategy for patients with cryptogenic stroke and PFO.

Methods: Between Jan 2000 and Apr 2007, 1,014 consecutive patients with stroke underwent transesophageal echocardiography (TEE) and PFO was documented in 323 patients (31.8%). Among them, 182 patients (18%, 51±14 years), in whom PFO was the only identifiable risk factor, were enrolled.

Results: Percutaneous closure of PFO was done in 20 patients (11%) and the remaining 162 patients received medical therapy including antiplatelet or warfarin. During follow-up (median 3.4 years), recurrent stroke developed in 14 patients (7.7%) and no recurrence was documented after PFO closure. Patients who received antiplatelet alone showed higher recurrence rate compared to the others (p=0.009). In multivariable analysis, atrial septal aneurysm (HR 7.42, 95% CI 2.17-25.28, p=0.001) and PFO size (HR 3.01, 95% CI 1.97-4.71, p<0.001) were independently associated with recurrence. The best cut-off value of PFO size was 3.05 mm and the recurrence-free survival rate was significantly different accordingly.

Conclusions: Risk stratification was possible based on TEE findings and the prophylactic benefit of percutaneous device closure of PFO in the selected patients needs further investigation.



1027-236

A Novel Method of Dense Speckle Tracking for Measuring Three-Dimensional Displacement of Ultrasound Targets on Four-Dimensional Echocardiogram Allows Evaluation of Right Ventricular Mechanics: An Experimental Study With Validation by Sonomicrometry

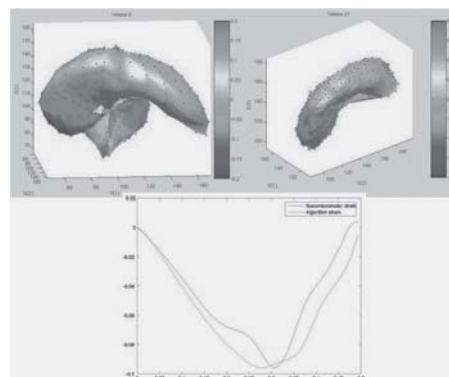
Xubo Song, Andriy Myronenko, Muhammad Ashraf, Robert I. Lowe, Ling Hui, David J. Sahn, Oregon Health & Science University, Portland, OR

Background: We have developed a new method to provide full displacement and strain from 4D cardiac images for study of right ventricular (RV) mechanics.

Methods: Initially 4D images were acquired in vitro using 6 cyclically expanded models of pig RV with balloons in them on a Philips IE 33 scanner with an X-7-2 matrix probe. We then studied the RV in 3 open-chest pigs. Polar coordinate envelope 4D data were downloaded and analyzed, yielding mapping of 3D locations of any arbitrary target. For computation, the displacement field between any two 3D volumes was modeled using B-splines, parameterized by the location of a set of control points. The optimal locations of the control points were obtained through volume-based registration by minimizing the sum of squared intensity differences between the two volumes, which yielded a spatially dense placement field. Distance strain or surface strain was computed for baseline strain mechanics as well as altered strains induced after proximal right coronary artery ligation in the pumped models and the 3 pigs.

Results: Given control point locations, the location of any target in the 3D volumes can be derived. Targets were processed to yield RV strains in 3D space (either distance strain or surface strain). 3D distance strain values could be matched to sonomicrometry computed longitudinal strains correlated with ($r^2 = 0.85$) in the pumped models and in the open-chest pigs.

Conclusions: This method provides an accurate, robust analysis of 4D RV strain mechanics from 4D echo data.



3:30 p.m.

1027-237

Echocardiographic Determinants of Exercise Capacity in Candidates for Cardiac Resynchronization Therapy

Chinami Miyazaki, Margaret M. Redfield, Raul E. Espinosa, Brian D. Powell, Fletcher A. Miller, Jr., David L. Hayes, Barry L. Karon, Jae K. Oh, Mayo Clinic, Rochester, MN

Background: Discrepant results between symptomatic response rate and reverse remodeling rate after cardiac resynchronization therapy (CRT) have been reported and were explained partly by a placebo effect. Previous works suggested a better correlation of diastolic than systolic function with exercise capacity in heart failure. We assessed the echocardiographic determinants of baseline exercise capacity and the improvement in exercise capacity in patients undergoing CRT. **Methods:** Cardiopulmonary exercise test and echocardiography were performed in 104 patients before CRT. Early diastolic velocity (E), deceleration time (DT), E/e', cardiac index (CI) and pulmonary artery pressure (PAP) were measured using echocardiography. Exercise capacity test and echocardiography were repeated 6 months after CRT in 70 patients. **Results:** EF, PAP and diastolic filling parameters showed a significant correlation with baseline max $\dot{V}O_2$. In multivariate analysis including EF, CI, E/e', DT, PAP as parameters, PAP and E/e' were independent predictors of $\dot{V}O_2$ when adjusted for age (p<0.001 for PAP, p=0.003 for E/e'). The improvement in $\dot{V}O_2$ was significantly correlated with the improvement in PAP, E/e' and DT, but not with the reverse remodeling. **Conclusions:** Pulmonary artery pressure and diastolic filling parameters are the main determinants of baseline exercise capacity. Diastolic filling parameters and pulmonary artery pressure should be considered for the follow-up evaluation of the patients after CRT.

Correlation between echo parameters and exercise capacity

Parameters	Correlation with baseline max $\dot{V}O_2$		Parameters	Correlation with Δ max $\dot{V}O_2$	
	r	p value		r	p value
EF, %	0.29	0.004	Δ EF, %	0.11	0.38
ESVI, ml/m ²	-0.11	0.26	% Δ ESV	0.08	0.54
CI, l/min/m ²	0.19	0.053	% Δ CO	0.23	0.06
E/e'	-0.45	<0.001	Δ E/e'	0.39	0.002

3:30 p.m.

1027-238

Left Ventricular Rotation and Torsion Can Distinguish Between Physiological and Pathological Left Ventricular Hypertrophy

Loira Toncelli, Sr., Francesco Cappelli, Jr., Cappelli Brunello, Sr., Maria Concetta Roberta Vono, Sr., Laura Stefani, Sr., Alessio De Luca, Jr., Giorgio Galanti, Sr., Sport Medicien Center, Florence, Italy

Background: Left ventricular hypertrophy (LVH) may be a physiological remodelling induced by physical training or the expression of a pathological disease like hypertension. Pathological LVH is correlated with an increase in cardiovascular risk and mortality. Echocardiography is very important to distinguish pathological or physiological hypertrophy because we can evaluate left ventricular diastolic function which is altered in pathological hypertrophy. Recently it has been proposed the use of speckle tracking echocardiography to study myocardial strain, rotation and torsion. The aim of our study was to assess if speckle tracking analysis derived LV function parameters (S, LVR and LVT) were different in physiological and in pathological hypertrophy. **Methods:** We enrolled 22 hypertensive subjects (Group A) and 59 well trained non professional endurance athletes (group B), matched for sex. We evaluated the following parameters: LV end diastolic diameter (LVED), LV septum (SIV) and posterior wall thickness (PW), LV mass (LVM), LV longitudinal strain (LVLS), Circumferential strain (LVCS), basal and apical rotation (ROT) and torsion. **Result:** No significant differences were found in LVED, SIV, PW and mass in the two groups. LVLS and LVCS were non statistical different in group A and Group B, too. Group A showed higher basal ROT and mainly higher apical ROT. Torsion was statistical higher in hypertensive subjects than in athletes. **Conclusion:** Subjects with physiological hypertrophy had similar LV dimension, wall thickness and mass if compared with subjects with pathological hypertrophy. Moreover speckle derived LVCS and LVLS were similar in both groups. On the contrary, basal ROT, apical ROT and torsion were significantly increased in hypertensive subjects. LV rotation and torsion can be useful parameters to distinguish physiological from pathological hypertrophy, particularly when sports eligibility certification is required by legal medical legislation as in Italy.

3:30 p.m.

1027-239

Radiofrequency-Based Three-Dimensional Echocardiography Speckle Tracking: Phantom Validation

Ping Yan, Qing Zhou, Congxian Jia, Donald P Dione, Kailasnath Purushothaman, Xenophon Papademetris, Lawrence Staib, Qifeng Wei, Karl Thiele, Matthew O'Donnell, James S Duncan, Albert Sinusas, Yale University, New Haven, CT, Congxian Jia, Seattle, WA

Background: The accurate quantification of complex myocardial deformations in 3-Dimensional (3D) space from real-time echocardiography is challenging. Application of a 3D correlation-based speckle-tracking algorithm using cross-correlation of phase-sensitive 3D ultrasound images offers a potential solution.

Methods: To validate our radiofrequency-based speckle tracking (RFST) algorithm for evaluation of displacements in 3D, real-time images of polyvinyl alcohol cryogels were acquired using a high-frequency (7 MHz) phase array probe (Philips, X7) and modified ultrasound system (Philips, IE33) that allows analysis of raw RF data. A tissue mimicking PVA phantom with an implanted rectangular array of ruby beads (0.4 mm diameter, n = 16) was placed in a precision displacement apparatus in a water bath for imaging. Beads were separated by 3 mm in axial direction (x), and 10 mm in both lateral (y) and azimuthal (z) direction. PVA phantom was imaged before and after progressive 0.5 mm displacements in all 3 directions. Regional displacements assessed using RFST algorithm and bead displacements were compared with true experimental displacements. PVA phantom was also imaged before and after progressive compressions along the axial direction at 0.2, 0.5, 1, 2, 3, 4, 5 mm increments. All four noncoplanar ruby beads forming small tetrahedral volumes were used to calculate finite normal, shear strains and principal strains. Regional strains derived from RFST algorithm and beads were compared.

Results: There were excellent correlations of RFST and beads derived displacements relative to experimental movements (p-values for all less than 0.008). The best correlations were seen with displacements in axial direction. An examination of the principal strains in a number of tetrahedras indicated that there was an excellent correlation of axial strain defined using the beads and RFST.

Conclusions: The tracking of beads within the PVA phantom provides a reliable quantitative method for validation of 3D RF-based speckle tracking. The RFST algorithm provided an excellent estimate of regional displacement with translation in all directions, and provided an excellent estimate of strain in axial direction.

3:30 p.m.

1027-240

Three-Dimensional Speckle Tracking Study of Myocardial Mechanics in Normal Humans: Demonstration of Regional and Segmental Heterogeneity in Radial, Circumferential and Longitudinal Strain

Antonietta Evangelista, Joachim Nesser, Stefano De Castro, Francesco Faletta, Carlo Gaudio, Alawi A. Alsheikh-Ali, Natesa Pandian, Tufts Medical Center, Boston, MA

Background: Reliable study of left ventricular (LV) mechanics by 2D speckle tracking and tissue Doppler is limited by through-plane movement, translational motion, and/or angle-dependency. These are overcome by 3D speckle tracking (3DST).

Methods: To evaluate the regional deformations associated with systolic function of

normal LV, we employed a novel 3DST imaging (Toshiba Artida) in 20 healthy subjects (15 males, age 34±10). From full volume speckle data sets, LV epicardial and endocardial borders were extracted, and peak systolic radial strain (PSRS), circumferential (PSCS), and longitudinal strain (PSLS) derived in 16 segments.

Results: Global LV values of strain (%) were (Mean, SD, Range): PSRS 36±10, (19 to 57); PSCS: -27±3 (-37 to -22), and PSLS -15±2 (-18 to -11). There was regional heterogeneity in PSRS and PSLS (Table), with a decreasing gradient of PSRS from base to apex (p<0.001), and a higher PSLS in the apex (p<0.001). PSCS was regionally homogeneous. Additionally, there was heterogeneity in segmental mechanics within each region.

Conclusion: 3DST echocardiography allows for the study of myocardial function without the flaws of 2D and tissue Doppler. The normal human ventricle has intrinsic heterogeneity in LV mechanics that needs to be considered while evaluating abnormal hearts.

Mean values of regional and segmental 3DST strain			
	Basal LV	Mid LV	Apical LV
Regional PSRS	51 ± 17	35 ± 10	18 ± 9
Segmental PSRS	BL 71 to BI 23	ML 46 to MI 23	AL 20 to AI 15
Regional PSCS	-28 ± 5	-27 ± 3	-26 ± 5
Segmental PSCS	BA -32 to BI -22	MAS -29 to ML -25	AS -30 to AA -22
Regional PSLS	-15 ± 4	-14 ± 3	-18 ± 3
Segmental PSLS	BL -18 to BAS -12	MAS -16 to MP -13	AS -24 to AA -10

BL=Basal Lateral, BI=Basal Inferior, ML=Mid Lateral, AL=Apical Lateral, AI=Apical Inferior, BA=Basal Anterior, MAS=Mid AnteroSeptal, AS=Apical Septal, AA=Apical Anterior, BAS=Basal Antero Septal, MP = Mid Posterior.

3:30 p.m.

1027-241

The Left Atrial Volume Index Over Late Diastolic Mitral Annulus Velocity (LAVI/A'): A New Echo Index for the Screening of Advanced Diastolic Dysfunction and a Predictor of Clinical Outcomes

Mahn Won Park, Hun-Jun Park, Hae-Ok Jung, Woo-Seung Shin, Pum Joon Kim, Ho-Joong Yoon, Sang-Hong Baek, Ki-Bae Seung, Jae-Hyung Kim, Kyu-Bo Choi, Joo Yeoul Baek, Sung Kyu Yoon, Jae Hong Park, Yoon Seok Koh, Division of Cardiology, College of Medicine, The Catholic University of Korea, Seoul, South Korea

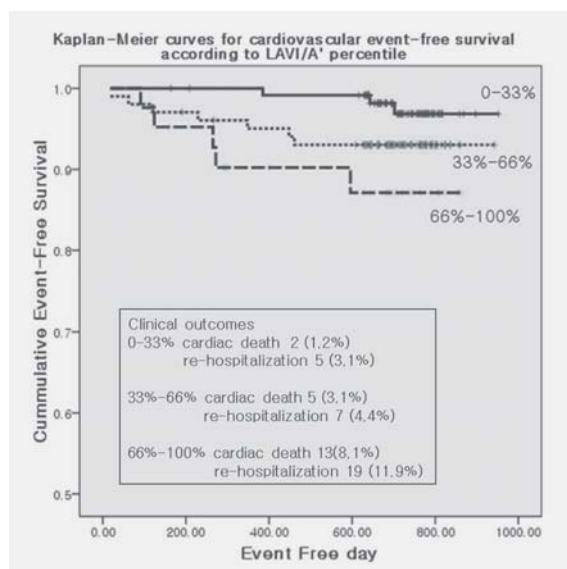
Background: As diastolic function deteriorates, left atrial volume index (LAVI) increases and late diastolic mitral annulus velocity (A') decreases progressively. Thus, information of A' with LAVI may have additional benefits to assess the diastolic dysfunction.

Objectives: We evaluated the clinical usefulness of LAVI/A' for screening of advanced diastolic dysfunction (ADD; pseudonormal to restrictive physiology) and predictor of clinical outcomes.

Methods: We enrolled 482 dyspneic patients who underwent 2-D Doppler echocardiography and BNP measurement. Additionally we correlated LAVI/A' with E/E', BNP and PCWP in 30 patients performing Rt. heart catheterization. Using ROC for the detection of ADD, we compared the area under the curves (AUC) of LAVI/A' with those of E/E' and BNP. We also compared the incidence of clinical outcomes (cardiac death and re-hospitalization for CHF) based on the tertile of LAVI/A' and identified independent predictors of clinical outcomes.

Results: LAVI/A' had a reasonable correlation with E/E' (r=0.65), BNP (r=0.62) and PCWP (r=0.68, all of them, p<0.001). The AUC of LAVI/A' was 0.88, which was comparable to those of BNP (0.91) or E/E' (0.89). During the median follow up of 23.6 months, the event rate was significantly increased based on the tertile of LAVI/A' (Fig.) and LAVI/A' ≥4 was an independent predictors of clinical outcomes (OR: 2.83, p<0.001).

Conclusions: A new echo index, LAVI/A' is useful for the screening of ADD and a significant predictor of clinical outcomes.



3:30 p.m.

1027-242

Direct Ultrasound Measurements of Circumferential, Longitudinal and Radial Strain Using Newly Developed Three-Dimensional Myocardial Tracking Image in Normal Adults

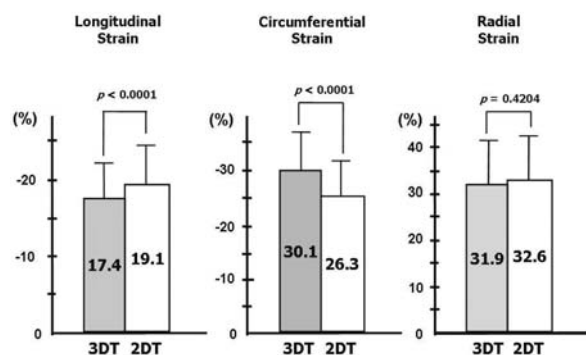
Ken Saito, Nozomi Watanabe, Koichiro Imai, Kikuko Obase, Nozomi Wada, Akihiro Hayashida, Youji Neishi, Takahiro Kawamoto, Hiroyuki Okura, Kiyoshi Yoshida, Kawasaki medical school, Kurashiki, Japan

Background: The assessment by 2-dimensional myocardial tracking (2DT) is based on the measurements of strain on the 2-dimensional (2D) image projection, ignoring 3-dimensional (3D) movement. Recently, 3-dimensional myocardial tracking (3DT) has been developed as a new application that can assess 3D wall motion. The aim of this study was to investigate feasibility of the 3DT to assess longitudinal (L), circumferential (C), and radial (R) strain values in normal subjects.

Methods: Echocardiographic exams were performed in 19 healthy subjects (mean 30±4 y.o.) using Artida™ (Toshiba, Japan). Using a dedicated software package, 3D volumetric images were analyzed to measure L, C and R strains. The results were compared with those obtained by the conventional 2DT method.

Results: Average time for analysis per subject by 3DT was significantly shorter than by 2DT (10 min vs. 34 min, $p < 0.0001$). The mean strain values of the 16 segments for L, C and R strains were shown in Figure. L strain value by 3DT was significantly smaller than 2DT, and C strain value by 3DT was significantly larger than 2DT. Intra- and inter-observer variabilities were 9.5 and 10.7% in 3DT, and 10.6% and 10.9% in 2DT, respectively.

Conclusions: The present study demonstrates that 3DT is a feasible and reproducible method to measure L, C and R strain. The discordant results between 3DT and 2DT may be, in part, explained by the 3D cardiac motion that 2DT can not take into account.



3:30 p.m.

1027-243

Age-Dependency of Left Ventricular Shape: Demonstration by Real-Time Three-Dimensional Transthoracic Echocardiography

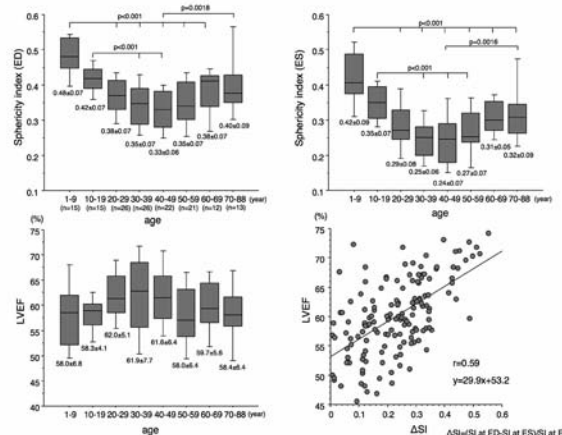
Kyoko Ootani, Masaaki Takeuchi, Lissa Sugeng, Hiromi Nakai, Kyoko Kaku, Nobuhiko Haruki, Hidetoshi Yoshitani, Nozomi Watanabe, Kiyoshi Yoshida, Yutaka Otsuji, Roberto M. Lang, 1-1 Iseigaoka Yahatanishi-ku, Kitakyushu, Japan

Background: Although left ventricular (LV) shape affects LV function, the impact of age-dependency on LV shape remains unknown. Real-time 3D transthoracic echocardiography (3DTTE) can reliably assess LV shape independently of geometric assumptions. The aim of this study was to determine the effect of aging on LV shape.

Methods: 3DTTE were acquired in 150 healthy subjects over a wide range of ages (mean age: 38±21 years, range: 1 to 88 years, 89 men). The LV endocardial border was traced semi-automatically using quantitative software (QLAB, Philips). LV volume and its corresponding long-axis diameter measured from the mitral annulus to the LV apex were measured in each frame throughout the cardiac cycle. LV sphericity index (SI) was defined as LV volume divided by the spherical volume calculated $0.52 \times (\text{long axis diameter})^3$. Data were grouped according to decade.

Results: SI was largest in the youngest decade then progressively declined until 4th decade. Thereafter a progressive increase was noted until the oldest decade (Figure). Although LVEF was non-significantly higher in the middle-decades, no age-dependency was noted. Delta SI, which was defined as SI at end-diastole minus SI at end-systole correlated with LVEF.

Conclusions: LV shape changes with age. In the younger ages the LV shape is characterized as spherical becoming more elliptical shape during the middle age decades. These age related LV shape changes probably correlate with the growing process of myocardial fiber arrangement.



3:30 p.m.

1027-244

Strain Dispersion Index and Global Longitudinal Strain in Differentiating Hypertrophic Cardiomyopathy From Other Forms of Left Ventricular Hypertrophy

Mengistu Alemayehu Simegn, Ashok Kondur, Pretti Ramappa, Tamam Mohammed, Luis Afonso, Division of Cardiovascular Medicine, Wayne State University and the Detroit Medical Center, Detroit, MI, Division of Cardiology the John D. Dingell VA Medical Center, Detroit, MI

Background: Differentiating variant forms of left ventricular hypertrophy (LVH) using conventional echocardiography can be clinically challenging. Deformational analysis using ultrasound speckle tracking (two-dimensional) strain appears promising as it permits characterization of global and regional perturbations of left ventricular systolic function.

Methods: Fifty-four subjects, 20 with hypertrophic cardiomyopathy (HCM), 16 with hypertensive (HTN) LVH and 18 healthy professional athletes (AT) with LVH underwent 2D strain imaging. Peak systolic longitudinal strain values in the apical long, two and four chamber views were measured offline to generate a 17-segment polar strain map (Automated Function Imaging software, EchoPAC, GE-Vingmed). Strain Dispersion Index (SDI) was then computed as the average of the standard deviations of segmental longitudinal strain values in the basal, mid and apical segments. Global longitudinal strain (GLS) was calculated as the average strain of all 17 segments

Results: Patients with HCM had significantly higher SDI compared to healthy athletes (4.9 ± 1.7 vs. 2.7 ± 0.74 , $P=0.001$) and patients with HTN (3.7 ± 1.3 , $P=0.02$) where as GLS was significantly attenuated (-12.25 ± 5.2 vs. -17.34 ± 2.6 , $P=0.001$) and (-16.6 ± 2.8 , $P=0.005$) respectively. There was no notable difference in GLS between healthy athletes and HTN LVH ($P=0.40$). Receiver-operator curve analysis showed a sensitivity and specificity of 70% and 82.4 % for SDI (for a cut-off value of 3.82) and 65 and 100 % respectively for GLS (cut of value of -13.0 %) for identifying patients with HCM

Conclusions: Heterogeneity of regional systolic deformation is frequent in patients with HCM and can be rapidly identified by longitudinal strain mapping. Objective quantification of regional and global systolic function using 2D strain imaging appears to a reliable complementary method of discerning variant forms of LVH.

3:30 p.m.

1027-245

Assessment of Left Atrial Appendage Function and Left Atrial Function by Velocity Vector Imaging Method Is Useful to Predict Left Atrial Appendage Thrombus in Patients With Nonvalvular Atrial Fibrillation

Takatomo Watanabe, Koji Ono, Ryuhei Tanaka, Noriyuki Oonishi, Tomoko Hirose, Tomonori Segawa, Toshiyuki Noda, Sachiro Watanabe, Masanori Kawasaki, Shinya Minatoguchi, Gifu Prefectural General Medical Center, Gifu, Japan, Gifu University Graduate School of Medicine, Gifu, Japan

Background: Left atrial appendage (LAA) thrombus is a high risk factor of embolism in patients with atrial fibrillation (AF) and echocardiographic parameters like spontaneous echo contrast (SEC) and LAA emptying velocity (LAAV) are predictors for thrombus. However, LAA and left atrial (LA) function such as LAA ejection fraction (EF) and LAEF should be an important determinant. Thus, we hypothesized that LAAEF and LAEF could be more useful predictors for thrombus in nonvalvular AF.

Methods: Using velocity vector imaging (VVI) (Siemens), time-LAA or LA volume curve can be automatically and rapidly provided. We measured LAAEF and LAEF by VVI and compared those with manual tracing method using transesophageal (TEE) and transthoracic (TTE) echocardiography in 82 patients with nonvalvular AF. LAAEF and LAEF were defined as (maximal - minimal volume) / maximal volume X 100% during a cardiac cycle using Simpson's method. Moreover, LAAV, SEC score and LA dimension (LAD) were measured in patients, who were grouped according to the existence of thrombus; AF with LAA thrombus ($n=25$, age 71 ± 8) and AF without thrombus ($n=57$, age 65 ± 11). Average values of 3 cardiac cycles were analyzed.

Results: There was an excellent correlation between VVI and manual method in LAAEF

and LAEF ($r=0.99$, $r=0.94$, $p<0.0001$, respectively) and also between LAAEF and LAEF by VVI ($r=0.87$, $p<0.0001$). LAAEF and LAEF in AF with thrombus were significantly reduced compared with those in AF without thrombus (17.0 ± 3.3 vs $28.4\pm8.8\%$, $p<0.0001$, 17.7 ± 3.5 vs $25.6\pm7.0\%$, $p<0.0001$, respectively). There was a significant difference in LAAV, SEC and LAD between two groups ($p<0.0001$, $p<0.001$, $p<0.01$, respectively). Using 20% of LAAEF as a cutoff value, sensitivity was 92% and specificity was 91% for thrombus by the optimum cutoff from the ROC curve. Using 21% of LAEF, sensitivity was 88% and specificity was 70%. Using 20cm/sec of LAAV, sensitivity was 84% and specificity was 60%.

Conclusions: The present study demonstrates that LAAEF and LAEF can be evaluated by VVI method in nonvalvular AF and that LAA function by TEE and LA function by TTE using VVI method will be novel and more useful markers to predict LAA thrombus than classic predictors such as LAAV, SEC and LAD.

3:30 p.m.

1027-246

Elevated Left Atrial Pressure Estimated by E/e' Ratio During Dobutamine Stress Echocardiography Is Independent of Changes in Blood Pressure

Jehangir N. Din, Stephen K. Glen, Stirling Royal Infirmary, Stirling, United Kingdom

Background: The measurement of the ratio of left ventricular early filling and mitral annular velocity (E/e') may be used to estimate left atrial pressure. However, the relevance of a high ratio during dobutamine stress echocardiography (DSE) is uncertain and may reflect acute haemodynamic effects of dobutamine rather than diastolic filling abnormalities due to cardiac disease. We therefore assessed the relationship between acute haemodynamic changes due to dobutamine stress and estimated left atrial pressure using the E/e' ratio.

Methods: DSE was performed for the detection of myocardial ischaemia in patients unable to exercise or with inconclusive treadmill test results. E/e' ratio was calculated using pulsed wave Doppler measurement at the tips of the mitral valve leaflets (E) and at the lateral annulus using tissue velocity imaging (e').

Results: We studied 1110 patients and the results are categorised in Table 1. Although there are significant differences between groups, regression analysis confirmed no significant relationship between peak systolic or diastolic blood pressure and E/e' ratio ($p=0.271$ and 0.236 respectively).

Conclusions: Changes in E/e' ratio occur independently from systolic blood and diastolic blood pressure during DSE. There is a significant relationship between a E/e' high ratio and patient symptoms. These results support the use of E/e' during DSE for the assessment of patients with symptoms suggestive of diastolic heart failure.

	Normal (E/e' <10)	Borderline (E/e' 10-15)	High (E/e' >15)	p
Number (male)	934 (422)	138 (63)	38 (19)	0.841
Age (years)	61.7±0.8	63.9±2.0	64.5±3.9	0.065
Baseline heart rate	74.3±0.9	74.9±2.5	79.4±4.8*	0.094
Baseline blood pressure	142±1.5 / 80±0.7	142±4.0 / 78±1.9*	151±7.7 / 82±3.7	0.073 / 0.03
Baseline pulse pressure	61±1.2	65±3.3	68±6.3*	0.029
Peak heart rate	131±1.1	124±2.9	106±5.5*	<0.001
Peak blood pressure	149±2.6 / 77±0.8	143±4.6 / 73±2.2	150±8.7 / 81±4.2*	0.073 / 0.001
Peak pulse pressure	61±1.2*	70±3.2	69±6.1	<0.001
Patient aware of dyspnoea during the test	55 (3.9%)	15 (11%)	8 (21%)*	<0.001

3:30 p.m.

1027-247

Afterload Augmentation Is Effective in the Identification of Recently Ischemic Myocardium: A New Method of Ischemic Memory Imaging With Speckle Tracking Echocardiography

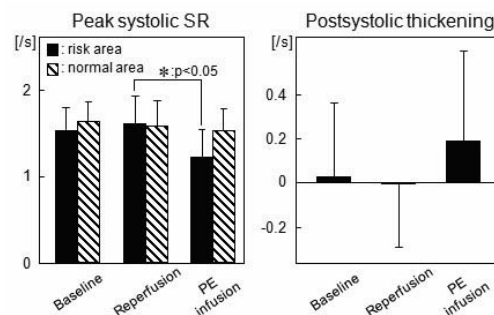
Kasumi Masuda, Toshihiko Asanuma, Mariko Iwasaki, Yumi Fukuta, Satoshi Nakatani, Osaka University, Suita, Japan

Background: Wall motion abnormalities induced by myocardial ischemia disappear shortly after its relief. Therefore, to identify recently ischemic myocardium, ischemic "memory" imaging is desirable. We evaluated whether speckle tracking echocardiography combined with mild afterload augmentation could detect recently ischemic myocardium using an ischemia-reperfusion model.

Methods: Left circumflex coronary artery was occluded for 4 minutes followed by 30-minute reperfusion in 8 open-chest dogs. After recovery of wall motion assessed visually, afterload was mildly increased with phenylephrine infusion (PE, 1.0 µg/kg/min). Short-axis images were acquired at baseline, during occlusion, after reperfusion, and during PE using Vivid 7 (GE). Peak systolic strain, peak systolic strain rate (SR), and peak SR during isovolumic relaxation (as a parameter of postsystolic thickening) were measured in the risk and the opposite normal areas using speckle tracking echocardiography.

Results: Each parameter returned to the baseline level after reperfusion. Left ventricular systolic pressure increased from 113 ± 10 to 144 ± 21 mmHg but peak systolic strain did not change in the risk and normal areas during PE. However, peak systolic SR significantly decreased only in the risk area (figure). Postsystolic thickening tended to increase in the risk area during PE.

Conclusion: Speckle tracking echocardiography during mild afterload augmentation is promising as ischemic memory imaging.



3:30 p.m.

1027-248

Single Center Report of Utility of Stress Echocardiography Stratified According to the 2008 Appropriateness Criteria From the ACCF/ASE/ACEP/AHA/ASNC/SCAI/SCCT/SCMR

Burhan Mohamedali, Dean Ferrera, Samip Vasaiwala, Nathan Bolden, Thomas Stamos, UIC, Chicago, IL

Background: The ACCF published appropriateness criteria for stress echocardiography (SE). An appropriateness score ranging from 1 to 9 was assigned to stress test indications as follows: accepted indications received a score of 7-9, unacceptable 1-3, and uncertain 4-6. Our objective was to report a single center experience in ordering discrepancies among cardiologists versus non-cardiologist in an academic medical center.

Methods: 236 subjects who underwent SE from Jan 2007 to April 2008 were studied. An indication score was assigned based on chart review. Subjects were separated into 2 groups based on the specialty of the ordering physician: Groups 1 (ordering physician was a cardiologist) versus Group 2 (ordering physician was a non-cardiologist). Chi-square testing for inter-group independence was conducted.

Results: Primary results are reported in Table 1

Indication Scores for Stress Echocardiograms ordered by Cardiologists (N=91)	Proportion of Patients %	Observations (N)
Acceptable (7-9)	70	64
Uncertain (4-6)	9	8
Unacceptable (1-3)	21	19
Total	100	91
Indication Scores for Stress Echocardiograms ordered by Non-Cardiologists (N=145)	Proportion of Patients %	N
Acceptable (7-9)	54	79
Uncertain (4-6)	9	13
Unacceptable (1-3)	37	53
Total	100	145
P Value for inter-group difference	0.03	

Conclusions: SE is an important method used routinely in the management of patients with known or presumed cardiovascular disease. We report a single center experience of ordering SE as it relates to the new appropriateness score set forth by the ACCF. In our experience, a majority of the studies were ordered did better at meeting the appropriateness criteria. Cardiologists were slightly better in ordering appropriate SE ($p=0.03$). Our data suggests that there is definite room for improvement in refining the ordering process. Improved education regarding this issue is indicated to reduce the number of unnecessary SE being ordered.

3:30 p.m.

1027-249

Higher Specificity of Stress-Contrast Echocardiography Than SPECT in Women With Suspected Coronary Artery Disease

Constantina Aggeli, Georgios Giannopoulos, Konstantinos Lampropoulos, Georgios Roussakis, Athanasios Aggelis, Euaggelia Christoforou, Maria Bonou, E. Gialafos, Christos Pitsavos, Christodoulos Stefanadis, 1st Department of Cardiology, University of Athens Medical School, Hippokraton Hospital, Athens, Greece

Background: The goal of the present study was to compare the diagnostic efficacy of the combination of dobutamine stress echocardiography (DSE) and myocardial contrast echocardiography (MCE) to that of thallium-201 single-photon emission computed tomography (SPECT) in women.

Methods: 113 women (mean age 68 ± 8 years), referred for coronary angiography (CAG), without known CAD, were submitted to DSE/MCE and SPECT within a two-week period without any intervening clinical events. The women had at least two major risk-factors for CAD and reported atypical or typical symptoms of angina. SPECT was performed with an exercise protocol, unless the patient was unable to exercise, in which case a dipyrindamole SPECT protocol was used. The DSE protocol consisted in four 3-minute stages of intravenous dobutamine infusion ($10-40$ mcg/kg/min) with atropine as needed to

achieve 90% of age-predicted maximal heart rate. An echo-contrast agent was infused at rest and at peak stress. All patients were submitted to CAG in less than 30 days, without any intervening event. Significant CAD was considered as one or more stenoses of at least 50% in a major epicardial artery.

Results: The prevalence of CAD in this population was 34%. In the per-patient analysis, the sensitivity of DSE/MCE and SPECT in detecting CAD was 91% and 87%, respectively ($p=NS$). Their specificity was 85% (DSE/MCE) vs. 73% (SPECT) ($p=0.016$). The overall accuracy was 88% (DSE/MCE) vs. 82% (SPECT) ($p=NS$). In the per-coronary-territory analysis, the higher specificity of DSE/MCE vs. SPECT was found to be attributed almost exclusively to higher specificity in the left anterior descending artery territory (86% vs. 73%, $p=0.014$). The differences between the two techniques were non-significant in the rest of the coronary artery territories.

Conclusions: The combination of DSE/MCE appears to be as sensitive and more specific than SPECT in detecting CAD in women. This may be due to such factors as smaller left ventricular size and breast attenuation in women. The observed higher specificity of DSE/MCE stems almost exclusively from its higher specificity in the left anterior descending artery territory.

3:30 p.m.

1027-250 Determinants of Exercise Induced Dynamic Left Ventricular Outflow Tract Obstruction

Jung Hyuk Kim, Ji Han Park, Sang Min Kim, Hye Jin Han, Jin-Oh Choi, Young Keun On, Sang-Chol Lee, Jae K Oh, Seung Woo Park, Samsung Medical Center, Seoul, South Korea

Background: The aim of the study is to investigate the determinants of the exercise-induced dynamic left ventricular outflow tract obstruction (LVOTO) and its clinical significances.

Methods: In 763 patients who underwent symptom-limited exercise echocardiography (ExE) for chest pain or dyspnea, dynamic LVOTO was assessed by continuous wave Doppler echocardiography at baseline and after exercise. 177 patients were excluded due to baseline wall motion abnormality, previous cardiac surgery or more than moderate valvular disease, and incomplete study with poor exercise tolerances. Dynamic LVOTO was defined as the peak pressure gradient at LVOT > 40 mmHg immediately after exercise with Valsalva or not. There were 139 patients (M:F=104:35) with dynamic LVOTO (group A), and 447 patients (M:F=248:199) without dynamic LVOTO (group B).

Results: In group A, the incidence of hypertension, male sex, diabetes, and negative ExE test were more frequent compared with group B. LV end systolic dimension and LVOT index (LVOT dimension/body surface area) were smaller in group A. There was no difference in the use of beta-blocker, ACE inhibitor, and diuretic. Resting and post exercise septal annular systolic velocity (S'), and left ventricular ejection fraction were higher in group A. In multivariable analysis, negative ExE test and LVOT index showed significant correlation with exercise-induced dynamic LVOTO ($p=0.001$, and $p=0.048$, respectively). Among the patients with negative ExE test, ECG was positive for ischemia in 14.9% (75/505) of the patients. The frequency of dynamic LVOTO was higher with positive exercise ECG (41.3% [31/75]) than with negative ECG (23.5% [101/430], $p<0.005$).

Conclusions: Vigorous left ventricular contraction and small LVOT index caused exercise-induced dynamic LVOT obstruction, which might be related to false positive exercise ECG test.

3:30 p.m.

1027-251 Longitudinal Two-Dimensional Strain of Left Ventricle at Rest Are Useful for the Diagnosis of Significant Coronary Artery Disease

Jin-Oh Choi, Joo-Yong Hahn, Seunghyuk Choi, Jin-Ho Choi, Young Keun On, Sang-Chul Lee, Hyeon-Cheol Gwon, Seung Woo Park, Eun-Seok Jeon, Duk-Kyung Kim, Sang Hoon Lee, Jeong Euy Park, Jae K. Oh, Samsung Medical Center, Sungkyunkwan University School of Medicine, Seoul, South Korea

Background: Longitudinal 2D strain of left ventricle (LV) might reveal subtle changes from myocardial ischemia. We sought to determine whether peak systolic longitudinal strain (PSLS) measured by 2D speckle tracking strain method could predict the presence of significant coronary artery disease (CAD) even in the patients with normal resting wall motion.

Methods: Consecutive 349 patients who underwent exercise echocardiography (ExE) as well as coronary angiography (CAG) and/or multi-detector computed tomography (MDCT) were evaluated. Exclusion criteria were as follows; previous cardiac surgery, abnormal resting wall motion, cardiomyopathy, valvular heart disease, variant angina, and atrial fibrillation. In the case of significant or equivocal MDCT results, CAG was performed. Using a cut off of percent diameter stenosis $> 50\%$, patients were grouped according to the coronary evaluation as CAD group versus normal. From resting images of ExE, the global and segmental PSLS of basal, mid and apical LV were analyzed offline.

Results: Total 193 patients (133 men, mean age 60 ± 10 years) were eligible for analysis. PSLS of all segments of LV could be obtained successfully with good tracking quality in 82% (159/193) patients. Global LV PSLS was significantly lower in CAD group ($n = 82$, mean age 60 ± 10 years) than in normal ($n = 77$, mean age 58 ± 10 years) ($-19.6 \pm 2.0\%$ versus $-21.8 \pm 2.1\%$, $p < 0.001$). Receiver operational characteristic curve demonstrated that global PSLS could predict CAD group with cutoff value of -21.2% (sensitivity 78%, specificity 71% and area under curve (AUC) = 0.79, 95%CI = 0.72-0.86). Segmental analysis showed that mid LV PSLS could predict CAD most efficiently with cutoff value of -19.3% (sensitivity 61%, specificity 83% and AUC = 0.77, 95%CI = 0.69-0.84). ExE could predict CAD group with sensitivity of 81% (62/77) and specificity of 82% (67/82). In multivariable logistic analysis, reduced PSLS (cutoff value of -21.2%) could predict significant CAD (OR = 4.6, 95%CI 1.77-11.7, $p = 0.002$) independently of ExE results (OR = 12.1, 95%CI, 5.05-29.0, $p < 0.001$).

Conclusions: Reduced LV PSLS at rest even in the patients with normal wall motion might be an independent predictor for the significant CAD.

1027-252

Neuropsychiatric Symptoms During 24 Hours After Dobutamine/Atropine Stress Testing

Punsak Wuthiwaropas, Julie A. Wiste, Robert B. McCully, Patricia A. Pellikka, Mayo Clinic, Rochester, MN

Background: Dobutamine/atropine stress testing (DST) is widely used for the detection of coronary artery disease. Neuropsychiatric (NP) symptoms have rarely been reported after the test but the incidence has not been systematically studied. We aimed to determine incidence and predictors of NP symptoms during 24 hours after DST.

Methods: Consecutive outpatients undergoing clinically indicated DST were prospectively enrolled. Trained registered nurses administered the Short Portable Mental Status Questionnaire (SPMSQ) and the Delirium Observation Screening Scale (DOSS) before and after DST. Patients were asked to return a follow up questionnaire regarding their symptoms during the 24 hours following DST.

Results: We included 902 patients (age 67 ± 12 years, 411 (46%) females) who completed SPMSQ & DOSS. Peak dose of dobutamine was 35 ± 7 mcg/kg/min and 301 (60%) received atropine. Of the 654 (73%) patients who returned their follow up questionnaires, 48 (7.3%) patients reported NP symptoms including amnesia, confusion, disequilibrium, or fall; 36 (75%) of these had received atropine. Four of these had seen their physician for NP symptoms. Spontaneous resolution within 24 hours was experienced in most symptomatic patients. Multiple logistic regression analysis demonstrated the following independent predictors of NP symptoms: atropine dose ≥ 1 mg (OR = 5.85, 95%CI = 3.10-11.31), history of NP disease (OR = 2.47, 95%CI = 1.27-4.78), and positive DOSS after DST (OR = 6.68, 95%CI = 1.69-24.87). Age, sex, dobutamine dose and SPMSQ were not associated with NP symptoms in univariate analysis.

Conclusions: NP symptoms occur in about 7% of patients during 24 hours after DST. Patients who had received ≥ 1 mg atropine, had underlying NP disease or positive DOSS after DST were at increased risk and should be accompanied by a relative or friend after the test.

3:30 p.m.

1027-253

Two-Dimensional Speckle Tracking Strain Imaging Can Predict Transmurality of Acute Myocardial Infarction Treated With Primary Percutaneous Coronary Interventions

Claudia Raineri, Margherita Calcagno, Sergio Leonardi, Fiorenza Fava, Mara Bonardi, Arturo Raisaro, Mario Previtali, IRCCS Policlinico S. Matteo University of Pavia, Pavia, Italy

Background: Two-dimensional Strain Imaging (2D-SI) can predict the transmural (TM) of ST-elevation myocardial infarction (STEMI) in the chronic phase, but its value in the acute phase is not as yet been demonstrated. The aim of this study was to evaluate the ability of basal and dobutamine stress 2D-SI to predict TM of STEMI, evaluated with cardiovascular magnetic resonance (CMR), in patients (pts) treated with primary (p) PCI.

Methods: 25 STEMI pts (mean age 58 years, 92% men, 68% anterior) reperfused with pPCI underwent contrast-enhanced CMR and baseline + low-dose (5-10 /Kg/min) dobutamine speckle tracking 2D-SI at a median of 5 days after STEMI. Longitudinal (L), radial (R), circumferential (C) Strain (S) and S Rate (SR) were evaluated on a 16-segment model of the left ventricle. TM was defined as a delayed enhancement (DE) extent $> 75\%$ in the infarcted segment at CMR.

Results: Of the 400 segments analyzed, 165 (41%) showed DE; of these, 57 (35%) showed DE $> 75\%$ and 108 (65%) DE $< 75\%$. The table shows the 2D-SI variables in the 2 groups. At multivariate analysis only basal LS ($p<0.0001$) and CS ($p<0.0001$) were independent predictors of TM. ROC analysis showed an area under the curve of basal LS of .79 (95% CI .69 -.90, $p<0.0001$) for detection of TM. A basal LS cut-off value of -6.9 had a 72% sensitivity and a 83% specificity for detecting TM.

Conclusions: 2D-SI can predict TM of STEMI and may be of clinical value for early clinical stratification. Baseline LS and CS are the best multivariate predictors of TM.

	DE < 75%	DE > 75%	p value
LS	-9.36 \pm 6.45	-5.00 \pm 6.96	<.001
LS Dob	-11.76 \pm 9.02	-6.34 \pm 8.75	.001
RS	24.00 \pm 16.36	14.81 \pm 15.45	.008
RS Dob	29.86 \pm 18.52	15.73 \pm 10.78	<.001
CS	-9.33 \pm 8.12	-2.96 \pm 7.85	<.001
CS Dob	-12.32 \pm 12.94	-5.10 \pm 8.53	.005
LSR	-0.81 \pm 0.33	-0.68 \pm 0.36	.022
LSR Dob	-1.20 \pm 0.50	-1.11 \pm 0.57	ns
RSR	1.79 \pm 0.68	1.36 \pm 1.04	<.014
RSR Dob	2.10 \pm 0.93	1.42 \pm 1.13	.002
CSR	-1.13 \pm 0.44	-0.80 \pm 0.57	.002
CSR Dob	-2.10 \pm 3.96	-1.17 \pm 0.55	ns

Explanatory Note: LS: Longitudinal Strain, LS Dob: Longitudinal Strain after Dobutamine, RS: Radial Strain, RS Dob: Radial Strain after Dobutamine, CS: Circumferential Strain, CS Dob: Circumferential Strain after Dobutamine, LSR: Longitudinal Strain Rate, LSR Dob: Longitudinal Strain Rate after Dobutamine, RSR: Radial Strain Rate, RSR Dob: Radial Strain Rate after Dobutamine, CSR: Circumferential Strain Rate, CSR Dob: Circumferential Strain Rate after Dobutamine.

3:30 p.m.

1027-254

Safety of Dobutamine Stress-Contrast Echocardiography: Experience From 22600 Studies

Constantina Aggeli, Georgios Giannopoulos, Konstantinos Lampropoulos, Georgios Roussakis, Euaggelia Christoforatos, Maria Bonou, Athanasios Aggelis, Amalia Chatziagianni, Christos Pitsavos, Christodoulos Stefanadis, 1st Department of Cardiology, University of Athens Medical School, Hippokraton Hospital, Athens, Greece

Background: The combination of perfusion assessment using myocardial contrast echocardiography with dobutamine-atropine stress testing has improved the diagnostic accuracy of traditional stress echocardiography. The aim of the present study is to provide evidence regarding the safety of real-time flash-contrast echocardiography combined with dobutamine stress echo.

Methods: 22600 individuals were submitted to dobutamine stress echocardiography (accelerated four-staged protocol at doses 10-20-30-40 mcg/kg/min with use of atropine as required to achieve 90% of age-adjusted heart rate), with concurrent myocardial contrast perfusion study using a low-mechanical index technique with administration of high-energy impulses in order to assess replenishment time. Sonovue, Bracco contrast agent was used and the studies were performed with a Sonos 5500 (Philips Medical Systems) echocardiography machine.

Results: Among 22600 examined subjects (68% male, mean age 61.5±9 years), 43.3% had known previous history of coronary heart disease (CHD), 38.1% were diabetics, 56% were hypertensive, 25% had family history of CHD and 33% were smokers. Sustained ventricular tachycardia (VT) or fibrillation requiring resuscitation occurred in 2 cases. The incidence of other arrhythmic events was: sustained VT not requiring resuscitation (N=15, 0.06%), non-sustained VT (N=36, 0.15%), supraventricular tachycardia at rate >180/minute (N=6, 0.02%), atrial fibrillation (N=52, 0.23%). Atrial fibrillation spontaneously reverted to sinus rhythm within 24 hours, except in 3 patients. Other observed adverse events included: Psychomotor agitation-disorientation during the study (N=5, 0.022%), intense headache (N=185, 0.8%), intense back-pain (N=210, 0.92%). Vagal reactions with systolic blood pressure fall <100mmHg were observed in 86 cases (0.38%). Finally, mild hypersensitivity reactions (skin rash, urticaria) within the first 24 hours after the study were reported in 118 cases (0.52%).

Conclusions: We report safety data regarding stress-contrast echocardiography in a large series of subjects, suggesting that this is an exceptionally safe technique.

3:30 p.m.

1027-255

Development of Atrial Fibrillation During Dobutamine Stress Echocardiography: Incidence, Clinical Course and Implications

Seth H. Sheldon, Wells Askew, Kyle Klarich, Patricia Pellikka, Robert McCully, Mayo Clinic Rochester, Rochester, MN

Background: As a synthetic catecholamine, dobutamine can precipitate both supraventricular and ventricular arrhythmias. The reported incidence of atrial fibrillation during dobutamine stress echocardiography (DSE) is 1-4%. Our objective was to determine the incidence, clinical course, and implications of atrial fibrillation precipitated during DSE.

Methods: Prospective data was obtained on consecutive patients (pts) in sinus rhythm who underwent DSE between November 1, 2003 and December 31, 2007. A review of the medical record was performed for pts who developed atrial fibrillation during DSE.

Results: Of 12,158 pts, 122 (1%) developed atrial fibrillation during DSE. Of these, 51 (42%) pts had a history of atrial fibrillation. Intravenous beta-blockers were administered to achieve heart rate control in the echocardiography laboratory (echo lab) in 98 pts (80%). Four pts (3%) developed hemodynamic instability during atrial fibrillation. The duration of dobutamine-induced atrial fibrillation was <1 hour in 74 pts (61%) and >24 hours in five pts (4%). Half the pts were discharged from the echo lab in sinus rhythm (n=61, 50%). The other pts had outpatient follow-up within 24 hours (n=26, 21%), were triaged to the emergency department or hospital (n=18, 15%), or were inpatients managed by their attending physician (n=17, 14%). Spontaneous cardioversion occurred in 114 (93%) pts. The other pts converted with an anti-arrhythmic drug (n=3, 2%) or direct-current cardioversion (n=1, 1%), or remained in stable atrial fibrillation (n=4, 3%). There were no reported cases of thromboembolic events, myocardial infarction, or death.

Conclusion: DSE-related atrial fibrillation is an infrequent complication (1%). Most episodes are of short duration. We recommend prompt heart rate control with intravenous beta-blockers with ECG monitoring in the stress-testing lab as the initial management strategy. Most pts with rate-controlled but persistent atrial fibrillation can be safely dismissed from the stress-testing area for outpatient follow-up within 24 hours. For pts with suboptimal rate control or a positive DSE, we recommend transfer to the emergency department or hospital for definitive treatment.

3:30 p.m.

1027-256

Right Heart Abnormalities by Stress Echocardiography Are Rarely Suspected by Clinicians and Rarely Evaluated in Women: A Supine Bicycle Stress Echocardiography Study

Steven C. Smart, Vicki L. McHugh, Kara J. Kallies, Kelly J. Ray, Bonnie Anderson, Gundersen Lutheran Medical Foundation, La Crosse, WI, Evanston Northwestern Healthcare, Evanston, IL

Background: Stress testing is performed to screen for coronary artery disease (CAD) and left heart abnormalities in patients with chest pain (CP) and shortness of breath (SOB). Supine bicycle stress echocardiography is an accurate test to screen these patients for epicardial CAD, cardiomyopathy, valvular disease, microvascular disease and

right heart abnormalities. It is unclear how right heart abnormalities are recognized and evaluated by clinicians.

Methods: We studied 638 women with CP and/or SOB who underwent supine bicycle stress echocardiography/Doppler imaging for left ventricular wall motion abnormalities (WMA) and ejection fraction (LVEF) analysis, right ventricular (RV) size and function with quantitative analysis of mitral regurgitation (MR), tricuspid regurgitation (TR), right heart pressures and valve function. We also identified coronary angiography, pulmonary function tests (PFT), ventilation perfusion scans (VQ), and polysomnography for CAD, lung disease, pulmonary emboli and sleep apnea data.

Results: Data was available on 606 women (age 63±13 years, LVEF 61±11%). Stress induced LV WMA and moderate to severe MR in 38% and 21%, as well as moderate to severe RV dilatation, dysfunction, TR and pulmonary hypertension in 30%, 31%, 42% and 43% of women, respectively. Only 88 women underwent polysomnography. Induced right heart abnormalities were very accurate (78%) for severe sleep apnea in this subset (TR volume AUC=0.575; RV function AUC=0.660; RV size AUC=0.701). There were 167 women with the combination of moderate to severe exercise induced RV dilatation, hypokinesis, TR and pulmonary hypertension; however, lower body mass, lower Epworth score and left heart abnormalities were deterrents for referral for most. PFTs, and VQ scans were performed in 7% and < 5% of women.

Conclusions: Complex right heart abnormalities by supine bicycle stress echocardiography identified severe sleep apnea in women who underwent polysomnography, but the majority of these women were not tested due to lower body mass, Epworth scores, and induced left heart abnormalities. Right heart abnormalities by stress echocardiography are rarely suspected, underappreciated, and rarely evaluated.

3:30 p.m.

1027-257

Relative Wall Thickness and Myocardial Ischemia Are the Most Important Factors in the Subendocardial Response to Stress

Tony Stanton, Charlotte Bjork Ingul, James L. Hare, Rodel Leano, Thomas H. Marwick, University of Queensland, Brisbane, Australia, University of Science & Technology, Trondheim, Norway

Background: Myocardial deformation parameters such as strain rate (SR) have been shown to be sensitive markers of global left ventricular (LV) systolic function. In particular they are thought to have the ability to reflect changes in myocardial interstitial fibrosis and subendocardial function. We wished to investigate the effect of relative wall thickness on myocardial deformation, both at rest and peak stress, and its subsequent interaction with coronary artery disease.

Methods: 126 patients with normal resting LV function undergoing dobutamine stress echocardiography had coronary angiography performed within 6 months. Relative wall thickness (RWT) and left ventricular hypertrophy (LVH) were calculated according to standard criteria. The presence and extent of coronary artery disease (CAD) was identified by quantitative coronary angiography.

Results: Individuals with raised RWT group had significantly lower peak SR (-2.3±0.4 vs -2.5±0.4 s⁻¹, p<0.05) and smaller change in SR (-1.0±0.4 vs -1.2±0.4 s⁻¹, p<0.05) with stress with no differences in resting values. Conversely subdivision by presence/absence of LVH, showed no difference in resting or peak myocardial deformation values between groups. Those with CAD, had significantly lower peak SR values (-2.3±0.4 vs -2.6±0.4 s⁻¹, p<0.05) and change in SR (-1.0±0.4 vs -1.3±0.4 s⁻¹, p<0.05) with no difference in resting measures. A linear regression model showed that RWT (β=0.14, p=0.1) and extent of CAD (β=0.35, p<0.01), but not LV mass index or LVH, were the strongest predictors of peak SR (overall model β=0.18, p<0.01). Similarly the strongest predictors of change in SR were RWT (β=0.19, p<0.05) and extent of CAD (β=0.30, p<0.01) were again the strongest predictors (overall model β=0.19, p<0.01). Increasing extent of CAD caused a steady degradation in peak SR and change in peak SR.

Conclusions: Markers of longitudinal myocardial deformation at peak stress are able to reflect both myocardial and interstitial properties. The main determinant of subendocardial function is wall thickness, as measured by relative wall thickness, and not LVH.

3:30 p.m.

1027-258

Is the Standard Weight-Based Protocol for Dobutamine Stress Testing Appropriate for Patients of Widely Varying Body Mass Index?

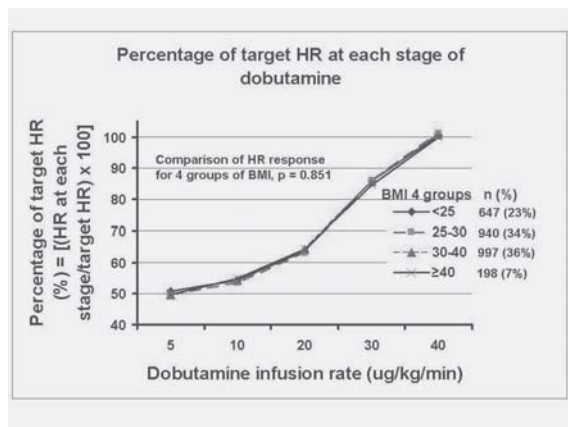
Maytinee Kittipovannon, Alain M. Bernheim, Christopher G. Scott, Clarence Shub, Marion E. Barnes, Patricia A. Pellikka, Mayo Clinic, Rochester, MN

Background: Dobutamine stress testing (DST) is performed according to a weight-based protocol. No data exists regarding the appropriateness of this dosing in situations of wide variation in body mass index (BMI). A gradual increase in heart rate (HR) during testing is desired. We sought to determine the effect of BMI on the rate of increase in HR.

Methods: Prospectively acquired data of consecutive patients who underwent DST according to a standard clinical protocol aimed at achieving 85% age-predicted maximum HR or administration of peak dose of dobutamine and atropine (64% patients) were reviewed. We classified patients into 4 groups of BMI (kg/m²): <25 (normal), 25-30 (overweight), 30-40 (obese), ≥ 40 (severely obese). The rate of increase of HR was compared for the 4 groups.

Results: Of the 2,782 patients, age 68 ± 12 years, 52% men, BMI was 29.8 ± 6.6 kg/m² (range 14.5 - 81.4) and 198 (7%) had BMI ≥ 40. The percentage of target HR achieved at each stage of dobutamine was essentially equivalent among 4 groups (figure). Target HR was achieved in 2,438 (88%). The percentage of patients with BMI <25, 25-30, 30-40, ≥ 40 who achieved target HR was similar: 87%, 88%, 88%, and 84%, respectively. Independent predictors of failure to achieve target HR included age, diabetes mellitus, treatment with chronotropic medications, and baseline HR; BMI was not a predictor (OR 0.98, p=0.072).

Conclusions: The current weight-based protocol of dobutamine dosing for DST results in similar increases in HR for patients of widely varying BMI.



3:30 p.m.

1027-259

High Prevalence of Stress-Induced Dynamic Diastolic Dyssynchrony in Heart Failure With Preserved Ejection Fraction

Cheuk-man Yu, PW Lee, JK Song, Gabriel WK Yip, Tian-gang Zhu, Qing Zhang, Jun-min Xie, Chun-mei Li, The Chinese University of Hong Kong, Hong Kong SAR, Hong Kong

Background: Recent studies suggested that left ventricular (LV) mechanical dyssynchrony is common in heart failure with preserved ejection fraction (HFpEF). It is, however, unclear whether and how LV dyssynchrony alters with hemodynamic stress in HFpEF. In this study, we measured LV mechanical dyssynchrony under resting and stress conditions in HFpEF using tissue Doppler echocardiography, and compared to asymptomatic hypertensive subjects and healthy controls.

Methods: Fifty-two consecutive patients (57 ± 14 years, 24 men) with prior history of heart failure, essential HTN, EF $\geq 50\%$ and without stress-induced ischemia (HFpEF group) were compared to 37 age, sex-matched asymptomatic HTN with EF $\geq 50\%$ (HTN group), and 50 healthy controls (Control group). All subjects underwent dobutamine stress echocardiography with tissue Doppler imaging to evaluate LV systolic and diastolic mechanical dyssynchrony by measuring the standard deviations of time to peak systolic (Ts-SD) and early diastolic (Te-SD) myocardial velocities, respectively, using a 12-segment model. The upper 2 standard deviations derived from healthy controls were used as cutoff for defining dyssynchrony (33ms for Ts-SD and 34ms for Te-SD).

Results: LV mechanical dyssynchrony did not alter with stress in the Control group. At rest, systolic and diastolic dyssynchrony were evident in 25.0% and 73.1% of HFpEF respectively, but this prevalence was similarly observed in HTN (systolic: 29.7%; diastolic: 59.5%, $p=NS$). During stress, the prevalence of systolic dyssynchrony increased to 36.5% in HFpEF and 48.6% in HTN ($p=NS$). Conversely, diastolic dyssynchrony increased significantly with stress only in HFpEF (94.2%) ($p<0.001$), but not in HTN or Controls. Furthermore, stress-induced diastolic dyssynchrony was more common in the HFpEF than HTN (94.2% vs 51.4%, $p<0.001$).

Conclusions: LV mechanical dyssynchrony is highly dynamic in hypertensive HFpEF. Notably, stress-induced exaggeration of LV diastolic dyssynchrony is frequently and characteristically observed in hypertensive HFpEF, as opposed to asymptomatic HTN, raising a possibility of its pathogenic role in progression of non-failing HTN to symptomatic HFpEF.

3:30 p.m.

1027-260

Abnormal Coronary Flow Reserve Is Related to Impairment of Left Ventricular Function During Adenosine Stress Echocardiography in Untreated Hypertensive Patients

Ignatios Ikonomidis, Stavros Tzortzis, Ioannis Paraskevaidis, John Lekakis, Helen Triantafyllidi, Costas Tsitlakidis, Costas Papadopoulos, Dimitrios T. Kremastinos, 'ATTIKON' University Hospital, Athens, Greece

Background: We investigated the effects of coronary flow reserve on the response of Left Ventricular (LV) systolic and diastolic function as assessed by Tissue Doppler Imaging during adenosine stress echocardiography in never-treated hypertensive patients

Methods: We studied 40 untreated consecutive patients (mean age: 53 ± 12 years), with newly diagnosed and untreated arterial hypertension by adenosine stress echocardiography and 22 healthy controls matched for atherosclerotic factors. We measured: a) time integral (VTI-Vd) of diastolic (Vd) coronary blood flow velocity at the distal tract of the LAD b) Ratio of VTI-Vd after adenosine infusion ($140 \mu\text{g/kg/min}$) to VTI-Vd at baseline to assess coronary flow reserve (CFR) c) E and A doppler, Sm, Em, Am lateral mitral annulus velocities with TDI, Em/Am ratio and E/Em ratio before and during adenosine infusion ($140 \mu\text{g/kg/min}$ for 6 min) to assess LV systolic and diastolic function, d) the percent % changes of the measured indices between baseline and peak adenosine infusion

Results: All patients had normal baseline ejection fraction. Compared to controls, patients with hypertension had lower CFR (2.3 ± 0.7 vs. 2.9 ± 0.9 , $p=0.03$).

At baseline, hypertensives compared to controls, had lower E/A ratio (0.9 ± 0.3 vs. 1.2 ± 0.3 , $p=0.08$), Em/Am ratio (0.9 ± 0.3 vs. 1.3 ± 0.4 , $p=0.002$), Sm ($p=0.07$), Em ($p=0.03$) and

higher Am ($p=0.03$). At peak adenosine infusion there was an increase in Sm, Em and Am in all patients, ($p<0.05$)

At peak adenosine infusion, a decreasing CFR was associated with a decreasing Em ($r=-0.46$, $p=0.05$), Em/Am ($r=0.49$, $p=0.048$) and increasing E/Em ($r=-0.4$, $p=0.04$). Furthermore a reduced CFR was related with a smaller % increase of Sm ($r=-0.40$, $p=0.049$), % increase of Em ($r=-0.5$, $p=0.033$) and higher % increase of E/Em ($r=-0.42$, $p=0.04$) at peak stress.

Patients with CFR <2.5 ($n=20$), compared to those with CFR ≥ 2.5 had lower % change of Sm ($27 \pm 20\%$ vs. $51 \pm 34\%$ $p=0.04$), % change of Em ($8 \pm 3\%$ vs. $46 \pm 3\%$, $p=0.05$) and higher % increase of E/Em ($24 \pm 3\%$ vs. $1 \pm 2\%$, $p=0.04$).

Conclusions: An abnormal response of left ventricular function during adenosine stress echocardiography is related with impaired coronary flow reserve in untreated hypertensive patients.

3:30 p.m.

1027-261

Prognostic Significance of ST-T-Wave Abnormalities on Baseline Electrocardiogram in Patients Without Known Coronary Artery Disease Referred for Dobutamine Stress Echocardiography

Pedone Chiara, Abdou Elhendy, Ron T. van Domburg, Stefan Nelwan, Arend F. Schinkel, Elena Biagini, Giuseppe Di Pasquale, Jeroen J. Bax, Don Poldermans, Erasmus University Medical Centre, Rotterdam, The Netherlands

Background: The prognostic significance of ST-T wave abnormalities in patients underwent dobutamine stress echocardiography (DSE) is not known. The aim of this study was to determine whether resting ST-T wave abnormalities provide incremental prognostic information relative to DSE in patients without known coronary artery disease (CAD).

Methods: We evaluated 1308 consecutive patients without known CAD underwent DSE. ST-T wave abnormalities were detected on resting electrocardiogram in 162 (12%) patients. Follow up (4.6 ± 3 yrs) for all cause deaths and hard cardiac events (cardiac death and/or non fatal myocardial infarction) was obtained.

Results: Patients with baseline ST-T wave abnormalities presented more frequently resting (52% vs 42% , $p=0.029$) and stress-induced (46% vs 28% , $p<0.0001$) wall motion abnormalities. Patients with resting ST-T wave abnormalities had a worse prognosis both in presence of abnormal (annual death rate 8.7% vs 4.9% and annual hard cardiac event rate 5.3% vs 3% , $p<0.05$) and normal DSE (annual death rate 4.7% vs 3.6% and annual hard cardiac event rate 3.1% vs 1.4% , $p<0.05$). Cox proportional modelling showed that these ECG findings added incremental value over clinical data, stress induced ischemia for the prediction of death (global χ^2 increased from 125 to 140 to 150 to; $p<0.05$) and hard cardiac events (global χ^2 increased from 79 to 100 to 111 to; $p<0.05$). Moreover in patients with normal DSE ST-T-wave abnormalities added incremental prognostic value over clinical data in predicting death (global χ^2 increased from 61 to 73; $p<0.05$) and hard cardiac events (global χ^2 increased from 21 to 28; $p<0.05$).

Conclusions: The presence of ST-T waves abnormalities independently increases the risk of hard cardiac events and all cause mortality over clinical data and DSE result. Patients with ST-T wave abnormalities have a higher risk, even in presence of normal DSE.

3:30 p.m.

1027-262

Strain as a Surrogate of Cardiac Contractility in Patients With Multivessel Coronary Artery Disease in Exercise Stress Echocardiography: A Novel Approach to Stress Echocardiographic Interpretation

Hector R. Villarraga, Peggy A. Kalmes, Fletcher A. Miller, Robert B. McCully, Patricia A. Pellikka, Mayo Clinic, Rochester, MN

Background: Exercise Stress Echocardiography (ESE) is an established subjective imaging modality for evaluating patients with suspected or known coronary artery disease (CAD). Strain (S) and systolic Strain Rate (SRs) derived from speckle tracking would allow us to quantify abnormalities in patients with multivessel disease. Our aim was to describe and compare S and SRs in patients with angiographically proven significant CAD and controls.

Methods: Off-line measurement of Digital Stored images from patients that had low pretest probability of CAD and a normal ESE (Group 1-42 patients [G1]) where compared to a cohort of individuals with significant multivessel disease (Group 2-42 patients [G2]) with $\geq 70\%$ stenosis in 2 or more vessels (LAD, CX or RCA). Syngo Velocity Vector Imaging (VVI) (Siemens Medical Solutions Malvern, PA) was utilized. Short axis (SAX) at mid level and apical 4 and 2 chamber views (Long) where used. All segments where analyzed for S, systolic SR; Anova, ROC and AUC were performed.

Results: A total of 84 patients and 3024 segments were analyzed. Peak values for SAX by coronary territory are shown in table 1. For Long S the apical segments values were -11.8 vs -7.6° (G1 vs G2) with an AUC of 0.73 ($p<0.02$). SRs values in SAX and Long were borderline or non-significant.

Conclusions: We show for the first time that Patients with multivessel disease that undergo ESE have lower circumferential as well as longitudinal apical S when compared with normal controls.

SAX Strain By coronary Territory and AUC (Area Under Curve) [G1 vs. G2, * $p<0.02$, # $p<0.05$]

Coronary Territory	SAX S (%) G1	SAX S (%) G2	AUC
LAD	-18.9	-13.0*	0.68*
CX	-19.6	-14.2#	0.66*
RCA	-22.7	-14.9*	0.71*
All territories	-20.3	-13.9*	0.70*

3:30 p.m.

3:30 p.m.

1027-263

Comparison of Coronary Blood Flow and Coronary Blood Flow Reserve in Hypercholesterolemia Before and After Atorvastatin Treatment Using Real-Time Myocardial Contrast Echocardiography

Fabio C. Lario, Marcio H. Miname, Jeane M. Tsutsui, Ingrid Kowatsch, Joao C. Sbrano, Raul D. Santos, Jr., Wilson Mathias, Jr., InCor - HCFMUSP, Sao Paulo, Brazil, FAPESP, Sao Paulo, Brazil

Background: Hypercholesterolemia induces functional and structural changes of the microvasculature and reduces coronary flow reserve in humans and experimental animals. Real time myocardial contrast echocardiography (RTMCE) may be used to determine myocardial blood flow (AxB) and its components: myocardial blood volume (A) and myocardial blood flow velocity (B). We sought to determine how hypercholesterolemia and its treatment with atorvastatin affect MBF using RTMCE in basal condition and after adenosine stress.

Methods: 16 patients with familial hypercholesterolemia without obstructive epicardial coronary disease (by multislice computed tomography) and 10 healthy volunteers were evaluated with RTMCE in two different moments (12 weeks apart). After the first evaluation, atorvastatin was prescribed to hypercholesteremic group. For MBF evaluation, the left ventricle was divided in 17 segments, and A, B, and their product AxB were calculated based on the ultrasound contrast agent refill curves for each myocardial segment in the resting condition and after adenosine maximal hyperemia. MBF reserve was calculated as the hyperemic to rest ratio.

Results: The two groups were comparable for sex, age, weight, resting and hyperemic heart rate and arterial blood pressure. The LDL-C (mg/dL) in the two moments were $101.14 \pm 34.65 \times 102.29 \pm 35.52$; $p=0.95$ for the control group and $279.50 \pm 60.02 \times 160.17 \pm 50.14$; $p<0.001$ for the hypercholesteremic individuals. HF patients before treatment had higher resting values of A ($0.56 \pm 0.08 \times 0.49 \pm 0.05$; $p=0.02$), B ($0.56 \pm 0.14 \times 0.45 \pm 0.04$) and AxB ($0.28 \pm 0.06 \times 0.20 \pm 0.02$; $p=0.002$), higher hyperemic value of A ($0.64 \pm 0.08 \times 0.57 \pm 0.06$; $p=0.04$) and lesser reserves of B ($2.59 \pm 0.61 \times 3.25 \pm 0.45$; $p=0.01$) and AxB ($2.78 \pm 0.71 \times 3.43 \pm 0.66$; $p=0.03$) as compared to healthy volunteers. After atorvastatin treatment no difference was observed in the resting, hyperemic and reserve values of A, B and AxB between the groups with a tendency of "normalization" of resting MBF.

Conclusions: In HF patients, MBF reserve is reduced mainly by augmented basal MBF velocity and MBV. Treatment with atorvastatin normalized these alterations.

3:30 p.m.

1027-264

Extensive No-Reflow Subsequently Induces a Decrease in the Epicardial Coronary Artery Lumen Diameter Downstream of the Initial Culprit Lesion in Reperfused Acute Myocardial Infarction

Tadamichi Sakuma, Masaya Otsuka, Tomokazu Okimoto, Mamoru Toyofuku, Hidekazu Hirao, Yuji Muraoka, Hironori Ueda, Yoshiko Masaoka, Yasuhiko Hayashi, Tsuchiya General Hospital, Hiroshima, Japan

Background: We hypothesized that the change in myocardial blood volume (MBV) downstream of the initial culprit lesion might influence an increase or decrease of the epicardial coronary artery lumen diameter (LD) at 6 months after primary percutaneous coronary intervention (PPCI).

Methods: The study included 97 consecutive first anterior acute myocardial infarction (AMI) patients(pts), who had >70% diameter stenosis even after selective coronary thrombus aspiration, and in whom PPCI with a metallic coronary stent was undertaken successfully within 12 h of symptom onset. The area of severe ischemia was measured on arrival by echocardiography. ECG-triggered 1.5 harmonic intravenous myocardial contrast echocardiography using Levovist was recorded to evaluate no-reflow (NR) at 2 weeks after PPCI. Group 1 was comprised of 47pts with $\geq 25\%$ of NR within the initial severely asynergic region, and group 2 consisted of the remaining 50 pts with < 25% of NR. LD was measured at 8 mm distal to the distal edge of the metallic coronary stent, after selective injection of nitrate, by coronary angiography with right and left cranial views. Additionally, corresponding LDs were also measured again at 6 months after PPCI in the same manner. Wall motion score indices (WMSI) within the left anterior descending coronary artery were calculated using the standard 16-segment model shortly before and 6 months after PPCI. **Results:** Percent change of LD, defined as (6 months LD - day 0 LD)/day 0 LD, was significantly lower in group 1 (-0.035 ± 0.11 vs. 0.068 ± 0.13 , $p=0.0016$; indicated by mean \pm SD). WMSI on day 0 was 2.66 ± 0.23 in group 1 and 2.55 ± 0.51 in group 2 ($p=0.45$), and WMSI 6 months after PPCI was 2.06 ± 0.59 and 1.63 ± 0.47 ($p=0.0007$), respectively. **Conclusions:** Extensive NR causes disuse reduction in LD of the downstream epicardial coronary artery 6 months after PPCI for first anterior AMI. Conversely, good reflow causes an increase in LD of the corresponding coronary artery subsequent to elimination of underlying flow limiting stenosis prior to PPCI. Myocardial viability and MBV within the risk area for infarction may influence the subsequent increase or decrease in epicardial coronary artery LD in the medium-term after PPCI.

1027-265

Survival in an Intensive Care Unit Population Undergoing Transthoracic Echocardiography With and Without Perflutren Containing Ultrasound Contrast Agents: Results in 39,189 Propensity Matched Cases

Michael L. Main, Amy C. Ryan, Teresa E. Davis, Maureen P. Albano, Lisa L. Kusnetzky, Mark Hibbard, Saint Luke's Mid America Heart Institute, Kansas City, MO, Premier, Inc., Charlotte, NC

Background: Lipid or Type A protein coated perflutren microsphere imaging agents improve image quality in technically inadequate baseline transthoracic echocardiograms (TTE). Although these imaging agents are widely used in acute care and intensive care unit settings where other diagnostic options are limited or unavailable, questions remain concerning the safety of these agents in the critically ill or mechanically ventilated patients.

Methods: A retrospective analysis was performed using the validated Premier Perspective™ Database which contains hospital billing data of primary and secondary diagnosis and procedure codes. All patients classified as critically ill who underwent a non-contrast (nTTE) or contrast (cTTE) study between 01 Jan 2002 and 31 Oct 2007 were included. Data included vital status within 2 days of imaging, baseline characteristics affecting short term survival, and co-morbid conditions. Propensity matching controlled for age, gender, race, severity of illness, and major co-morbidities. Multivariate logistic regression (MLR) analysis was used to compare short term mortality (<48 hours) between cTTE patients and their propensity matched nTTE controls.

Results: A total of 145,882 clinically matched patients underwent resting TTE. Of those, 39,189 were critically ill and in the ICU when the echo was performed (nTTE n=19,871; cTTE n=19,318). Short-term mortality rates were 2.98% (n=592 deaths) for patients after nTTE and 2.30% (n=445 deaths) for patients after cTTE. MLR analysis revealed that short term mortality among critically ill patients was 23% less in patients receiving a contrast agent (adjusted odds ratio=0.786 (95% CI = 0.678-0.870)). A subset of 12,572 patients on mechanical ventilation was also examined (n=6,250 nTTE and n=6,322 cTTE). Two-day mortality rates were 6.11% (n=382 deaths) for nTTE, and 4.59% (n=290 deaths) for cTTE ($p=0.0001$).

Conclusion: In comparison with nTTE, cTTE is associated with higher short term survival in critically ill patients, including patients requiring mechanical ventilation.

3:30 p.m.

1027-266

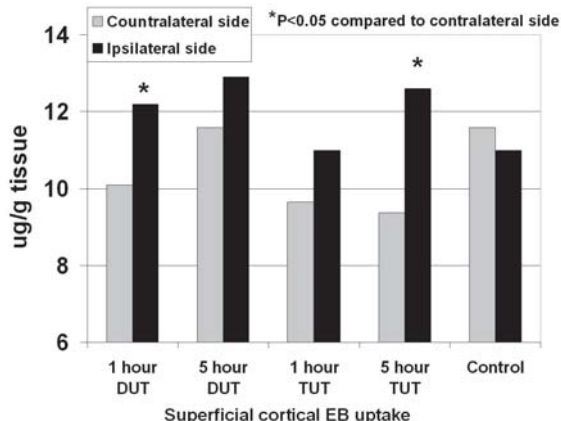
Transtemporal Ultrasound-Induced Alterations in Blood Brain Barrier Permeability During an Intravenous Microbubble Infusion

Feng Xie, John Lof, Terry Matsunaga, Reena Zutshi, Evan Unger, Thomas R. Porter, University of Nebraska Medical Center, Omaha, NE

Background: Although diagnostic (DUT) and therapeutic ultrasound (TUT) transducers combined with intravenous (IV) microbubbles (MB) have been utilized to target drug delivery, their ability to create therapeutic effects in transcranial diseases is unknown due to attenuation and scattering across temporal bone.

Methods: In 12 pigs, blood brain barrier (BBB) permeability was examined following 30 minutes of transtemporal ultrasound using either a DUT (Siemens 1.5 MHz; <1% duty cycle; 1.9 mechanical index or MI) or a TUT (1 MHz, Richmar; 10% duty cycle; 1.0 MI). MB (ImaRx Therapeutics) were administered as a 3% continuous IV infusion. A low MI pulse sequence detected when MB were traversing the capillary bed and guide delivery of high MI impulses from either transducer. Evans Blue (EB) uptake was measured at one and five hours post insonation within superficial and deep cortex bilaterally. **Results:** Superficial ipsilateral EB uptake was increased with DUT at one hour after insonation (Graph), but not at five hours. EB uptake with the DUT was also increased in the deep cortex at one hour ($p<0.05$ compared to contralateral). With the TUT, increased uptake was only in superficial cortex and persisted at five hours. Contralateral EB uptake was not different than control pigs.

Conclusions: Guided high MI impulses from a DUT can transiently alter BBB permeability in both superficial and deep locations of the cortex. This may be a method of non-invasive targeted drug delivery in degenerative or metastatic brain disease.



3:30 p.m.

3:30 p.m.

1027-267

Contrast-Enhanced Ultrasound Assessment of Microvascular Responses to Anti-VEGF Therapy: An Investigation of the Pathophysiologic Basis for Hypertension Associated With Antiangiogenic Therapy

Todd Belcik, Qi Yue, Beat Kaufmann, Weihui Shentu, Sherry Bullens, Ganesh Koluman, Stuart Bunting, Jonathan Lindner, Oregon Health & Sciences University, Portland, OR, Genentech, Inc., South San Francisco, CA

Background: Anti-angiogenic therapy with vascular endothelial growth factor (VEGF) inhibitors is increasingly used in cancer treatment. Major adverse effects of anti-VEGF therapy are hypertension and ischemic complications. The aim of this study was to determine whether hypertension during anti-VEGF therapy is secondary to diffuse peripheral microvascular rarefaction.

Methods: We studied 20 wild-type (WT) mice and 20 mice with atherosclerosis produced by double knockout (DKO) of the LDL receptor and Apo-B mRNA editing peptide. Echocardiography and contrast ultrasound assessment of microvascular blood volume (MBV) and flow (MBF) in the myocardium and limb skeletal muscle were performed at baseline (10 wks of age) and after 5 wks of therapy with a functional blocking anti-VEGF-A monoclonal antibody (AVA) or vehicle (1:1 randomization). Skeletal muscle MBF decrease during contractile exercise and left heart catheterization for hemodynamics were performed. In an additional 7 WT mice, ambulatory BP monitoring was performed weekly during AVA treatment.

Results: After therapy, mean arterial and LV systolic pressure were 15-20% greater ($p < 0.05$) in WT and DKO mice receiving AVA compared to placebo. Ambulatory monitoring indicated that BP increased by 2 wks of anti-VEGF therapy. After controlling for treatment group, there were no differences in pressures between WT and DKO mice. Hypertension in the AVA group was associated with a higher aortic stiffness index (4.8 ± 1.9 vs 8.5 ± 3.6 , $p = 0.006$), an increase in LV wall thickness (0.65 ± 0.11 vs 0.75 ± 0.12 mm, $p = 0.001$), and decrease in E' velocity (13.7 ± 4.4 vs 9.9 ± 3.8 cm/s, $p = 0.003$). There were no significant changes in skeletal muscle or myocardial MBF or MBV, or MBF reserve in any of the treatment groups. Microvascular density on histology was similar among all groups. After 5 weeks, plasma angiotensin-II levels were higher in AVA vs. control group.

Conclusions: Hypertension complicating anti-VEGF therapy is not secondary to anatomic or functional microvascular rarefaction. The rapid increase in BP and development of secondary hypertrophy and reduced aortic compliance suggest activation of neurohormonal pathways as an alternative mechanism.

3:30 p.m.

1027-268

Safety of Contrast Agents During Stress Echocardiography in Patients With High Right Ventricular Systolic Pressure: A Study of 16,434 Patients

Sahar S. Abdelmoneim, Mathieu Bernier, Christopher G. Scott, Abhijeet Dhole, Stuart Moir, Robert B. McCully, Patricia A. Pellikka, Sharon L. Mulvagh, Mayo Clinic, Rochester, MN

Background: Microbubble safety concerns led to changes in product recommendations in patients (pts) with pulmonary hypertension. Pulmonary artery systolic pressure equals right ventricular systolic pressure (RVSP) in absence of pulmonary obstruction. We evaluated short and long-term safety in pts with increased RVSP undergoing clinical stress echo (SE) with and without contrast

Methods: From 11/03 -12/07 we studied 26,774 SE pts. RVSP was measured in 16,434 pts: 10,270 (63%) had no contrast, 6,164 (38%) contrast (Optison or Definity). Short-term (<72 hrs, <30 days) & long-term (0.1 - 4.3 years) endpoints were death & myocardial infarction (MI). RVSP analysis at levels ≥ 35 , >50 & ≥ 60 mmHg was done. Cox regression models were used

Results: Contrast-SE cohorts were older (67 ± 12 vs 64 ± 14 yrs, $P < 0.001$), male (53 vs 49%, $P < 0.001$) & with positive SE (35 vs 30%, $P < 0.001$) vs no contrast-SE, Table. Short-term events for contrast & no contrast-SE cohorts were comparable. For RVSP ≥ 50 mmHg, there was no significant difference in long-term events in contrast vs no contrast-SE cohorts [adjusted hazard ratio (HR 95% CI): death = 1.1 (0.8, 1.5), $P = 0.56$; MI = 0.34 (0.11, 1.0), $P = 0.06$ and combined = 1.01 (0.75, 1.3), $P = 0.94$]. Similarly RVSP ≥ 35 & ≥ 60 mmHg showed no significant differences for all endpoints [HR=1.02 (0.85, 1.2), $P = 0.85$ and 0.94 (0.55, 1.6), $P = 0.82$] for combined events, respectively)

Conclusions: Microbubble use in SE is not associated with increased risk of death/MI in pts with increased resting RVSP up to 60mmHg

Demographics & short-term events in 16,434 SE pts stratified by RVSP from Nov 2003-Dec 2007

Variable	RVSP > 50 mmHg (N=1,025)			RVSP < 50 mmHg (N=15,409)		
	Contrast (N=414)	No Contrast (N=611)	P-value	Contrast (N=5750)	No Contrast (N=9659)	P-value
Dobutamine Exercise	363(88%) 51(12%)	467(76%) 144(24%)	<0.001 <0.001	3410(59%) 2340(41%)	3596(37%) 6063(63%)	<0.001 <0.001
Age, years	73.8 \pm 10	73.3 \pm 12	0.57	67 \pm 12	64 \pm 14	<0.001
Males	210(51%)	287(48%)	0.24	3081(54%)	4777(50%)	<0.001
BMI, kg/m2	31 \pm 7	27 \pm 6	<0.001	31 \pm 6	27 \pm 5	<0.001
Diabetes	141(34%)	167(28%)	0.04	1381(24%)	1280(14%)	<0.001
Hypertension	324(79%)	463(78%)	0.81	3980(69%)	5282(56%)	<0.001
Hyperlipidemia	290(70%)	350(59%)	<0.001	3937(69%)	5645(59%)	<0.001
Prior Myocardial Infarction	89(22%)	106(18%)	0.14	763(13%)	854(9%)	<0.001
Prior Coronary Bypass	88(21%)	102(17%)	0.09	795(14%)	686(7%)	<0.001
Death \leq 72 hrs after SE	0(0.0%)	0(0.0%)	--	0(0.0%)	2(0.0%)	0.28
Death \leq 30 days of SE	0(0.0%)	10(2%)	0.72	18(0.3%)	28(0.3%)	0.80
MI \leq 72 hrs after SE	0(0.0%)	2(0.3%)	0.24	4(0.1%)	3(0.0%)	0.28
MI \leq 30 days of SE	1(0.2%)	2(0.3%)	0.80	9(0.2%)	12(0.1%)	0.60

1027-269

Development and In Vivo Testing of a Novel Microbubble Agent Capable of Both Gene Payload Delivery and Microvascular Targeting: Implications for Site-Specific Transfection

Aris Xie, Todd Belcik, Shivam Champinieri, Qi Yue, Weihui Shintu, Sarah Taylor, Jonathan Lindner, Oregon Health & Sciences University, Portland, OR, University of Virginia, Charlottesville, VA

Background: Ultrasound mediated gene delivery (UMGD) with microbubble (MB) vectors relies on controlled bioeffects caused by cavitation energy. Proximity of gene-laden MB to the vessel wall is a critical determinant of UMGD and could be optimized by targeting MBs to the endothelium. Our aim was to test the targeting efficiency of MBs designed for cDNA payload delivery.

Methods: In vitro attachment to plated streptavidin was assessed in a flow chamber (shear stress 0.6 and 1.5 dyne/cm²) using biotinylated cationic or neutral MB, with and without surface coupling of plasmid cDNA. Intravital microscopy was used to evaluate in vivo vascular attachment of ICAM-1-targeted cationic MB, with and without cDNA in TNF- α -stimulated murine cremaster muscle. For imaging studies, contrast ultrasound imaging of the hindlimb of mice after brief (10 min) ischemia and reperfusion (30 min) was used to assess attachment of P-selectin-targeted cationic MB, with and without cDNA.

Results: On quantitative fluorometry, the amount of cDNA charge-coupled to cationic MB was not affected by the presence of targeting moiety (≈ 0.04 pg/MB). *In vitro* flow chamber studies demonstrated that attachment efficiency for cationic biotinylated MB with cDNA was higher than without cDNA (141 ± 19 vs 58 ± 14 mm², $p < 0.01$), and was similar to neutral biotinylated MB (140 ± 22 mm²). On intravital microscopy, attachment of ICAM-1-targeted cationic MB to inflamed venules was similar for MB with and without surface coupling of cDNA (≈ 130 mm² for both agents) with minimal attachment for non-targeted preparations (< 5 mm²). Imaging of post-ischemic hindlimb skeletal muscle demonstrated a 4-fold increase in the retention fraction of cationic P-Selectin-targeted compared with control non-targeted cationic MB. Signal for P-selectin targeted MB was similar for preparations with and without surface coupling of cDNA (36 ± 22 vs 36 ± 14 AU, $p = 0.983$).

Conclusions: The binding of plasmid DNA to cationic MBs does not interfere with the ability to target these agents to counterligands on the vascular endothelium. The ability to target MB to disease-related molecules may increase both efficiency and tissue specificity of UMGD.

3:30 p.m.

1027-270

Optimization of Targeted Microbubbles With Adhesive Dynamics Modeling

Timothy M. Maul, Michael T. Beste, Daniel A. Hammer, Drew D. Dudgeon, John S. Lazo, William R. Wagner, Flordeliza S. Villanueva, University of Pittsburgh, Pittsburgh, PA, University of Pennsylvania, Philadelphia, PA

Background: Ultrasound molecular imaging using targeted microbubbles (MB) is limited by low signal to noise ratios, partly due to relatively few MB binding events. To maximize MB binding to the endothelial cell (EC) target, we used computational modeling to define ideal MB designs incorporating the multivariate factors governing adhesion.

Methods: Adhesive Dynamics (AD) to model the stochastic interaction of leukocytes and ECs under fluid shear stress was used to calculate a MB optimized to bind via sialyl LewisX (sLe^x) and an ICAM-1 binding molecule to ECs overexpressing E-selectin and ICAM1, respectively. MB properties (radius [R_c], kinetics and densities of targeting ligand) and the intravascular physical environment (shear rate [SR] and E-selectin and ICAM1 density) were modeled. Kinetic rates for sLe^x:E-selectin interactions derived by surface plasmon resonance and estimated values for an anti-ICAM1 molecule were used.

Results: Firm adhesion (MB velocity < 2% of the free stream velocity) occurs readily for ligands with high on rates and is independent of radius at R_c > 0.4 μ m and SR < 900 s⁻¹ (Fig 1A). Decreasing the on rate shows a relationship between R_c and SR, where velocity is minimum at R_c = 1.5 μ m (Fig 1B).

Conclusions: AD defines optimal properties of currently available ligands and MBs and the kinetic parameters required for new targeting ligands. This approach may allow flexible, prospective design of MBs optimized for binding and enhance clinical translation of ultrasound molecular imaging.

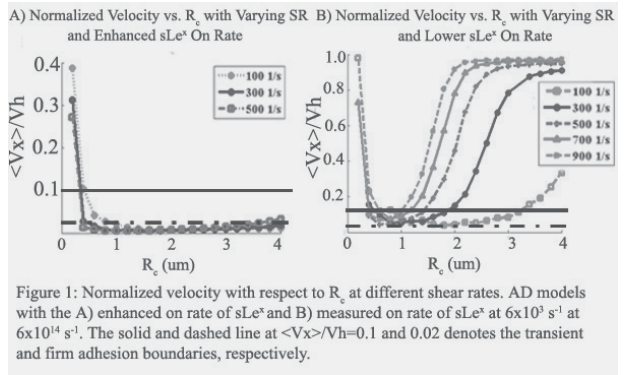


Figure 1: Normalized velocity with respect to R_c at different shear rates. AD models with the A) enhanced on rate of sLe^x and B) measured on rate of sLe^x at 6x10³ s⁻¹ at 6x10¹⁴ s⁻¹. The solid and dashed line at <Vx>/Vh=0.1 and 0.02 denotes the transient and firm adhesion boundaries, respectively.

3:30 p.m.

1027-271

Optison™ Does Not Increase Mortality in Critically Ill Patients: Preliminary Results From a Retrospective Matched Case-Control Study

Michael L. Main, Alex Exuzides, Chris Colby, Steven B. Feinstein, Jonathan H. Goldman, Anne Waaler, Paul A. Grayburn, Saint Luke's Mid America Heart Institute, Kansas City, MO, ICON Medical Imaging, Warrington, PA

Background: Due to serious cardiopulmonary reactions reported immediately following administration of perflutren containing contrast agents, the United States Food and Drug Administration (FDA) required a Black Box Safety warning for this class of agents including Optison™ (Perflutren Protein-Type A Microspheres Injectable Suspension, USP). FDA has requested a database analysis to compare in-hospital mortality in critically ill patients undergoing echocardiography with and without Optison. This study provides preliminary results of the retrospective analysis.

Methods: The study utilized the largest available hospital service-level database in the U.S. (Premier Perspective™, Charlotte, NC). Patients were characterized by diagnoses, dates of treatments, and outcomes. All adult patients undergoing inpatient echocardiography between Jan. 2003 and Oct. 2005 were identified (n=2,588,722 of which 22,499 received Optison). Of those administered Optison, 2,900 had diagnoses meeting defined criteria for critical illness (heart failure, acute myocardial infarction, arrhythmia, respiratory failure, pulmonary embolism, emphysema, and pulmonary hypertension). Outcomes for these patients were compared to 11,600 case-matched controls who received echocardiography without contrast. Controls were matched by level of care (e.g., intensive care unit or cardiac care unit), and mechanical ventilation status. Adjustments were made for demographic factors, hospital-specific factors, and co-morbidities using a conditional logistic regression model.

Results: Optison was not associated with an increase in same-day mortality (odds ratio=1.22, P=0.29) in critically ill patients. This was in spite of a higher Deyo-modified Charlson comorbidity index (P<0.0001) and incidence of coronary artery disease (P<0.0001) in Optison patients.

Conclusions: There is no increase in mortality in critically ill patients undergoing echocardiography with Optison compared to case-matched controls, despite the fact that Optison patients demonstrated greater comorbidity, including coronary artery disease.

3:30 p.m.

1027-272

Safety of Ultrasound Contrast Agents During Echocardiography in Patients With Pulmonary Hypertension

Rubin S. Gabriel, Yvonne M. Smyth, Richard A. Grimm, James D. Thomas, Venu Menon, Allan L. Klein, Ellen Mayer Sabik, Cleveland Clinic, Cleveland, OH

Background:

Despite the revision of the "Black Box" warning by the Federal Drug Administration (FDA) on the safety of ultrasound contrast agents in echocardiography, there remains concern the risk of serious cardiopulmonary reactions are increased in patients with pulmonary hypertension. This audit reviews the rate of adverse events in patients with underlying pulmonary hypertension receiving ultrasound contrast agents at the Cleveland Clinic.

Methods: All patients undergoing transthoracic (TTE) or exercise (ESE) or dobutamine (DSE) stress echocardiography who received perflutren based contrast agents at the Cleveland Clinic between 1998 and 2007 were included. Pulmonary hypertension was estimated from continuous wave Doppler interrogation of the tricuspid regurgitant jet. Mild-moderate pulmonary hypertension was defined as a right ventricular systolic pressure (RVSP) of 30-50 mmHg and severe pulmonary hypertension as an RVSP of greater than 50 mmHg. Serious adverse events were defined as: death within 24 hours of contrast administration and cardiac arrest, anaphylaxis and sustained ventricular arrhythmias within 30 minutes of contrast administration.

Results: 10010 patients received intravenous ultrasound contrast during echocardiography at the Cleveland Clinic between 1998 and 2007. An accurate measurement of RVSP was obtained in 3479 (35%) of patients. Mild pulmonary hypertension was documented in 1921 (19%) patients and severe pulmonary hypertension in 346 patients (3%) patients. 60% of patients received Definity, 37% Optison and 3% were unknown. There were 1514 TTE, 399 ESE and 354 DSE performed with contrast in patients with pulmonary hypertension. There was no death within 24 hours of contrast administration, no cardiac arrest, no anaphylaxis and no sustained ventricular arrhythmias noted in patients with pulmonary hypertension.

Conclusions: No serious adverse events were noted in 2267 patients with documented pulmonary hypertension who received ultrasound contrast agents during echocardiography over a 10 year period at the Cleveland Clinic. These findings have major implications to the revised black box warning by the FDA.

3:30 p.m.

1027-273

Registration of 3D Ultrasounds (US) of Carotid Endarterectomy (CEA) Specimens With Corresponding Magnetic Resonance Images (MRI)

Eric Y. Yang, Venkateshwar R. Polsani, Michael J. Washburn, William Zang, Anne L. Hall, Salim Virani, Christie M. Ballantyne, Joel D. Morrisett, Vijay Nambi, Baylor College of Medicine, Houston, TX

Background: Co-registration of images obtained from different imaging modalities is critical to directly comparing modalities. We compared ultrasound (US) and MR images of CEA specimens using a novel position sensing technology that uses an electromagnetic

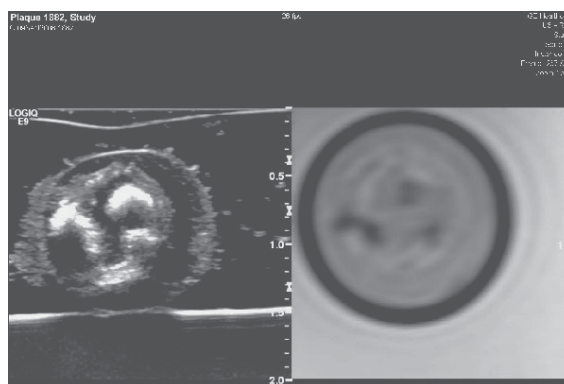
(EM) transmitter placed near the scan area and a pair of EM sensors attached to a bracket connected to the US transducer. Both the transmitter and sensors in turn connect to a position sensing unit embedded in the US machine.

Methods: After imaging 11 CEA specimens with 3.0 Tesla EXCITE GE MRI scanner, images were loaded on a Logiq E9 3D (GE Healthcare) US system. The US and MRI images were registered (figure) by identifying 2-3 common points. The position sensors then mapped the US position to multiplanar reconstructed MR images using a transformation matrix.

To verify registration, 2 observers jointly recorded 2-3 fiducial markers for each CEA sample on MRI and noted the frame numbers; they then identified the same frames on US, blinded to the MRI frame numbers.

Results: There was a mean of 21 (SE 2.3) frames per MRI slice. The mean difference over 27 registration markers between MR and US images for observers 1 and 2 was 7.6 frames (SE 1.3) and 5.7 frames (SE 1.1) respectively. Of 27 markers, only 2 of 54 were outside the same MRI slice (inter-observer reliability 93%).

Conclusions: Accurate co-registration between US and MRI is feasible. This technology should be applicable to other imaging modalities and has significant clinical and research applicability.



3:30 p.m.

1027-274

Comparison of Velocity Vector Imaging and a Prototype Radiofrequency-based Speckle Tracking Echocardiography System to Tissue Doppler-based Strain Imaging

Theodore J. Kolias, Nicole M. Kline, Lingling Zhang, Matthew O'Donnell, James D. Hamilton, University of Michigan, Ann Arbor, MI

Background: Conventional strain imaging has relied on tissue Doppler (TDI) for determination of strain. Velocity vector imaging (VVI) is a newer non-Doppler method for measuring strain, but data comparing it to TDI are lacking. In this study, we compared VVI to TDI for measurement of longitudinal strain (ϵ). In addition, we also compared a prototype radiofrequency-based speckle tracking system (RF) to TDI and VVI for measurement of ϵ . This prototype operates at a high frame rate of 100 frames/sec and uses the signal phase information from the RF-signal to improve tracking quality.

Methods: 20 subjects (age 55 ± 16 , 40% female) underwent echocardiography using color TDI and VVI (Siemens Sequoia), and RF-based speckle tracking using the prototype system (Pixel Velocity, Inc). Longitudinal ϵ was measured offline in 18 segments derived from 3 standard apical views using each modality (n=360 segments). Pearson's correlation testing was used to compare the different modalities for measurement of ϵ .

Results: Longitudinal ϵ could be measured in 64% of segments using TDI, 98% using VVI, and 89% using the RF prototype. VVI- ϵ did not have a significant correlation with TDI- ϵ ($r = 0.024$; $p = 0.713$). RF- ϵ had a modest but significant correlation with TDI- ϵ ($r = 0.172$; $p = 0.012$). There was also a mild correlation between RF- ϵ and VVI- ϵ ($r = 0.138$; $p = 0.014$).

Conclusions: Longitudinal strain measured by VVI did not significantly correlate with TDI-derived strain, whereas strain measured from the RF-based prototype had a modest correlation with TDI-derived strain. These data suggest that further development and validation of these techniques are needed before they are ready for widespread clinical application. RF-based speckle tracking for measurement of strain appears feasible, however, and may be a step in the right direction.

3:30 p.m.

1027-275

Utility of Tissue Doppler and Strain Imaging in the Early Detection of Trastuzumab and Anthracycline Mediated Cardiomyopathy

Davinder S. Jassal, Song-Yee Han, Anita Sharma, Tielan Fang, Roien Ahmadi, Matthew Lytwyn, Andrew Czarnecki, Tarek Moussa, Pawan K. Singal, University of Manitoba, Winnipeg, MB, Canada

Background: Trastuzumab (Trast) provides considerable therapeutic benefits in the adjuvant setting of breast cancer. Its use however is limited by an elevated incidence of cardiotoxicity when used in combination with doxorubicin (Dox). Although Myocet (liposomal encapsulated doxorubicin) is less cardiotoxic, its cardiac safety profile with Trast has not been thoroughly evaluated.

Objective: To determine if early sensitive indices of left ventricular (LV) dysfunction, specifically tissue Doppler imaging (TDI), would be useful for addressing the cardiotoxic

effects of Trast in combination with either conventional Dox or Myocet.

Methods: In an acute murine model of chemotherapy induced cardiomyopathy, wild-type C57Bl/6 mice (n=55) received one of the following drug regimens intraperitoneally; i) Control; ii) Dox; iii) Myocet; iv) Trast; v) Dox+Trast; or vi) Myocet+Trast. TDI-derived peak endocardial systolic velocity (Vendo), strain rate (SR), and LV ejection fraction (EF) were measured serially for five days. On day 5, the hearts, lungs and livers were removed for histopathological and Western blot analyses.

Results: Mice treated with Myocet+Trast demonstrated minimal cardiotoxicity in comparison to Dox alone or Dox+Trast. Progressive LV dilatation and LV systolic dysfunction was observed by day 4 of treatment with Dox+Trast, as compared to preserved LVEF in the remaining groups. TDI parameters decreased within 24 hours in the Dox alone or Dox+Trast groups and predicted early mortality. There was a significant increase in the proapoptotic index (Bax/Bcl ratio) in the Dox+trastuzumab group as compared to the other groups. The survival rate was only 20% at day 5 of the experiment in the Dox+Trast group, whereas 100% of mice receiving Trast, Myocet or Myocet+Trast survived the 5 days.

Conclusion: TDI can detect early LV dysfunction prior to alterations in conventional echo indices and predicts early mortality in mice receiving Dox+Trast as compared to Myocet+Trast. The latter combination is a relatively safer in an acute model of chemotherapy induced cardiotoxicity.

3:30 p.m.

1027-276

The Usefulness of Myocardial Tissue Doppler Imaging to Distinguish Right Ventricular Volume Overload From Right Ventricular Pressure Overload

Tomoko Tani, Atsushi Kobori, Koichi Tamita, Makoto Kinoshita, Natsuhiko Ehara, Shuichi Kaji, Atsushi Yamamoto, Shigefumi Morioka, Yutaka Furukawa, Kobe City Medical Center General Hospital, Kobe, Japan

Background: Tissue Doppler imaging (TDI) has provided new insight into right ventricular (RV) function assessment. Recent study only suggested that RV-myocardial performance index and RV-TDI were useful to differentiate RV pressure overload from volume overload. The objective of this study was to evaluate the effects of TDI parameters in the differential diagnosis between RV volume and pressure overloads.

Methods: Patients with primary pulmonary arterial hypertension (RV-pressure-overload group: Group A, n=14) and patients with atrial septal defects (RV-volume-overload group: Group B, n=14) have been subjected to this study. Pulsed TDI sample of the RV was obtained at the basal segment of the tricuspid annular lateral wall in a four-chamber view. Optimum parallel Doppler angle was maintained during TDI acquisition. A peak systolic TDI velocity (S), transtricuspid early diastolic wave (Ea) and the wave of atrial contraction (Aa) were measured. Left ventricular (LV) diastolic and systolic dimension (LVDd, LVDs), were measured. LV end-diastolic and end-systolic volume (EDV, ESV) and ejection fraction (EF) were measured by modified Simpson's method. Right ventricular systolic pressure (RVp) was estimated by Doppler echocardiography.

Results: As shown in Tables. S-TDI velocity of Group A was significantly lower than that of Group B.

Conclusion: TDI measurements of tricuspid annulus may be useful to differentiate RV pressure overload from volume overload.

	Group A	Group B	p-value
LVDd (cm)	4.1 ± 0.7	4.1 ± 0.4	0.87
LVDs (cm)	2.4 ± 0.7	2.5 ± 0.4	0.54
EDV(ml)	57 ± 20	59 ± 16	0.82
ESV(ml)	22 ± 9	20 ± 6	0.53
EF(%)	63 ± 8	65 ± 4	0.38
E/A	1.1 ± 1.0	1.1 ± 0.6	0.96
RVp (mmHg)	60 ± 22	41 ± 11	0.02
S (cm/s)	10.4 ± 1.7	16.3 ± 4.1	<0.0001
Ea (cm/s)	10.1 ± 4.3	13.7 ± 3.2	0.02
Aa (cm/s)	13.2 ± 2.9	16.3 ± 4.2	0.04

3:30 p.m.

1027-277

Comparison of Magnetic Resonance with Intravascular Ultrasound and With Pathology in Coronary Arteries Segments of Human Hearts

Luiz A. Machado Cesar, Everli P. Gomes, Pedro A. Lemos Neto, Paulo S. Gutierrez, Miguel A. Moretti, Jose A. Franchini Ramires, Carlos E. Rochitte, Heart Institute (Incor), University of Sao Paulo Medical School, Sao Paulo, Brazil

Background: Magnetic resonance (MR) may be the method of choice to evaluate coronary arteries (CA) in the future. So, we aimed to evaluate its capability to identify and measure arteries wall and lumens, in comparison with intravascular ultrasound (IVUS) and pathology (PAT) in human CA.

Methods: We selected 13 consecutive hearts from individuals died of acute coronary syndromes. Hearts were injected with 10% formalin into both right and left CA, under 80 mmHg. After, the right, the left anterior descending and left circumflex arteries were dissected and both ostia and part of the aorta wall were preserved. Specimens were studied first with IVUS; then at MR, and lastly the PAT study was performed. We have made three measures at each cm, in each of the first three cm of all three CA. Some were lost due to technical problems, so we studied 38 arteries (355 segments). The following measures were obtained: total area of artery (TAA), luminal area (LA), maximum artery

diameter(MxAD), minimum artery diameter(MiAD), Mx and Mi lumen diameter (MxLD, MiLD) and Mx and Mi wall thickness (MxWT, MiWT). Statistics: We did correlations of Pearson and Bland Altman.

Results: only 22 arteries (187 segments) were submitted to IVUS because of occluded arteries; MR was realized in all 38 (218 segments); and 107 segments were evaluated by all three methods. Considering MR and IVUS, the better correlations obtained were for: TAA (r=0.84, p<0.001, n=112), LA (r=0.77, p<0.001; n=107), MaxAD (r=0.73, p<0.001; n=107) and MiAD (r=0.64, p<0.001; n=107). Correlations of MR with PAT were lower for the same variables, except for LA (r=0.80, p<0.001; n=207). However, MR compared with PAT overvalued the TAA and the MiAD, respectively (15.46 ± 4.83 vs 11.87 ± 4.57; 4.23 ± 0.73 vs 3.48 ± 0.70; p<0.001 n=110). The best correlation for TAA was IVUS with MR in the left anterior descending (r=0.89, p<0.001, n=25).

Conclusions: Compared to pathology, both image techniques overestimate areas and lumens but MR images is very close to that of IVUS to visualize arterial wall and lumen.

3:30 p.m.

1027-278

Can Two-Dimensional Strain Imaging Determine Changes In Left Ventricle Wall Motion With Simulated Dyssynchrony Between the Left and Right Ventricles?

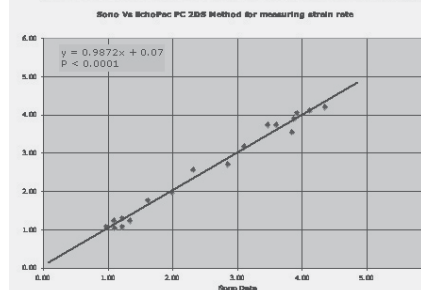
Ethan Muldoon, Ana Badua, Cong Tin P. Le, Cole Streiff, Galym Imanbayev, Sydney Prescott, Rohini Deb, Minjuan Zheng, Pengyuan Zhang, Xiaokui Li, David J. Sahn, Oregon Health & Science University, Portland, OR

Background: Our study aimed to compare the wall motion in the left ventricle (LV) between simulated synchronized and dyssynchronized LV and right ventricle (RV) pump settings in a dynamic biventricular model using a 2D speckle tracking method.

Methods: Dissected pig hearts were used to simulate the human heart. Two balloons were added separately to each ventricle. The two balloons were connected to two separate pulsatile pumps. Five stroke volumes (30-50 ml/beat) were studied in synchronized and dyssynchronized settings. For dyssynchrony, the RV was pumped to begin 20%-30% of cycle length before the LV. Three sonomicrometry (sono) crystals were inserted near the base of the LV free wall. Sono data was recorded at baseline and each hemodynamic stage to obtain reference longitudinal strain. Echo scanning was performed with a GE Vivid 7 (7 MHz). Data was analyzed with EchoPac PC 2D strain (2DS) for circumferential strain on the LV free wall. This data was also compared with sono data.

Results: Mean global LV circumferential strain rate derived by 2DS decreased a mean of 0.27/sec, an exaggerated change of -10.1% ± 3% when the RV was pumped first. Linear regression between sono measurement and 2DS showed good correlation (P < 0.0001, r = 0.97).

Conclusion: In our study, the model revealed interventricular mechanics of dyssynchrony, and the 2DS method was accurate and detected mechanical changes associated with dyssynchrony.



3:30 p.m.

1027-279

Detection of Myocardial Ischemia Using a New Technique of Transthoracic Tissue Doppler Imaging: DADI

Rei Yajima, Nobusada Funabashi, Miyuki Kawakubo, Maiko Takahashi, Kwangho Lee, Akihisa Kataoka, Yoshio Kobayashi, Issei Komuro, Chiba University, Chiba, Japan

Background: In the initial phase of the ischemic myocardium, delay of dilation of the left ventricular (LV) myocardium occurs and post systolic shortening (PSS), which indicates diastolic abnormality in isometric relaxation period, may be present. Using Displacement by tissue Doppler imaging (TDI), we evaluated the utility of a new technique, "DADI (detection of diastolic abnormality by displacement Imaging)" which evaluates PSS at

rest without any loads for detection of myocardial ischemia.

Methods: Consecutive subjects (19 male, mean 66.7 yrs) referred with chest pain underwent TDI (Aplo, Toshiba) at rest with no loads. Cross sectional LV images at 2, 3, and 4 chamber views from apical LV were divided into 16 segments by AHA classification, and peak phases of Displacement at each sample volume were detected, time from end-systole to peak phase on Displacement was measured, and presence of PSS was defined as time of more than 70msec. Among sample volumes supplied by each coronary artery, the cite with PSS in at least one segment was diagnosed as positive myocardial ischemia in DADI and compared with significant stenosis in conventional coronary angiogram (CAG) performed soon after TDI.

Results: Among the 304 segments, 6 were excluded due to poor measurements. Of the remaining 298 segments, 113 were diagnosed as significant stenosis in DADI with sensitivity 42%, specificity 81%, positive predictive value (PPV) 89% and negative predictive value (NPV) 25% in comparison with CAG. Among 128 segments supplied by left anterior descending branch, 51 were stenotic in DADI with sensitivity 43%, specificity 74%, PPV 86% and NPV 74%. Among 94 segments supplied by left circumflex, 30 were stenotic in DADI with sensitivity 35%, specificity 79%, PPV 87% and NPV 23%. Among 76 segments supplied by right coronary artery (RCA), 32 were stenotic in DADI with sensitivity 48%, specificity 100%, PPV 97% and NPV 27%.

Conclusions: In the subjects referred with chest pain, specificities and PPV for detecting significant stenosis in DADI compared with CAG were high, especially in RCA. Detection of PSS using Displacement by TDI may provide a non invasive diagnosis of myocardial ischemia without any loads with high specificity and PPV.

3:30 p.m.

1027-280 Transmural Gradient in Myocardial Deformation Revealed by a Multi-layer Approach Using Advanced Two-Dimensional Speckle Tracking Echocardiography

Cheuk-man Yu, Qing Zhang, Fang Fang, Yu-jia Liang, Jun-min Xie, Yue-yi Wen, Gabriel WK Yip, Joseph YS Chan, Jeffrey WH Fung, The Chinese University of Hong Kong, Hong Kong SAR, Hong Kong

Background: Two-dimensional (2D) speckle tracking echocardiography detects myocardial deformation based on grayscale B-mode images and hence allows angle-independent assessment on various components. Recently, a new offline system also provides a multi-layer approach which helps to observe if transmural gradient exists.

Methods: The study enrolled 80 subjects of 4 groups (n=20 in each): group 1, normal controls; group 2, acute coronary syndrome (ACS) with ejection fraction (EF) >45%; group 3, right ventricular apical (RVA) pacing with EF >45%; and group 4, heart failure with EF <45% (SHF). Mean circumferential strain (ϵ -circum) and torsion (Tor) in subendocardial and subepicardial layer was assessed by QLab 6.0, Philips.

Results: The subendocardial and subepicardial deformation had a good linear correlation in both ϵ -circum ($r=0.955$, $p<0.001$) and Tor ($r=0.939$, $p<0.001$). However, in each group, a transmural gradient was also revealed in ϵ -circum and Tor, with higher values in the subendocardium (Table). Moreover, within the normal, ACS, RVA pacing and SHF group, a 27%, 30%, 28% and 25% transmural difference in ϵ -circum was consistently existed, whereas the figures were 22%, 25%, 24% and 10% for Tor which showed a lesser degree in SHF. When compared to the others, SHF also had a marked reduction in ϵ -circum and Tor in both layers.

Conclusion: A transmural gradient of circumferential strain and torsion exists in normal and disease conditions, even when cardiac function become significantly reduced.

1

Parameters	Normal	ACS	RVA pacing	SHF
ϵ -circum, subendocardial, %	-25.7 \pm 4.1	-24.1 \pm 4.6	-22.3 \pm 6.6†	-10.6 \pm 3.2‡\$Δ
ϵ -circum, subepicardial, %	-18.7 \pm 3.8*	-16.9 \pm 4.0*	-15.9 \pm 4.7**	-7.9 \pm 2.4*‡\$Δ
Tor, subendocardial, degree	13.9 \pm 5.6	14.9 \pm 3.6	13.5 \pm 5.8	5.6 \pm 3.4‡\$Δ
Tor, subepicardial, degree	10.9 \pm 4.6*	11.3 \pm 3.4*	10.2 \pm 4.4*	4.8 \pm 3.2*‡\$Δ

* $p<0.05$ vs subendocardial layer.

† $p<0.05$, ‡ $p<0.001$ vs normal; \$ $p<0.001$ vs ACS; Δ $p<0.001$ vs RVA pacing.

2

3:30 p.m.

1027-281 Impact of Infarct Transmurality on Layer Specific Impairment of Myocardial Function: A Myocardial Deformation Imaging Study

Michael Becker, Jan Balzer, Harald Kuehl, Malte Kelm, Rainer Hoffmann, Cardiology Department, Aachen, Germany

Background. To evaluate deformation parameters of an endocardial, mid-myocardial and epicardial myocardial layer in different transmuralities of myocardial infarction and assess whether layer specific deformation analysis allows definition of infarct transmuralities.

Methods. 56 patients (mean age 55 \pm 9 years, 38 men) with chronic ischemic left ventricular dysfunction underwent 2D echocardiography and ceMRI. The extent of myocardial infarction was determined as relative amount of hyperenhancement by ceMRI in a 16 segment LV model (0%: no infarction, 1-50% non-transmural infarction, 51-100%: transmural infarction). Based on 2D echocardiographic parasternal short axis views peak systolic circumferential strain was determined for the total wall thickness and for each of three myocardial layers (endo-, mid-myo- and epicardial) using an automatic frame-by-frame tracking system of acoustic echocardiographic markers (EchoPAC, GE Ultrasound).

Results. In non-transmural infarction impairment of circumferential strain was greater in the endocardial than the epicardial layer, relative decrease 45% vs. 28% ($p<0.001$), respectively, compared to control segments. In transmural infarction additional impairment of circumferential strain was greater in the epicardial than the endocardial layer, relative decrease 28% vs. 8% ($p<0.001$), respectively, compared to non-transmural infarction. Endocardial layer circumferential strain allowed distinction of non-transmural vs. no infarction with higher accuracy than total wall thickness strain (AOC 0.842 vs. 0.774, $p=0.005$). Epicardial layer circumferential strain allowed distinction of transmural from non-transmural infarction with higher accuracy than total wall thickness strain (AOC 0.819 vs. 0.762, $p<0.001$).

Conclusions. Non-transmural infarction results in greater functional impairment of the endocardial than of the epicardial myocardial layer. In transmural infarction both layers are affected similarly compared to controls. A layer specific analysis of myocardial deformation allows accurate discrimination between different transmuralities categories of myocardial infarction.

3:30 p.m.

1027-282

Use of Strain and Strain Rate Imaging in the Assessment of Regional Right Ventricular Deformation: A Study in Adult Unoperated Patients With Marfan Syndrome

Anatoli Kiotsekoglou, George R. Sutherland, James C. Moggridge, Venedictos Kapetanakis, Bart H. Bijnens, Michael J. Mullen, Dariush K. Nassiri, John Camm, Anne H. Child, St. George's, University of London, London, United Kingdom

Background: Marfan syndrome (MFS) is an inherited connective tissue disorder caused by mutations in the fibrillin-1 gene that encodes for the protein fibrillin-1. Fibrillin-1 has been identified as a regulator of transforming growth factor- β (TGF- β) bioactivity in the extracellular matrix. TGF- β dysregulation has been linked to reduced left ventricular (LV) stroke volume in the MFS mouse model. LV dysfunction has also been demonstrated in humans but little attention has been paid to the right ventricle (RV). We aimed to assess RV function in adult unoperated MFS patients.

Methods: Forty-three MFS patients, 25 men and 18 women (mean age 30 \pm 12 years) and 49 controls without significant differences in age, sex and body surface area, were studied. No patient had more than mild tricuspid regurgitation. All subjects underwent an echocardiographic examination at rest. Dp/Dt was measured for all patients. 2D colour Doppler data was recorded using a 4-chamber apical view to evaluate longitudinal systolic strain/strain rate (ϵ SYS/SRsys) in the RV free lateral wall. Diastolic strain rate was also assessed in the same region. Measurements were averaged over 3 consecutive cardiac cycles.

Results: Values are presented as mean \pm SD. Dp/Dt values were significantly lower in MFS patients compared to controls (746.79 \pm 322.34 mmHg vs 1086.20 \pm 226.57 mmHg, $p<0.001$). Both longitudinal ϵ SYS and SRsys were significantly reduced in the basal, mid- and apical segments of RV free lateral wall in MFS patients when compared to controls ($p<0.001$). Diastolic strain rate values were also significantly lower in the MFS group ($p<0.001$). In a multiple regression analysis including age, sex, heart rate and pulmonary systolic pressure, MFS was negatively associated with reduced RV free lateral wall regional deformation ($p<0.001$).

Conclusion: These findings showed reduced regional RV systolic and diastolic deformation in MFS patients. This could be attributed to fibrillin-1 deficiency in the cardiac extracellular matrix. Treatment may need to be tailored to prevent further deterioration by supporting RV function.

3:30 p.m.

1027-283

High Resolution Echocardiography May Be Used to Monitor the Response to Cardiotoxic Medication: Two-Dimensional Strain Studies in Open-Chest Instrumented Pigs

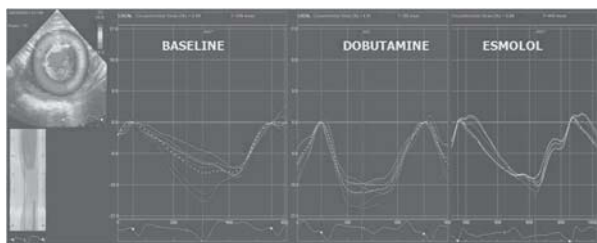
Muhammad Ashraf, Wei Zhou, Elizabeth Sanchez, Jennifer Corniea, Aman Mahajan, David J. Sahn, Oregon Health & Science University, Portland, OR, University of California, Los Angeles, CA

Background: Dobutamine and beta blockers are commonly used in clinical practice with anticipated effects on heart function. With the introduction of speckle tracking methods, it is now possible to noninvasively assess left ventricular mechanics in detail. We studied the effect of these drugs in an open chest animal model.

Methods: In 7 open-chest adult pigs, high-resolution high frame rate apical and basal short-axis images were acquired directly from the heart surface with a 10 MHz VIVID 7 Dimension ultrasound system. Left ventricular pressure and dP/dt were obtained with a solid state catheter. After acquisition of baseline data, pigs were subjected to pharmacological interventions using escalating doses of dobutamine and then doses of esmolol. Both apical and basal short-axis images for each state were obtained and exported to EchoPac PC for offline analysis of cardiac mechanics using the speckle tracking method. Hemodynamic data was analyzed in custom software.

Results: Dobutamine increased maximum dP/dt by 30-50% and shortened the time to peak contraction ([circumferential strain] 31.35% \pm 2.65% to 18.90% \pm 3.35%) of the RR' interval, increased the period of sustained contraction at peak (16.45% \pm 1.60% to 38.90% \pm 3.5%). Esmolol decreased maximum dP/dt by 30-50% and increased the time to peak strain (52.90% \pm 3.5%) and decreased the time of sustained contraction (8.90% \pm 4.65%).

Conclusions: Speckle tracking analysis may provide a useful tool to monitor response to cardiotoxic medications.



3:30 p.m.

1027-284

The Impact of Arterial Stiffness on Ventricular Torsion and Global Strain Rate Assessed by Speckle Tracking Imaging in Patients With Hypertension

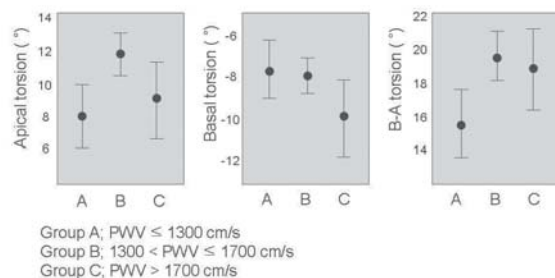
Soo-Jin Kang, Jungwon Hwang, Hong-Seok Lim, Byung-Joo Choi, So-Yeon Choi, Myeong-Ho Yoon, Gyo-Seung Hwang, Joon-Han Shin, Seung-Jea Tahk, Ajou university hospital, suwon, South Korea

Background: Ventricular-arterial coupling is a key determinant of cardiovascular performance. We studied how the arterial stiffening affects the myocardial function in hypertensive patients with normal EF.

Methods: In 63 patients with hypertension (47±14 years), brachial-ankle pulsed wave velocity (PWV) was measured. Using 2D-speckle tracking imaging, longitudinal and circumferential global strain rate (SRs, SRe) and ventricular torsion were obtained.

Results: PWV was significantly related to age, body mass index, systolic BP and pulse pressure. Moreover, PWV correlated with early diastolic SRe ($r=0.434$, $p<0.001$) on the longitudinal global SR curve and septal E' velocity ($r=-0.573$, $p<0.001$) as markers of relaxation abnormality. A linear correlation was found between PWV and basal torsion ($r=-0.433$, $p<0.001$), and basal-to-apical torsion ($r=0.331$, $p=0.008$), whereas the change in apical torsion showed biphasic pattern (Fig). In 49 patients with PWV <1700 cm/s, PWV was significantly related to apical torsion ($r=0.377$, $p=0.009$) and basal-to-apical torsion ($r=0.500$, $p<0.001$). On multivariate analysis, PWV ($\beta=0.668$, $p<0.001$), peak systolic SRs on the longitudinal global SR curve ($\beta=0.318$, $p=0.001$) and basal-to-apical torsion ($\beta=-0.208$, $p=0.030$) were independent determinants for E'/E' ratio.

Conclusions: Increased PWV correlated with impaired relaxation and high filling pressure. Compensatory increase of ventricular torsion may be diminished in advanced stage of arterial stiffening.



3:30 p.m.

1027-285

Effects of Myocardial Infarction and Reperfusion Therapy on Left Ventricular Rotational Mechanics

Gaetano Nucifora, Nina Ajmone Marsan, Victoria Delgado, Matteo Bertini, Jacob M. van Werkhoven, Eduard R. Holman, Hans-Marc J. Siebelink, Martin J. Schalij, Ernst E. van der Wall, Jeroen J. Bax, Leiden University Medical Center, Leiden, The Netherlands

Background: LV twist, defined as the net difference between counterclockwise rotation of LV apex and clockwise rotation of LV base during systole, is an important determinant of LV systolic function. In the present study we assessed the changes of LV twist after AMI and its relationship to global and regional LV systolic function, AMI site and efficacy of reperfusion therapy.

Methods: A total of 100 patients with a first ST-elevation AMI (59±11 years, 79% male) were included. All patients underwent primary PCI. 2D speckle tracking echocardiography was performed within 48 hours of PCI for the assessment of apical and basal rotation and LV twist. Immediately after, myocardial contrast echocardiography (MCE) with Perflutren was performed to evaluate post-AMI reperfusion. MCE perfusion was scored (1=normal; 2=reduced; 3=absent) on a 16 segment LV model; myocardial perfusion was considered incomplete when absence of perfusion involved ≥25% of the LV.

Results: LV EF, apical and basal rotation and LV twist were significantly lower among AMI patients, as compared to controls (48±10 vs. 61±7, $p<0.001$; 8.6±4.6 vs. 11.6±2.8, $p<0.001$; -5.1±2.8 vs. -6.8±2.7, $p=0.02$ and 13.0±5.1 vs. 17.7±2.1, $p<0.001$, respectively). LV EF, extent of wall motion abnormalities, infarct site (anterior vs. inferoposterior) and extent of absent perfusion were significantly related to LV twist ($r=0.73$, $p<0.001$; $r=0.65$, $p<0.001$; $r=-0.42$, $p<0.001$; $r=0.70$, $p<0.001$, respectively). Apical and basal rotation and LV twist among AMI patients with incomplete perfusion after primary PCI ($n=15$) were significantly lower as compared to the remaining AMI patients with complete perfusion

(2.8±2.0 vs. 9.7±4.1, $p<0.001$; -3.6±3.2 vs. -5.4±2.6, $p=0.02$ and 5.6±2.7 vs. 14.3±4.3, $p<0.001$, respectively).

Conclusions: LV twist is significantly decreased after AMI and is significantly related to global and regional LV systolic function, AMI site and efficacy of reperfusion therapy. Moreover, incomplete perfusion after PCI significantly widens the detrimental effects of AMI on LV twist and apical rotation.

3:30 p.m.

1027-286

Safety and Efficacy of XperSwing Dual-Axis Rotational Coronary Angiography Versus Standard Coronary Angiography

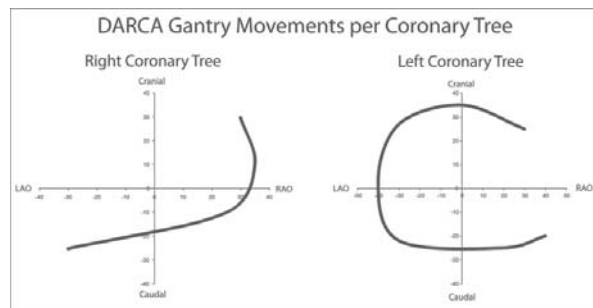
Andrew J. Klein, Michael S. Kim, Ivan P. Casserly, Onno Wink, S.Y. James Chen, John C. Messenger, Paul A. Hudson, Adam Hansgen, John D. Carroll, Joel A. Garcia, University of Colorado Denver, Aurora, CO

Background: Standard coronary angiography (SA) requires multiple angiographic acquisitions while rotational angiography (RA) employs the use of automated gantry acquisitions. RA uses 2 simple arcs (LAO to RAO with a fixed cranial or caudal angulation) for the left (cranial & caudal) and 1 of the right coronary tree. Dual-axis rotational coronary angiography (DARCA), named XperSwing is a novel acquisition method wherein the gantry automatically swings in a trajectory involving a constantly changing LAO/RAO and cranial/caudal angulation (Figure 1) permitting complete visualization of a coronary tree with a single injection. We sought to evaluate the safety and efficacy of DARCA vs. SA.

Methods: 15 patients underwent SA and DARCA for both coronary trees. Contrast, dose-area product (DAP) and time (mean ±SD) were recorded for each and compared using a Student's t-test. For DARCA, blood pressure, heart rate, symptoms and ectopy were recorded for each prolonged injection.

Results: DARCA significantly reduced the amount of contrast used (28.9±4.2 vs. 55.3±12ml; $p=0.0002$), radiation dose (23.9±6.3 vs. 38.5±11.7 Gy/cm2: $p=0.0003$) and procedural time (158.5±40.2 vs. 221.9±61.5 seconds; $p=0.0028$) when compared to SA. Neither significant hemodynamic changes nor the development of symptoms/ectopy occurred during DARCA.

Conclusions: DARCA is a novel, safe and effective angiographic acquisition technique which significantly reduces contrast, radiation exposure and procedural time when compared to SA.



3:30 p.m.

1027-287

Analysis of Left Ventricular Lead Position to Predict Success of Cardiac Resynchronization Therapy

Michael Becker, Ertunc Altioek, Christian Meyer, Patrick Schauer, Malte Kelm, Rainer Hoffmann, Cardiology Department, Aachen, Germany

Background: To evaluate whether myocardial deformation imaging during pure left ventricular (LV) pacing allows definition of the LV lead position with improved effectiveness of cardiac resynchronization therapy (CRT) on LV function and reverse remodeling.

Methods: In 56 patients (53±5 years, 34 men) undergoing CRT fluoroscopy and two myocardial deformation imaging based approaches were applied to determine the LV lead position in a 17-segment model. The myocardial deformation imaging based techniques relied on tracking of acoustic markers within 2D echocardiographic images to determine (1) the maximal temporal difference of peak circumferential strain before-to-on biventricular CRT and (2) the earliest peak systolic circumferential strain during LV pacing. At 12 months follow-up echocardiography was performed to determine improvement in LV function and remodeling. Optimal LV lead position was defined as concordance or immediate neighbouring of the segment with latest systolic strain prior to CRT and segment with assumed LV lead position. The modality with best predictive power for improvement in LV function and remodeling based on optimal definition of LV lead position was determined.

Results: LV lead position determined during LV pacing correlated to the position determined by fluoroscopy. Patients with optimal LV lead position defined during LV pacing had greater improvement in LV function and reverse remodeling than those with non-optimal LV lead position. Determination of the optimal LV position based on myocardial deformation imaging analysis during LV pacing showed the best discriminatory power for LV remodeling (13.86, $p<0.001$ vs. 6.63, $p=0.0551$ for biventricular pacing and 7.59, $p=0.0273$ for fluoroscopy) and improvement in ejection fraction (4.64, $p<0.0001$ vs. 3.03, $p=0.0723$ for biventricular pacing and 2.22, $p=0.0528$ for fluoroscopy).

Conclusions: Analysis of circumferential strain imaging during pure LV pacing allows determination of the LV lead position in CRT. Improvement in LV function and remodeling as indicator of optimal LV lead position can be best predicted by LV lead position analysis during LV pacing.

3:30 p.m.

1027-288

Reduced Left Atrial Function in Patients With Hypertension, Breathlessness and Normal Ejection Fraction

Frauke WG Wenzelburger, Yu Ting Tan, Eveline SP Lee, Grant Heatlie, Francisco Leyva, Michael P. Frenneaux, John E. Sanderson, Cardiovascular Medicine, University of Birmingham, Birmingham, United Kingdom, North Staffordshire University Hospital, Stoke on Trent, United Kingdom

Background: Hypertension is a risk factor to develop heart failure with normal ejection fraction (HFNEF). This is often combined with atrial fibrillation. Little is known about atrial function in patients with HFNEF who are still in sinus rhythm (SR). We hypothesize that these patients have reduced atrial function and this is unmasked on exercise.

Methods: 40 hypertensive patients with dyspnoea on exertion, SR and LVEF>50% (72±7 years, 30female), and 25 age-matched controls (69±7years, 19 female) were recruited. Supine rest and exercise echocardiography was performed to comparable heart rates and images were analysed off-line. Peak early (Em) and late diastolic annular velocities (Am) were assessed by Colour Tissue Doppler Imaging at the mitral annular level at septal and lateral wall at rest and exercise; septal and lateral values were averaged and an atrial functional reserve index was calculated by using the following equation: (Am on exercise- Am at rest)*(1-1/Am at rest). Left atrial volume index (LAVI) and left ventricular mass index (LVMI) were derived from M-Mode or 2D pictures.

Results: Am was already significantly reduced at rest in patients compared to controls (6.9±1.6cm/s versus 7.8±1.7cm/s, p=0.033). This difference was even more marked at exercise (8.1±1.7cm/s versus 10.0±2.3cm/s, p=0.000) due to a significantly reduced atrial functional reserve index (0.98±1.44 versus 1.92±1.47, p=0.033). LAVI and LVMI were significantly higher in patients (LAVI 31.6±9.8ml/m² versus 23.9±8.7ml/m², LVMI (92.6±34.4g/m² versus 77.9±19.3g/m²). Am at exercise correlated with LAVI (p=0.006), LVMI (p=0.004) and the ratio of early mitral inflow velocity to Em at exercise (E/Em, p=0.000).

Conclusions: Atrial function is reduced in breathless, hypertensive patients with HFNEF. On exercise these patients show a significantly reduced atrial function reserve index. This is related to E/Em as a surrogate parameter for left atrial pressure and also related to left atrial size. Reduced LA function may contribute to breathlessness in HFNEF patients.

ACC.ORAL CONTRIBUTIONS

902

Exercise Testing/Stress Imaging

Monday, March 30, 2009, 8:00 a.m.-9:30 a.m.

Orange County Convention Center, Room W308C

8:00 a.m.

0902-3

High Intensity Interval Training Reduces Late Luminal Loss Following Percutaneous Coronary Intervention With Stent Implantation

Peter S. Munk, Eva M. Staal, N. Butt, Kjetil Isaksen, Alf I. Larsen, Stavanger University Hospital, Stavanger, Norway, University of Bergen, Bergen, Norway

Background: Even though regular exercise after myocardial infarction reduces morbidity and mortality, training after percutaneous coronary intervention (PCI) is not part of the standard treatment. We hypothesized that regular high-intensity interval training following PCI for stable or unstable angina reduces late luminal loss in the stented coronary segment.

Methods: We prospectively randomized 40 patients after PCI with implantation of a bare metal stent (N=22) or drug eluting stent (N=23) to a 6 months supervised interval training program or to a control group. All patients underwent an incremental exercise stress test with breath-by-breath gas exchange analysis, brachial artery ultrasound assessment of flow-mediated vasodilation and quantitative coronary angiography at baseline and after 6 months.

Results: Training resulted in a significant increase in peak oxygen uptake (17.6% versus 0.5%; p<0.001) and flow-mediated dilation (6.5% versus 0.3%; p=0.005) compared to the control group. A reduction in in-segment late luminal loss of the stented coronary area (0.21±0.39 mm versus 0.55±0.41 mm, p=0.011) was observed. Late luminal loss was smaller after implantation of a drug eluting stent compared to bare metal stent (0.26±0.41 mm versus 0.41±0.52 mm, p=0.17). Reduction of late luminal loss in the training group was consistent in both stent types.

Conclusions: Regular high intensity interval exercise significantly increases aerobic capacity and improves endothelium dependent vasodilation in patients following PCI for stable or unstable angina. This effect is associated with a reduction in late luminal loss in the stented coronary segment independent of stent type implanted. This beneficial effect of training might translate into clinical benefit.

8:15 a.m.

0902-4

Exercise Capacity Predicts Overall Mortality Beyond the Framingham Risk Score in Patients Without Established Coronary Artery Disease

Firas J. Al Badarin, Stephen L. Kopeckey, Thomas G. Allison, Mayo Clinic, Rochester, MN

Background: Cardiovascular disease (CVD) is largely a preventable disease. Exercise capacity is a predictor of CVD incidence and mortality but isn't included in current risk prediction rules, like Framingham risk score (FRS). Whether functional aerobic capacity (FAC) adds incremental risk prediction beyond FRS is unknown. **Methods:** We identified

patients with no history of CVD referred for exercise stress testing (1993-2003) from a computer database at a tertiary care center. Patients were stratified according to their predicted 10-year CVD risk into 5 groups using FRS (Table). FAC (% of predicted for age and sex) was used to stratify patient according to their exercise capacity into 5 groups (Table). National death registry was used to ascertain vital status of included patients. Mortality rates were compared using χ^2 test and cox model was used for multivariate regression analysis. **Results:** 18406 patients identified, 69% were males. Mean age was 52.8 ± 10.4 yrs and mean follow up was 8.4±3.7 yrs. Total mortality increased with increasing FRS category and was inversely related to FAC (p<0.0001, Table). Within each FRS risk group, lower FAC predicted a higher mortality (Table). All of the FAC-FRS interactions were statistically significant. FAC was an independent predictor of mortality (HR 0.97, p <0.0001). **Conclusion:** Exercise capacity predicts risk beyond FRS and identifies patients at higher risk for CVD who might benefit from aggressive risk factor reduction.

Table. Mortality according to FRS and FAC.

FRS Group	FAC Group (% predicted)					Overall
	>110%	90-109%	70-89%	50-69%	<50%	
< 5%	0.7	1.2	1.7	5.0	14.1	1.67
5 - 9.9%	1.7	2.4	3.6	9.6	22.1	3.47
10 - 14.9%	2.3	4.0	7.2	11.5	22.3	5.86
15 - 19.9%	5.6	6.7	10.6	13.9	32.5	9.36
≥ 20%	5.4	10.8	15.5	20.0	27.2	13.8
Overall	1.84	3.41	5.92	11.04	22.62	

8:30 a.m.

0902-5

Diagnostic Accuracy of Single-Photon Emission Computed Tomography Myocardial Perfusion Imaging and Stress Echocardiography for the Diagnosis of Left Main and Triple Vessel Disease: A Comparative Meta-Analysis

Nitin Mahajan, Latha Polavaram, Hema Vankalaya, Yun Wang, Joel Agar, Brian Ference, Luis Afonso, Wayne State University, Detroit, MI

Background: Limited comparative data on Single Photon Emission Computed Tomography (SPECT) and Stress Echocardiography (SE) for the detection of left main (LM) and triple vessel disease (TVD) exists. This study compares the diagnostic performance of SE and SPECT for the diagnosis of LM and high risk disease (LM+TVD).

Methods: Quantitative meta-analysis was performed using studies identified by MEDLINE search. Data was extracted using "any reversible perfusion deficit, electrocardiographic changes, transient ischemic dilatation, or other ancillary data" for SPECT and "any reversible wall motion abnormality" for SE. The sensitivity and specificity were computed. Summary receiver operating characteristic (SROC) analysis and metaregression were performed.

Results: Twenty nine studies met inclusion criteria. We found that SE has a significantly higher sensitivity but similar specificity compared to SPECT for identification of LM. The pooled diagnostic odds ratio (DOR) for SPECT and SE were 4.11(2.52-6.71) and 4.21(1.80-9.89) respectively. SE had higher sensitivity and superior diagnostic performance (Table 1) for the detection of high risk disease. The pooled DOR for SPECT and SE were 5.04 (3.20-7.93) and 10.44 (7.16-15.23) respectively.

Conclusions: In the absence of a direct head-to-head comparison of the diagnostic accuracies of SE and SPECT, our findings indicate that SE is the preferred screening modality for high risk disease.

Table 1: Comparison of diagnostic performance of SPECT and SE.

Coronary Vessel	Sensitivity (95% CI)		p	Specificity		p	Area Under SROC curve (Standard Error)		p	Meta Regression
	SPECT	SE		SPECT	SE		SPECT	SE		
LM	0.80 (0.68-0.92)	0.92 (0.87-0.98)	<0.05	0.50 (0.36-0.64)	0.39 (0.22-0.56)	NS	0.71 (0.05)	0.73 (0.06)	NS	NS
High risk disease (LM+TVD)	0.84 (0.76-0.91)	0.94 (0.92-0.96)	<0.05	0.47 (0.34-0.60)	0.45 (0.39-0.52)	NS	0.74 (0.04)	0.83 (0.02)	<0.05	SE>SPECT

8:45 a.m.

0902-6

Incremental Value of Adenosine-Induced Stress Myocardial Perfusion Imaging Using Dual Source Computed Tomography on Coronary Computed Tomography Angiography

Jose A. Rocha-Filho, Leon Shturman, Ian S. Rogers, Ron Blankstein, David R. Okada, Wilfred S. Mamuya, Hiram G. Bezerra, Ammar Sarwar, Udo Hoffmann, Gudrun Feuchtnr, Thomas J. Brady, Ricardo C. Cury, Massachusetts General Hospital, Boston, MA

BACKGROUND: Coronary computed tomography angiography (CTA) with its high negative predictive value can accurately exclude coronary artery disease (CAD) but is often limited in determining significance of a plaque. We aim to evaluate whether incorporation of stress-induced perfusion and myocardial functional assessment via adenosine stress CT can improve the evaluation of equivocal segments.

METHODS: 22 subjects with high-likelihood of CAD undergoing a cardiac catheterization (cath) underwent adenosine-induced stress myocardial perfusion imaging using dual source CTA. Two experienced readers initially analyzed the CTA alone and graded each segment for evaluability and presence of significant stenosis (>70%). All non evaluable segments were considered as positive for stenosis.

Next, readers reanalyzed all segments but were permitted to include data from stress and rest myocardial perfusion imaging and regional wall motion. When a perfusion defect or a wall motion abnormality was present and corresponded to the equivocal coronary segment, readers redefined this segment as stenotic. Per vessel analysis, were then compared to quantitative coronary angiography, as the gold standard.

RESULTS: The prevalence of significant stenoses in 22 subjects (age: 62.9±10.7 years, 82% males, average BMI 30.7kg/m²) was 48% on the first CTA reading, 45% on the second and 26% for cath.

During initial analysis, 35% vessel segments were originally scored as indeterminate with sensitivity 83%, specificity 65%, PPV 47% and NPV 91%. Following integration of stress perfusion and wall motion, global sensitivity, specificity, PPV and NPV improved to 89%, 71%, 53% and 94%, respectively. Summary test characteristics revealed an increase in the c-statistic from 0.74 to 0.80 despite requiring readers to define all segments as stenotic or non-stenotic regardless of limitations.

CONCLUSION: Our results demonstrate that integration of stress perfusion and ventricular function assessment with CTA can permit evaluation of coronary segments for significant stenosis that might otherwise be non-evaluable. The incremental value is most likely to benefit patients with a high incidence of calcific CAD.

9:00 a.m.

0902-7

Additional Value of First Pass Magnetic Resonance Myocardial Perfusion Imaging to Computed Tomography Coronary Angiography for Detection of Significant Coronary Artery Disease

Jan G. Groothuis, Aernout M. Beek, Stijn L. Brinckman, Martijn R. Meijerink, Simon C. Koestner, Marco J. Götte, Mark B. Hofman, Albert C. van Rossum, VU Medical Center, Amsterdam, The Netherlands

Background: As computed tomography coronary angiography (CTCA) has a reported excellent negative predictive value for detection of significant coronary artery disease (CAD), it is increasingly used as first line technique in the evaluation of patients with suspected CAD. However, positive predictive value is low and CTCA lacks information about myocardial perfusion. As first pass magnetic resonance myocardial perfusion imaging (MRMPI) can accurately assess myocardial perfusion and does not involve ionizing radiation, it may be a valuable additional technique to CTCA in the evaluation of patients with suspected CAD. The additional value of MRMPI to CTCA for detection of significant CAD was investigated using invasive coronary angiography (CAG) as the standard of reference.

Methods: Patients with chest pain and intermediate pre-test probability CAD underwent both 64-slice CTCA (Sensation, Siemens, Erlangen) and adenosine stress and rest first pass MRMPI (1.5 Tesla MR scanner, Siemens, Erlangen). CTCA was scored per segment as: normal; non-obstructive CAD (0-50% diameter stenosis) and abnormal (>50% stenosis). MRMPI was analyzed qualitatively and was assessed as abnormal in case of any segment with a perfusion defect. In case of abnormal CTCA and/or abnormal MRMPI, CAG was performed. Significant CAD was defined as > 70% stenosis on CAG.

Results: A total of 106 patients (mean age 57±10; 53 males) underwent both CTCA and MRMPI within 2 weeks. Consequently, 43 patients underwent CAG.

Of 69 patients with normal or non-obstructive CTCA, 6 patients had abnormal MRMPI. None of these patients had significant CAD on CAG. Of 37 patients with abnormal CTCA, 13 patients had significant CAD on CAG (positive predictive value 35%). Of 37 patients with abnormal CTCA, 15 (41%) patients had normal MRMPI. In 14 of these 15 patients absence of significant CAD was confirmed by CAG.

Conclusions: By using MRMPI as additional technique in case of abnormal CTCA findings, significant CAD could be ruled out in 14 of 37 (38%) patients with abnormal CTCA. In case of normal CTCA however, the additional value of MRMPI for detection of significant CAD is low.

ACC.POSTER CONTRIBUTIONS

1036

Tissue Imaging; CT Coronary Angiography

Monday, March 30, 2009, 9:30 a.m.-12:30 p.m.
Orange County Convention Center, West Hall D

9:30 a.m.

1036-233

Usefulness of Early End Diastolic Wall Thickness Changes After Reperfusion in ST-Elevation Acute Myocardial Infarction to Predict Late Transmurality as Assessed by Cardiac Magnetic Resonance

Marinela Chaparro-Muñoz, Alejandro Recio-Mayoral, Nicholas Bunce, George R. Sutherland, Department of Cardiology, St George's Hospital, London, United Kingdom

Background: Experimental studies have shown that complete reperfusion of acutely infarcted segments results in an immediate increase in end-diastolic wall thickness (EDWT), that are caused by reflow-induced myocardial edema. We aimed to determine whether early changes in EDWT after successful percutaneous coronary intervention can predict transmural necrosis at follow up, as assessed by delayed enhancement imaging.

Methods: We assessed EDWT and wall motion abnormalities in 26 consecutive patients with a first acute myocardial infarction (MI) by standard M Mode and 2D echocardiogram performed within first 12 hours after successful primary angioplasty. After 3 months of follow up, a repeat echocardiogram was carried out to assess changes in EDWT and contractile function and Cine-magnetic resonance imaging (MRI) was performed to evaluate location and size of the infarct zone. Necrosis was judged as transmural when delayed enhancement after gadolinium contrast was extended >50%.

Results: 416 segments were analysed. Compared with remote myocardium, dysfunctional segments in the infarct territory (n=144) had an increased EDWT (11±1.9 versus 9.4±1.1 mm, p<0.001) after primary angioplasty. At 3 months, 50% of dysfunctional segments showed an improvement in contractility. Segments that showed no improvement were thicker in the acute phase of the MI but thinner at 3 months of follow up than segments that recovered function (11.1±2.0 versus 10.4±1.7 mm, p = 0.023 and 8.9±1.2 versus 9.2±1.2 mm, p = 0.014, respectively). Delayed enhancement MRI identified transmural infarction in 41 segments. These segments had a significant increased EDWT in the acute phase of the MI compared with no transmural dysfunctional segments (11.8±1.9 versus 10.3±1.6 mm, p<0.001).

Conclusions: An early increased left ventricular wall thickness after full reperfusion of acute MI could indicate transmural necrosis and lack of recovery in contractility at follow up.

9:30 a.m.

1036-234

Strain Mapping by Speckle Tracking Echocardiography: A Novel Approach for Detailed Quantification of Infarct Transmurality Irregularities After STEMI

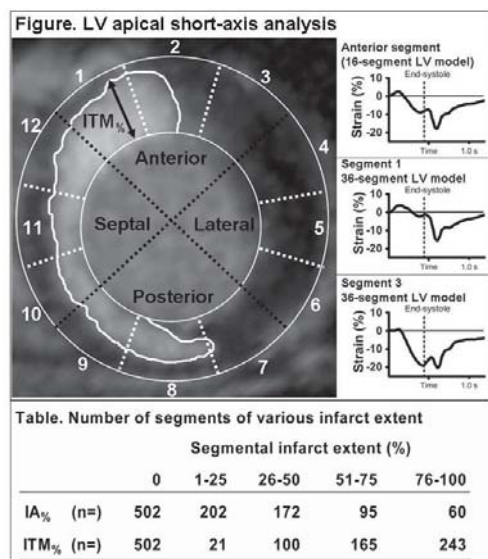
Thomas M. Helle-Valle, Eirik Pettersen, Trond Vartdal, Erik Lyseggen, Anders Opdahl, Espen W. Remme, Hans-Jørgen Smith, Ketil Lunde, Halfdan Ihlen, Otto A. Smiseth, Thor Edvardsen, Rikshospitalet University Hospital, Oslo, Norway, University of Oslo, Oslo, Norway

Background: Assessment of myocardial infarct morphology is clinically important. However, the conventional distinction between transmural and non-transmural infarcts has been challenged by reports of irregular morphology. We sought to characterize transmural intra-infarct distribution and determine whether the morphology could be quantified from detailed strain mapping by speckle tracking echocardiography (STE).

Methods: In 62 patients revascularized after acute LAD occlusion (STEMI), infarct transmurality was quantified by contrast MRI according to a standard 16-segment LV model. In each segment infarct extent was measured as infarct area in percentage of total segment area (IA%) and as maximal endo- to epicardial infarct transmurality (ITM%). In 15 patients circumferential strain and IA% were measured according to a detailed 36-segment LV model.

Results: There was a striking difference in transmurality grading between the two MR methods: Non-transmural and transmural infarction was 23 vs. 77% by ITM% and 71 vs. 29% by IA%. In segments classified as non-transmural by IA%, 66% were transmural by ITM%. Strain mapping by STE could differentiate between segments of 0, 1-25, 26-50, 51-75 and >75% IA% (P<0.05).

Conclusions: Due to the irregular distribution of infarct transmurality in reperfused infarcts, the conventional distinction between infarcts of transmural or non-transmural extent is ambiguous. However, strain mapping by STE allows detailed characterization of infarct morphology.



9:30 a.m.

1036-235 Subclinical Left Ventricular Dysfunction in Subjects Without Coronary Heart Disease is Related to the Number of Major Cardiovascular Risk Factors

Dragos Vinereanu, Gherghinescu Carmen, Andrea Ciobanu, Natalia Niculescu, Mircea Cinteza, Christopher Madler, Alan Fraser, University of Medicine and Pharmacy Carol Davila, Bucharest, Romania, Wales Heart Research Institute, Cardiff, United Kingdom

Atherosclerotic coronary disease is related to the number of major risk factors (RF). Similarly, number of RF might affect the function of heart, however, this is not clarified yet in asymptomatic patients, without coronary disease. **Aim:** To measure regional left ventricular (LV) function, at rest and during stress, in order to assess if subclinical myocardial dysfunction in asymptomatic patients, as assessed by tissue Doppler, is related to the number of major RF. **Methods:** 243 subjects (54±12 yrs, 54% men) were included in 5 groups according to the presence of 6 major RF (diabetes, hypertension, obesity - BMI ≥30 kg/m², dyslipidemia - LDL-cholesterol ≥3.4 mmol/l, smoking, and family history): group 1 (no RF) = 38; group 2 (1 RF) = 49; group 3 (2 RF) = 53; group 4 (3 RF) = 64; group 5 (>3 RF) = 39. All subjects had echo at rest and during dobutamine stress. Longitudinal function was assessed from the mean velocities of 4 basal segments, and radial function from the velocities of the basal posterior wall. Systolic functional reserve was calculated as the absolute increase in velocity from baseline. **Results:** Age and global ejection fraction (EF) were not different between groups. Longitudinal peak systolic velocity was decreased with the number of RF, at rest (6.7±1.5 vs. 6.2±1.6 vs. 5.9±1.5 vs. 5.4±1.3 vs. 5.2±1.5 cm/s for group 1, 2, 3, 4, and 5, respectively), and at peak stress (14.5±3.3 vs. 13.1±3.1 vs. 12.0±3.5 vs. 11.5±2.5 vs. 11.2±2.4 cm/s for group 1, 2, 3, 4, and 5, respectively) (both p<0.0001). Longitudinal functional reserve was also impaired with the number of RF, whereas radial peak systolic velocity and functional reserve were increased compensatory. By stepwise multivariate regression analysis, determinants of reduced longitudinal LV systolic function at rest were age, BMI, baseline DBP, cholesterol, and triglycerides (r = 0.60, r² = 0.35, p<0.0001); at peak stress were age, BMI, and baseline SBP (r = 0.56, r² = 0.31, p<0.0001). **Conclusion:** Subjects without clinical heart disease have impaired subendocardial function of the LV at rest and peak stress, which is related to the number of major RF. This is compensated by the radial function, maintaining the EF.

9:30 a.m.

1036-236 Validation of Speckle Tracking Based Strain Analysis for Study of Dynamic Function of the Heart by Sonomicrometry

Muhammad Ashraf, Aman Mahajan, Kalyanam Shivkumar, Petra S. Niemann, Tara Gu, Xiao-Yue Han, Thomas L. Lee, Galym Imanbayev, David J. Sahn, Oregon Health & Science University, Portland, OR, University of California, Los Angeles, CA

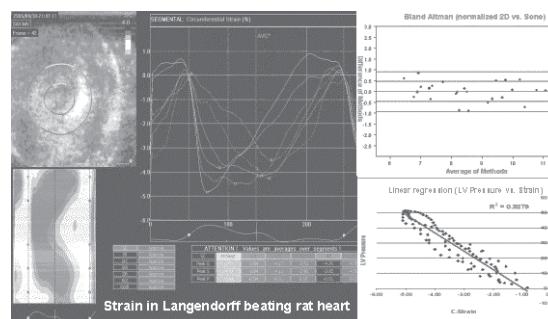
Background: 2D strain computation from speckle tracking allows direct assessment of global segmental dynamic myocardial function.

Methods: We studied 5 fresh pig hearts on a model designed to simulate cardiac motion. Five calibrated stroke volumes (30-70 ml) were delivered into the left ventricular (LV) cavity while rotating the LV 15° at 60 beats/min. Three sonomicrometry crystals were embedded in the myocardium across the circumference of the heart. We also studied 25 rat hearts using a Langendorff preparation modified for ultrasonic imaging. Heart rate was controlled by pacing the right atrium. LV pressure was recorded using a high fidelity tip catheter. We acquired short axis views on a Vivid 7 ultrasound system at 100-300 FPS. Images were exported to EchoPac PC for offline strain analysis using the speckle tracking method. Sonomicrometry data was analyzed in SonoMetrics® software.

Results: Increasing stroke volume in both models increased systolic and diastolic circumferential strain in the LV wall in short axis. A good correlation was detected between

sonomicrometry and speckle tracking based strain measurements both in the Langendorff beating hearts and the pig heart model studies (R²=0.85, R²=0.87, p=0.02), respectively. LV pressure dP/dt also showed a good correlation with strain computed by sonomicrometry and speckle tracking method in the Langendorff model (R²=0.92, p=0.01).

Conclusions: Our studies validate the speckle tracking program for study of dynamic cardiac function.



9:30 a.m.

1036-237 Two Dimensional Speckle Tracking Imaging Can Detect Subclinical Cardiac Dysfunction After Anthracycline-Based Chemotherapy

Wan Xian Chan, Lingli Gong, Raymond Cc Wong, Soo Chin Lee, Hla Yee Daw, Siew Eng Lim, Ross Soo, Boon Cher Goh, Lieng H. Ling, National University Hospital, Singapore, Singapore

Background: Anthracycline-based chemotherapy (ABC) can cause dose-related cardiomyopathy and heart failure. Myocardial tissue Doppler imaging can detect early left ventricular (LV) dysfunction in pts receiving ABC but is limited by angle dependency and translational motion artefact. Angle-independent 2-dimensional speckle tracking imaging (STI) may provide an alternative method to detect cardiotoxicity.

Methods: We performed echocardiography and measured plasma aminoterminal pro-B-type natriuretic peptide (NT-proBNP) before and within 4 weeks after completing ABC. Longitudinal, circumferential and radial STI indices were obtained using EchoPac software from 4-chamber and short-axis LV images acquired at optimal frame rates.

Results: We studied 38 pts (35 female; mean age 50.6±9.5 yrs) whose median anthracycline dose was 240 mg/m². Mean LV ejection fraction was 67±4% before and 61±6% after ABC (P=0.002) and corresponding mean NT-proBNP levels, 76±88 and 173±233 pg/ml (P=0.01). All peak strain values and longitudinal and circumferential early diastolic strain rate decreased significantly post-ABC (Table 1).

Conclusions: Serial changes in systolic and diastolic STI indices are demonstrable in pts receiving ABC, in tandem with reduction in LV ejection fraction and elevation of NT-proBNP. These findings suggest that STI can detect subclinical LV dysfunction in these pts.

Table 1

	Pre-ABC	Post-ABC	P
Longitudinal systolic strain rate, s-1	1.1±0.2	1.1±0.2	0.14
Longitudinal early diastolic strain rate, s-1	1.6±0.5	1.4±0.3	0.002
Longitudinal peak strain, %	20±2.7	17.9±2.4	<0.001
Circumferential systolic strain rate, s-1	1.6±0.3	1.5±0.3	0.16
Circumferential early diastolic strain rate, s-1	2.0±0.5	1.7±0.5	0.004
Circumferential peak strain, %	21.4±4.0	18.1±3.8	0.001
Radial systolic strain rate, s-1	2.1±0.5	2.0±0.5	0.34
Radial early diastolic strain rate, s-1	2.3±0.8	2.1±0.7	0.25
Radial peak strain, %	60.3±15.3	52.1±16.9	0.007

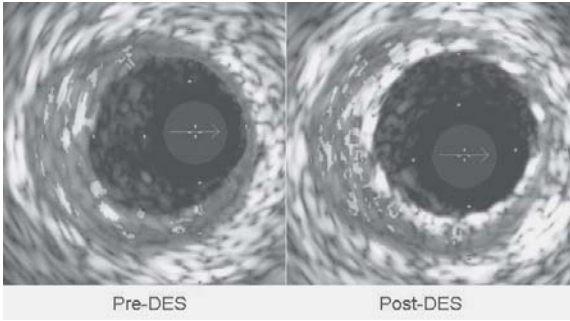
9:30 a.m.

1036-238 The Impact of Necrotic Core in Thin-Capped Fibroatheroma on Post-DES Implantation: Virtual Histology Intravascular Ultrasound Analysis

Sang-Wook Kim, Gary S. Mintz, Wang-Soo Lee, Gi-Hwan Kim, Young-Mi Jo, Kyung-Sook Park, Kwang-Je Lee, Tae-Ho Kim, Chee-Jeong Kim, Wang-Seong Ryu, Neil J. Weissman, Chung-Ang University Hospital, Seoul, South Korea, Washington Hospital Center, Washington, DC

We assessed 100 pts treated with DES. Virtual histology intravascular ultrasound (VH-IVUS) imaging was performed before and after DES implantation. Thin-capped fibroatheroma (TCFA) was defined as NC >10% of plaque area within a plaque burden of >40% and NC in contact with the lumen for at least 3 image slices. TCFA were compared to non-TCFA lesions (all other VH-IVUS lesion types including thick-capped fibroatheromas and fibrocalcific plaques). Stent strut artifacts were manually excluded. Positive remodeling was defined as a remodeling index >1.05. **Results:** Pt age was 62±10yrs and 70% were males in TCFA group; pt age was 60±13yrs and 75% were males 75% in non-TCFA group. Greyscale IVUS showed that TCFA and non-TCFA had similar distal reference lumen area (7.05±2.15mm² vs 6.97±2.44mm², p=0.92) and lesion length (19.1±7.36mm vs 19.5±6.52mm, p=0.77). Remodeling index was 1.01±0.13 in TCFA vs 0.97±0.12 in non-TCFA, p=0.46. Pre-DES %average NC (p=0.013) and %maximal NC (p=0.001) were higher in TCFA vs non-TCFA (Table). After DES implantation VH-IVUS showed that the NC was more often in contact with lumen in TCFA (13/30 [43%]) than

in non-TCFA (6/32 [18.7%], $p=0.034$). Similarly, post DES implantation, the %maximal NC was still larger in TCFA than non-TCFA (44.37 ± 11.57 vs 33.50 ± 11.77 , $p=0.005$). **Conclusion.** DES implantation into a TCFA results in NC in contact with the lumen in almost 50% of lesions. These may be at higher risk of subsequent events because of impaired healing response.

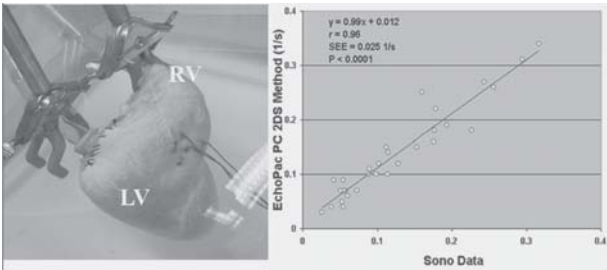


9:30 a.m.

1036-239 Accuracy of Two-Dimensional Speckle Tracking Strain to Determine Right Ventricular Dyssynchrony

Rohini Deb, Cong Tin P. Le, Ethan Muldoon, Sydney Prescott, Galym Imanbayev, Cole Streiff, Ana Badua, Ann Carver, Ryan Townsend, Minjuan Zheng, Pengyuan Zhang, Muhammad Ashraf, Xiaokui Li, David J. Sahn, Oregon Health & Science University, Portland, OR

Background: There is little published data about the accuracy of 2D strain methods to evaluate synchrony of the thin-walled right ventricle (RV). We compared the wall motion in the RV in a dynamic biventricular heart model with synchronized and dyssynchronized pumping of the left ventricle (LV) and RV. **Methods:** Three dissected pig hearts were filled with 2 separate balloons in both ventricles, connected to two pulsatile pumps, with 5 stroke volumes (30-50 ml/beat) and studied in synchronized and dyssynchronized settings. Three sonomicrometry crystals were inserted along the long axis of the RV free wall in a triangular pattern. Echo imaging was performed with a GE Vivid 7 Dimensions system using a 7 MHz probe. Data was analyzed with EchoPac PC 2D strain (2DS) for longitudinal strain/strain rate (SrL) for the RV free wall and compared with sonomicrometry data. **Results:** Mean strain and strain rate for RV free wall synchrony and dyssynchrony were $11.34 \pm 5.69\%$ vs. $9.37 \pm 5.38\%$; 0.16 ± 0.1 vs. 0.13 ± 0.08 1/s; mean percentage difference for strain is $16 \pm 20\%$, and for strain rate is $8 \pm 58\%$ as compared with synchrony. Linear regression of strain rate between crystal and 2DS derived data showed good correlation ($y = 0.99x + 0.012$, $r = 0.96$, $SEE = 0.025$ 1/s, $P < 0.0001$). **Conclusions:** RV strain was decreased when RV work was delayed until after the LV was filled in our model.



9:30 a.m.

1036-240 Effect of Alcohol Septal Ablation on Left Ventricular Deformation and Cardiac Twist

Jianwen Wang, Karla Kurrelmeyer, William A. Zoghbi, Vera Veerasamy, Yelena P. Ashtou, Miguel A. Quinones, Sherif F. Nagueh, The Methodist Research Institute and Methodist DeBakey Heart Center, Houston, TX

Background: Alcohol septal ablation (ASA) treats dynamic obstruction, and improves dyspnea and angina symptoms in patients with obstructive hypertrophic cardiomyopathy (HCM). However, there is a paucity of data regarding its effects on myocardial deformation and cardiac twist. **Methods:** Forty-one HCM patients underwent transthoracic echocardiography. Two-dimensional loops of left ventricular (LV) apical 4, 2, and long axis views and short axis views at the level of the mitral valve, papillary muscle, and apex were obtained for analysis of global longitudinal (GSII), radial (GSIR), and circumferential (GSIC) strains using 2D speckle tracking. In 14 patients with dynamic gradient ≥ 30 mmHg, ASA was performed. Echocardiography was performed in these patients at rest, and 3-6 months after ASA. Twenty healthy age-matched normal subjects were included as a control group. **Results:** LV global longitudinal and radial strains were significantly reduced in HCM patients ($P < 0.01$) compared to controls, but not circumferential strain or twist. After ASA, LV global longitudinal, and radial strains improved significantly (table, both $P \leq 0.05$), but circumferential

strain was of borderline significance ($p=0.05$), and twist did not show change. **Conclusions:** In general, HCM patients have depressed longitudinal and radial strains, but preserved circumferential deformation. ASA significantly improves longitudinal and radial strains but does not affect LV twist.

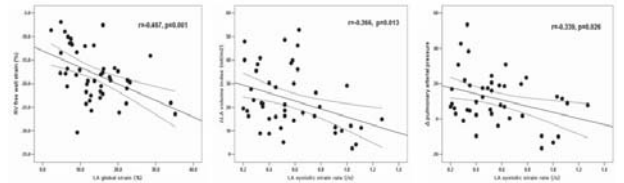
Variables	Control group	HCM group				
		Total group	P value	with obstruction		
			Control vs HCM	Prior ASA	Post ASA	P (prior vs post)
GSII (%)	-18.6 (2.4)	-12.2 (3.4)	<0.001	-11.4 (2.7)	-13.3 (2.0)	0.03
GSIC (%)	-21.3 (2.5)	-19.7 (3.1)	0.06	-16.4 (4.1)	-18.9 (3.6)	0.05
GSIR (%)	45.4 (4.4)	31.6 (9.1)	<0.001	29.8 (5.9)	39.8 (6.8)	<0.001
Twist (%)	14.4 (4.6)	14.5 (6.8)	0.91	15.1 (7.2)	14.9 (5.1)	0.68

9:30 a.m.

1036-241 Prediction of Left Atrial Reverse Remodeling after Mitral Valve Surgery with Speckle Tracking Imaging

Ae-Young Her, Eui-Young Choi, Sung-Ai Kim, Sang-Jae Rhee, Chi-Young Shim, Jong-Won Ha, Namsik Chung, Yonsei Cardiovascular Center and Cardiovascular Research Institute, Seoul, South Korea

Background: Left atrial (LA) reverse remodeling and pulmonary arterial pressure reduction is important prognostic factor after mitral valve (MV) surgery. We sought to investigate whether LA function and compliance measured by speckle tracking imaging might predict the future reduction of LA volume and pulmonary arterial pressure after MV surgery. **Methods:** Patients who had planned to MV surgery underwent echo-Doppler evaluation. Global strain and strain rate of LA were measured in apical 4- and 2-chamber views using 2D speckle tracking image analysis. Seven to fifteen days after MV surgery, LA volume and right ventricular systolic pressure were re-evaluated. **Results:** 51 patients were studied (27 patients with predominant mitral stenosis and 24 patients with mitral regurgitation). LA global strain was significantly correlated with LA volume index ($r = -0.608$, $p < 0.001$), pulmonary arterial systolic pressure ($r = -0.328$, $p = 0.02$) and right ventricular free wall strain ($r = -0.467$, $p = 0.001$). In multivariate analysis, preoperative LA systolic global strain rate was significantly correlated with degree of LA volume reduction ($\beta = -0.715$, $p = 0.003$) and right ventricular systolic pressure decline ($\beta = -0.490$, $p = 0.042$) after surgery independent of age, presence of atrial fibrillation (AF), preoperative predominant pathology or modality of valve surgery. **Conclusion:** Preoperative LA global strain rate could predict the degree of postoperative LA volume reduction and pulmonary arterial pressure decline.

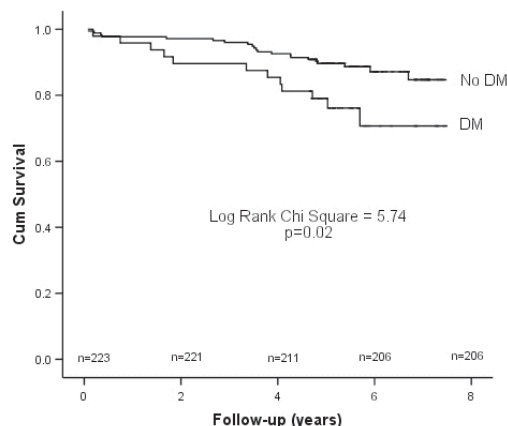


9:30 a.m.

1036-242 Peak Systolic Strain Rate Is Predictive of Mortality in Patients With Diabetes Undergoing Dobutamine Stress Echocardiography

Tony Stanton, Charlotte Bjork Ingul, David J. Holland, James L. Hare, Rodel Leano, Thomas H. Marwick, University of Queensland, Brisbane, Australia, University of Science & Technology, Trondheim, Norway

Background: Deformation imaging detects subclinical myocardial changes that parallel fibrosis and collagen deposition in diabetes mellitus (DM). We sought whether this technique predicts mortality in patients with DM undergoing dobutamine stress echo (DSE). **Methods:** Of 223 consecutive individuals with normal resting left ventricular (LV) function undergoing DSE, 48 (22%) had DM. Standard echocardiographic measures and ischemia were recorded. Mean peak systolic strain rate (SR) was calculated in 18 segments. Patients were followed for all-cause mortality over 5.4 ± 1.4 years. **Results:** Patients with and without DM showed no significant differences in LV mass, ejection fraction, ischemia or peak systolic SR. Patients with DM had worse survival (see figure). In a Cox Proportional Hazards Model the strongest predictors of mortality in DM were peak systolic SR (HR 2.50, 95%CI 1.04-5.98, $p < 0.05$) and peak systolic blood pressure (HR 0.47, 95%CI 0.24-0.9, $p < 0.05$). These variables were superior to and independent of LV mass index (HR 1.20, 95%CI 0.94-2.17, $p = 0.15$) and ischemia (HR 0.98, 95%CI 0.44-2.17, $p = 0.96$). **Conclusions:** Peak SR during DSE is a significant and independent predictor of all-cause mortality in DM. The independence of this from ischemia suggests that SR is a marker of myocardial changes that influences outcome.



9:30 a.m.

1036-243

Demonstration of Transmural Dispersion of Myocardial Relaxation in Humans Assessed With Tissue Strain Imaging: Comparison of Normal Subjects and Hypertension

Makoto Amaki, Satoshi Nakatani, Hideaki Kanzaki, Jun Tanaka, Toshiyuki Tanaka, Masafumi Kitakaze, National Cardiovascular Center, Suita, Japan

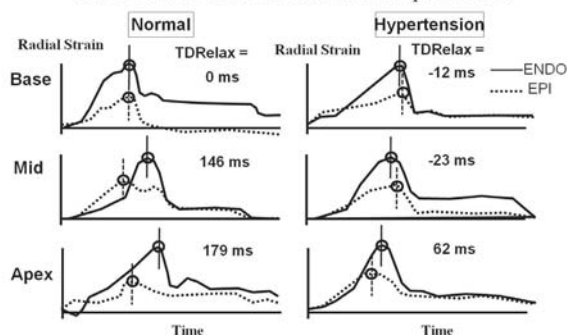
Background: Myofiber relaxation begins from subepicardium (Epi) to subendocardium (Endo) creating transmural dispersion of myocardial relaxation (TDRelax). It has been reported in animals but not in humans so far.

Methods: To demonstrate TDRelax in humans, 20 normals (NL) and 20 age-matched patients with hypertension (HT) were studied using tissue strain imaging (TDI-Q, Toshiba). Endo and Epi temporal strain profiles during a cardiac cycle were obtained at the basal, mid and apical posterior wall in the left ventricular (LV) short-axis image. Time to peak radial strain (TTP) of Endo and Epi were measured, and normalized to the cycle length ($\approx 100\%$ at the end of the cycle). TDRelax was defined as the difference between TTP Epi and TTP Endo.

Results: In NL, TTP Epi was shorter than TTP Endo in the apex (30 ± 7 vs $42 \pm 6\%$, $p < 0.001$) and the mid (36 ± 7 vs $42 \pm 6\%$, $p < 0.01$), but they were almost similar at the base. In HT, TTP Epi, not TTP Endo, was delayed at the apex and the mid making the beginning of relaxation coincident at both layers. Consequently, TDRelax in NL was largest at the apex and progressively decreased towards the base (12 ± 6 vs 7 ± 5 vs $2 \pm 5\%$, $p < 0.001$), whereas it was constantly small in HT (3 ± 6 vs 2 ± 7 vs $3 \pm 4\%$, n.s.).

Conclusions: Epi relaxation began earlier than Endo relaxation at the mid and the apex in NL. Delayed timing of peak strain at Epi but not Endo created less TDRelax both at the apex and the mid in HT. This may indicate the ineffective relaxation in hypertensive heart.

Transmural dispersion of myocardial relaxation between subendocardium and subepicardium



9:30 a.m.

1036-244

Left Ventricular Global Strain Is More Accurate Than EF as a Marker of Arrhythmic Events After Myocardial Infarction

Kristina H. Haugaa, Marit Kristine Smedsrud, Erik Kongsgaard, Otto A. Smiseth, Jan P. Amlie, Thor Edvardsen, Rikshospitalet University Hospital, Oslo, Norway, University of Oslo, Oslo, Norway

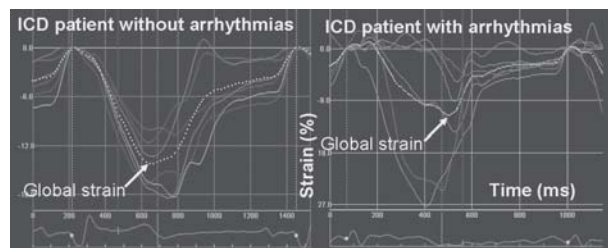
Background: Currently, left ventricular ejection fraction (EF) is the primary parameter used to select patients for ICD therapy after myocardial infarction (MI). Myocardial strain by echocardiography can quantify regional myocardial function. We hypothesized that

analyses of myocardial strain can better identify susceptibility for ventricular arrhythmias compared to EF.

Methods: We included 58 patients with an ICD according to secondary prevention post MI. After 3.8 ± 3.6 years follow up, 28 had no and 30 patients had one or more recorded arrhythmias requiring appropriate ICD therapy. Strain measurements were assessed by speckle tracking echocardiography. The average value of peak negative strain in a 16 LV segments model was assessed as global LV strain.

Results: EF did not discriminate ICD patients with arrhythmias from those without ($39 \pm 10\%$ vs. $40 \pm 12\%$, $P=0.94$). Left ventricular end diastolic (LVEDV) and end systolic volumes (LVESV) were not significantly different between arrhythmic and non-arrhythmic patients (LVEDV 182 ± 63 ml vs. 160 ± 62 ml, $P=0.19$ and LVESV 113 ± 49 ml vs. 100 ± 52 ml, $P=0.31$). Global LV strain was lower in the arrhythmic patients compared to the non-arrhythmic ($-10.8 \pm 4.7\%$ vs. $-13.3 \pm 4.2\%$, $P=0.03$). Figure demonstrates lower global strain in an arrhythmic ICD patient (right panel) compared to a non-arrhythmic.

Conclusions: Global LV strain by echocardiography was more accurate than EF in identifying dependency of ICD therapy in post MI patients.



9:30 a.m.

1036-245

Adenosine Stress Dual-Energy CT of the Heart for Diagnosing Myocardial Ischemia and Viability Compared With Cardiac MRI and SPECT: Initial Experience

Balazs Ruzsics, Michael Rosenblum, Peter Zwerner, Salvatore Chiamaramida, Joseph Abro, Sebastian Vogt, Joseph Schoepf, Medical University of South Carolina, Charleston, SC

Purpose: To evaluate the feasibility and accuracy of dual-energy CT (DECT) including rest-, stress-, and delayed enhancement-imaging for diagnosing fixed/reversible myocardial ischemia and viability compared with cardiac MRI (cMRI) and SPECT-myocardial perfusion imaging (MPI).

Method And Materials: With IRB approval we prospectively enrolled 10 patients with known or suspected coronary artery disease who underwent 1) Clinically indicated adenosine stress/rest SPECT-MPI 2) Contrast (Magnevist, Bayer) enhanced adenosine stress/rest perfusion and delayed enhancement cMRI (1.5T Avanto, Siemens) 3) Contrast (Ultravist) enhanced, retrospectively ECG-gated adenosine stress/rest and delayed enhancement DECT. DECT was performed by independently operating the two tubes of a dual-source CT system (Definition) at 140kV and 100kV. In each patient all three DECT data sets were analyzed for blood pool deficits and delayed enhancement by mapping the iodine content within the myocardium based on the different x-ray spectra. Two independent, blinded observers evaluated SPECT-MPI, cMRI and DECT for fixed/reversible ischemia and cMRI and DECT for delayed enhancement based on the AHA segmental model.

Results: All patients (5 female, mean age 67 years) were successfully imaged with all three modalities without adverse events. 170 myocardial segments were analyzed of which 15 were abnormal at cMRI. Interreader agreement for detection of fixed/reversible ischemia and delayed enhancement at DECT was moderate to excellent ($k=0.5-k=1$). Compared with cMRI, DECT and SPECT-MPI had 100% (88%) sensitivity, 99% (100%) specificity, and 99% (98%) accuracy for detecting myocardial segments with fixed ischemia, respectively. Reversible ischemia was detected with 100% (100%) sensitivity, 100% (90%) specificity, and 100% (92%) accuracy by DECT and SPECT-MPI. Compared with cMRI, DECT detected myocardial segments showing delayed enhancement with 100% sensitivity, 100% specificity, and 100% accuracy.

Conclusion: Our initial experience suggests that adenosine stress and delayed enhancement DECT is feasible. Compared to cMRI as the reference standard DECT shows good agreement for delayed enhancement and equal or better performance than SPECT-MPI for detection of myocardial ischemia.

9:30 a.m.

1036-246

Segmental Twisting Synchrony Provides a Noninvasive Marker of Cardiac Performance During Cardiac Resynchronization Therapy

Muhammad Ashraf, Nicole Chang, Wei Zhou, Elizabeth Sanchez, Jennifer Corniea, Kalyanam Shivkumar, David J. Sahn, Aman Mahajan, Oregon Health & Science University, Portland, OR, University of California, Los Angeles, CA

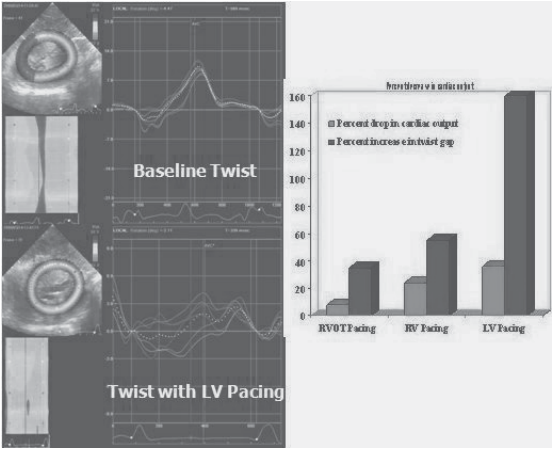
Background: Cardiac pacing is often used to improve dynamic heart function in patients with underlying rhythm disorders. Lead placement is an important consideration. Imaging based mechanical parameters and segmental synchrony have been related to hemodynamic indices of heart function.

Methods: Seven pigs underwent midline sternotomy to expose the heart. Continuous hemodynamic monitoring was performed. Left ventricular (LV) pressure-volume curves

were obtained with an intraventricular conductance catheter. Rapid ventricular pacing was performed from multiple right ventricular (RV) epicardial sites (apex and RV outflow tract [RVOT]) and LV (basal lateral wall) at a constant heart rate. Apical and basal short axis 2D views were acquired directly from the heart surface. Images were exported to EchoPac PC for offline analysis of strain and twist using speckle tracking based methods. Differences of peak segmental twist and strain were recorded at each pacing site.

Results: Cardiac output dropped with each pacing method compared to sinus rhythm. The difference in timing of maximal twist between segments was computed as an index of twisting synchrony (twist gap). Percent increase in twist gap showed good correlation with percent drop in cardiac output (R=0.74). The changes in hemodynamics and twist gap were minimal with RVOT pacing and worse with LV pacing.

Conclusions: Segmental twisting synchrony provides an index of cardiac performance during pacing in this model. The RVOT was an optimal pacing site.



9:30 a.m.

1036-247 Defining Characteristics of Subjects With Exclusively Noncalcified Plaque: The Pitfall of Screening Strategy Based on Coronary Artery Calcification

Kihyun Jeon, Iksung Cho, Yeonyee E Yoon, Juan J. Rivera, Khurram Nasir, Sang Il Choi, Eunju Chun, Hyung-Kwan Kim, Yong-Jin Kim, Dae-Won Sohn, Hyuk-Jae Chang, Cardiovascular Center, Seoul National University Hospital, Seoul, South Korea

Background: Coronary artery calcium scoring (CACS) is widely used to differentiate an asymptomatic individual at high risk. However, CACS only detect calcified plaque as a surrogate marker of coronary atherosclerosis, and the absence of calcified plaque alone does not be enough to exclude future cardiac events. We, therefore, define the prevalence of the subjects with exclusively noncalcified plaque (NCP) using coronary CT angiography (CCTA), and their characteristics comparing to normal and those with different types of plaque.

Methods: We enrolled 3100 asymptomatic subjects (53.9 ± 7 years, male 60%) free of known cardiovascular disease or symptom who had underwent both CACS and CCTA as a part of routine health check-up. Cardiovascular risk factors, CACS as a whole and presence of atherosclerotic plaque and significant stenosis (≥ 50% diameter stenosis) for each coronary segment were determined.

Results: Atherosclerotic plaques were identified in 924 (30 %) subjects. 226(7.3%) subjects had exclusively NCP without CAC: 28 (11%) of those had significant stenosis. Most of them had single vessel disease (89%) and most (53%) of the significant lesions were located in the left anterior descending coronary artery. Comparing to subjects with normal coronary artery, those with exclusively NCPs were characterized by male gender (<0.001), older age (p<0.001), higher Triglyceride (p=0.03) and lower HDL-cholesterol (p<0.001) as well as more diabetes (p=0.03) and hypertension (p=0.026). However after adjusting conventional risk factors (LDL, HDL, Triglyceride, hypertension, diabetes and smoking), there were significant difference only in male gender (OR3.561; 95%CI: 2.289-5.540), age (OR 1.045; 95% CI: 1.028-1.062) and incidence of diabetes (OR 1.798; 95%CI: 1.135-2.848).

Conclusions: Our study demonstrated that incidence and severity of exclusive NCPs are not negligible. Although current screening method guided by CACS could detect calcified plaques efficiently in asymptomatic subjects, it can miss NCPs which can elicit future cardiac events. Screening of subclinical coronary atherosclerosis using CCTA could be considered as an alternative especially in young with several risk factors.

9:30 a.m.

1036-248 Accuracy Of 64-Slice Computed Tomography in Assessing Coronary Artery Stenoses in Segments With Mild, Moderate, or Extensive Calcification: A Subanalysis of the CORE-64 Trial

Andrea L. Vavere, Armin Arbab-Zadeh, Julie M. Miller, Carlos E. Rochitte, Marc Dewey, Hiroyuki Niinuma, Ilan Gottlieb, Melvin Clouse, David Bush, John Hoe, Albert de Roos, Christopher Cox, Joao AC Lima, Johns Hopkins University, Baltimore, MD

Background: The diagnostic capability of any imaging modality is critically dependent upon image quality. Blooming artifacts due to coronary artery calcification interfere with

image interpretation in computed tomography angiography (CTA). The aim of this study is to evaluate the influence of segment calcification on the diagnostic accuracy CTA as compared to conventional coronary angiography (CCA).

Methods: 291 patients (3782 segments; 76 women; age 59.3 ± 10.0 yrs) with ≤600 coronary calcium score were included in the CorE-64 Multicenter International Trial, which compared 64-detector CTA with CCA. An independent observer visually assessed cross-sectional arc calcium using an ordinal scale: non-calcified, mild (<90°), moderate (90-180°), and extensive (>180°). Two independent blinded readers assessed diameter stenosis quantitatively using semi-automatic measurement tools. Disagreements were consensed by a third experienced reader. Positive segments were defined as ≥50% and negative segments were <50% by quantitative CCA. By definition, an accurate diagnosis was agreement between CCA and CTA. Data were analyzed using logistic regression with generalized estimating equations to account for within-patient clustering.

Results: Table

Conclusions: By multi-variable analysis, extensive coronary artery segment calcification is the strongest predictor of disagreement between computed tomography and conventional angiography for the assessment of coronary artery disease severity.

Crude and Adjusted Odds Ratio for Diagnostic Disagreement between CTA and CCA

	OR	Crude 95% CI	P value	OR	Adjusted* 95% CI	P value
Gender (male vs female)	1.9	(1.4-2.7)	<0.001	1.8	(1.2-2.5)	0.001
Age	1.0	(1.0-1.0)	0.49	1.0	(1.0-1.0)	0.79
Arc Calcium			<0.001			<0.001
None (reference)	n=2945	1.0		1.0		
Mild (<90°)	n=490	1.8	(1.3-2.5)	1.4	(1.0-1.9)	
Moderate (90-180°)	n=227	2.5	(1.7-3.7)	1.7	(1.1-2.6)	
Extensive (>180°)	n=120	4.7	(2.9-7.6)	3.0	(1.7-5.1)	
CNR			0.055			0.052
0-10 (reference)		1.0		1.0		
11-20		0.6	0.4-0.9	0.7	(0.5-0.9)	
21-30		0.8	0.4-1.3	0.9	(0.6-1.5)	
>30		0.7	0.4-1.4	0.7	(0.4-1.2)	
Acquisition HR			0.052			0.001
<60 (reference)		1.0		1.0		
60-70		1.1	0.8-1.6	1.3	(0.9-1.7)	
>70		2.1	1.3-3.3	2.2	(1.4-3.3)	

Abbreviations: CTA: computed tomography angiography; CCA: conventional coronary angiography; OR, odds ratio; CI, confidence interval; CNR, contrast to noise ratio; HR, heart rate
* Adjusted model includes gender, age, race, segment calcium, contrast to noise ratio, acquisition heart rate, and the interaction of age and coronary calcium

1036-249 Extent and Distribution of Mixed Plaque Type by Coronary CT Angiography Predicts Individuals With Obstructive Coronary Artery Stenosis: Results From the Multicenter ACCURACY Trial

James K. Min, Matthew J. Budoff, Cornell University Medical Center, New York, NY, Harbor UCLA Medical Center, Los Angeles, CA

Background: Coronary computed tomographic angiography (CCTA) is able to assess plaque composition in addition to stenosis severity. Prior studies have focused on stenosis severity without accounting for plaque composition.

Methods: 230 consecutive outpatients (136 men, 94 women; CAD 34% vs. 11%, age 57±10 years) with stable chest pain underwent CCTA and invasive coronary angiography (ICA) at 16 sites. Coronary arteries were assessed using a 15-segment AHA model for obstructive (≥70%), non-obstructive (<70%) or no coronary plaque. Plaques were graded as non-calcified, calcified or "mixed" composition. "Mixed" composition was defined as either segments with mixed plaque type or a non-dominant pattern of calcified and non-calcified plaques (i.e., <5 segments each). Patients were classified into 7 categories: no evident plaque and ≥5 or <5 segments with calcified plaque, non-calcified plaque or mixed plaque.

Results: 32 individuals were noted to have obstructive CAD by ICA. Individuals classified by plaque composition are listed in table 1. In contrast to other groups, those exhibiting ≥5 segments with mixed plaque demonstrated higher rates of obstructive plaque (17/32; 53.1%, p<0.0001). Individuals with ≥5 segments with calcified plaque had no obstructive plaque (0/32; 0%).

Conclusions: Increasing numbers of segments with mixed plaque predict individuals with obstructive CAD. Conversely, increasing numbers of segments with calcified plaque are not associated with obstructive CAD.

Plaque composition and Obstructive CAD

	No plaque	>or= 5 calcified segments	<5 calcified segments	<5 mixed segments	<5 non-calcified segments	>or=5 non-calcified segments	>or=5 mixed segments
Obstructive CAD	0	0	3	5	4	3	17
No obstructive CAD	59	6	20	49	30	6	25
Total	59	6	23	54	34	9	42

9:30 a.m.

9:30 a.m.

1036-250

Impact of Procedure Volume and Operator Experience on the Diagnostic Accuracy of Computer Tomographic Coronary Angiography

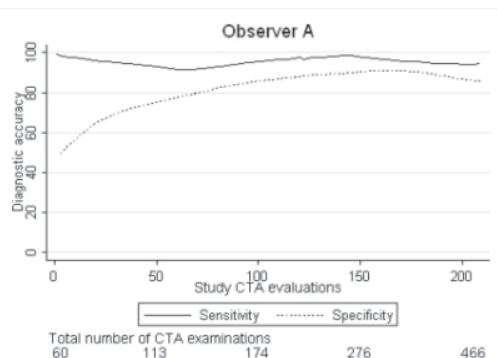
Kristian A. Oevrehus, Morten Boettcher, Henrik M Larsen, Hans E Boetkaer, Bjarne L Noergaard, Vejle Hospital, Vejle, Denmark, Aarhus University Hospital, Aarhus, Denmark

Background: Studies demonstrating a high diagnostic accuracy of CT coronary angiography (CTA) in identifying coronary artery disease (CAD) derive primarily from experienced high volume centres. Whether this accuracy applies to centres with less CTA experience is unknown.

Methods: For two cardiologists with limited CTA experience (60 examinations), diagnostic accuracy (64-slice, n=94 and dual source, n=115) in 209 patients recruited from August 2006 until November 2007 was calculated. CAD was defined as > 1 stenoses > 50% at invasive CAG. The influence of observer experience on accuracy and interobserver variability was evaluated. Kappa values at different time points defined as 1 (patients 1-47), 2 (48-94), 3 (95-151), and 4 (152-207) were compared.

Results: On a patient level (CAD prevalence 35 %) sensitivity was 98 % (92-100), specificity 81 % (74-87), PPV 74 % (64-82), and NPV 99 % (95-100). Diagnostic specificity improved with observer experience ($p < 0.05$) (figure). The agreement between readers also improved with observer experience (time point 1: $\kappa = 0.35$; 2: $\kappa = 0.54$; 3: $\kappa = 0.63$; 4: $\kappa = 0.89$; $p < 0.01$).

Conclusions: At a level of CTA competence 1, both diagnostic specificity and interobserver agreement was poor, however, with increasing observer experience a significant improvement in both measures were demonstrated. Following a total of 400 CTA examinations (CTA level of competence 3), estimates of accuracy and interobserver agreement were comparable to the results from CTA high volume centres.



9:30 a.m.

1036-251

Novel Dedicated Automated Approach for Quantification of the Degree of Stenosis on 64-Slice Multislice Computed Tomography Angiography: Validation With Quantitative Coronary Angiography

Mark M. Boogers, Joanne D. Schuijff, Jacob. M. van Werkhoven, Isabel M. Adame, Albert de Roos, J. Wouter Jukema, Johannes H.C. Reiber, Jeroen J. Bax, Leiden University Medical Center, Leiden, The Netherlands

Background: Multi-slice computed tomography (MSCT) angiography is an increasingly used technique in the evaluation of patients with known or suspected coronary artery disease (CAD). Thus far, previous attempts to quantify stenosis severity on MSCT have been discouraging. This study aimed to demonstrate the feasibility of a novel dedicated algorithm for automated quantification of stenosis severity in comparison to quantitative coronary angiography (QCA).

Methods: Patients who underwent both 64-MSCT angiography and invasive coronary angiography within two months were included. Using dedicated quantitative computed tomography angiography (CTA) software, the most severe lesion was quantified in each coronary artery. After accurate segment definition, automatic contour detection was performed in longitudinal and transversal planes. Next, automatic quantification was based on interrelation of reference line (estimate of normal tapering of coronary vessel) and luminal contours. An independent observer, blinded to CTA data, performed QCA similar to MSCT.

Results: In total, 100 patients (38 men, 59.9 ± 8.1 yrs, mean coronary calcium score 331.1 ± 729.7 , ranging from 0 - 4441) were analyzed. A total amount of 284 (94.7 %) vessels could be evaluated. Exclusion of 16 (5.3 %) vessels of 16 patients was based on motion artefacts ($n = 11$), total occlusion ($n = 3$) or poor contrast arrival ($n = 2$). In 8 patients the severest lesion was affected. Good correlations for diameter stenosis were observed for vessel-based ($n = 284$, $r = 0.82$, $p < 0.01$) and patient-based ($n = 92$, $r = 0.83$, $p < 0.01$) analysis. Bland-Altman analysis showed a mean difference (\pm standard deviation) between QCA and MSCT of 3.3 ± 12.9 % and 5.2 ± 14.5 %, respectively. In addition, subanalysis of lesions containing calcium also showed good correlations on vessel-based ($n = 140$, $r = 0.79$, $p < 0.01$) and patient-based ($n = 61$, $r = 0.80$, $p < 0.01$) analysis with a mean difference between QCA and MSCT of 2.8 ± 15.1 % and 5.7 ± 15.9 %, respectively.

Conclusions: Automated quantification of coronary stenosis severity can be performed using novel dedicated software and correlates well to QCA.

1036-252

Clinical Appropriateness, Economic Impact and Adverse Events Associated With Coronary Computed Tomography Angiography

Jeffrey J. Fine, Gerald G. Blackwell, Cardiovascular Associates, PC, Kingsport, TN

Background: We analyzed the clinical and economic impact of Coronary CT Angiography (CCTA) using the nation's largest data set (CCTA Data Registry). Questions remain from payors and clinicians regarding the clinical appropriateness, adverse event rates, and economic impact of CCTA. Data to answer these questions have not been previously available.

Methods: 64-slice CCTA cases from 34 practices/hospitals ($n=26,492$) from November, 2005 through March, 2008 were included. Demographic data, clinical indications, adverse events, and radiation exposure were obtained from databases and uniform data collection forms. We determined if patients had additional diagnostic procedures 30 days pre through 30 days post CCTA. This period defines a diagnostic episode. Mathematically, 11 imaging combinations exist. We grouped 6 combinations, which include three modalities into "layered tests". From frequency data, substitutions or additions can be derived. Mean reimbursements values were: nuclear perfusion (\$1311), diagnostic angiography (\$2800), CCTA (\$1000).

Results: Seventy-seven percent of CCTA studies were ordered due to chest pain, dyspnea, abnormal function study, or known CAD. Only 6% of CCTA studies were ordered based upon screening indications.

CCTA was used predominantly (74%) as a substitute for nuclear perfusion testing as the initial test ordered for the symptomatic patient. Significantly, CCTA was the solitary diagnostic test ordered for 66% of patients. Savings among the 34 practices to the healthcare system were \$14,931,228 over 3 years after subtracting the costs incurred due to layered testing, which only occurred in 3% ($n = 826$) of all cases. Savings per patient for imaging were \$563. Renal insufficiency and contrast allergy incidence were rare (0.1% and 0.4%, respectively). Mean radiation exposure was 7.2 mSv.

Conclusions: Our results suggest CCTA is utilized appropriately and provides savings for the health care system. This is supported by narrowly defined clinical indications and economically beneficial substitutions demonstrated. CCTA provides a less invasive, cost-effective strategy for diagnosis of coronary disease.

9:30 a.m.

1036-253

Cardiovascular Risk Scores and Coronary Plaque Burden as Detected by Computed Tomography for Detection of Acute Coronary Syndrome

Maros Ferencik, Christopher L. Schlett, Fabian Bamberg, John H. Nichols, Antonio J. Pena, Michael D. Shapiro, Ian S. Rogers, Sujith Seneviratne, Quynh A. Truong, Blair Alden Parry, Ricardo C. Cury, Claudia U. Chae, Thomas J. Brady, David F. Brown, John T. Nagurney, Udo Hoffmann, Massachusetts General Hospital, Boston, MA

Background: The value of risk scores to predict acute coronary syndrome (ACS) in patients presenting to the emergency department (ED) with acute chest pain appears to be limited. We determined the association of low, intermediate, and high risk categories of three scoring systems with the outcome of ACS and examined whether this association persisted after adjustment for coronary plaque burden as determined by cardiac CT.

Methods: We enrolled 368 subjects presenting to the ED with a chief complaint of acute chest pain and inconclusive initial evaluation (negative biomarkers, non-diagnostic ECG changes) and no history of CAD. All subjects underwent contrast-enhanced 64-slice cardiac CT and then completed standard care to rule out ACS with both patients and caregivers blinded to the CT results. CT data sets were evaluated for the presence of plaque in 17 coronary artery segments. The end-point of ACS (NSTEMI or unstable angina) was adjudicated by an independent committee according to AHA guidelines. Three cardiovascular risk scores were calculated: Goldman, TIMI and Sanchis score. Univariate and logistic regression analyses were performed in three models to determine the crude and adjusted (for the number of coronary artery segments with plaque) predictive value of each risk score stratified into low, intermediate and high risk categories for ACS.

Results: Among 368 subjects (53 ± 12 yrs, 61% men), 31 (8%) subjects were diagnosed with ACS. The risk for ACS increased significantly across categories of risk from low to intermediate to high. In unadjusted analysis the odds increased with each category for Goldman (OR 3.35, 95%CI 1.64-6.84, $p < 0.001$, AUC 0.62), Sanchis (OR 6.10, 95%CI 3.40-10.88, $p < 0.001$, AUC 0.79) and TIMI (OR 8.24, 95% CI 3.20-21.24, $p < 0.001$, AUC 0.63) scores. Goldman (OR 3.18, 95% CI 1.37-7.39, $p = 0.007$, AUC 0.89) and Sanchis (OR 4.30, 95% CI 2.26-8.17, $p < 0.001$, AUC 0.90) scores remained independent predictors of ACS even after adjustment for coronary plaque burden.

Conclusions: Goldman and Sanchis scores predict risk for ACS independent of coronary plaque burden. The combined information on risk scores and coronary plaque burden has excellent discriminatory power for ACS.

9:30 a.m.

1036-254

Assessment of Plaque Burden and Plaque Composition Using Multislice Computed Tomography Coronary Angiography: Implications for Risk Stratification

Jacob Van Werkhoven, Joanne D. Schuijff, Oliver Gaemperli, J. Wouter Jukema, Eric Boersma, Gabija Pundziute, Arthur Scholte, Ernst E. Van der Wall, Philipp Kaufman, Jeroen J. Bax, Leiden University Medical Center, Leiden, The Netherlands, University Hospital Zurich, Zurich, Switzerland

Background: Non-invasive multi-slice computed tomography coronary angiography (MSCT) allows assessment of plaque burden as well as plaque composition. The purpose of this study is to assess the prognostic value of these variables determined on MSCT.

Methods: 64-slice MSCT was performed in 474 patients (47% male, age 58±12 years) with suspected coronary artery disease (CAD) referred for cardiac evaluation. MSCT was scored using a 17 segment model for the presence and severity of atherosclerosis and for plaque composition (non-calcified, calcified and mixed plaque). The following events were recorded: all cause death, non-fatal infarction, and unstable angina requiring hospitalization.

Results: MSCT was normal in 155 patients (33%). In the 319 patients with atherosclerosis, non-significant CAD was observed in 203 (43%) and significant CAD (≥50% stenosis) in 116 (25%) patients. An event was observed in 23 patients (4.9%). Using univariate analysis, optimal segment cutoff values were obtained for plaque burden and plaque composition. After correction for baseline clinical variables the extent of CAD and the extent of non-calcified and mixed plaques remained independent predictors of events, whereas the extent of calcified plaques was not (Table).

Conclusions: Our observations suggest that plaque burden and plaque composition assessed with MSCT may be important prognostic markers. Potentially, integration of these variables in risk models may further improve risk stratification.

	HR (95%-CI)	p-value
Plaque burden		
≥8 diseased segments	6.9 (1.5-31.4)	0.013
≥6 obstructive segments	12.2 (2.2-69.5)	0.005
Plaque composition		
≥4 non-calcified plaque	4.7 (1.4-16.0)	0.014
≥4 mixed plaques	3.9 (1.1-13.1)	0.03
≥4 calcified plaques	1.6 (0.5-5.9)	ns

9:30 a.m.

1036-255

Three-Dimensional Coronary Venous Imaging With Computed Tomographic Angiography Facilitates Cardiac Resynchronization Therapy

Marc J. Givsky, Jerold S. Shinbane, Naser Ahmadi, Fred Flores, Songshao Mao, Matthew J. Budoff, Harbor-UCLA Medical Center, Torrance, CA, University of Southern California Keck School of Medicine, Los Angeles, CA

Background: Cardiovascular CT angiography (CTA) can visualize the coronary veins. We sought to assess the ability of CTA to facilitate resynchronization therapy (CRT) procedures.

Methods: Patients underwent CTA for characterization of cardiomyopathy prior to biventricular ICD implant. Randomization was performed with operator review of the CTA for coronary venous anatomy prior to CRT in one half of the cases. Invasive coronary venous angiograms were used in all procedures. Analysis included procedure times and utilization of contrast, fluoroscopy and guide catheters.

Results: Characteristics of the 26 patients enrolled were: mean age 55±11 years, male 76.9%, ischemic etiology 35%, ejection fraction 25±3%, Class III CHF 100%, and QRS duration 179±29 msec. Of patients enrolled, 22 had both CTA and procedure initiation. Three patients (2 with CTA review and 1 without CTA review) had aborted procedures due to hemodynamic issues. Analysis of the 19 remaining patients (7 with preprocedure CTA review and 12 without CTA review) demonstrated that preprocedure review of CTA coronary venous anatomy led to significantly decreased procedure times and utilization of contrast, fluoroscopy and guide catheters (Table 1).

Conclusions: Preprocedure review of CTA coronary venous anatomy leads to decreased procedural times and decreased procedural utilization of contrast fluoroscopy and guide catheters. These preliminary results will need to be evaluated in larger heart failure populations undergoing CRT.

Lab Times and Utilization With and Without Review of Coronary Vein Findings on CTA Prior to CRT

Variables	CRT with CTA Review N=7	CRT without CTA Review N=12	P Value
Venous Access to CS Cannulation Time (min)	38.3±4.1	41.2±5.3	0.04
CS Cannulation to Lead Placement Time(min)	33.4±4.5	38.5±3.4	0.01
Total Procedure Time (min)	122.1±5.3	136.1±6.3	0.01
Successful Final Lead Position	100%	100%	---
Total Contrast (cc)	83.2±13.2	108.1±12.1	0.01
Fluoroscopy Time (min)	18.1±3.4	24.4±3.4	0.01
Number of Guide Catheters Used	2±1	4±2	0.01

9:30 a.m.

1036-256

320-Slice Computed Tomography for Detection of Coronary Artery Stenoses

Marc Dewey, Elke Zimmermann, Florian Deissenrieder, Michael Laule, Hans-Peter Döbel, Wolfgang Rutsch, Bernd Hamm, Charité, Berlin, Germany

Background: For 16-slice and 64-slice coronary CT angiography, radiation exposures of 15 mSv on average have been reported. This high radiation exposure is a cause of concern, which might be alleviated by prospective scanning using volume CT with 320

simultaneous detector rows and acquisition of the entire cardiac anatomy in a single heartbeat.

Methods: Twenty-eight patients with suspected coronary artery disease (8 women, 20 men; mean age 60.8 ± 10 years) underwent coronary CT angiography using a 320-slice scanner (0.35 s gantry rotation time, 120 kV, and 350-450 mAs) prior to clinically indicated conventional coronary angiography (CCA). CT images were manually reconstructed in motion-free phases with 0.5-mm slice thickness and 0.25-mm slice increment. Blinded quantitative analysis of CT and CCA was performed by two independent readers to detect significant (at least 50%) diameter stenoses.

Results: Of the 28 patients, in 19 patients, single-heart beat CT acquisition was performed, resulting in an effective dose of 4.3 ± 0.9 mSv and an image reconstruction window length of 175 msec. The effective dose of CT in these patients was significantly smaller than that for CCA (4.3 ± 0.9 mSv vs. 8.9 ± 3.8, p<0.01). In the other 9 patients, because of higher heart rates (above 65 beats per minute), 2 or 3 heart beats were used for acquisition, resulting in higher radiation exposure (on average 16 mSv) and the possibility to perform multisegment reconstruction with improved temporal resolution (88 and 58 msec image reconstruction windows, respectively). Per-patient sensitivity and specificity for CT compared to CCA were 100% and 94%. Per-vessel sensitivity and specificity were 93% and 97%, respectively. Intraindividual comparison of CT with CCA revealed a significantly smaller contrast agent amount (80 ± 0 ml vs. 111.6 ± 16.2 ml, p<0.01) for 320-slice CT.

Conclusion: 320-slice coronary CT significantly reduces the contrast agent amount compared to CCA while radiation exposure is reduced in patients with slow heart rates. The diagnostic accuracy of coronary CT angiography using up to 320 simultaneous detector rows remains high on the per-vessel and per-patient levels as compared with CCA as the reference standard.

9:30 a.m.

1036-257

Predicting the Hemodynamic Significance of Coronary Stenoses With Multi-Detector Computed Tomographic Coronary Angiography

Benjamin J. W. Chow, Paul Galiwango, Arun Abraham, Robert deKemp, Rob S. Beanlands, Yeung Yam, Jean DaSilva, Terrence D. Ruddy, University of Ottawa Heart Institute, Ottawa, ON, Canada

Introduction: Studies have demonstrated that CT coronary angiography (CTA) has good operating characteristics for the detection of obstructive coronary artery disease (≥50% stenosis). Though CTA is able to assess coronary anatomy, there is a disparity between anatomical and hemodynamically significant stenoses, particularly in lesions with 50-69% stenosis. N-13 ammonia positron emission tomography (PET) has the ability to quantify myocardial blood flow and coronary flow reserve (CFR). The establishment of better anatomical predictors of hemodynamically significant lesions would be desirable. The objective of this study was to determine if various anatomical measures of stenosis can reliably predict the hemodynamic significance of coronary lesions as determined with quantitative N-13 ammonia PET.

Methods: Between January and May 2008, 24 consecutive patients with obstructive coronary stenoses (≥ 50%) detected with cardiac CT were prospectively enrolled and underwent quantitative N-13 ammonia PET MPI. CFR of < 2.3 was defined as abnormal flow. CTA anatomic measures were compared to CFR, and operating characteristics were determined.

Results: A total of 29 lesions (13 visually moderate and 16 visually severe) were analyzed. The agreement between visual stenosis assessment and regional CFR was fair (kappa = 0.65; 95%CI: 0.39-0.92). However, minimum cross-sectional area (CSA) appeared to be a better predictor of abnormal CFR with an AUC of 0.94 (95% CI: 0.83-1.0) and CSA of ≤1.35 mm² had a sensitivity of 92% and a specificity of 94% for a CFR < 2.3 (kappa = 0.91; CI: 0.77-1.0; p <0.0001).

Conclusions: We introduce a promising anatomic measure (minimum lesion CSA) which may accurately detect hemodynamically significant obstructive CAD.

9:30 a.m.

1036-258

A Novel Index of Coronary Artery Disease Severity by Multi-detector Computed Tomography

Hiroyuki Niinuma, Yasuko Fujisawa, Julie M. Miller, Kunihiro Yoshioka, Edward P. Shapiro, David E. Bush, Joanna J. Wykrzykowska, Pedro A. Lemos, Wolfgang Rutsch, Joao A.C. Lima, Armin Arbab-Zadeh, Iwate Medical University, Morioka, Japan, Johns Hopkins University, Baltimore, MD

Background: The severity of coronary artery disease (CAD) is currently expressed as diameter stenosis by conventional coronary angiography (CCA), requiring normal segments for reference which frequently have CAD. In contrast to CCA, multi-detector computed tomography (MDCT) is able to evaluate the entire vessel wall, including atherosclerotic plaque. We sought to investigate how coronary lumen volume, vessel wall volume, and total vessel volume by MDCT relate to CAD severity by CCA.

Methods: Eighty MDCT studies from the CORE-64 trial were selected for this analysis based on good image quality. Three indices were obtained from cross-sectional lumen and outer wall contours of all segments within the three coronary arteries with lumen diameter ≥ 2.0 mm in one mm intervals: 1) Lumen volume/ Vessel volume (LV/VV), 2) Wall volume/ Vessel volume (WV/VV), 3) Wall volume/Lumen volume (WL/LV). The maximum logarithmically transformed variables per artery and per patient were compared to CAD severity by modified Duke coronary artery disease index (DCADI) and quantitative CCA to three categories: no/mild disease (N) <30% (n=25), moderate disease (M) 50-70% (n=28), and severe disease (S) >70% (n=27).

Results: Data are shown in the Table.

Conclusions: An index of WV/LV obtained semi-automatically by MDCT showed excellent discriminative power to assess CAD severity by DCADI and CCA. This atherosclerotic

index could become an effective tool to evaluate patients with CAD in the clinical and epidemiological setting.

Relationship between atherosclerotic indices and DCADI

	correlation coefficient	p value
LV/VV	-0.16	ns
WV/VV	0.66	<0.001
WV/LV	0.71	<0.001

Discrimination power of atherosclerotic indices for severity of coronary artery disease

	N (n=25)	M (n=28)	S (n=27)	N vs. M	N vs. S	M vs. S
	(mean±SD)				(p value)	
Patient based						
LV/VV	-0.14±0.03	-0.18±0.03	-0.16±0.04	<0.01	ns	<0.05
WV/VV	-0.17±0.06	-0.07±0.03	-0.03±0.03	<0.001	<0.001	<0.001
WV/LV	0.36±0.19	0.83±0.24	1.47±0.54	<0.001	<0.001	<0.001
Vessel based						
LV/VV	-0.18±0.05	-0.20±0.05	-0.20±0.04	<0.01	<0.05	ns
WV/VV	-0.19±0.08	-0.10±0.05	-0.06±0.06	<0.001	<0.001	<0.001
WV/LV	0.33±0.24	0.67±0.26	1.18±0.61	<0.001	<0.001	<0.001

Abbreviations: DCADI: Duke coronary artery disease index, LV/VV: lumen volume/vessel volume, WV/VV: wall volume/vessel volume, WV/LV: wall volume/lumen volume, N: normal disease, M: moderate disease, S: severe disease.

9:30 a.m.

1036-259 Gender Differences in Coronary Plaque Composition by Coronary Computed Tomography Angiography

Michael Blaha, Juan Rivera, E. K. Choi, S. I. Choi, S. A. Chang, E. J. Chun, H. K. Kim, D. J. Choi, Roger S. Blumenthal, H. J. Chang, Khurram Nasir, Johns Hopkins Hospital, Baltimore, MD

Background: Coronary computed tomography angiography allows the differentiation of non-calcified, calcified, and mixed coronary artery plaques. While males have a higher total plaque burden for a given age, there is currently little data regarding age-adjusted gender differences in plaque morphology and composition.

Methods: The study population consisted of 1,043 asymptomatic South Korean subjects (49±10 years, 62% men) referred for 64-slice MDCTA. Plaque characteristics were analyzed on a per-segment basis according to the modified AHA classification. Multiple regression analysis was employed to describe the relationship between gender and plaque type prevalence (≥2 affected segments) after adjustment for age and other cardiovascular risk factors.

Results: Males had a greater prevalence of coronary plaque (13% vs. 3%, p<0.0001). Men were more likely to have calcified (4% vs. 1%, p=0.004) and mixed (5% vs. 1%, p<0.0001) plaque, while the prevalence of non-calcified plaque was similar across gender (2% vs. 1%, p=0.24). After multivariable adjustment, men were 7-8 times more likely to have calcified and mixed coronary plaque, while no gender difference was observed for non-calcified plaque (see table).

Conclusion: There were significant gender differences in plaque composition. Future studies will determine if these differences contribute to the accelerated cardiovascular risk observed in men.

	Females	Males (Age-adjusted)	Males (Model 1*)
Prevalence of ≥2 coronary segments with plaque		OR (95% CI)	OR (95% CI)
Non-calcified	1 (ref)	2.23 (0.71-6.97)	0.87 (0.20-3.92)
Calcified	1 (ref)	7.81 (2.27-26.95)	8.17 (2.21-30.16)
Mixed	1 (ref)	6.17 (2.29-16.59)	6.92 (2.17-22.08)

* Model 1: Adjusted for age, diabetes mellitus, hypertension, smoking, LDL-C, HDL-C, triglycerides, BMI, and family history of premature CHD

9:30 a.m.

1036-260 Accuracy of Aortic Distensibility Index Measured by Computed Tomography: Association With Vascular Dysfunction and Coronary Artery Calcification

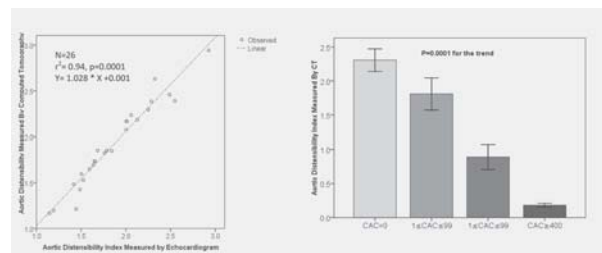
Naser Ahmadi, Hussain Ismaeel, Wahid Nabavi Larjani, Fereshteh Hajsadeghi, Manzoor Bevinall, Ferdinand Flores, Song S. Mao, Gary P. Foster, Matthew Budoff, Los Angeles Biomedical Research Institute at Harbor UCLA Medical Center, Torrance, CA

Introduction: Previous studies have evaluated the relation between aortic distensibility index (ADI) and conventional cardiovascular risk factors. The purpose of this study was to evaluate the relationship between ADI measured by computed tomographic angiography (CTA) and 2 dimensional transthoracic echocardiography (2DTE) and to correlate these findings with coronary artery calcification (CAC).

Methods: 229 subjects (age 63±9 years, 42% female) underwent CAC and CTA. End-systolic and end-diastolic diameter of aortic cross section area (CSA) were measured 16 mm above the left main coronary ostium. Aortic distensibility index (ADI) was defined as: ADI = Δlumen CSA/(lumen CSA at end diastole x systemic pulse pressure). In a sub-study, the CTA measured ADI was compared with 2DTE measured ADI in 26 subjects without CAC.

Results: ADI measured by CTA correlated closely with ADI measured by echocardiography ($r^2 = 0.94$, $p=0.0001$). CTA measured ADI decreased proportionally from CAC=0 ($2.64±0.49$) to CAC ≥1, ≤99 ($1.81±0.41$) to CAC ≥100, ≤399 ($0.89±0.32$) to CAC ≥400 ($0.18±0.09$) ($p=0.001$). After adjustment for age, gender and cardiac risk factors, the odds ratio of lowest vs. 2 upper tertiles of ADI was 1.54 for CAC ≥1, ≤99, 3.64 for CAC ≥100, ≤399 and 5.44 for CAC ≥400 compared to CAC=0.

Conclusion: ADI measured by CTA correlates well with ADI measured by 2DTE and decreased proportionally with the extent of CAC.



9:30 a.m.

1036-261 Prospective Randomized Trial On Radiation Dose Estimates of CT Angiography In Patients Scanned With a 100kV Protocol: The PROTECTION II Study

Jörg Hausleiter, Tanja Meyer, Franziska Hein, Martin Hadamitzky, Eugenio Martuscelli, Iris Pschierer, Gudrun Feuchtnner, Benedict Czernak, Paz Catalan, Bernhard Bischoff, Stefan Martinoff, Stephan Achenbach, Deutsches Herzzentrum München, Munich, Germany

Background: Concerns have been raised about the exposure to ionizing radiation associated with coronary CT angiography (CCTA) which is increasingly used as a non-invasive method for the detection of obstructive coronary artery disease. A reduced tube voltage of 100 kV has been shown to be an effective means to reduce radiation exposure, but the diagnostic image quality of 100kV scans has been questioned. The Prospective Randomized Trial On Radiation Dose Estimates Of CT Angiography In Patients Scanned With A 100kV Protocol (PROTECTION II) study is an international, multicenter and multivendor study investigating the impact of a 100kV tube voltage on image quality and radiation exposure.

Methods: Non-obese patients (body weight <90 kg) with a stable sinus rhythm were randomized to either CCTA with a tube voltage of 120 kV (control group) or 100 kV. Image quality is assessed using a 4-point score (1: nondiagnostic - 4: excellent image quality). The primary study endpoint of this non-inferiority study is to demonstrate that the diagnostic image quality of the 100kV tube voltage protocol is not inferior to the standard 120 kV tube voltage protocol (non-inferiority margin: 0.2 points in image quality score), while radiation exposure is significantly reduced. Among others, the secondary endpoints comprise the clinical need for additional diagnostic tests within 30 days after CCTA. Radiation dose estimates are derived from the dose length product (DLP) and a conversion coefficient for the chest ($0.014 \text{ mSv} \cdot \text{mGy}^{-1} \cdot \text{cm}^{-1}$).

Results: The enrollment process, which started in January 2008, has been successfully completed with the targeted 400 randomized patients in October 2008. The data analysis is currently ongoing.

Conclusions: The final data of the PROTECTION II - study which investigates the impact of a 100kV tube voltage on image quality and dose reduction in CCTA will be presented.

9:30 a.m.

1036-262 Incidence of Contrast-Induced Nephropathy With Intravenous Administration of Contrast Medium Iodixanol for Computed Tomographic Angiography

Carsten Matthias Schmalfuss, CTA Investigator Panel, University of Florida, Gainesville, FL

Background: To report renal function information in a large number of patients undergoing computed tomographic angiography (CTA) following intravenous (IV) administration of iso-osmolar iodixanol.

Methods: In five prospective, multi-center, open-label CTA studies, patients with known or suspected coronary artery disease, known or suspected peripheral arterial occlusive disease, or known or suspected abdominal visceral vascular (renal and hepatic arteries) disease, underwent cardiac or peripheral/visceral CTA with a single IV bolus administration of iodixanol 320 mg-I/mL. Patient hydration protocol was standardized across all studies and centers. Serum creatinine (SCr) values were measured at baseline and 24 hours (peripheral and abdominal CTA studies) or 48 hours (3 cardiac CTA studies) as part of overall safety monitoring. Contrast-induced nephropathy (CIN) was determined by two definitions: SCr increase of ≥25% or of ≥0.5 mg/dL from baseline. Occurrence of CIN was correlated with factors known to increase risk for CIN.

Results: 887 patients (mean age: 58.9 y; 64.9% men) had complete SCr measurements. CIN developed in 4.4% patients (39/887) using definition of ≥25%; and 0.7% patients (6/887) using ≥0.5 mg/dL. Rate of CIN was higher in patients with baseline renal insufficiency, diabetes, age >75 years, use of NSAIDs, and history of cardiovascular disease. The only factor associated with a significant difference was history of cardiovascular disease using SCr increase of ≥25% ($p=0.006$).

Conclusion: The incidence of CIN in patients undergoing CTA following IV administration of iodixanol was low. Only history of cardiovascular disease significantly increased risk for CIN.

9:30 a.m.

9:30 a.m.

1036-263

Diagnostic Efficacy of 320-Multislice Cardiac Computed Tomography in Patients With Atrial Fibrillation

Atsushi Hirohata, Keitao Senoh, Masaaki Murakami, Eiki Hirose, Keisuke Ohkawa, Shinji Sato, Ryotaro Yamada, Koichi Yoshimura, Yasuhiro Imai, Minako Ohara, Masatoshi Tsunoda, Keizo Yamamoto, The Sakakibara Heart Institute of Okayama, Okayama, Japan

Backgrounds: Despite its substantial efficacy in diagnosing coronary artery disease, multislice coronary CT is still discouraged in patients with atrial fibrillation (AF) due to image quality. The purpose of this study was to assess the diagnostic value of 320 multislice CT angiography (320-CTA) in AF patients.

Methods: Three-hundred-twenty multislice coronary CTA procedures were performed in 87 consecutive AF patients with suspected coronary artery disease. In order to perform CTA with the lowest heart rate possible, 20-40mg of oral metoprolol was administered to all study patients one hour prior to CTA. Image quality was evaluated by 2 isolated investigators using a blinded fashion, and images were scored using: 1 (unacceptable), 2 (acceptable) and 3 (excellent). In addition, the relationships between image quality and heart rate (HR), or coronary artery calcification score (agatston score, CACS), and calcium volumetric score (CVS) were also examined.

Results: Mean patient age was 71±9 (years) and 66% (57) were male. Mean HR of AF was 61±14 (/min), and maximum / minimum HR, due to AF fluctuation effect, was 64±19 / 58±15 (/min). Mean CACS and CVS were 511 ± 971 and 431 ± 785, respectively. ECG gated reconstruction CTA images were adapted for 48 (55%) patients from one cardiac beat, 37 (43%) from two beats, and 2 (2%) from three beats. With respect to scored image quality analysis, 64 (74%) patients obtained 3 points, 22 (25%) patients for 2 points, and only 1 (1%) patient for 1 point. Although there was no relationship between image quality and HR or AF fluctuation effect, low image quality (scored 1 or 2) cases were frequently observed in higher CACS (>700) and CVS (>600) cases (22/23, 96%, for CACS > 700 and 22/23, 96% for CVS > 600).

Conclusions: In using 320 multislice CT angiography for AF patients, image quality was not interrupted due to optimal patient preparation combined with an imaging reconstruction strategy. However, severely calcified lesions still pose a challenge in image acquisition for this state-of-the-art modality.

9:30 a.m.

1036-264

Vascular Dysfunction Measured by Digital Thermal Monitoring Strongly Correlates With the Extent of Coronary Artery Disease Diagnosed by 64 Slice Multidetector Computed Tomography

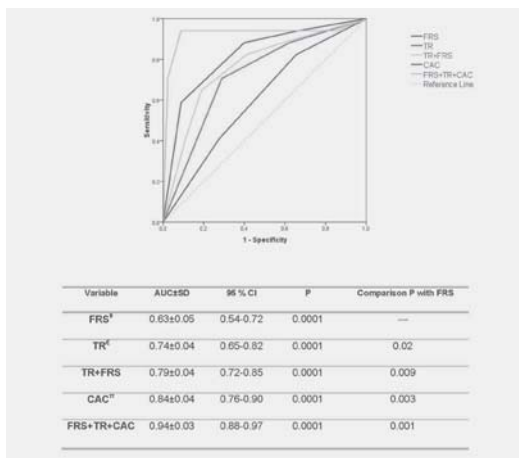
Naser Ahmadi, Sumithra Tirunagaram, Vahid Nabavi Larijani, Vivek Nuguri, Manzoor Bevinall, Anila Saeed, Fereshteh Hajsadeghi, Nudrat Usman, Harvey Hecht, Morteza Naghavi, Matthew Budoff, Los Angeles Biomedical Research Institute at Harbor UCLA Medical Center, Torrance, CA

Background: Previous studies have demonstrated the correlation between vascular dysfunction measured by digital thermal monitoring (DTM) and Framingham Risk Score (FRS) as well as coronary artery calcification (CAC). This study evaluates the correlation between DTM and the extent of coronary artery disease (CAD) measured by computed tomography angiography (CTA).

Methods: 181 patients, age 63±9 years, 68% male, underwent DTM (during a 5 minute arm-cuff induced reactive hyperemia), CAC scoring and CTA. Fingertip temperature rebound (TR) was used as DTM index of vascular reactivity and FRS was calculated. Obstructive CAD was defined as ≥50% luminal stenosis.

Results: TR decreased significantly from normal coronaries (0.99±0.12) to non-obstructive CAD (0.67±0.09) to obstructive CAD (0.15±0.08) (P<0.05). After adjusting for age, gender and cardiac risk factors using logistic regression analysis, the odds ratio for lowest vs. 2 upper tertile of TR was 3.8 (95% CI 1.1- 14.4, p=0.008) for non-obstructive CAD and 8.5 (95% CI 1.8-19.8, p=0.006) for obstructive CAD compared to normal coronaries. The combination of TR, FRS and CAC resulted in the area under ROC curve equal to 0.94 to diagnosis of obstructive CAD.

Conclusions: In patients suspected of coronary artery disease, severely impaired vascular reactivity is strongly associated with obstructive CAD. Further studies are needed to corroborate our findings and define the clinical utility of DTM for cardiovascular risk assessment.



1036-265

Asymmetrical Distribution of Shear Stress Is Related to Plaque Accumulation in Coronary Atherosclerosis: A Study With In Vivo Color Mapping of Shear Stress Using Coronary Multi-detector Computed Tomography

Yusaku Fukumoto, Takafumi Hiro, Mitsuyuki Hiromoto, Masakazu Tanaka, Michio Yamada, Masunori Matsuzaki, Shuto General Hospital, Yanai, Japan, Yamaguchi University Graduate School of Medicine, Ube, Japan

Background: Shear stress is one of the most important physical factors in the process of atherosclerosis. However, noninvasive in-vivo visualization of shear stress distribution along the coronary luminal surface has been technically difficult. We previously demonstrated a novel noninvasive way of color mapping of shear stress in coronary artery using a 64-row multi-detector computed tomography (MDCT) (Circulation 116, II-342, 2007). The purpose of this study was to investigate the relationship between shear stress distribution and pattern of coronary plaque accumulation with using in-vivo color mapping of shear stress with MDCT.

Methods: A total of 180 proximal cross sections of LAD and LCx from 30 patients were imaged with MDCT. The outer-curvature (out-Th) and inner-curvature (in-Th) thickness of plaque were measured, and then plaque eccentricity index (P-ecc) was calculated as in-Th divided by out-Th. The color mapping of shear stress distribution was performed as we recently documented (J Am Coll Cardiol, 51:645, 2008). The spatial resolution was 0.05 mm². The flow was considered to be a constant laminar one, and the pulsatile motion was neglected. The value of shear stress as well as its asymmetry (shear stress of a plaque surface divided by the value of its counterpart wall) were then measured. The relationship between these values and patient's risk factor profiles was also evaluated.

Results: The plaque thickness was significantly inversely correlated with shear stress value (r=-0.36, p<0.0001). Shear stress asymmetry for each vessel cross-section was significantly correlated with P-ecc (r=0.57, p<0.0001). Especially, these relationships were more remarkable in patients (n=80) without diabetes mellitus (DM) (r=-0.56, p<0.0001 and r=0.72, p<0.0001, respectively), whereas less significant in patients with DM.

Conclusions: Our original noninvasive color mapping way of shear stress distribution using MDCT indicated that the degree and pattern of local coronary plaque accumulation was significantly related to the value and the asymmetrical distribution of shear stress. This relationship might be modified by general factors such as DM.

9:30 a.m.

1036-266

GFR Independently Predicts the Presence of Coronary Plaque, by 64-MDCT, Among Patients With GFR>60 ml/min and Normal LV Ejection Fraction

Hussain Isma'eel, Vahid Larijani, Yasmin S. Hamirani, Jigar Kadakia, Mathew J. Budoff, Harbor-UCLA, Torrance, CA

Background: Lower glomerular filtration rate (GFR) has been associated with adverse cardiovascular outcomes. Using 64-MDCT we are capable of visualizing 3 types of plaques -calcified, mixed and non-calcified- with very high sensitivity and specificity. We investigated the association of GFR and coronary plaque in a group of patients with 'normal kidney function' (GFR>60 ml/min/1.73 m²) and normal left ventricular (LV) function. **Methods:** One hundred eighty patients (Age 61.96 (+/-12.17) yrs.; 61.7% Males) were randomly selected from a group of 1085 patients scanned at our outpatient center. GFR was calculated using the MDRD equation (ml/min/1.73m²) correcting for ethnicity and gender. **Results:** In our cohort 20.6% patients had DM type II; 2.8% were currently smokers; 35% were dyslipidemic; 47.8% had hypertension; and 55.6% had positive family history of coronary artery disease (CAD). Of the classical risk factors for CAD: male gender, DM type II, and smoking were significantly associated with the presence of any plaque (Pearson Chi²: 6.5, 6.0 and 7.0; p<0.05 respectively). Patients with no plaque had a GFR of 89.73 (+/-21.53) in comparison to 81.24 (+/-15.81) in patients with plaque; p<0.01. In multi-logistic regression, only increased GFR (OR 1.028; p<0.03) and female gender (OR 2.78; p<0.03) were independently associated with normal coronaries. **Conclusion:** Early decrease in GFR is independently associated with the presence of plaque detected by 64-MDCT, even among patients categorized within "normal" range.

9:30 a.m.

1036-267

Diagnostic Accuracy of 320-Slice Multi-Detector Row Computed Tomography to Detect Coronary Artery Disease: A Direct Comparison to Invasive Coronary Angiography

Jonathan Chan, Sheryar Sarwar, Faisal Khosa, Milliam Kataoka, Marie-Claire Paicopolis, Roger Laham, Melvin E. Clouse, Beth Israel Deaconess Medical Center, Harvard Medical School, Boston, MA

Background: The aim of this study was to evaluate the diagnostic accuracy of 320-slice multi-detector row computed tomography (MDCT) to identify significant coronary artery disease. The new 320-slice MDCT has improved spatial and temporal resolution and allows acquisition of the whole heart by single rotation over one heart beat.

Methods: Forty-seven consecutive patients were referred for cardiac MDCT to investigate for coronary artery disease. All examinations were performed with 320-slice MDCT using retrospective ECG gating with half-scan reconstruction method with a single cardiac cycle. All acquisitions could be achieved by a single rotation with coverage width of 16cm. Ten out of 47 patients (mean age 70±13, Body mass index 26±3 kg/m²) with abnormal MDCT results underwent invasive coronary angiography. The diagnostic accuracy of MDCT to detect significant coronary artery stenosis (>50%) was compared with invasive coronary angiography as the standard of reference. Results were analyzed by 2 independent

observers using the 15 coronary segment model of the American Heart Association.

Results: Of 145 segments, 96% could be assessed by both MDCT and invasive coronary angiography. The mean time interval between the 2 procedures was 10±5 days. The mean heart rate during MDCT acquisition was 60±5/min. The mean calcium score was 815 Agatston Units with 30% of patients above calcium score of 400. Specificity, sensitivity, positive and negative predictive values by segment analysis to detect significant coronary artery stenosis were 98%, 80%, 89%, and 97% respectively. Overall diagnostic accuracy was 96%.

Conclusion: The 320-slice MDCT is a robust potential diagnostic tool for non-invasive coronary artery assessment with novel single rotation and single cycle acquisition capabilities. It has excellent diagnostic accuracy with high positive and negative predictive values.

9:30 a.m.

1036-268

The Diagnostic Accuracy of 64-Slice Cardiac Computed Tomography Compared With Stress Nuclear Imaging and Exercise Treadmill Test in Patients Undergoing Cardiac Catheterization

Yasmin Hamirani, Paul Drury, Wayland Lim, Hussain Isma'eel, Mathew J. Budoff, Los Angeles Biomedical Research Institute at Harbor-UCLA, Torrance, CA

Background: Compared with conventional coronary angiography (CCA), Multidetector Cardiac Computed Tomography (MDCT) has shown promising accuracy in the detection and confirmation of coronary stenosis. Myocardial perfusion imaging (MPI) using SPECT is an established method for noninvasively assessing the functional significance of coronary stenosis. This retrospective analysis compared the accuracy of MDCT, MPI and treadmill exercise test (TMT) in the detection of hemodynamically relevant lesions of coronary arteries.

Methods: 52 symptomatic patients with cardiac catheterization who also had MPI and MDCT evaluations done within 6 months period at our center were included in the study. TMT was used for stress in 41 (79%) patients for MPI. Lesion stenosis reported >70% was considered to be significant on both MDCT and CCA

Results: Seventy three percent of the patients were males, 26% with diabetes, 49% with hypertension and 18% were smokers. The sensitivity, specificity and negative and positive predictive values in detecting significant coronary lesions on CCA for MDCT were 84%, 65%, 86.5% and 60% respectively and for MPI 52%, 57%, 76% and 31% respectively. Amongst the 14 patients with normal CCA 5 patients (35%) had disease documented on CTA and amongst them 3 patients who also had TMT done had normal results. Sixteen patients (42%) with positive CCA had both abnormal MPI and MDCT.

Conclusion: Compared with MPI, MDCT provided important information and identified significant lesions in symptomatic intermediate to high risk patients. Use of Prospective multi-centered studies is needed to further evaluate these findings. TMT can complement CTA in its diagnostic accuracy, which should be evaluated by further studies.

9:30 a.m.

1036-269

Comparison of Prospective ECG: Triggering Versus Retrospective Gating for Computed Tomography Coronary Angiography and Evaluation of Stress-Only SPECT/CT Hybrid Imaging

Lars Husmann, Bernhard A. Herzog, Oliver Gaemperli, Fuminari Tatsugami, Nina Burkhard, Ines Valenta, Patrick Veit-Haibach, Christophe A. Wyss, Ulf Landmesser, Philipp A. Kaufmann, University Hospital Zurich, Zurich, TN, Switzerland

Background: To determine diagnostic accuracy, effective radiation dose, and potential value of computed tomography coronary angiography (CTCA) for hybrid imaging with single-photon emission computed tomography (SPECT) comparing prospective electrocardiogram (ECG)-triggering versus retrospective ECG-gating.

Methods: Two hundred patients underwent myocardial SPECT perfusion imaging, which served as standard of reference. One hundred consecutive patients underwent 64-slice CTCA using prospective ECG-gating, and were compared to 100 patients who had previously undergone CTCA using retrospective ECG-gating.

Results: For predicting ischemia CTCA with prospective ECG-triggering and a stenosis cut-off >50% had a per-vessel sensitivity, specificity, positive and negative predictive value of 100%, 84%, 100%, and 30%, respective values for CTCA with retrospective ECG-gating were similar ($P=n.s.$): 86%, 83%, 98%, and 33%. Combining CTCA with stress-only-SPECT revealed 100% clinical agreement with regard to perfusion defects, and provided additional information in half the patients on preclinical coronary findings. Effective radiation dose was 2.2±0.7mSv for CTCA with prospective ECG-triggering, and 19.7±4.2mSv with retrospective ECG-gating ($P<0.001$) (5.4±0.8 vs. 24.1±4.3mSv for hybrid imaging).

Conclusions: Prospective ECG-triggering for CTCA reduces radiation dose by almost 90% without affecting diagnostic performance. Combined imaging with stress-only-SPECT is an attractive alternative to standard stress/rest-SPECT for evaluation of coronary artery disease, offering additional information on premature atherosclerosis.

9:30 a.m.

1036-270

UKPDS Coronary Heart Disease Risk Score Correlates With Extent and Type of Plaque on 64 Slice Coronary CT Angiography in Asymptomatic Type II Diabetics

David A. Halon, Idit Dobrecky-Meri, Tamar Gaspar, Mali Azencot, Nathan Peled, Basil S. Lewis, Lady Davis Carmel Medical Center, Haifa, Israel

Background: Features of coronary arterial plaque may predict subsequent coronary events in asymptomatic high risk individuals. We examined differences in extent and characteristics of coronary plaque in type 2 diabetics and their relation to 10 yr risk for late events defined by the UK Prospective Diabetic Study (UKPDS) score.

Methods: Coronary CT angiography (64 slice) was performed in 120 asymptomatic diabetics (63% women, age 55-74 (mean 63.7) yrs) enrolled in an ongoing prospective outcomes trial. Coronary arteries were examined using a 17 segment model and presence or absence of plaques was assessed on a segmental basis and plaques characterized as calcified (≥50% calcium), non-calcified (no calcium) or mixed (<50% calcium).

Results: Plaque was present in 105/120 (87.5%) pts. UKPDS risk correlated with total number of coronary segments with plaque, calcified plaque and non-calcified plaque but not with mixed plaque (Table). Plaque causing luminal narrowing (>25%) showed similar correlation with UKPDS for total and non-calcified plaque only.

Conclusions: In asymptomatic type 2 diabetics: 1. Overall extent of coronary plaque and of segmental luminal narrowing correlated with UKPDS risk score for adverse clinical outcome events. 2. Extent of non-calcified and calcified plaque correlated individually with risk score for adverse clinical outcome events. 3. In presence of plaque causing appreciable luminal narrowing only extent of total and non-calcified plaque correlated with patient risk score.

UKPDS risk score and prevalence and characteristics of coronary plaque

	Total	Calcified	Non-calcified	Mixed
N of coronary segments with plaque (mean±1SD)				
UKPDS risk				
Low (N=23)	2.2±2.1	1.3±1.8	0.39±0.89	0.57±0.84
Medium (N=46)	3.7±2.7	1.9±2.0	1.2±1.4	0.74±1.1
High (N=38)	5.6±3.3	3.4±3.0	1.3±1.4	1.1±1.6
p-value	<0.001	0.012	0.006	0.232
Coronary segments with luminal narrowing >25%				
p-value	<0.001	0.202	0.007	0.095

9:30 a.m.

1036-271

Multidetector Computed Tomography for Detecting Coronary Artery Disease: Experience and Follow-up in 900 Consecutive Patients in a Single Center

Ricardo Baeza, Alvaro Huete, Luis Meneses, Nicolas Ahumada, Jose Vidal, Ercilia Vasquez, Bernardita Gaete, Cristian Cabrera, Catholic University Hospital, Santiago, Chile

Background: Multidetector computed tomography coronary angiography (64-MDCT-CA) is a well established method for evaluating coronary anatomy and the presence of coronary artery disease (CAD). We sought to evaluate the usefulness of MDCT to predict clinical outcome in a long term follow up, based on the information provided by a single center registry.

Methods: We did include, in prospective fashion, all the patients referred to our center to undergo a 64-MDCT-CA, from January 2007 till August 2008. All demographic and clinical information were included in a database to perform clinical follow up until one year after the exam. Previous to the 64-MDCT-CA, a Coronary Calcium Score (CCS) was acquired only in patient without previous PCI or CABG. The images were acquired after the administration of 80 cc of iodated contrast intravenously, that was followed by 20 cc of a saline solution. All the images were analyzed in a dedicated working station, using multiplanar and 3D reconstruction. For purposes of this analysis, the result was presented as: NORMAL= without evidence of CAD; NS= for non significant (<50%) stenosis; and POSITIVE= for significant (≥ 50%) coronary stenosis. Follow-Up (F/U) was done by telephone in every patient at 30 day, 6 month; and 12 months.

Results: We included 900 patients during the aforementioned period of time. The most common reasons to be referred for a 64 MDCT-CA, were non typical chest pain (58 %); non diagnostic ergometry (35%) and abnormal resting ECG (15 %). Main characteristic of the analyzed population were: Male 72%; Mean Age 55 ±9 y/o; Diabetes 29 %; Tobacco 32%; previous CABG 9%; previous PCI 12%. Mean CCS was 78 ± 233. Mortality was 0.3 % for the whole population. During the F/U 10 % of patient had new chest pain episode, and a 15 % of patients needed a revascularization procedure. Patients with one or more events during the F/U had a higher mean CCS compared with patients without events (238 vs 66). Also patients with clinical events had more POSITIVE (88%) vs those without events (10%), $p=0.023$

Conclusions: Beyond the anatomic information provided by 64 MDCT-CA, having a normal or non significant CAD result, is associated with a good clinical outcome.

9:30 a.m.

1036-272

Frequency of Immediate and Short-Term Procedure-Related Complications in a Large Ongoing Prospective Registry of Patients Undergoing Coronary Computed Tomography Angiography

Aiden Abidov, Kavitha M. Chinnaiyan, Michael Gallagher, Gilbert L. Raff, William Beaumont Hospital, Royal Oak, MI

Background:

Most of the safety data related to use of the coronary CTA (CCTA) protocols was obtained from small studies with limited and highly selected study populations. We report results of the analysis of immediate and short-term (3 months) complications based on data acquired from the unique ongoing community-based prospective registry enrolling patients undergoing CCTA in order to develop quality improvement (QI) strategies and stimulate best-practice utilization of CCTA.

Methods: According to our last monitoring results in September 2008, the registry included data of 2767 patients (54% men; age 57±13 yrs, BMI 29.3±6.0) who had CCTA at William Beaumont Hospitals since July 2007. Amount of IV contrast given during CTA was 89±18 ml; 97% of pts were given sublingual nitroglycerin. Total of 87% pts received heart-rate lowering medications before the scan. Of those, 97% had beta-blockers

(intravenous-25%) and 3% had calcium-channel blockers.

Results: There was a very low incidence of the complications reported (Table). Only 0.3% of all CTA scans were aborted due to the complications or technical problems. We observed a significant decrease in frequency of the complications in 2008 compared to the initial studies obtained in 2007.

Conclusions: CCTA protocols currently used in the real-world cardiac imaging practice are safe and have a very low incidence of complications. These results demonstrate importance of ongoing QI control and education measures in improving CCTA safety and effectiveness.

	2007 (n=1272)	2008 (n=1495)	Overall population (n=2767)
Any Complications from CTA	1.4%	0.2% (p<0.001 vs. 2007)	0.7%
Contrast Infiltration	0.3%	0.1%	0.2%
Rash/hives	0.3%	0.1%	0.2%
Symptomatic Bradycardia	0.1%	0	0.04%
Respiratory distress	0.1%	0	0.04%
ER Visit/Hospitalization	0.3%	0	0.2%
Anaphylaxis	0.1%	0	0.04%
Other Complications	0.2%	0	0.1%
Contrast-induced nephropathy (documented on 3 months follow-up)	0.1%	0	0.04%

9:30 a.m.

1036-273

The Value of Clinical Risk Stratification by the Morise Score in Assessing the Presence of Obstructive and Nonobstructive Coronary Artery Disease in Symptomatic Women

Susie N. Hong, Jennifer H. Mieres, Jill E. Jacobs, Parag Patel, Camille A. Pearte, Monvadi B. Srichai, New York University Medical Center, New York, NY

Background: Coronary artery disease (CAD) is the leading cause of morbidity and mortality in the U.S. Early identification of CAD, particularly among symptomatic women, is critical given their worse outcomes as compared to men. We evaluated the predictive role of the Morise Score, a simple clinical risk score incorporating estrogen status and family history, in the assessment for obstructive and non-obstructive CAD as determined by computed tomography coronary angiography (CTCA) in women at risk for ischemic heart disease.

Methods: For 140 consecutive symptomatic women with no known CAD referred for CTCA imaging, Morise scores were calculated and risk stratified accordingly to likelihood of CAD. CTCA studies were evaluated for the presence and degree of CAD, defined by the existence of any atherosclerotic plaque, and classified as normal, non-obstructive (<50% stenosis), or obstructive (>50% stenosis). Total calcium score was calculated based on Agatston score. Statistical analyses were performed using t-tests and analysis of variance.

Results: By Morise score, 10 (7%) women were stratified as low, 60 (43%) as intermediate, and 70 (50%) as high risk. There was no CAD by CTCA in 45 (32%) women. CAD was present in 95 (68%) women, with 73 (52%) classified as non-obstructive and 22 (16%) as obstructive. Morise scores significantly correlated with calcium score (p<0.00001), as well as the presence of normal (mean 12.7) versus non-obstructive (mean 16.1) or obstructive (mean 17.0) CAD (p<0.00001). There was no significant difference for distinguishing non-obstructive versus obstructive CAD, although a slight trend was noted (p=0.12). All women deemed low risk by the Morise score were without evidence of CAD.

Conclusion: An intermediate or high risk Morise score demonstrates an excellent correlation with the presence of CAD in women. Given the higher mortality and challenges in assessing atherosclerotic burden among women with CAD, clinical risk stratification using the Morise score, with further characterization by CTCA, may play a role in the early identification of any CAD in symptomatic women.

9:30 a.m.

1036-274

Serum Uric Acid Levels Predict the Severity and Morphology of Atherosclerotic Plaques in Coronary Arteries Detected by Multidetector Computed Tomography

Ergun Baris Kaya, Hikmet Yorgun, Ugur Canpolat, Hamza Sunman, Aysegül Ülgen, Tuncay Hazırolan, Musturay Karcaaltınca, Ahmet Hakan Ates, Hakan Aksoy, Kudret Aytemir, Giray Kabakçı, Lale Tokgözoğlu, Nâsîh Nazlı, Hilmi Özkutlu, Deniz Akata, Ali Oto, Hacettepe University Faculty of Medicine, Department of Cardiology, Ankara, Turkey, Hacettepe University Faculty of Medicine, Department of Radiology, Ankara, Turkey

Background: There are several studies, showing the relationship between elevated serum uric acid (UA) levels and increased risk of cardiovascular disease. The aim of this study was to evaluate whether serum UA levels were associated with the severity and morphology of atherosclerotic plaques in coronary arteries, shown by multidetector computed tomography.

Methods: A total of 821 consecutive patients (mean age 57.5 ± 11.6 years, 410 men) who underwent MDCT for the assessment of coronary artery disease in our hospital were involved in the study. All demographic parameters and MDCT data of patients were collected. MDCT parameters were used for the assessment of the severity and morphology of the coronary atherosclerosis. Serum UA levels were determined using commercially available assay kits.

Results: The critical atherosclerotic lesions (>50 % narrowing of luminal diameter) were

detected in 264/821(32.2%) subjects by MDCT. Basal characteristics of two groups categorized according to the severity of coronary atherosclerotic lesions detected by MDCT, were similar. Serum UA levels were found to be higher in patients with critical stenosis (5.3±1.3 mg/dl vs 5.8±1.5 mg/dl, p<0.001). When patients were stratified into having primarily mixed, non-calcified and calcified plaques (defined as > 70% of all segments including coronary atherosclerotic plaque), subjects having primarily calcified plaques have higher serum UA levels compared to other patients having other types and normal coronary arteries (6.04±1.6 vs 5.29±1.3 for normal coronaries, 5.45±1.4 for noncalcified plaques, 5.52±1.3 for mixed plaques, respectively, p=0.005).

Conclusions: These findings have shown that serum UA level was significantly associated with coronary artery disease severity and coronary plaque morphology, detected by MDCT angiography. Our study provides insight into the relation of serum uric acid levels to both plaque characteristics and degree of coronary stenosis.

9:30 a.m.

1036-275

Prospective-Triggered 64 Slice CT Compared to Invasive Cardiac Catheterization in Patients With a High Prevalence of Coronary Artery Disease

Kelley R.H. Branch, Arzang Fallahi, David Lockhart, Justin Strote, Lee M. Mitsumori, William P. Shuman, Janet May, James H. Caldwell, University of Washington, Seattle, WA

Introduction: Prospective ECG-triggered cardiac CT (P-CT) using a 64 slice scanner provides at least equivalent image quality with significantly less radiation than retrospective-gated CT. However, P-CT diagnostic capabilities are not well established.

Methods: This retrospective study compared 37 patients with both P-CT and ICA. 64 slice P-CT used 0-30% R-R padding with max mA 600, kVp 120, and 0.625 mm/slice. All patients received beta blockers. Twenty segment coronary models were visually scored for the presence of CAD and quintiles of % stenosis. P-CT's diagnostic ability was compared to ICA, the imaging standard, at patient, vessel, and segmental levels using >50% and >70% stenosis thresholds for "significant" CAD. P-CT radiation dose was calculated from dose-length products.

Results: Prevalence of CAD (ICA stenosis >50%) was 72%. CT indications included possible ischemia (31%), pre-sternotomy (25%), chronic occlusion (14%), or anomalous coronary or equivocal stress test (6% each). 380 total segments were compared. Overall diagnostic performance is outlined in the Table. Non-evaluability of segments was 3% in CT and 6% in ICA (OR 3.1, p=.12). Overall, PPV was lower than the NPV and similar between 50% or 70% stenosis cutoffs. The ROC area under the curve was 0.87 for segmental analysis. Average radiation dose was 8.6±4.0 mSv.

Table: Diagnostic Performance of Prospective Triggered CT Compared to ICA

	Sensitivity	Specificity	Positive Predictive Value	Negative Predictive Value
>50%				
Patient	1.00	0.70	0.90	1.00
Vessel	0.86	0.84	0.76	0.91
Segment	0.79	0.92	0.70	0.95
>70%				
Patient	0.96	0.67	0.85	0.89
Vessel	0.78	0.88	0.73	0.90
Segment	0.65	0.95	0.70	0.94

Conclusions: PCT compares favorably to ICA with few non-evaluable segments with a relatively low radiation dose. P-CT has a high NPV and modest PPV in a high CAD population.

9:30 a.m.

1036-276

Obstructive Coronary Plaque Is Less Calcified Than Nonobstructive Plaque on 64 Slice Cardiac Computed Tomography in Asymptomatic Type II Diabetics

David A. Halon, Tamar Gaspar, Idit Dobrecky-Meri, Mali Azencot, Nathan Peled, Basil S. Lewis, Lady Davis Carmel Medical Center, Haifa, Israel

Background: We prospectively examined 64 slice coronary CT angiograms (CTA) in an asymptomatic patient cohort at high risk for coronary events to examine differences in characteristics of coronary plaque between pts with non-obstructive disease and pts with coronary luminal narrowing.

Methods: Type 2 diabetics, 55-74 yr, with no history of coronary disease underwent CTA in the confines of a prospective, ongoing, outcomes study. Coronary luminal narrowing was assessed visually as <25%, 25-50% or >50% and plaque as absent, calcified (≥50% calcium), non-calcified (no calcium) or mixed (<50% calcium) using a 17 segment coronary arterial model.

Results: In 120 pts (44, 36.7% men, age (men and women) 63.7 yr) coronary plaque was present in 40 (90.9%) men and 65 (85.5%) women (ns) but was more extensive in men (5.7±3.4 vs 3.2±2.2 coronary segments, p=0.001; total plaque length 56±56 vs 30±31 mm, p=0.02). In plaques <25% narrowed calcified plaque was predominant (70.9%), whereas in segments narrowed >50% non-calcified plaque was commonest (50.0%) and calcified plaque the minority (11.1%) (p<0.001) (Table). Findings were similar for men and for women.

Conclusions: In asymptomatic type 2 diabetics: 1. Coronary plaques were present on 64 slice cardiac CTA in most patients (>85% women, >90% men). 2. Obstructive (>50%) coronary plaques were less often calcified than minimal or intermediate non-obstructive plaques. 3. Progression of plaque to luminal stenosis appears to be due to mechanisms unrelated to calcification.

Plaque characteristics in relation to severity of luminal narrowing

	Total segments with plaque	Calcified	Non-calcified	Mixed
Narrowing	N (% total)	N (% within narrowing)		
<25%	258 (55.4)	183 (70.9)	29 (11.2)	46 (17.8)
25-50%	156 (33.5)	58 (37.2)	44 (28.2)	54 (34.6)
>50%	52 (11.1)	6 (11.5)	26 (50.0)	20 (38.5)
	P<0.001	P<0.001		

9:30 a.m.

1036-277

Elevated High Sensitive C-Reactive Protein and White Blood Cell Count Are Strongly Associated With Mixed Coronary Plaque Burden Assessed by Noninvasive Cardiac Computed Tomography Angiography in Asymptomatic Subjects

Juan J. Rivera, Khurram Nasir, Eue-Keun Choi, Sang-il Choi, Sung Chang, Eun-Ju Chun, Hyung-Kwan Kim, Dong-Joo Choi, Roger S. Blumenthal, Hyuk-Jae Chang, Johns Hopkins University, Baltimore, MD, Seoul National University Bundang Hospital, Seoul, South Korea

Background: The purpose of this investigation was to assess the association between coronary plaque sub-types and increasing CRP and WBC count, both markers of inflammation, using non-invasive coronary computed tomography angiography (CCTA).

Methods: The study population consisted of 1043 asymptomatic Korean individuals (mean age: 49±10 years, 63% males) free of known cardiovascular disease who underwent 64-slice CCTA. The study population was divided according to tertiles of CRP and WBC count. Multivariable logistic regression analysis was employed to investigate the association between CRP level and WBC count with plaque sub-types, after adjusting for traditional risk factors.

Results: No coronary plaque was observed in 826 (79%) study participants, whereas 115 (11%) and 102 (10%) had 1 or ≥2 segments with atherosclerotic plaques, respectively. Unadjusted analyses demonstrated a positive relationship between increasing number of coronary segments with mixed coronary plaques (MCAP) and increasing levels of CRP (<0.00001) and WBC count (0.0007). The table illustrates that the association persisted after adjusting for CV risk factors.

Conclusions: Increase inflammation is associated with the presence of MCAP, which in turn has been associated with a higher degree of vulnerability. Clinical outcomes studies are needed to establish if individuals with this biochemical and coronary anatomic profile are at an increase risk to develop a coronary event.

Increasing levels of CRP and WBC were independently associated with MCAP burden

Prevalence of 2 or more segments with coronary plaque	CRP 1st tertile<br OR (95% CI)	CRP 2nd tertile<br OR (95% CI)	CRP 3rd tertile OR (95% CI)
Non calcified	1 (ref)	1.6 (0.3-8.3)	1.5(0.5-4.5)
Calcified (> 50% of plaque area calcified)	1 (ref)	1.0(0.3-3.7)	0.6(0.2-1.5)
Mixed (< 50% of plaque area calcified)	1 (ref)	2.8(0.7-10.8)	3.9(1.7-9.2)
Total	1 (ref)	1.3(0.6-3.0)	1.5 (0.9-2.6)
Prevalence of 2 or more segments with coronary plaque	WBC 1st tertile OR (95%CI)	WBC 2nd tertile OR(95% CI)	WBC 3rd tertile OR(95% CI)
Non calcified	1 (ref)	1.1(0.3-4.2)	1.2(0.3-4.4)
Calcified (> 50% of plaque area calcified)	1 (ref)	0.5(0.2-1.5)	0.3(0.1-0.9)
Mixed (< 50% of plaque area calcified)	1 (ref)	2.5(0.8-7.9)	4.0(1.3-12.0)
Total	1 (ref)	0.8(0.4-1.6)	1.1(0.6-2.0)

9:30 a.m.

1036-278

Saphenous Vein Graft Plaque Characterization by Multidetector Computed Tomography With Histopathological Correlation of Embolic Debris During Intervention

Gary Y. Liew, Christopher J. Hammett, Anthony C. Thomas, Benjamin K. Dundon, Matthew I. Worthley, Azfar G. Zaman, Stephen G. Worthley, Royal Adelaide Hospital, Adelaide, Australia, Flinders Medical Centre, Adelaide, Australia

Background: Recent studies have shown encouraging results in ability of multi-detector computed tomography (MDCT) to quantify and characterize coronary plaques. We sought to investigate the relationship between saphenous vein graft (SVG) plaque volume and density determined on MDCT, and the composition and amount of embolic debris during SVG intervention.

Methods: Sequential patients (n=27) undergoing SVG stenting for angina were consented in this study and had MDCT scanning. In all cases a distal protection device, FilterWire EZ (Boston-Scientific, USA) was used. All MDCT images were analysed by two investigators blinded to the results. Amount of embolic debris captured by the FilterWire were weighed then fixed and stained for histopathological assessment by a pathologist blinded to results. High resolution digital images of histopathology slides were analysed using computer software (ImagePro Plus, Media Cybernetics, USA) to measure absolute

and percentage areas of each plaque component: fibrous, thrombus, lipid, red blood cells and cholesterol clefts. Spearman's correlations were used as appropriate.

Results: Data were obtained in 25 patients (n=27 lesions). The inter-observer variability for MDCT plaque volume and Hounsfield Unit measurements were 3.6% and 7.2% respectively. Every FilterWire yielded some embolic material. Plaque volumes correlated with embolic weight (r=0.463; p=0.015) and total area of material on histology (r=0.514; p=0.007). Plaque volume also correlated well with embolic material containing thrombus (r=0.74; p=0.001) and lipid (r=0.613; p=0.009). Plaque density on MDCT had an inverse relationship with embolic weight (r=-0.508; p=0.007) and lipid content of embolic material (r=-0.539, p=0.026).

Conclusion: We have demonstrated that greater plaque volumes tend to produce greater embolic material during SVG intervention. There are good correlations between larger plaque volumes and embolic debris that contain more thrombus and lipid components. Plaques with higher density tend to produce less embolic debris and have less lipidic content. Use of MDCT for atherosclerotic plaque characterisation warrants further investigation.

9:30 a.m.

1036-279

Low Framingham Risk Score Category: How Abnormal Are Carotid Ultrasound and Coronary Computed Tomography Angiogram Results?

Dennis P. Doan, Rabeea Aboufakher, Susanna Szpunar, Renee Bess, Howard Rosman, Gerald Cohen, St. John Hospital & Medical Center, Detroit, MI

Background: Carotid intimal-medial thickness (IMT) and calcium score by coronary computed tomography angiogram (CCTA) have also been shown to predict cardiovascular risk. Framingham risk score (FRS) may not identify patients with low short-term but high lifetime risk for coronary heart disease. We determined the prevalence of abnormal findings in the low FRS group and evaluated the association between FRS, carotid ultrasound, and CCTA.

Method: 136 non-diabetic patients (72% male, age 58±10 years) underwent CCTA for calcium scoring and degree of coronary artery stenosis. Carotid ultrasound was performed to measure IMT. FRS was divided into 3 risk categories according to Adult Treatment Panel III.

Result: Of 136 patients, 57% were in low, 32% in moderate, and 11% in high FRS risk. A high percentage of low FRS patients had abnormal imaging findings (table A). From logistic regression, FRS was a significant predictor for increased carotid IMT, Ca⁺⁺ score >100, and coronary stenosis. Compared to the low FRS group, patients in moderate and high-risk groups had higher odd ratios for increased carotid IMT, elevated Ca⁺⁺ score, and coronary stenosis (table B). The inverse association with LDL is most likely a result of treatment effect.

Conclusion: A high percentage of low FRS patients had abnormal imaging findings. Therefore, FRS alone may significantly underestimate long-term cardiovascular risk. Further study is needed to determine whether combining FRS and non-invasive imaging can better evaluate long-term risk.

A. Abnormal Findings in Low FRS Group			
Carotid IMT > 1.5 mm	Ca++Score > 100	Coronary Stenosis > 0%	Coronary Stenosis > 50%
49%	14%	37%	8%
B. Odds Ratios from Multiple Logistic Regression			
	Carotid IMT ≥1.5mm	Ca++Score > 100	Coronary Stenosis >0%
FRS			
Intermediate vs. Low	5.1 (p=0.001)	7.3 (p<0.0001)	4.5 (p<0.0001)
High vs. Low	13.0 (p=0.016)	10.5 (p=0.001)	8.8 (p=0.004)
LDL	NS	0.99 (p=0.017)	0.99 (p=0.014)

9:30 a.m.

1036-280

Diagnostic Efficacy of 64-Slice CT Coronary Angiography in the Evaluation of In-Stent Restenosis: A Meta-Analysis

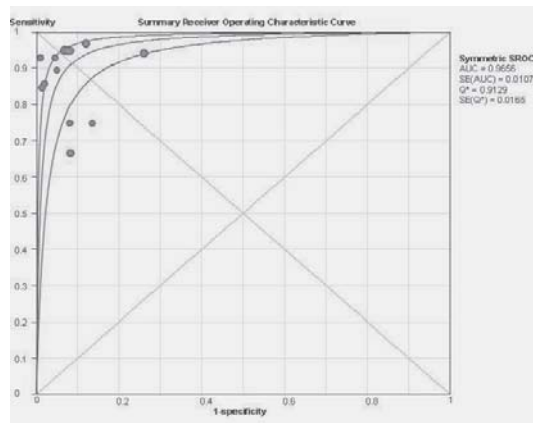
Dharam J. Kumbhani, Christopher P. Ingelmo, Paul Schoenhagen, Ronan J. Curtin, Scott D. Flamm, Milind Y. Desai, Cleveland Clinic, Cleveland, OH

Background: Multi-slice computed tomography (MSCT) allows non-invasive assessment of coronary vessels. However, artifacts limit evaluation of stented segments. We conducted a meta-analysis using available studies to study the diagnostic efficacy of 64 MSCT in evaluating in-stent restenosis (ISR).

Methods: We included studies that utilized 64 MSCT for evaluation of ISR. We pooled efficacy estimates across studies using random effects models.

Results: We identified 12 studies, with 785 patients (1,171 stents; mean diameter = 3.1 mm). Of these, 90% were adequately assessed by MSCT. Overall sensitivity was 91% (95% CI 86 - 94), specificity was 91% (95% CI 89 - 93), positive predictive value (PPV) was 69% (95% CI 63 - 75), and negative predictive value (NPV) was 98% (95% CI 97 - 99). The summary ROC graph showed a symmetric area under the curve of 0.97 (Figure). On inclusion of non-assessable segments, the sensitivity decreased to 86% (95% CI 79 - 91), specificity to 86% (95% CI 83 - 89), PPV to 57% (95% CI 0.50 - 0.63), and NPV to 97% (95% CI 0.95 - 0.98). Meta-regression indicated that the diagnostic performance improved by 67% per mm increase in stent diameter (95% CI 3 - 170, p=0.04).

Conclusions: 64 MSCT detects (high sensitivity and specificity) or excludes ISR (high NPV) with a high-degree of confidence; however, precise quantification of ISR is not accurate (low PPV). Efficacy estimates are even lower when non-assessable segments are included. Diagnostic performance is enhanced with increasing stent diameter.



9:30 a.m.

1036-281

High Risk Subclinical Coronary Atherosclerosis Is Associated With Impaired Macro and Micro-Vascular Reactivity

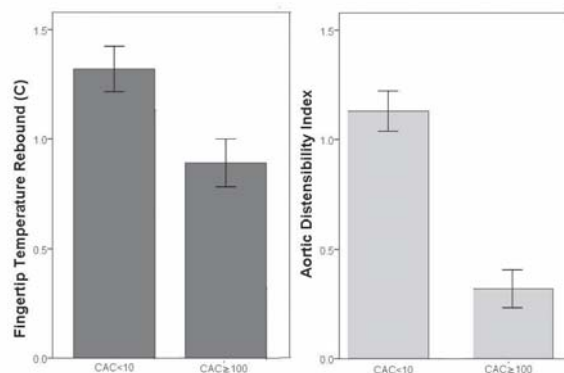
Naser Ahmadi, Vahid Nabavi Larijani, Fereshteh Hajsadeghi, Manzoor Bevinall, Ferdinand Flores, Song S. Mao, Harvey Hecht, Morteza Naghavi, Matthew Budoff, Los Angeles Biomedical Research Institute at Harbor UCLA Medical Center, Torrance, CA

Introduction: Aortic distensibility index (ADI) is a measure of macrovascular reactivity, and reactive hyperemia index (RHI) is a measure of microvascular reactivity. We investigated whether ADI measured by CT angiography and RHI measured by Digital Thermal Monitoring (DTM) correlate with coronary artery atherosclerosis measured by coronary artery calcium (CAC).

Methods: 116 subjects (age 59±6 years, 38% female) underwent DTM, CAC and CTA. DTM was done during a 5-minute arm-cuff occlusion induced reactive hyperemia procedure. Fingertip temperature rebound (TR) was studied as the index of microvascular reactivity. End-systolic and End-diastolic diameter of aortic cross-sectional area (CSA) were measured 16 mm above the left main coronary ostium. Aortic distensibility index (ADI) was defined as: $ADI = \Delta \text{lumen CSA} / (\text{lumen CSA in diastole} \times \text{pulse pressure})$.

Results: TR correlated well with ADI ($r = 0.738$, $p = 0.001$). ADI and TR reduced significantly in $CAC \geq 100$ compared to $CAC < 10$ ($P < 0.05$) (Figure). After adjustment for age, gender and cardiac risk factors, the odds ratio of lowest vs. 2 upper tertiles of ADI was 3.52 in $CAC \geq 100$ and 4.76 in the lowest tertile of TR. Addition of TR to ADI increased area under ROC curve from 0.70 to 0.81 to predict $CAC \geq 100$.

Conclusion: High risk coronary artery calcification is associated with reduced micro and macro vascular reactivity. Further studies are needed to evaluate the predictive value of concomitant low ADI and low RHI for identification of high risk coronary patients.



9:30 a.m.

1036-282

Coronary Risk Stratification in Women: Correlation With Coronary CT Angiography

Kavitha M. Chinnaiyan, Aiden Abidov, Gilbert Raff, William Beaumont Hospital, Royal Oak, MI

Background: Clinical risk assessment for coronary artery disease (CAD) may fail to identify women with CAD. Coronary computed tomography angiography (CCTA) has high diagnostic accuracy when compared to invasive coronary angiography and may be of use to reliably risk stratify women.

Methods: This retrospective study included women with no prior history of CAD who underwent CCTA. Significant (SIG) CAD was defined as calcium score (CAS) >400 units and/or coronary stenosis of >50%. Pre-test probability of CAD was determined by the

ACC/AHA criteria. SIG and non-significant (defined as no CAD, CAS <400 and/or stenosis <50%) groups were compared for pre-test likelihood scores and binary logistic regression model used to evaluate the strongest predictors of SIG CAD.

Results: The cohort consisted of 681 women (mean age 56 ± 10 yrs). Indications for CCTA were symptoms of CAD, non-diagnostic stress test and/or unfavorable risk factor profile. CAD and SIG-CAD were found in 278 (41%) and 99 (15%), respectively. The strongest univariable predictors of SIG-CAD were age ($p < 0.001$), diabetes or metabolic syndrome ($p < 0.001$), dyslipidemia ($p < 0.001$), and hypertension ($p = 0.002$), the strongest multivariable predictors of SIG CAD displayed in Table. Presence and/or type of symptoms were not predictive of CAD and 62% women of SIG CAD had low or intermediate pre-test likelihood of disease.

Conclusions: Nearly two-thirds of women with SIG CAD do not have a high pre-test probability of CAD and symptoms are not predictive of CAD on CCTA.

MULTIVARIABLE PREDICTORS OF SIG-CAD

SIG-CAD	p VALUE	ODDS RATIO	95% CI
AGE	<0.0001	1.07	1.04-1.09
DIABETES	<0.0001	2.15	1.54-3.00
DYSLIPIDEMIA	0.0066	2.07	1.23-3.49
FAMILY HX CAD	0.0564	1.59	0.99-2.55

9:30 a.m.

1036-283

The Detection of Cancer With Multidetector Computed Tomography Coronary Angiography

Seiji Habara, Hiroyuki Yamamoto, Kazuaki Mitsudo, Kazushige Kadota, Tsuyoshi Goto, Satoki Fujii, Harumi Kato, Naoki Oka, Yasushi Fuku, Shingo Hosogi, Akitoshi Hirono, Toru Kawakami, Takeshi Maruo, Hiroyuki Tanaka, Daiji Hasegawa, Masao Imai, Otsuru Suguru, Chinatsu Yamada, Yoji Okamoto, Masakazu Miyamoto, Naoki Saito, Kentaro Shibayama, Yuki Tsujimoto, Kurashiki central hospital, Kurashiki, Japan

Purpose: The purpose of the present study was to determine the prevalence of cancer in asymptomatic patients undergoing 64-multidetector computed tomography coronary angiography (CTCA).

Methods: The study group consisted of 1646 consecutive patients who received CTCA between October 2006 and June 2008 at our institute. Patients with known cancers were excluded from the analysis. The scan volume was determined from the neck level to the diaphragmatic level. Experienced cardiologist and radiologist evaluated both cardiac and non-cardiac structures.

Results: A total of 59 patients (3.0%) had suspected cancer requiring further investigations. Of 59 patients, cancers were revealed in 18 patients (1.0%), including 8 lung cancers, 3 renal cell cancers, 3 breast cancers, 2 hepatic cancers, 1 pancreas cancer and 1 bladder cancer. Six patients diagnosed with cancer have significant coronary artery stenosis. These non-cardiac findings influenced the strategy for management of coronary artery disease. **Conclusions:** The detection of cancer with CTCA is more important, concerning antiplatelet therapy in the setting of PCI.

9:30 a.m.

1036-284

Does Minimal Dose Radiation in CT Coronary Angiography Radiation Dose Have Implications for Clinical Image Quality?

John R. Lesser, Peter Eckman, Carolina Masri, Bjorn Flygenring, Thomas Knickelbine, Terry Longe, Robert S. Schwartz, Minneapolis Heart Institute Foundation, Minneapolis, MN

Background: Reducing radiation exposure without compromising image quality is critical in CT angiography. This study assessed the effect of weight-based scanning protocols on imaging quality compared to a conventional protocol.

Methods: Radiation doses were calculated in 3 cohorts of consecutive patients referred for assessment using a dual source scanner. Cohort 1 (C1) included 180 patients. EKG modulation included a "pulsed" window of 30-70% of R-R interval. KVP remained at 120 and mA (450-850) was adjusted to chest diameter. KVP was decreased to 100 for weight <85 kg in cohort 2 (C2, n=155). The window of full radiation exposure was narrowed according to heart rate (65-65% up to 40-65%) and "non-pulsed" period of dose modulation was reduced between 4-20% if LV function was desired. Cohort 3 (C3, n=256) used a weight-based protocol for KVP and injection rate (80 KVP + 5 cc/s if 100 kg). Dose of 4% was used in the "non-pulsed" period of radiation dose modulation for all patients. Scan quality was assessed quantitatively with signal-to-noise and contrast-to-noise ratios and qualitatively by comparison to angiography when available.

Results: Patients were well matched (50% F, mean weight 87 kg and BMI 30 kg/m²). Dose declined significantly across cohorts: C1-19.5±7 mSv, C2-9.8±5 mSv, C3-7.3±4 mSv. Signal-to-noise ratios in the left main coronary artery was significantly different between C1/C2 and C3, respectively: 24.3±20, 24.4±22, and 17.0±8 ($p < 0.0004$). However, contrast-to-noise ratios was improved in C3 compared to C1/C2, 11.0±4 versus 9.7±4, 9.2±4. 59/591 patients subsequently underwent angiography (11.7%, 9.0%, and 5.4% in the 3 cohorts). No significant difference in concordance using a patient based CTA assessment with angiographic findings was found.

Conclusions: A protocolized weight based approach to radiation exposure using helical CCTA resulted in important dose reduction in a heterogeneous consecutive population without significant decrement in image quality or reading accuracy

9:30 a.m.

9:30 a.m.

1036-285

Increased Epicardial Adipose Tissue in Patients With Acute Coronary Syndrome and Association With Non-Calcified Plaque With Positive Remodeling as Assessed by Multislice Computed Tomography

Norihiro Ohashi, Hideya Yamamoto, Toshiro Kitagawa, Futoshi Tadehara, Tomoki Shokawa, Hiroki Teragawa, Takafumi Ishida, Yasuki Kihara, Hiroshima university, Hiroshima, Japan

Background: Epicardial adipose tissue (EAT) is reported to be associated with calcified coronary plaque. However, no study has measured EAT volume in patients with acute coronary syndrome (ACS) or investigates its association with vulnerable plaque by 64-slice computed tomography (CT).

Methods: This is a cross-sectional study of consecutive 115 male patients (mean 65±11 yrs) who were suspected of coronary artery disease and underwent 64-slice CT coronary angiography. We assigned patients to the ACS (non-ST-segment elevation myocardial infarction [NSTEMI], and unstable angina, n = 21) or the non-ACS group (equivocal or positive cardiac stress test, atypical chest pain, or stable angina, n = 94). Sixty-four-slice CT was used to measure EAT volume and abdominal visceral adipose tissue (VAT) area and to determine the characteristics of coronary plaque. Each non-calcified plaque (NCP) was evaluated with the minimum CT density, vascular remodeling index (RI), and morphology of adherent calcium deposits.

Results: The EAT volume was highly correlated with the VAT area ($r=0.64$, $p<0.001$) and was associated with traditional cardiovascular risk factors. Patients with ACS had a greater EAT volume compared with non-ACS subjects ($193\pm86\text{ml}$ vs. $101\pm51\text{ml}$, $p<0.001$). The prevalence of patients having NCP with positive remodeling ($RI>1.05$) was significantly different between ACS and non-ACS groups (100% [21/21] vs. 22% [21/94], $p<0.001$). Patients with positive remodeling also had a greater EAT volume than those without ($148\pm53\text{ml}$ vs. $105\pm68\text{ml}$, $p<0.001$). In multivariable logistic regression analysis, EAT remained as an independent predictor of ACS status (OR [95%CI] per 1-SD increase in EAT: 3.9 [2.2-9.1]) and positive remodeling lesions (1.6 [1.2-2.2]) even after adjustment for traditional risk factors and VAT.

Conclusions: EAT volume is increased in patients with ACS and is associated with vulnerable plaque characterized by 64-slice CT.

9:30 a.m.

1036-286

Measurement of Coronary Atherosclerotic Plaque Volumes by Contrast-Enhanced Multi-detector CT: Correlation to IVUS

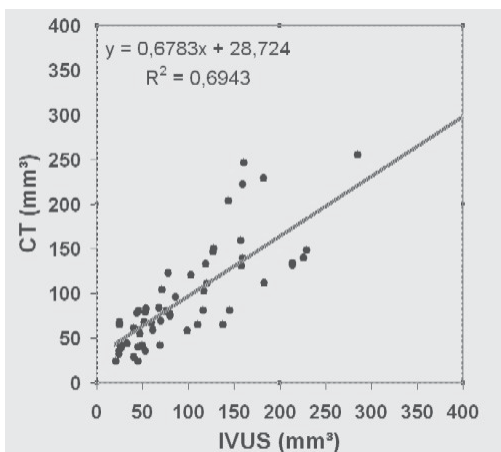
Stephan Achenbach, Martin Seltmann, Mohamed Marwan, Tobias Pfleiderer, Tiziano Schepis, Dieter Ropers, Werner G. Daniel, Department of Cardiology, University of Erlangen, Erlangen, Germany

Very limited data is available concerning the accuracy of CT angiography to quantify coronary atherosclerotic plaque. We therefore validated the accuracy of multi-detector CT (MDCT) to measure the volume of coronary plaques against intravascular ultrasound (IVUS).

Methods: 40 patients who underwent contrast-enhanced MDCT and invasive coronary angiography with IVUS were analyzed. CT data were acquired using Dual-Source or 64-slice CT (64x0.6mm collimation, 330ms rotation) with i.v. contrast (70 ml, 5 ml/s). Beta blockers were given to all patients with a heart rate > 60/min. IVUS (40 MHz) was performed with motorized pullback (0.5 mm/s). MDCT data sets were analyzed to identify single coronary atherosclerotic plaques that had distinct proximal and distal borders in the coronary artery that was studied by IVUS. The volume of these plaques were independently measured in CT by manually tracing plaque contours in serial cross-sectional reconstructions and in IVUS by manual tracing of plaque borders.

Results: 58 coronary atherosclerotic plaques were identified in MDCT and IVUS (LM: 9, LAD: 32, LCX: 2, RCA: 15). Mean plaque volume was $97\pm40\text{ mm}^3$ in MDCT (24 mm^3 - 278 mm^3) and $101\pm74\text{ mm}^3$ in IVUS (21 mm^3 - 401 mm^3 ; $p = \text{n.s.}$). Correlation between IVUS and MDCT was close ($r^2 = 0.69$, $p < 0.001$, see graph). Bland-Altman Analysis revealed a mean absolute difference of 31 mm^3 (35%) and significant influence of plaque size on CT accuracy.

Conclusion: MDCT allows volumetry of coronary plaques with close correlation to IVUS.

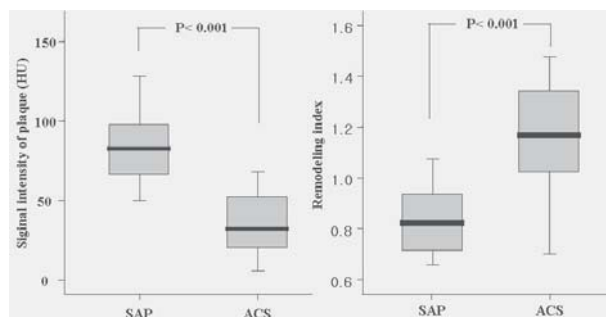


1036-287

Noninvasive Assessment of Coronary Artery Lesions Between Stable Angina and Acute Coronary Syndrome by Multislice Computed Tomography

So Yeon Kim, Kee Sik Kim, Young Soo Lee, Jin Bae Lee, Jae Kean Ryu, Ji Young Choi, Sung-Gug Chang, Daegu Catholic University Hospital, Daegu, South Korea

Background: Disruption of coronary artery plaque is the primary cause of acute coronary syndrome (ACS). The vulnerable, rupture-prone plaques are characterized by large plaque volumes and large necrotic cores with thin fibrous caps. The positive remodeled vessels and small calcific concretions in fibrous cap have been shown to contribute to plaque instability. We evaluated characteristics of culprit coronary lesions between ACS and stable angina pectoris (SAP) using multislice computed tomography (MSCT). **Methods:** 64-slice MDCT was conducted on 37 patients with 18 patients with ACS and 19 patients with SA before percutaneous coronary intervention (PCI). The culprit coronary lesions were evaluated for signal intensity of plaque, spotty calcification, outer vessel diameter and area in culprit lesion characteristics and remodeling index (RI). The remodeling index was defined as the ratio of lesion diameter and mean of proximal and distal reference diameter. **Results:** In patients with ACS, culprit coronary lesions had significantly higher remodeling index than patients with SA ($p < 0.001$). The plaque of culprit coronary lesions in patients with ACS were predominantly non-calcified (46% vs 32%, $p=0.02$). In addition, lower SI and more spotty calcification were observed in the plaque of culprit lesions in patients with ACS ($p = 0.02$, $p < 0.001$). **Conclusions:** In our study, the culprit lesions of ACS had higher remodeling index, lower SI of plaque and spotty calcification.



9:30 a.m.

1036-288

Cardiac Events Predicted by Computed Tomography Coronary Angiography

Robert Donnino, Jill E. Jacobs, Jay V. Doshi, Seema Pursnani, James S. Babb, Danny C. Kim, Steven P. Sedlis, Monvadi B. Srichai, New York University School of Medicine, New York, NY, Veterans Affairs NYHCS New York Campus, New York, NY

Background: Although computed tomography coronary angiography (CCTA) is a widely used and sensitive imaging modality for the detection of coronary artery disease (CAD), its prognostic utility remains uncertain. Our objective was to evaluate clinical outcomes based on CCTA findings.

Methods: We evaluated outcomes in 201 consecutive out-patients (mean age 57±11 years; 64% male) who underwent 64-slice CCTA (Sensation 64 or Definition, Siemens) between February 2005 and July 2006 for coronary evaluation. Patients were divided into 3 groups based on CCTA findings: 1) "Normal" patients had no detectable plaque in any coronary artery; 2) "non-obstructive CAD" patients had plaque with less than 50% luminal stenosis in at least one major coronary artery; and 3) "obstructive CAD" patients had greater than 50% luminal stenosis in at least one coronary artery. Patients were assessed for clinical events at a minimum of six months after the CCTA.

Results: Patients were followed for a mean of 18 months (range 8 to 29). There were no cardiac events (non-fatal myocardial infarction, coronary revascularization, or cardiac death) in the normal group, and only one cardiac event (revascularization) in the non-obstructive CAD group (see Table). In contrast, 15 of 62 patients with obstructive CAD (24%) had cardiac events.

Conclusion: A normal CCTA is associated with an excellent short-term prognosis. Outcomes worsen as the severity of CAD detected on CCTA increases.

Clinical Outcome	Normal Coronaries (N=33)	Non-obstructive CAD (N=104)	Obstructive CAD (N=63)
Any Cardiac Event	0	1%	24%
Coronary Revascularization	0	1%	21%
Myocardial Infarction	0	0	2%
Cardiac Death	0	0	2%
Any non-cardiac event	0	3%	0
Stroke	0	2%	0
Non-cardiac Death	0	1%	0

ACC.ORAL CONTRIBUTIONS

905

Echocardiography: New Applications

Monday, March 30, 2009, 10:30 a.m.-Noon

Orange County Convention Center, Room W308C

10:30 a.m.

0905-3

Left Atrial Volume Index and Left Ventricular Geometry Independently Predict Mortality in 16,904 Elderly Patients With Preserved Ejection Fraction

Dharmendrakumar A. Patel, Carl J. Lavie, Jr., Richard V. Milani, Hector O. Ventura, Ochsner Clinic Foundation, New Orleans, LA

Background: LV geometry predicts Cardiovascular (CV) events but it is unknown whether left atrial volume index (LAVi) predicts mortality independent of LV geometry in elderly patients with preserved ejection fraction (EF).

Methods: We evaluated 16,904 patients aged ≥ 70 years with preserved EF to determine the impact of LAVi and LV geometry on mortality during an average follow-up of 1.7 ± 1.0 years.

Results: Deceased patients ($n=2,404$) had significantly higher LAVi (37.2 ± 15.7 vs. 33.7 ± 13.8 , $p<0.0001$) and abnormal LV geometry (62% vs. 53%, $p<0.0001$) than survivors ($n=14,500$). LAVi was an independent predictor of mortality in all four LV geometry groups [Hazard ratio: Normal= 1.010 (1.002-1.011), $p<0.0001$; concentric remodeling=1.007 (1.001-1.012), $p=0.005$; eccentric hypertrophy= 1.008 (1.006-1.018), $p=0.03$; concentric hypertrophy=1.012 (1.008-1.022), $p<0.0001$]. Comparison of models with and without LAVi for mortality prediction was significant suggesting increased mortality prediction by addition of LAVi to other independent predictors (Table).

Conclusion: LAVi is higher and LV geometric abnormalities are more prevalent in deceased patients with preserved EF and are independently associated with increased mortality. LAVi predicts mortality independent of LV geometry and has synergistic influence on all cause mortality prediction in large cohort of elderly patients with preserved ejection fraction.

Table: Predictors of Mortality in 16,904 Elderly Patients with Preserved EF:

Variables	Hazard Ratio (95% CI)	
	Model without LAVi	Model with LAVi
Age	1.001 (1.001 - 1.006), $p<0.0001$	1.001 (1.001 - 1.008), $p<0.0001$
Gender	0.933 (0.912 - 1.040), NS	0.963 (0.932 - 1.066), NS
BMI	0.978 (0.961 - 0.990), $p<0.0001$	0.977 (0.962 - 0.991), $p<0.0001$
Ejection Fraction	0.986 (0.981 - 0.993), $p=0.0008$	0.989 (0.981 - 0.993), $p=0.005$
LV mass index	1.001 (1.003 - 1.006), $p=0.0002$	1.001 (1.000 - 1.004), NS
Relative wall thickness	3.449 (2.639 - 4.014), $P<0.0001$	3.479 (2.846 - 4.327), $p<0.0001$
Left Atrial Volume Index	---	1.011 (1.006 - 1.015), $p<0.0001$
Likelihood Ratio Test (comparing models with and without LAVi): $P<0.0001$		

10:45 a.m.

0905-4

Prediction of Myocardial Viability in Acute Myocardial Infarction: Two-Dimensional Global Longitudinal Strain Imaging by Echocardiography

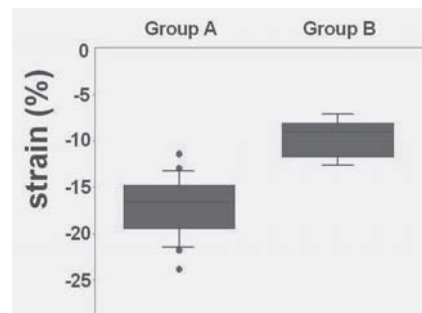
Woo-Shik Kim, Seok Jae Hwang, Il Suk Sohn, Soo Joong Kim, Myung-Gon Kim, Jong-Hoa Bae, Kwon-Sam Kim, Kyung Hee University, Seoul, South Korea

The aim of the study was to assess whether global peak systolic longitudinal strain obtained by 2-dimensional (2-D) speckle tracking method is useful for myocardial viability assessment in patients with acute myocardial infarction (AMI).

Methods: Thirty-eight patients with AMI were examined before myocardial revascularization. The 2-D strain measurements from standard 16-segments were averaged to obtain a global strain value for the entire left ventricle. Myocardial viability was assessed six months after percutaneous coronary intervention (PCI) using 2-D echocardiography and dobutamine stress echocardiography. Patients were classified into 2 groups according to follow-up echocardiography study: group A; normal or viable myocardium ($n=28$), group B; nonviable myocardium ($n=10$).

Results: Group A showed higher value of global strain compared with group B (-17.0 ± 3.1 vs. -9.7 ± 2.2 , $P<0.001$) (Figure). On the basis of receiver operating characteristic (ROC) curve analysis, optimal cutoff values of -12.5 for global strain value were chosen to predict viable myocardium (sensitivity=0.80, specificity=0.96). Global strain was proportionate to wall motion score index, both before and after PCI ($r=0.739$, $p<0.001$; $r=0.699$, $p=0.001$, respectively).

Conclusions: The 2-dimensional strain echocardiography is a useful tool in distinguishing viable myocardium from nonviable myocardium and may therefore be an important clinical tool for risk stratification in the acute phase of myocardial infarction.



11:00 a.m.

0905-5

Quantification of Mitral Regurgitation by Real-Time Three-Dimensional Echocardiography: Head-to-Head Comparison With Three-Dimensional Velocity-Encoded Magnetic Resonance Imaging

Nina Ajmone Marsan, Jos J M Westenberg, Claudia Ypenburg, Victoria Delgado, Rutger J. van Bommel, Stijnje D. Roes, Rob J. van der Geest, Ernst E. van der Wall, Martin J. Schalij, Jeroen J. Bax, Leiden University Medical Center, Leiden, The Netherlands

Background: accurate grading of mitral regurgitation (MR) severity is crucial for appropriate patient management, but remains challenging. Velocity-encoded (VE) magnetic resonance imaging (MRI) with 3-dimensional (3D) 3-directional (3-dir) acquisition has been recently proposed as the reference method. The aim of this study was to evaluate feasibility and accuracy of real-time three-dimensional echocardiography (RT3DE) for quantification of MR, in a head-to-head comparison with VE-MRI.

Methods: a total of 51 patients with functional MR were included. A 3D 3-dir VE-MRI acquisition was applied to quantify mitral regurgitant volume (Rvol-MRI). Color Doppler RT3DE was applied for direct measurement, in 'en face' view, of mitral effective regurgitant orifice area (EROA-3D); the regurgitant volume (Rvol-3D) was subsequently calculated as EROA-3D multiplied by the velocity time integral of the regurgitant jet on the continuous-wave Doppler. To assess the relative potential error of the conventional approach, color Doppler 2D echocardiography was performed: vena contracta width (VCW) was measured in the 4-chamber view and EROA calculated as circular (EROA-4CH); EROA was also calculated as elliptical (EROA-ellipt), measuring VCW also in the 2-chamber view. From these EROA measurements, the regurgitant volumes (Rvol-4CH and Rvol-ellipt) were also calculated.

Results: EROA-3D was significantly higher than EROA-4CH ($p<0.001$) and EROA-ellipt ($p=0.02$) with a significant bias between these measurements (0.11cm² and 0.07cm², respectively). Rvol-3D showed excellent correlation with Rvol-MRI ($r=0.93$) without a significant difference between these techniques (mean difference -0.7 ml/beat). Conversely, Rvol-4CH significantly underestimated Rvol ($p=0.017$) as compared to Rvol-MRI (mean difference 3.9 ml/beat). Rvol-ellipt demonstrated a better agreement with VE-MRI (mean difference 2.4 ml/beat).

Conclusions: quantification of EROA and Rvol of functional MR using RT3DE is feasible and accurate as compared to 3D 3-dir VE-MRI; the currently recommended 2D echocardiographic approach significantly underestimates both EROA and Rvol.

11:15 a.m.

0905-6

Assessment of Aortic Stiffness in Marfan Syndrome Using Two-Dimensional and Doppler Echocardiography

Anatoli Kiotsekoglou, George R. Sutherland, James C. Moggridge, Venedictos Kapetanakis, Michael J. Mullen, Dariush K. Nassiri, John Camm, Anne H. Child, St George's, University of London, London, United Kingdom

Background: Fibrillin-1 deficiency, dysregulated cytokine transforming growth factor- β and increased collagen deposition related to fibrillin-1 gene mutations cause increased aortic stiffness in Marfan syndrome (MFS). Pulse wave velocity (PWV) probably constitutes the best indirect measure of aortic stiffness. We aimed to assess PWV in adult MFS patients using two-dimensional (2D) and Doppler echocardiography.

Methods: Twenty-six un-operated MFS patients, 12 men and 14 women (mean age 31 ± 14 years) and 26 normal controls matched for sex, age and body surface area were studied. 2D and Doppler measurements were taken from a supra-sternal view. Blood flow was recorded with the sample volume placed in the centre of the aorta near the aortic valve and after 10 seconds in the most distal displayed point of the descending aorta with simultaneous ECG. The time from the beginning of QRS to the onset of ascending (T1) and descending (T2) aortic flow and the difference between these time intervals (TD = T2-T1) were measured. PWV was then calculated by dividing the distance between the two points of Doppler recordings by the TD. B-stiffness and peak aortic flow were also measured.

Results: PWV was significantly higher in MFS patients compared to controls; 7.20 m/s ($5.12, 9.43$) vs 4.64 m/s ($3.37, 6.24$), $p<0.001$. B-stiffness was also increased in MFS patients; 5.15 (3.69, 7.65) vs 2.44 (1.82, 3.66), $p<0.001$. Systolic blood pressure and peak aortic flow values showed no differences; MFS patients: 111.5 mmHg (110, 120) and 359 ml/s (304, 399) vs controls: 110 mmHg (110, 120) and 379 ml/s (333, 402). Nine out of 26 MFS patients were on b-blockers. Heart rate (HR) was lower in MFS patients, (56 bpm ± 8 vs 62 bpm ± 8 , $p=0.035$) but there was no difference in HR between controls and patients off b-blockers. Lower HR could be attributed to b-blockade effect. Multiple regression analysis was not performed due to the pilot character of this study.

Conclusion: Aortic stiffness was significantly higher in MFS patients. Our preliminary data demonstrated that PWV measurements can be easily performed in adults as part of an echocardiogram. This technique can be helpful in diagnosis, long-term follow-up and management of MFS patients.

11:30 a.m.

0905-7

Molecular Imaging of High-Risk Atherosclerotic Plaque With Targeted Ultrasound Imaging of Activated von Willebrand Factor

Weihui Shentu, Robert Conley, Aris Xie, Todd Belcik, Qi Yue, Chad Carr, Boya Fang, Owen McCarty, Jonathan R. Lindner, Oregon Health & Science University, Portland, OR

Background: Activated von Willebrand factor (vWF) on the endothelial cell surface has been linked to vascular inflammation and susceptibility to thrombus formation in atherosclerotic diseases. We hypothesized that molecular imaging of activated vWF with contrast-enhanced ultrasound (CEU) could be used to detect high-risk vascular phenotype.

Methods: Microbubbles targeted to vWF (MB_v) were prepared by surface conjugation of recombinant GPIIb/IIIa, the major platelet glycoprotein receptor for activated vWF. Flow chamber studies were performed to assess attachment of MB_v and control microbubbles (MB_c) to botrocetin-stimulated vWF (shear rate: 75s⁻¹) and to platelet aggregates on surface-bound fibrillar collagen (shear rate: 500 s⁻¹). CEU molecular imaging of vWF was performed in an *ex vivo* in blood-perfused mouse thoracic aorta with crush injury; and *in vivo* in the thoracic aorta of a murine model of severe atherosclerosis produced by genetic deletion of the LDL receptor and the ApoBec-1 mRNA editing peptide (DKO mice).

Results: In flow chamber experiments, there was greater (P<0.05) attachment of MB_v compared to MB_c to activated vWF (126±62 vs 46±26 per mm²) and to platelet aggregates (530±115 vs 56±27 per mm²). In the *ex vivo* aortas from wild type mice, selective attachment at the crush site for MB_v over MB_c was indicated by higher CEU signal enhancement (66±34 vs 24±21 AU, p<0.05) and greater area of enhancement (35±9% vs 18±8 % of total pixels, p<0.05). There was minimal enhancement in the non-crush region for both agents. In the DKO mice at 40 weeks of age, histology showed severe atherosclerotic lesions with necrosis and severe inflammation in the thoracic aorta. CEU imaging at these sites demonstrated a trend toward greater enhancement for MB_v over MB_c (38±23 vs 15±15 % pixel enhancement, p=0.04) when imaged 10 min after IV injection.

Conclusions: Activated vWF can be detected by CEU molecular imaging with microbubbles bearing recombinant GPIIb/IIIa. This strategy may be useful for non-invasive detection of high risk atherosclerotic phenotype.

ACC.POSTER CONTRIBUTIONS

1045

CT Coronary Angiography; CT Coronary Calcium and Noncoronary CT Applications; MRI; Nuclear Cardiology/PET

Monday, March 30, 2009, 1:30 p.m.-4:30 p.m.

Orange County Convention Center, West Hall D

3:30 p.m.

1045-233

Coronary CT Angiography Is a More Cost-Effective Strategy Than Myocardial Perfusion Imaging as an Initial Diagnostic Test in Clinical Practice

Jason H. Cole, Vance M. Chunn, Cardiology Associates, Mobile, AL, University of South Alabama, Mobile, AL

Background: Myocardial perfusion imaging (MPI) is commonly used as an initial diagnostic test for patients with chest pain in clinical practice. Coronary CT angiography (CCTA) is an emerging technology that may be considered in the same patient population. Cost implications of the different tests remain unclear. **Methods:** A large group cardiology practice that performs both MPI and CCTA established a clinical database to review indications and results of all CCTA studies. Costs for performing MPI and CCTA were determined from reimbursement levels. Downstream costs were modeled based on results (normal versus abnormal) for both CCTA and MPI. Total costs were expressed as cost per initial patient studied. Multi-level sensitivity analysis was performed on the variables of abnormal CCTA and MPI rates. Costs were also modeled for CCTA as a gatekeeper after abnormal MPI. Results: Over 1 year, 913 patients underwent CCTA as an initial diagnostic test for coronary artery disease. 398 (43.6%) were normal, and 290 (31.8%) were diagnosed with nonobstructive coronary disease. 225 (24.6%) were diagnosed with potentially obstructive disease and referred for downstream testing. Over the same period of time, 7246 patients underwent myocardial perfusion imaging. 30% of MPI patients were referred to cardiac catheterization. Total costs were \$1586/patient for CCTA and \$2153/patient for MPI. Sensitivity analysis revealed CCTA to be a cost-saving strategy so long as catheterization rate after MPI was greater than 15%. Additional cost savings could be realized by the use of CCTA after MPI. Conclusion: In a large cardiology practice with experience in both nuclear cardiology and computed tomography, an initial diagnostic strategy for chest pain using CCTA saved \$567 over a strategy using MPI. Cost savings were preserved over a large range of variables.

1045-234

Diagnostic Accuracy of In-stent Restenosis Detection With 64- Multi-detector Row Computed Tomography: A Meta-analysis

Nazario Carrabba, Filippo Cademartiri, Nico R. Mollet, Guido Parodi, Gabriele Accetta, David Antoniucci, Division of Cardiology, Careggi Hospital, Florence, Italy

Background: Currently stents are used in almost all percutaneous coronary interventions. Following the recent introduction of drug eluting stents (DES) the occurrence of in-stent restenosis (ISR) was reduced. However, the ISR may still occur causing potential adverse events, and frequently a conventional coronary angiography (CCA) is required for ISR diagnosis. Because a substantial number of these CCA are not followed by intervention, the need of non-invasive alternative approach for ISR detection is unquestionable. We sought to evaluate the diagnostic accuracy of 64- multi-detector row computed tomography (MDCT) compared with the standard CCA for ISR detection.

Method and Results: Based on a systematic search, 9 studies including 518 patients were eligible for meta-analyses. The mean age was 62 years. Males and diabetics constituted 82% and 17% respectively. Overall 978 stents were included, out of 9% were unassessable (range from 0% to 42%). Accuracy tests with 95% confidence intervals comparing 64-MDCT vs CCA showed that pooled sensitivity, specificity, positive and negative likelihood ratio (random effect model) values were: 0.86% (95% CI 0.80 to 0.91; heterogeneity chi-squared = 8.80, df = 8, p=0.360), 0.93% (95% CI 0.91 to 0.95; heterogeneity chi-squared = 25.81, df = 8, p=0.0011), 12.32 (95% CI 7.26 to 20.92; heterogeneity chi-squared = 24.91, df = 8, p=0.002), 0.18 (95% CI 0.12 to 0.28; heterogeneity chi-squared = 8.34, df = 8, p=0.401) for binary ISR detection (>50% ISR). The calculated positive and negative predictive values were 74% and 96%, respectively. The symmetric area under the curve value was 0.95 (SE AUC=0.02), showing a high degree of agreement between 64-MDCT and CCA for ISR detection.

Conclusions: The 64-MDCT provides a high diagnostic performance for ISR detection in high selected patients deemed ideal candidate for MDCT. However, a substantial number of unassessable stents (9%) were excluded from the analysis underscoring the shortcomings of MDCT, and the sensitivity remained moderate. Thus, in clinical practice the diagnostic role of this emerging technology for ISR detection remains to be demonstrated.

3:30 p.m.

1045-235

Gender Comparison of Diagnostic Accuracy of 64-Multidetector Row Coronary Computed Tomographic Angiography: Results From the Multicenter ACCURACY Trial

Janet C. Tsang, James K. Min, Matthew J. Budoff, Fay Y. Lin, Los Angeles Biomedical Research Institute at Harbor-UCLA, Torrance, CA, Weill Medical College of Cornell University and New York Presbyterian Hospital, New York, NY

Background: Diagnosis of coronary artery disease (CAD) in women remains a challenge, due to a lower prevalence of obstructive disease and the suboptimal performance of traditional non-invasive tests (exercise electrocardiography and stress myocardial perfusion imaging). Coronary computed tomographic angiography (CCTA) is a promising method for detection and exclusion of obstructive coronary artery stenosis. The purpose of this study was to compare the diagnostic accuracy of electrocardiographically-gated 64-detector row CCTA in men and women without known coronary artery disease using invasive coronary angiography (ICA) as the reference standard.

Methods: We prospectively evaluated subjects with chest pain at 16 sites who were clinically referred for ICA. CCTAs were scored by consensus of 3 independent blinded readers. ICAs were evaluated for coronary stenosis based upon quantitative coronary angiography (QCA).

Results: 230 subjects (136 men and 94 women with CAD prevalence of 34% vs. 11%, mean age 57 ± 10 years) underwent both CCTA and ICA. For a patient-based model for stenosis >50%, sensitivity, specificity, and positive and negative predictive values in men vs. women were 96%, 78%, 69%, 100% and 90%, 88%, 47%, 99%, respectively. For stenosis >70%, sensitivity, specificity, positive and negative predictive values in men vs. women were 96%, 73%, 48%, 99% and 83%, 94%, 50%, 99%, respectively. For either 50 or 70% stenosis thresholds, men had significantly higher specificity (for either 50% or 70% threshold) and women had high specificity (p<0.02 for all measures).

Conclusions: In this prospective multicenter trial of symptomatic patients without known CAD, 64-multidetector row CCTA demonstrates improved specificity and mildly reduced sensitivity for women as compared to males. Importantly, the >99% negative predictive values in both genders support the use of CCTA as an effective noninvasive test for reliably ruling out obstructive disease.

3:30 p.m.

1045-236

Semi-automated Noninvasive Coronary Plaque Volumetry by 64-Row Multidetector Computed Tomography

Yoshiyuki Kijima, Osamu Akutagawa, Taku Sakai, Kiyoshi Kume, Akira Okura, Takeshi Hata, Higashi-osaka City General Hospital, Osaka, Japan

Background: Improved spatial resolution of MDCT visualized not only vessel lumen but also vessel wall of coronary arteries. We measured coronary plaque volumes in patients with stable angina pectoris employing the SUREPlaque software on 64-row multidetector computed tomography (MDCT). The volumetric parameters were compared with those by three-dimensional intravascular ultrasound (IVUS).

Methods: Twenty-nine coronary lesions were enrolled from 21 patients. Excluded

were vessels with in-stent stenosis, calcified lesions, and chronic total occlusion. The ^{SURF}Plaque tentatively defined each tissue on the color map based on CT number. Vessel lumen was green [131 to 350Hounsfield units (HU)]. Calcified tissue was yellow (> 350HU). Vessel wall was divided into two portions, i.e. red (-100 to 50HU) and blue area (51-130HU). The ^{SURF}Plaque determined vessel area, lumen area, and plaque area in each 0.5mm-thick cross sectional slice. Integral of each area was defined as each volume.

Results: MDCT successfully determined volumetric parameters of 17 lesions. Good positive correlations were observed between MDCT and IVUS for vessel volume ($r = 0.93$, $P < 0.0001$), lumen volume ($r = 0.87$, $P < 0.0001$), and plaque volume ($r = 0.79$, $P = 0.0002$). MDCT overestimated vessel volume versus IVUS (386.2 ± 176.4 vs. $337.2 \pm 137.0\text{mm}^3$, $P < 0.05$) and lumen volume (247.3 ± 117.7 vs. $151.6 \pm 78.9\text{mm}^3$, $P < 0.01$), whereas MDCT underestimated plaque volume (140.7 ± 66.6 vs. $187.4 \pm 82.4\text{mm}^3$, $P < 0.01$).

Conclusions: Non-invasive MDCT-based coronary plaque volumetry is an alternative method for evaluation of coronary plaque progression and regression in humans.

3:30 p.m.

1045-237 **Increasing Coronary Artery Disease Severity as Detected by Coronary Computed Tomographic Angiography Is Associated With Enhanced Medical Treatment and Improved Control of Cardiovascular Risk Factors**

Troy M. LaBounty, Richard B. Devereux, Fay Y. Lin, Jonathan W. Weinsaft, James K. Min, Weill Cornell Medical College, New York, NY

Background: While coronary computed tomographic angiography (CCTA) can accurately diagnose coronary artery disease (CAD), its impact on downstream medical treatment and risk factor control is not known.

Methods: We evaluated 204 consecutive outpatients undergoing CCTA (age 57 ± 16 years; 40% male) for suspected CAD for whom comprehensive electronic medical records were available. Blood pressure (BP), lipid levels, and medications were compared before versus after CCTA. CAD was graded as absent, non-obstructive (<50% stenosis) or obstructive ($\geq 50\%$).

Results: Medication changes were evaluated at a mean follow-up of 2.0 ± 2.5 months (Table). Independent of risk factors, increased CAD severity was associated with downstream increased aspirin initiation ($p < 0.001$), BP medication initiation/increase ($p = 0.009$), and statin initiation/increase ($p < 0.001$). Independent of risk factors and baseline values, increasing CAD severity (absent vs. non-obstructive vs. obstructive) during an extended follow-up (8.9 ± 5.4 months) was associated with lower post-CCTA total cholesterol (184 ± 37 vs. 196 ± 48 vs. 154 ± 33 mg/dl, $n = 90$, $p = 0.001$), low-density lipoprotein (108 ± 35 vs. 106 ± 45 vs. 78 ± 23 mg/dl, $n = 80$, $p = 0.007$), and diastolic BP (76 ± 9 vs. 73 ± 11 vs. 73 ± 9 mmHg, $n = 134$, $p = 0.03$), but not systolic BP.

Conclusions: Increasing grades of CAD severity as detected by CCTA favorably impacts medical treatment of CAD, with enhanced control of hypertension and dyslipidemia.

Univariate Evaluation of Management Impact

Medications after CCTA	No CAD (n=73)	Non-obstructive CAD (n=66)	P-value (non-obstructive vs. no CAD)	Obstructive CAD (n=65)	P-value (obstructive vs. no CAD)
Aspirin start (%)	0 (0%)	6 (9%)	0.01	18 (28%)	<0.01
Total on aspirin (%)	26 (36%)	40 (61%)	<0.01	54 (83%)	<0.01
Statin start/increase (%)	1 (1%)	16 (24%)	<0.01	25 (38%)	<0.01
Total on statin (%)	12 (16%)	40 (61%)	<0.01	53 (82%)	<0.01
BP medication start/increase (%)	6 (8%)	6 (9%)	NS	19 (29%)	<0.01
Total on BP medication (%)	33 (45%)	45 (68%)	0.01	55 (85%)	<0.01
Any medication start/increase (%)	6 (8%)	24 (36%)	<0.01	40 (62%)	<0.01

3:30 p.m.

1045-238 **Stress Perfusion Cardiac CT Permits Simultaneous Evaluation of the Coronary Arteries, Myocardial Perfusion, and Left Ventricular Function With Similar Radiation Exposure to Rest/Stress Single Photon Emission Computed Tomography**

Ian S. Rogers, Ron Blankstein, Ammar Sarwar, Leon Shtruman, Anand V. Soni, Ricardo Loureiro, Hiram Bezerra, Milena Petranovic, David R. Okada, Thomas J. Brady, Wilfred S. Mamuya, Ricardo C. Cury, Massachusetts General Hospital, Boston, MA

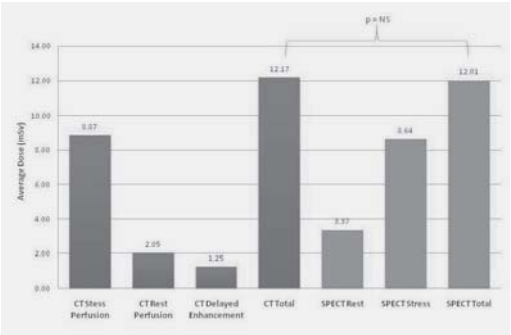
INTRO: Our group recently demonstrated the feasibility of adenosine stress myocardial perfusion imaging using dual source CT (DSCT), which permits assessment of the coronary arteries, myocardial perfusion, and left ventricular (LV) function in one test. Our aim was to compare the radiation dose subjects received from this technique with the exposure they received from rest/stress single photon emission computed tomography (SPECT).

METHODS: Subjects underwent rest/stress SPECT using technetium Tc 99m sestamibi followed by stress DSCT, which included 3 components: stress perfusion (CT-SP), rest perfusion (CT-RP) and delayed enhancement (CT-DE). Prospective triggering was used for CT-RP and CT-DE. Retrospective triggering with tube current modulation was used for CT-SP. Total radiation was calculated as follows: SPECT: total megabecquerel converted to millisievert (mSv); DSCT: dose-length product multiplied by conversion factor 0.017 mSv/mGy/cm.

RESULTS: 26 subjects (Age: 63 ± 10 years; 85% men, BMI: 31 ± 5 kg/m²) underwent

both SPECT and DSCT (SP/RP/DE) imaging. The calculated radiation dose for each modality is presented in Table 1. Average dose for stress DSCT (12.17 ± 4.04 , 95% CI 10.54 - 13.8) did not differ from SPECT (12.01 ± 0.36 , 95% CI 11.87 - 12.16), $p = 0.84$.

CONCLUSION: Adenosine stress cardiac CT can provide simultaneous evaluation of the coronaries, myocardial perfusion, and LV function with similar radiation exposure to the perfusion data provided by SPECT.



3:30 p.m.

1045-239 **The First Direct Demonstration That Whole-Heart and Lesion-Based Coronary Artery Calcium Scores Predict Plaque Volume and Composition on Intravascular Ultrasound and Radiofrequency Analysis (VH)**

Gustavo Vasquez, Sarah Rinehart, Zhen Qian, Idean Marvasti, Laura Murrieta, Hunt Anderson, Szilard Voros, Piedmont Heart Institute, Atlanta, GA

Background. Coronary artery calcium scoring (CAC) quantifies whole-heart plaque burden; it predicts events and obstructive disease. Intravascular ultrasound (IVUS) with radiofrequency analysis (VH) invasively quantifies plaque volume/composition. CAC and IVUS/VH have not previously been compared.

Methods. 24 pts had CAC and IVUS/VH; Framingham Risk Score (FRS) was calculated. On CAC scans, we determined 2D and 3D Agatston and volume score (AS, VS). We scored each lesion individually and determined lesion-specific AS, lesion-specific VS, width and length. Minimal lumen diameter (MLD) and area (MLA), percent atheroma volume (PAV) and percent area stenosis (%AS) were measured on IVUS. Fibrous (FI), fibrofatty (FF), necrotic core (NC) and dense calcium (DC) volume and percent were measured on VH. We determined correlation coefficients (r); $p < 0.05$ was significant.

Results. FRS was not predictive of IVUS/VH parameters. Whole-heart 2D and 3D Agatston and volume score significantly correlated with PAV on IVUS, but not with measures of lumen stenosis (Table). However, lesion-specific measures correlated with MLD and %AS; they also correlated with PAV (Table). Furthermore, whole-heart measures did not correlate with VH parameters, except VS vs FF%. However, several lesion-specific values correlated with NC and DC volume (Table).

Conclusions. Whole-heart CAC values correlate with plaque burden on IVUS, while lesion-specific scores correlate with values of lumen stenosis and plaque composition by VH.

Whole-Heart and Lesion-Specific CAC vs IVUS/VH Parameters

	CAC	IVUS/VH	r-value	p-value
Whole-Heart Score	Agatston	PAV	0.6059	0.0046
	Volume Score	PAV	0.5869	0.0065
Lesion-Specific Score	Lesion Width	MLD	-0.5490	0.0122
	Lesion Length	PAV	0.4376	0.0325
	Agatston	%AS	-0.4780	0.0330
	Lesion Width	%AS	-0.4641	0.0393
	Volume	%AS	-0.5041	0.0234
	Volume	DC Volume	0.5463	0.0057
	Volume	NC Volume	0.4071	0.0483

3:30 p.m.

1045-240 **Comprehensive Valvular Assessment by Cardiac Computed Tomography: A Comparison to Transesophageal Echocardiography**

Troy M. LaBounty, Sunil Mirchandani, Richard B. Devereux, Fay Y. Lin, Jonathan W. Weinsaft, James K. Min, Weill Cornell Medical College, New York, NY

Background: Cardiac computed tomography (CCT) has been reported accurate for evaluation of isolated valvular lesions; however the efficacy of CCT to concurrently assess all significant valvular findings is not known. We compared CCT to transesophageal echocardiography (TEE) for detection of significant valvular lesions.

Methods: Valvular function was compared in 61 consecutive patients undergoing both 64-detector ECG-gated CCT and TEE. Blinded comparisons were performed for aortic and mitral valve thickening; aortic and mitral valve stenosis (valve area $< 2.0\text{cm}^2$ for both); mitral valve prolapse; and \geq moderate mitral, tricuspid, or aortic regurgitation (MR, TR,

AR, respectively). AR or MR by CCT was defined as any regurgitant orifice area; TR was defined as a Hounsfield Unit ratio >0.4 of the inferior vena cava compared to the right heart during mid-diastole.

Results: The mean age was 58.4 ± 11.7 yrs, 24.6% were female, and ejection fraction was $<50\%$ in 9 patients. A complete valvular assessment was possible in 53 patients (Table 1). Prosthetic valves (n=5) and non-evaluable valves (n=3) were excluded from the analyses.

Conclusions: CCT exhibits high diagnostic performance for detection of aortic stenosis, mitral stenosis, and aortic regurgitation, with less robust performance for other valvular lesions. Importantly, the sensitivity of CCT to detect and the negative predictive value of CCT to exclude any significant valvular lesions at a per-patient basis are high.

	Sensitivity	Specificity	Positive Predictive Value	Negative Predictive Value
Aortic valve thickening (n=59)	11/16 (69%)	26/43 (60%)	11/28 (39%)	26/31 (84%)
Aortic stenosis (n=59)	2/2 (100%)	55/57 (96%)	2/4 (50%)	55/55 (100%)
Aortic regurgitation (n=58)	4/4 (100%)	51/54 (94%)	4/7 (57%)	51/51 (100%)
Mitral valve thickening (n=56)	7/10 (70%)	30/46 (65%)	7/23 (30%)	30/33 (91%)
Mitral stenosis (n=54)	1/1 (100%)	52/53 (98%)	1/2 (50%)	52/52 (100%)
Mitral valve prolapse (n=56)	3/9 (33%)	45/47 (96%)	3/5 (60%)	45/51 (88%)
Mitral regurgitation (n=54)	0/5 (0%)	48/49 (98%)	0/1 (0%)	48/53 (91%)
Tricuspid regurgitation (n=61)	5/7 (71%)	31/54 (57%)	5/28 (18%)	31/33 (94%)
Any valvular abnormality (n=53)	24/24 (100%)	8/29 (28%)	24/45 (53%)	8/8 (100%)

3:30 p.m.

1045-241 Visualization of Myocardial Ischemia and Infarction Using Adenosine Triphosphate Stress Myocardial Perfusion CT in Patients With Coronary Artery Disease

Akira Kurata, Teruhito Kido, Fumiaki Shikata, Hiroshi Imagawa, Hideki Okayama, Jitsuo Higaki, Kohei Hosokawa, Yuma Inoue, Hiroshi Higashino, Teruhito Mochizuki, Ehime University Graduate School of Medicine, Ehime, Japan

Background: Since our preliminary data showed that there was some time-difference (4–15 s) to peak contrast enhancement between arterial and myocardial perfusion phase using multi-slice spiral computed tomography (MSCT), the aim of this study was to test the myocardial perfusion specific CT scan protocol in a clinical setting.

Methods: Eighteen patients with CAD (8 female; mean age, 70 years) gave informed consents and enrolled the approved study. They underwent ATP stress myocardial perfusion CT using 16-slice CT and 201-Thallium single photon emission computed tomography (SPECT), and coronary angiography (CAG), respectively. Twelve patients underwent gadolinium magnetic resonance imaging (MRI) as required. The ATP-stress myocardial perfusion CT was performed as follows: 1) intravenous ATP (0.16 mg/kg/min) infusion for 5 min, 2) the slow infusion of contrast medium at a rate of 2 ml/min for 100 ml (370 mg-iodine/ml) in 3 min later, 3) the stress image was acquired without bolus tracking after the contrast-injection, 4) the late image was acquired without additional contrast administration after 15 min from the stress image. Myocardial perfusion was semi-quantitatively evaluated by the CT-attenuation based color coded images (hot color as hyper-enhanced; cold color as hypo-enhanced). Hypo-perfusion area (HPA) of perfusion CT and early defect (ED) of SPECT in each stress image, late iodine-enhancement (LIE) and gadolinium enhancement (LGE) in each late image were compared, respectively.

Results: Twelve patients had 54 (18*3) coronary territories and 30 stenoses proved by CAG. Perfusion CT described 39 HPAs and SPECT described 29 EDs in the stress images. The agreement between perfusion CT and SPECT was 74 % (40/54, $p<0.05$). CAG revealed 21 stenoses in 27 HPA(+)/ED(+) matched territories, 9 stenoses in 12 HPA(+)/ED(-) mismatched territories, 0 stenosis in the other 15 HPA(-) territories, respectively. The LIE could describe 4/7 LGEs and the agreement was 89% (32/36, $p<0.05$).

Conclusion: The ATP stress myocardial perfusion CT is promising for simple and robust assessment of myocardial ischemia and infarction (late enhancement) just like SPECT and MRI in patients with CAD.

3:30 p.m.

1045-242 Coronary Artery Calcium Using 64-MDCT Compared With Invasive Coronary Angiography: Data From the Accuracy Trial

Matthew J. Budoff, James G. Jollis, David Dowe, James Min, Los Angeles Biomedical Research Institute, Torrance, NY, Cornell University, New York, NY

Background: Although numerous trials have demonstrated the diagnostic accuracy of coronary artery calcium (CAC) scanning for prediction of obstructive disease, virtually all studies have been performed using Electron Beam CT (EBCT). We evaluated the diagnostic accuracy of CAC by 64-row CT to detect obstructive coronary stenosis compared to quantitative coronary angiography (QCA) in the ACCURACY multicenter trial.

Methods: 16 sites prospectively enrolled 232 patients (pts) [59.5% male, 57 yrs] with chest pain referred for invasive coronary angiography (ICA). Pts underwent CAC scan and CT angiography prior to ICA. Total CAC scores were correlated with angiographically

documented stenoses using common cutpoints of $CAC>0$, >100 and >400 . Significant obstructive disease was defined as $>50\%$ luminal stenosis by QCA.

Results: $\geq 50\%$ stenoses were identified in 49 (21.3%) pts. The per-patient accuracy of CAC by 64-row CT compared to QCA is reported in Table 1. With $CAC>0$, >100 , and >400 , the sensitivity to predict stenosis was 94%, 84%, and 53%, whereas the specificity was 42%, 69%, and 86%, respectively.

Conclusions: This prospective multicenter results comparing 64-row CAC to QCA demonstrate that CAC using 64-row CT scanner, similar to previously published reports using EBCT, is highly sensitive and moderately specific test to predict significant coronary artery stenosis. Whether this information is complementary to CTA data remains to be validated.

Table 1.

Calcium Threshold	Sensitivity %	Specificity %	Positive Predictive Value %	Negative Predictive Value %
CAC >0	46/49 94%	75/180 42%	46/151 30%	75/78 96%
CAC >100	41/49 84%	125/180 69%	41/96 43%	125/133 94%
CAC >400	26/49 53%	154/180 86%	26/52 50%	154/177 87%

3:30 p.m.

1045-243 Nonalcoholic Fatty Liver Disease Under the Influence of Statin Therapy: The Saint Francis Heart Study

Matthew J. Budoff, Junichiro Takasu, Naser Ahmadi, Craig Gordon, Alan D. Guerci, Los Angeles Biomedical Research Institute, Torrance, CA, Saint Francis, Roslyn, NY

Non-Alcoholic Fatty liver disease (NAFLD) is an increasingly prevalent disease, especially given the rise in metabolic syndrome, obesity and diabetes in the population. There is preliminary evidence in small studies that statin use may have a beneficial effect on this disease state. Non-contrast CT is a useful modality to evaluate fatty liver by comparing the density of spleen (control) to the liver, and has been validated using both autopsy and biopsy. The lower the attenuation in the liver as compared to the spleen, the more fat is present. Autopsy and biopsy studies have demonstrated that L:S ratio <1 is consistent with NAFLD. Coronary calcium scans typically include some visualization of the liver and spleen in approximately 90% of cases.

Methods: The Saint Francis Heart Study was a double-blind, placebo-controlled randomized clinical trial of atorvastatin 20 mg daily, vitamin C 1 g daily, and vitamin E 1,000 U daily (active therapy), versus matching placebos in 1,005 asymptomatic, apparently healthy men and women age 50-70 years. Of these, 877 (88%) persons had CT data for analysis (both liver and spleen present on the scan). Patients underwent multiple non-contrast CT scans (mean interval of first to third scan 45 months). Liver:spleen (L:S) ratios were compared at baseline and follow-up scan, and results compared between treatment and placebo.

Results: Baseline L:S ratio was 1.23 and 1.22 in placebo and treatment groups ($p=ns$). The mean L:S ratio did not change under the influence of atorvastatin+antioxidants, but worsened with placebo (1.22 and 1.17 respectively, $p<0.01$). 17% of patients had NAFLD (L:S ratio <1) at baseline in both groups. At follow-up, CT showed resolution of fatty liver in 29% of patients on placebo and 74% on active therapy ($p<0.0001$). No patients on active therapy formed NAFLD, while 11% of patients on placebo developed CT evidence of NAFLD ($p<0.001$).

Conclusions: In this double-blind randomized trial, use of atorvastatin+antioxidants significantly improved fatty liver as compared to placebo, and halted decline of L:S ratio over almost 4 years of therapy.

3:30 p.m.

1045-244 Dipyridamole Stress and Rest Myocardial Perfusion by 64 Detector-Row Computed Tomography in Patients With Suspected Coronary Artery Disease and Positive SPECT Scintigraphy: A Feasibility Study

Roberto C. Cury, Tiago A. Magalhães, Anna C. Borges, José Soares, Jr., José R. Parga, Luiz F. Ávila, Afonso A. Shiozaki, Pedro A. Lemos, Carlos E. Rochitte, Heart Institute (InCor), University of São Paulo Medical School, São Paulo, Brazil

Background: Multiple detector-row computed tomography (MDCT) used for coronary angiography (CTA) is useful for diagnosis of coronary artery disease (CAD). Recently, MDCT myocardial perfusion (CTperf) was shown to detect CAD. Our objectives were to compare dipyridamole MDCT and SPECT perfusion defects with CTA and conventional angiography (CCA).

Methods: Fourteen patients (59.7 \pm 8.7 years old, 8 males) with suspected CAD and <2 months prior positive SPECT underwent a customized MDCT protocol with rest/stress myocardial perfusion evaluation and CTA. MDCT was performed in a 64 scanner (Aquilion 64, Toshiba) with stress perfusion during 0.56mg/kg/4min of dipyridamole (100mA, 120kV, 32x1mm collimation, 60 ml 370mg/ml iodinated contrast at 3ml/s) followed by aminophylline and metoprolol infusion prior to a second rest perfusion/CTA acquisition (270-400mA, 120kV, 64x0.5mm collimation, 80-90ml contrast at 5ml/s). Independent observers with no knowledge of clinical data or other exams performed visual and semi-quantitative analysis of myocardial perfusion, CTA and CCA.

Results: All 14 patients completed the protocol with no adverse events, <20 mSv dose and with interpretable scans. CTperf was positive in 10 of 14 patients (71.4%). From the 4 disagreements with normal CTperf and positive SPECT, 3 patients had normal CTA or CTA and 1 had an occluded branch with collateral flow. Comparison between CTperf and SPECT on a per territory analysis showed good agreement at rest (kappa 0.63) and

during stress (κ 0.62, $p < 0.001$ for both). Sensitivity, specificity, positive and negative predicted values using CTA as reference were for CTperf 83.3, 87.5, 83.3, 87.5% and for SPECT 77.8, 79.2, 73.6 and 82.6%, respectively. In 10 patients with CCA as reference, diagnostic values were similar.

Conclusions: Rest and dipyridamole-stress myocardial perfusion combined to angiography by MDCT is feasible and results are similar to SPECT scintigraphy. The combined anatomical and perfusional information may allow identification of false-positives on perfusion scans. Our data corroborate the need for further investigation of this protocol in a routine clinical scenario.

3:30 p.m.

1045-245

Progression Rates of Coronary Artery Calcification in Diabetic Subjects Compared to Matched Controls

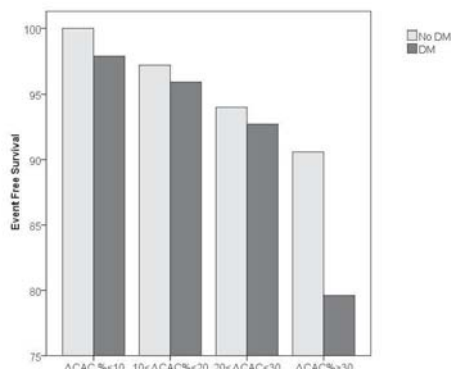
Sarkis Kiramijyan, Naser Ahmadi, Ferdinand Flores, Khuram Nasir, Matthew Budoff, Los Angeles Biomedical Research Institute at Harbor-UCLA Medical Center, Torrance, CA

Background: Coronary artery calcium (CAC) is a marker that is correlated with the presence of coronary artery disease (CAD). This study evaluates the rates of CAC progression between diabetics (DM) and matched controls.

Methods: 296 asymptomatic DM and 300 matched controls (age 59 ± 6 years, 29% female) underwent baseline and follow-up electron beam computed tomography within a 2 year interval. The controls were matched to the DM with age, gender, CAD risk factors and baseline CAC. Measurements of baseline CAC, annual changes in CAC and $\Delta\text{CAC}(\%)$ ($[\text{annual changes in CAC}/\text{baseline CAC}] \times 100$) were assessed. Follow-up was completed 56 ± 11 months after the 2nd scan. Multivariable Cox proportional hazards models were developed to predict all-cause mortality.

Results: Annual change in CAC was 34.3 ± 4.8 in matched controls vs. 80.6 ± 10 in DM ($p = 0.0001$). The $\Delta\text{CAC}(\%)$ was 10.2 ± 6.7 in matched controls vs. 29.4 ± 8.7 in DM ($p = 0.0001$). Hazard ratios of death in matched controls vs. DM was 1.88 (95% CI 1.51-2.36, $p = 0.0001$) for $10 \leq \Delta\text{CAC} \leq 20$, 2.29 (95% CI 1.56-3.38, $p = 0.0001$) for $20 \leq \Delta\text{CAC} \leq 30$, and 6.95 (95% CI 2.23-11.53, $p = 0.0001$) for $\Delta\text{CAC} > 30$ compared to $\Delta\text{CAC} < 10\%$ independent of age, gender and CAD risk factors. The event free survival decreased more in DM than in matched controls in proportion to the rate of CAC progression (Figure).

Conclusions: CAC progression rate is higher in DM compared to matched controls and event free survival decreased more in DM than in matched controls in proportion to the rate of CAC progression.



3:30 p.m.

1045-246

Epicardial Adipose Tissue and Cardiac Prognosis in a Community Sample

Tanya Dutta, Mark J. Goldman, Dipti Gupta, Ali Salah, Jing Han, Marguerite A. Roth, Alan D. Guerci, Nathaniel Reichel, St. Francis Hospital, Roslyn, NY, Stony Brook University Medical Center, Stony Brook, NY

Background: Epicardial adipose tissue (EAT) accumulates between the visceral and parietal pericardium and is associated with coronary risk factors including metabolic syndrome, coronary calcium score and vascular disease.

EAT correlates with the presence and extent of coronary disease. It is unknown whether EAT has any independent prognostic value.

Methods: Subjects enrolled in the St. Francis Heart Study, ages 50 through 70 with no history of coronary disease, underwent electron beam CT and were treated with atorvastatin and antioxidants or placebo. 316 of the 532 subjects with calcium scores greater than 350 were randomly selected for EAT volume measurement. EAT volume was compared to coronary disease risk factors, calcium score, all cardiac events (coronary death, nonfatal myocardial infarction, coronary revascularization) and vascular events (non-hemorrhagic stroke and peripheral vascular surgery). Spearman correlation and Wilcoxon test were performed to estimate the relationship of EAT with demographic characteristics and risk factors. ROC analysis was performed to detect the effect of EAT on cardiac, vascular, and all events.

Results: There were 38 events among 316 participants (34 cardiac, 4 vascular events) over a mean follow up of 4.3 years. EAT volume ranged from 10 to 413 cc (mean 82 ± 41 cc, median 75 cc). EAT volume was correlated with weight ($r = 0.47$ $p < 0.0001$), body mass index ($r = 0.44$ $p < 0.001$), systolic blood pressure ($r = 0.19$ $p = 0.001$), diastolic blood pressure ($r = 0.12$ $p = 0.03$), triglycerides ($r = 0.2$ $p = 0.0003$), and HDL ($r = -0.25$ $p < 0.0001$), as

well as male gender ($p = 0.0008$) and hypertension ($p = 0.01$) but not diabetes or calcium score. Although not robustly powered for cardiac events (AUC=0.58, $p = 0.096$, power = 0.35) there did not appear to be an association between EAT and all-cause mortality or cardiac events. However, EAT appeared more associated with vascular events, which were few in number ($n = 4$, threshold 117 cc, sensitivity 75%, specificity 87%, AUC 81.3, $p = .0171$, power = 0.59).

Conclusions: Although EAT was associated with cardiovascular risk factors and vascular events, in this high risk group, EAT volume did not provide prognostic information regarding cardiac events.

3:30 p.m.

1045-247

Assessment of Local Myocardial Stress and Function in Ischemic Cardiomyopathy: A New Method Using Multidetector Computed Tomography and Novel Software System

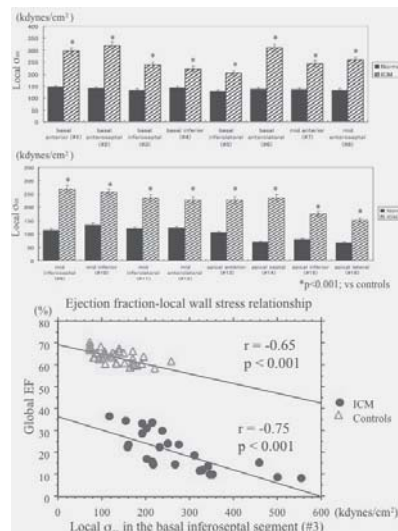
Yasuhiro Shudo, Goro Matsumiya, Hajime Matsue, Koji Takeda, Koichi Toda, Kazuhiro Taniguchi, Yoshiaki Sawa, Osaka University Graduate School of Medicine, Suita, Osaka, Japan, Japan Labour Health and Welfare Organization, Osaka Rosai Hospital, Sakai, Osaka, Japan

Background: Local myocardial stress is an important index of ventricular loading conditions, though it is very difficult to measure reliably in clinical settings, especially in an infarcted ventricle. We developed a novel software system to use with multidetector computed tomography (MDCT), which allowed us to estimate local circumferential stress of the infarcted ventricle. In this pilot study, we investigated local end-systolic stress (σ_{es}) in pts with ischemic cardiomyopathy (ICM) due to broad antero-septal myocardial infarction.

Method: We studied 30 consecutive ICM pts (age 65 ± 10 years, EF $21 \pm 9\%$) and 38 normal control subjects (age 66 ± 11 years, EF $63 \pm 6\%$). Left ventricular MDCT angiograms (4-, 3-, 2-chamber views) were acquired as AVI files, transferred to a software-installed computer for offline analysis and analyzed using Janz's method to estimate local σ_{es} in 16 segments, based on AHA/ASE segmentation criteria. End-systolic pressure was obtained from calibrated carotid pulse tracing measured just before the MDCT angiography.

Results: Local σ_{es} in each segment was significantly higher in ICM pts than the controls (Figure). A highly significant relation was found between global EF and local σ_{es} in the basal inferoseptal non-infarcted segment (#3) in ICM pts, while the same relation was present in the controls, though lower (Figure).

Conclusion: These results suggest that our newly developed software system with MDCT may be useful to assess local σ_{es} and systolic ejection in ICM pts.



3:30 p.m.

1045-248

Multidetector Computed Tomographic Cardiac Venography for Noninvasive Coronary Sinus Imaging in Ischemic Cardiomyopathy: Implications for Cardiac Resynchronization Therapy in the Setting of Prior Myocardial Infarction

Thananya Boonyasirinant, Paul Schoenhagen, Sandra S. Halliburton, Scott D. Flamm, Cleveland Clinic, Cleveland, OH

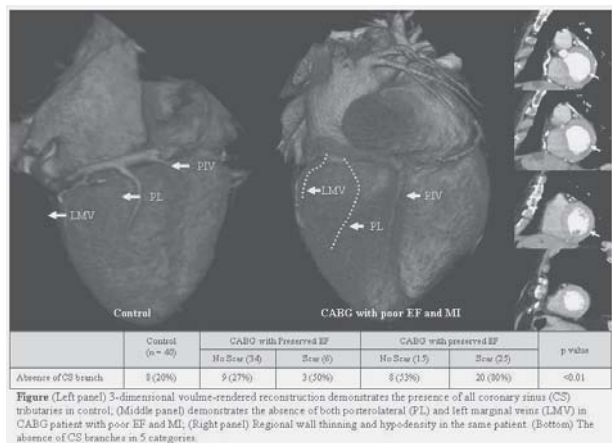
Background: Cardiac resynchronization therapy (CRT) is a therapeutic strategy in severe heart failure, however non-response rate remains 30%, particularly in ischemic cardiomyopathy. Coronary sinus (CS) tributaries may be absent in infarct myocardium owing to thrombosed veins. We sought to assess the absence of CS branches in patients with coronary bypass graft (CABG) with poor ejection fraction (EF), and the relationship with evidence of myocardial infarction (MI).

Methods: The CS and its tributaries were assessed by multidetector computerized tomography (MDCT) in 120 patients: 40 CABG with poor EF, 40 CABG with preserved

EF, and 40 controls. Regional wall thinning with hypodensity was categorized as MI, then summed scar score was calculated using a 17 segment model.

Results: MI was present in 25 CABG with poor EF and 6 CABG with preserved EF. The absence of posterolateral or left marginal vein was greater in patients with MI vs no MI (80% vs 53% in CABG with poor EF, and 50% vs 27% in CABG with preserved EF), and 20% in controls ($p<0.01$). The extent (higher summed scar score) and inferolateral MI was correlated with lack of CS branches ($p<0.001$).

Conclusions: The absence of CS branches was substantially greater in CABG patients with poor EF, particularly with prior MI. This is the first to relate the absent CS branches with evidence of MI, and also its extent and location, using MDCT. The absence of amenable CS hinders proper LV lead positioning, thus provides MDCT as a potential effective screening tool for CRT candidates.



3:30 p.m.

1045-249

Correlation Between Left Ventricular Size by Computed Tomography and Thoracic Aortic Distensibility Measured by MRI: Multiethnic Study of Atherosclerosis (MESA) Study

Mouaz H. Al-Mallah, Khuram Nasir, Ronit Katz, Junichiro Takasu, Song Shou Mao, João Lima, Juan J. Rivera, David A. Blumke, William Gregory Hundley, Roger Blumenthal, Mathew J. Budoff, Henry Ford Hospital, Detroit, MI, Harbor-UCLA Medical Center, Torrance, CA

Background: The correlation between decreased arterial compliance and left ventricular size (LVS) on CT, a marker of LV dysfunction, has not been well demonstrated. We tested the hypothesis that decreasing aortic compliance and increasing arterial stiffness is independently associated with increased LVS.

Methods: The final study population consisted of 3,540 subjects from the MESA study (61±10 years, 46% males) who underwent aortic distensibility (AD) assessment on MRI. The CT derived LVS was defined as the sum of LV mass and LV intracavitary volume. The calculated LVS was taken from a measurement of a single slice from noncontrast images and indexed by body surface area (BSA). Linear regression models for the correlation between LVS and AD were calculated.

Results: The mean AD was 1.84 ± 1.26 mmHg⁻¹, while the mean adjusted LVS was 100.3 ± 25.3 ml. After adjusting for demographic and atherosclerotic risk factors, there was a significant negative correlation between LVS and AD. The table shows the odds ratio of LVS>75th percentile across the AD quartiles. As distensibility decreases, the odds of LVS more than 75th percentile increased.

Conclusion: Our analysis has demonstrated that increased arterial stiffness is independently associated with increased LVS after adjusting for race and other atherosclerotic risk factors. This may potentially provide a new tool that correlates with diastolic dysfunction.

	Regression coefficient for AD per SD Increase	Quartile 4 (>2.33 mmHG-1)	Quartile 3 (1.57-2.32 mmHG-1)	Quartile 2 (1.05-1.56 mmHG-1)	Quartile 1 (<1.04 mmHG-1)
Model 1: adjusted for age, gender, race	-2.3 (1.44,-3.16)	Ref group	1.19 (0.94-1.55)	1.65 (1.28-2.13)	1.76 (1.330-2.33)
Model 2: adjusted for age, gender, race, hypertension, diabetes mellitus, cigarette smoking, LDL cholesterol levels, cholesterol lowering medications	-1.62 (-0.77,-2.47)	Ref group	1.19 (0.94-1.51)	1.67 (1.29-2.15)	1.78 (1.3-2.36)
Model 3: Model 2, log (CAC+1), log CRP	-1.59 (-0.75,-2.43)	Ref group	1.26 (1.0-1.59)	1.82 (1.42-2.32)	2.05 (1.58-2.65)

1045-250

Visual Estimation of Coronary Artery Calcium from Low-Dose CT Attenuation Correction Scans Shows Close Agreement With Standard Agatston Score in Hybrid SPECT/CT and PET/CT

Andrew J. Einstein, Lynne L. Johnson, Randall C. Thompson, Timothy M. Bateman, Sean W. Hayes, Daniel S. Berman, Columbia University Medical Center, New York, NY, Mid America Heart Institute, Kansas City, MO

Background: Hybrid SPECT and PET cameras incorporating multi-detector row CT scanners have become more widely available in recent years. At the time of myocardial perfusion imaging, such systems obtain a low-dose, non-ECG-gated CT scan that is used to perform attenuation correction. The utility of this CT attenuation correction (CTAC) scan in estimating actual coronary artery calcium (CAC) as measured by the Agatston score (AS) on standard ECG-gated CAC scans has not been previously studied.

Methods: 493 patients from 3 centers performing hybrid SPECT/CT or PET/CT were studied retrospectively (Columbia University: Philips Precedence 16P SPECT/CT, Mid-America Heart: Siemens Biograph 16 PET/CT, Cedars-Sinai: Siemens Biograph 64 PET/CT). Each patient had received both a myocardial perfusion study with CTAC and a CAC scan performed on the same day. At each site, experienced readers blinded to the AS reviewed CTAC images and visually estimated CAC on a six point scale: 1=AS 0, 2=1-9, 3=10-99, 4=100-300, 5= 400-999, 6= ≥ 1000 . Agreement between visually-estimated CAC (VECAC) on CTAC and AS, measured on the standard CAC scan and converted to the same six point scale, was determined using weighted kappa statistics, with linear weighting and bootstrap with 1000 replications for confidence intervals. Statistical analysis was performed using STATA 10.1 (StataCorp, College Station, TX).

Results: Although CTAC images are not considered diagnostic quality, a high degree of association was observed between VECAC and AS, with 92.7% of VECACs within one category of the AS category. Weighted kappa was 0.77 (95% confidence interval 0.73 to 0.80, $p<0.0001$). High weighted kappa statistics were observed for each site (range 0.71 to 0.80), for each scanner vendor (0.75 and 0.78), and for women and men (0.76 and 0.77, respectively).

Conclusions: Coronary artery calcium can be visually assessed from low-dose CTAC scans with outstanding agreement with AS. CTAC scans should be routinely assessed for VECAC. These data may allow the development of protocols for both performing attenuation-corrected myocardial perfusion imaging and assessing CAC using lower radiation dose.

3:30 p.m.

1045-251

Radial Strain Mapping Using Multidetector Computer Tomography Cine Recordings Reflects Regional Myocardial Function: A Multimodality Tissue Tracking (MTT) Study

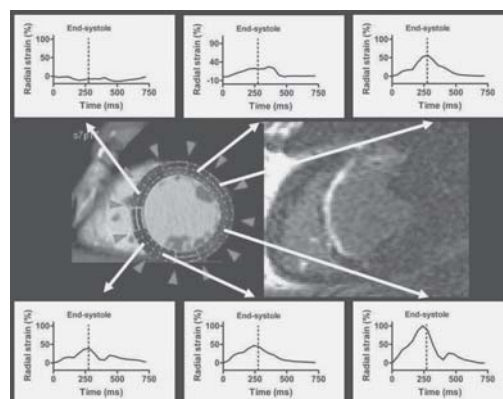
Thomas M. Helle-Valle, Verônica R S Fernandes, Boaz D. Rosen, João A C Lima, Johns Hopkins University, Baltimore, MD

Background: Detection of regional left ventricular (LV) dysfunction has important clinical consequences. Multidetector computer tomography (MDCT) has become a useful noninvasive clinical tool for assessment of coronary artery disease, but evaluation of regional myocardial function is restricted to visual assessment of wall motion. We have recently introduced and validated multimodality tissue tracking (MTT) as a new automated pixel based pattern matching software that allows quantification of cardiac and vascular deformation from cine ultrasound, MRI and MDCT. We hypothesized that radial strain mapping by MTT MDCT could identify segmental infarct extent determined by delayed enhancement MRI.

Methods: In 12 patients with ischemic heart disease radial strain by MTT was measured from midventricular short-axis recordings (12 segments) obtained by a 64-slice MDCT scanner. To compensate for differences between patients in LV contractility, strain values were normalized in each patient with reference to the segment of maximum strain. Segmental infarct extent was determined by delayed gadolinium enhancement MRI.

Results: Segmental strain differed significantly between remote, border-zone and infarcted segments (74.2 ± 23.1 , 42.5 ± 33.2 and $17.9 \pm 2.3\%$, respectively, $P<0.05$), and showed good correlation with segmental infarct extent ($r=-0.61$, $P<0.0001$).

Conclusion: To our knowledge this is the first study to demonstrate that regional LV function can be quantified from MDCT images.



3:30 p.m.

3:30 p.m.

1045-252

Correlation of Breast Artery Calcification by Mammography With Coronary Artery Calcification Using 64 Slice CAT Scan: The BAC-CAT Study

Michael A. Rossi, James Newcomb, Kenneth Harris, Lee Phillips, Crystal Maksimik, James Reed, Lehigh Valley Hospital and Health Network, Allentown, PA, Penn State University College of Medicine, Hershey, PA

Background: The clinical significance of breast artery calcification (BAC) detected on routine mammography (MMG) has not been well established. Identification and quantification of coronary artery calcium (CAC) using multi-slice Computed Tomography (MSCT) has been shown to correlate with the presence and extent of coronary artery disease (CAD). The purpose of our study is to assess the correlation between the presence of BAC on MMG and CAC by MSCT.

Methods: A random sample of 192 asymptomatic women without known CAD who underwent MMG were identified with (n=88) or without (n=104) BAC. All underwent CAD risk factor questionnaires and MSCT for CAC scoring.

Results: The women with BAC were older than those without BAC. Otherwise, there was no difference between the groups of women with and without BAC for traditional risk factors of diabetes, hypertension, hyperlipidemia, smoking, and family history. There was no definite correlation found between the presence of BAC on MMG and CAC on MSCT (p=0.33). However, among women with CAC, if BAC was present then the degree of CAC was likely to be severe, with a CAC score >400 (p=0.001).

Without BAC (n=104) With BAC (n=88)

Risk Factors:

Age 57.6 60.8 p=0.006

DM 11.5% 13.6% p=0.661

HTN 26.9% 39.8% p=0.059

Chol 33.7% 43.2% p=0.175

Smoking 29.8% 36.4% p=0.499

Fam Hx 49.0% 53.4% p=0.546

CAC Score:

0 54.8% 47.7% p=0.328

>0 45.2% 52.3% p=0.435

>400 1.0% 12.5% p=0.001

Conclusions: Our study demonstrates the lack of association between the presence of BAC on MMG and CAC by MSCT, independent of traditional CAD risk factors. Given the frequency of BAC on screening MMG, it is useful to know that the finding of BAC does not appear to correlate with the presence of subclinical CAD.

3:30 p.m.

1045-253

Ultra-Low Dose Intra-Arterial Contrast Injection for Ilio-femoral Computed Tomographic Angiography: A Novel Imaging Protocol

Subodh B. Joshi, Dorinna D. Mendoza, Daniel H. Steinberg, Cristian F. Lopez, Arnold Raizon, Gaby Weissman, Joseph Hutter, Lowell F. Satler, Augusto D. Pichard, Guy Weigold, Washington Hospital Center, Washington, DC

Background: Assessment of iliac and femoral artery anatomy is important prior to cardiac interventions that use large bore catheters, such as percutaneous aortic valve replacement. We developed a novel protocol for ilio-femoral computed tomographic (CT) angiography using ultra-low dose intra-arterial contrast injection to follow diagnostic cardiac catheterization.

Methods: Thirty-seven patients underwent standard iliac angiography during cardiac catheterization. A pigtail catheter was left in situ in the infrarenal abdominal aorta. Forty cc of a 1:3 to 1:4 dilution contrast to saline mixture was injected intra-arterially via the pigtail catheter while a spiral CT was acquired. Fluoroscopic and CT angiography images were analyzed independently for tortuosity, calcification and vessel caliber to assess suitability for large bore (7 mm diameter) arterial access.

Results: Excellent CT image quality was obtained in 34 patients (92%). The mean contrast dose was 12 ± 2 cc. In 9 patients (24%), CT changed the fluoroscopic assessment of femoral access feasibility. Furthermore, in another 7 patients (19%), unfavorable anatomy as demonstrated by CT directed the avoidance of a particular side. Overall, CT findings would have altered the interventional approach in 16 patients (43%).

Conclusion: High quality aorto-ilio-femoral CT angiography can be obtained with 10-15 cc of contrast injected via a pigtail catheter in the abdominal aorta, and may alter management when performed after cardiac catheterization.



1045-254

Gender Differences in the Assessment of Coronary Artery Stenosis Risk Using Coronary Calcium Scores in Patients Undergoing Conventional Coronary Angiography

Shah Azmoon, Ramin Ebrahimi, Naser Ahmadi, Matthew Budoff, Harbor-UCLA, Torrance, CA

B: Currently calculation of probability of coronary artery stenosis (CAS) based on coronary artery calcium score (CAC) levels does not take into account the potential effects of gender variation. We sought to evaluate the effect of gender on the probability of significant (>50% luminal stenosis) CAS at same CAC levels in patients undergoing conventional coronary angiography (CCA).

M: 1851 consecutive patients who underwent CAC quantification prior to CCA were evaluated for CAC scores and obstructive coronary disease. Computed tomography (CT) and invasive angiography readers were blinded to results of other tests and demographics.

R: The prevalence of obstructive CAS was significantly lower in females compared to males (40.2% vs. 60.7% respectively, p < 0.001). Women were on average 4 years older than men within every CAC score group. With the exception of CAC score interval of >1000, males had a higher prevalence of significant CAS at every CAC score interval (p < 0.01).

Table 1. Gender and CAC Score in Association to Significant CAS

	0	0	1-10	1-10	11-100	11-100	101-400	101-400	400-1000	400-1000	>1000	>1000
	m	f	m	f	m	f	M	f	m	f	m	f
Cohort (#)	185	200	105	65	222	110	287	165	214	99	156	43
Age (mean)	48	53	52	56	55	60	58	62	62	65	64	67
CAC (ave)	0	0	4	4	49	52	230	216	645	646	1951	1845
CAS (#)	24	11	37	10	116	41	215	92	180	79	137	41
(#)	(13.0%)	(5.5%)	(35.3%)	(15.4%)	(52.3%)	(37.3%)	(74.9%)	(55.8%)	(84.1%)	(79.8%)	(87.8%)	(95.3%)
P value	0.004		0.001		0.002		0.001		0.006		0.03	

C: These data point to the potential influence of gender in the overall assessment of probability of significant CAS based on standard CAC scores. Incorporation of gender may enhance the predictive value of risk of significant CAS based on CAC scores.

3:30 p.m.

1045-255

Relationship of Oxidized LDL Biomarkers, Persistent Vascular Dysfunction Measured by Fingertip Digital Thermal Monitoring and Progression of Coronary Artery Calcification

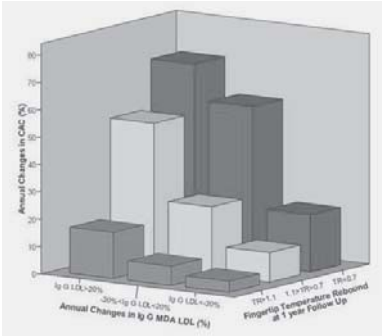
Naser Ahmadi, Fereshteh Hajsadeghi, Ferdinand Flores, Sotirios Tsimikas, Harvey Hecht, Morteza Naghavi, Matthew Budoff, Los Angeles Biomedical Research institute at Harbor UCLA Medical Center, Torrance, CA

Background: Oxidized low density lipoproteins (OxLDL) are pro-inflammatory and pro-atherogenic. This study evaluated the relationship of changes in biomarkers of OxLDL to vascular dysfunction measured by digital thermal monitoring (DTM) and to progression of coronary artery calcium (CAC).

Methods: 60 asymptomatic intermediate risk patients (age 61±9 years, 78% Male) on chronic statin therapy underwent CAC and DTM vascular function assessment measured by fingertip temperature rebound (TR) after a 5-minute arm-cuff reactive hyperemia test (VENDYS™, Endothelix Inc.) at baseline and 12 months. Autoantibodies to malondialdehyde (MDA)-LDL, and oxidized phospholipids (OxPL) on apolipoprotein B-100 (OxPL/apoB) were measured and baseline and 1 year follow up. CAC-progression was defined as an increase in CAC>15% per year.

Results: At one year, OxPL/apoB levels increased and IgG and IgM MDA-LDL autoantibody levels decreased more in CAC non-progressors and in patients with improved TR (TR>1.1 vs. TR<0.7) (P<0.001 for both). CAC increased proportionally with decreasing TR and OxPL/apoB levels. The change in TR correlated well with changes in OxPL/apoB (r = 0.71, p=0.0008) and CAC (r = -0.89, p=0.001).

Conclusion: Increases in OxPL/apoB and decreases in IgG and IgM MDA-LDL autoantibodies are associated with improved vascular function and lack of progression of CAC. This study documents a robust pathophysiological relationship between pro-inflammatory OxPL, vascular function and progression of CAC.



3:30 p.m.

1045-256

Modification of Global Coronary Heart Disease Risk by Coronary Calcium Scanning: Preliminary Results from the Early Identification of Subclinical Atherosclerosis Using Noninvasive Imaging Research (EISNER) Study

Johanna HM Kim, Heidi Gransar, Nathan D. Wong, Leslee J. Shaw, Romalisa S. Miranda-Peats, Daniel S. Berman, Cedars-Sinai Medical Center, Los Angeles, CA, University of California, Irvine, CA

Background: Current evidence is inconclusive as to whether undergoing a coronary calcium (CC) scan results in improved CHD risk or outcomes. **Methods:** We assessed Framingham Risk Score (FRS) change in asymptomatic, intermediate-risk subjects randomized 2:1 to undergo CC scan vs. no scan at baseline in the EISNER prospective randomized trial. FRS was calculated on 510 subjects (mean age 59±9 yrs, 47% female) who had a baseline and 1-year followup risk assessment. Subjects were divided into those with no CC scan (n=144), CC score (CCS) of 0 (n=157), 1-99 (n=126) or ≥100 (n=83). **Results:** At baseline, 48% of the subjects had low (<6% FRS), 15% moderate (6-10%), 29% moderately high (10-20%), and 8% high (>20%) risk. Overall mean FRS was 8.0% at baseline and 7.9% at follow-up ($\Delta = -0.1 \pm 4\%$, $p=0.64$), where mean changes in FRS were $0.1 \pm 4.4\%$ in the no scan vs. $-0.2 \pm 3.9\%$ in the scan group ($p=0.47$). Age and gender-adjusted logistic regression showed the odds ratio and 95% CI for a FRS reduction was 1.25 (0.80-1.93, $p=0.33$) for the scan vs. no scan group. However, when comparing CCS categories to the no scan group, the adjusted odds ratio for FRS reduction was 1.05 for CCS 0 ($p=0.84$), 1.14 for CCS 1-99 ($p=0.64$), and 1.81 for the CCS ≥100 group ($p=0.04$). Further, when changes by ≥1 FRS category were considered, the CCS 1-99 and CCS ≥100 groups had significantly greater frequency of improved FRS scores as compared to the CCS 0 group (17.6% vs. 7.4% ($p=0.01$) and 16.5% vs. 7.4% ($p=0.03$), respectively). Other baseline factors associated with FRS reductions included (in order of importance) elevated total cholesterol, elevated systolic blood pressure, being male, current smoking, and low HDL-cholesterol levels. **Conclusion:** Among asymptomatic, intermediate-risk individuals, CC scanning did not alter changes in 1-yr FRS compared to controls. However, improvements in FRS were evident in patients with CCS ≥100, suggesting that identification of moderately extensive subclinical coronary atherosclerosis by the CCS may result in short-term improvements in global estimated risk of CHD.

3:30 p.m.

1045-257

Marked Decrease in Epicardial Fat Volume Five Years After Gastric Bypass Surgery: Relationship to Visceral Fat Volume and Coronary Calcification

Nathaniel Hall, Tiffany Priestler, Travis Ault, Theophilus Owan, Richard Gress, Ted Adams, Steven Hunt, Sheldon E. Litwin, University of Utah, Salt Lake City, UT

Background: Visceral fat within the abdominal cavity is widely believed to contribute to development of the metabolic syndrome and also to increase the risk of cardiovascular disease. More recently, some groups have suggested that epicardial fat may behave similarly to visceral fat and increase the risk of CAD. No previous studies have evaluated the effect of gastric bypass surgery (GBS) on epicardial fat volume.

Methods: We performed gated, noncontrast CT scans of the heart and abdomen (at L4-5) in a subset of patients enrolled in a registry that is prospectively following severely obese patients (n=1156) treated with GBS or nonsurgical therapy. We studied 67 patients returning for 5 year follow up visits. 40 subjects were in the nonsurgical group (Nonsurg) and 27 were in the GBS group. The 2 groups were well-matched at baseline in terms of age, gender, BMI and cardiac risk factors.

Results: At the 5 year visit, GBS subjects had a mean BMI of $33.8^* \pm 46.6$ in Nonsurg subjects ($*p < .05$ vs. Nonsurg). Epicardial fat volume was lower in the GBS group ($89 \pm 38^* \text{ cc}$) vs. the Nonsurg group ($150 \pm 60 \text{ cc}$). Visceral fat volume was also lower ($60 \pm 42^* \text{ vs. } 147 \pm 57 \text{ cc}$). There was a positive correlation between visceral fat and epicardial fat for all subjects ($r=0.8$, $p < 0.001$) and within each group (GBS $r=0.71$, $p=0.002$; Nonsurg $r=0.72$, $p < 0.001$). Epicardial fat volume also correlated with BMI ($r=0.63$, $p < 0.0001$) and waist circumference ($r=0.69$, p zero CAC score (112 ± 54 vs. $155 \pm 68 \text{ cc}$, $p=0.23$). Similarly, we did not find significant correlations between epicardial fat volume and CAC score in those patients who had detectable coronary calcium.

Conclusion: Marked weight loss with GBS is associated with lower epicardial and visceral fat volumes. Visceral fat volume declines by a greater proportion than epicardial fat. Epicardial fat volume is related to BMI, waist circumference and visceral fat volume. However, we did not find a clear link between epicardial fat volume and coronary artery calcification.

3:30 p.m.

1045-258

Systemic Inflammatory Marker Improve the Prediction of Coronary Calcifications

Christoph D. Garlachs, Atilla Yilmaz, Thomas Frank, Dorette Raaz, Iwona Cicha, Stephan Achenbach, Piotr Lewczuk, Jens Wiltfang, Werner Daniel, Medical Clinic II, University Clinic Erlangen, Erlangen, Germany, Clinic for Psychiatry, University Clinic Erlangen, Erlangen, Germany

Background: Coronary calcification is a marker of coronary atherosclerosis. Since atherosclerosis is a chronic inflammatory disease, we investigated whether the evaluation of systemic inflammatory parameters can predict coronary calcification and improve the predictive value of lipids and age for coronary calcification.

Methods: Plasma was obtained from 230 patients (~60 years, 146 male, 84 female) with clinical indication for performing cardiac CT, and analysed with a Luminex Laser-based Fluorescence Analyser. Quantification of coronary calcification was performed by

applying the Agatston Score to the MDCT data. To identify predictive biomarkers, we compared 144 coronary calcifications patients (CAC) with a control group (C; n=86).

Results: CAC had significantly enhanced plasma concentrations of IL-7 ($10.92 \pm 7.60 \text{ pg/mL}$ in C; $p=0.009$) and IL-13 ($60.55 \text{ vs } 48.20 \text{ pg/mL}$; $p<0.02$) as well as the chemokines eotaxin ($p<0.5$), MCP-1 ($p<0.01$) and IP-10 ($p<0.0001$). Adjustment for sex eliminated association of eotaxin and MCP-1 with coronary calcification, whereas IL-7, IL-13 and IP-10 remained significant predictors. In a sex- and age- and risk factor-adjusted model, IL-7, IL-13, and IP-10 remained significantly associated with coronary calcification. When CAC age and biomarkers' levels were divided into tertials, patients >63 years showed a 5-fold elevated risk of coronary calcifications as compared to patients <56 years, whereas in patients with a IP-10 concentration of >121 pg/mL the risk was increased 4-fold as compared to patients with a IP-10 <79 pg/mL. MCP-1, eotaxin, IL-13, and, at the borderline significance, IL-7 were also associated with elevated risk. Taken MCP-1, eotaxin, and IP-10 together, a 4-fold increase in risk of coronary calcification existed at the upper tertial concentrations of the 3 chemokines. The established biomarkers, lipids, hsCRP, and IL-6 did not show significant differences between C and CAC.

Conclusions: The inflammatory parameters IL-7, IL-13, and IP-10 allow the prediction of CAC independent of age and serum lipids. In combination with age, IL-7 and IL-13 showed a strong association with elevated risk for coronary calcification.

3:30 p.m.

1045-259

Usefulness of 64-Row Multidetector Computed Tomography for the Evaluation of Patients With Variant Angina

Kyohei Yamaji, Takeshi Arita, Yoshimitsu Soga, Shinichi Shirai, Koyu Sakai, Hiroyoshi Yokoi, Masashi Iwabuchi, Hideyuki Nosaka, Masakiyo Nobuyoshi, Kokura Memorial Hospital, Kitakyushu, Japan

Background: Invasive coronary angiography is useful in patients with suspected variant angina to document an episode of coronary artery spasm with provocative test. The aim of this study was to clarify the relation between 64-row Multi-detector Computed Tomography (MDCT) findings of coronary artery and vasospasm.

Methods: A total of 77 patients with suspected variant angina (42 females and 35 males, aged 49 to 87 years, mean 65 ± 9 years) who have no evidence of luminal narrowing in major coronary artery with MDCT and underwent ergonovine test to detect the presence of coronary artery spasm were enrolled in this study. Two patients were excluded because of poor images of MDCT. The criteria of positive ergonovine test was total occlusion or localized occlusive spasm associated with chest pain and ST segment elevation after administration of ergonovine into the left coronary artery. The presence of plaques and calcifications in major coronary artery were evaluated with MDCT.

Results: 26 of 75 (34.7%) patients were positive with ergonovine test. 10 of 26 (38.5%) were total occlusion and 16 of 26 (61.5%) were localized spasm. Using MDCT, atherosclerotic lesions were observed at all coronary spasm sites. Presence of plaques was significant factor for positive ergonovine provocation test ($p = 0.006$).

Conclusions: Patients with positive ergonovine test had coronary artery plaques at the site of coronary spasm sites. Absence of coronary artery plaques with MDCT could rule out variant angina.

Association of CT findings with the result of ergonovine provocation test

Ergonovine provocation test	All plaques	Calcified plaques	Plaques in left anterior descending	Plaques in left circumflex	Plaques in right coronary artery	Plaques in left main trunk
Positive	26/26 (100%)*	15/26 (57.7%)	25/26 (96.2%)**	6/26 (23.1%)	11/26 (42.3%)	2/26 (7.7%)
Total occlusion	10/10 (100%)	5/10 (50.0%)	9/10 (90.0%)	3/10 (30.0%)	6/10 (60.0%)	1/10 (10.0%)
Focal spasm	16/16 (100%)	10/16 (62.5%)	16/16 (100%)	3/16 (18.8%)	5/16 (31.3%)	1/16 (6.3%)
Negative	37/49 (75.5%)*	29/49 (59.2%)	37/49 (75.5%)**	18/49 (36.7%)	24/49 (49.0%)	6/49 (12.2%)
	* p = 0.006		** p = 0.025			

3:30 p.m.

1045-260

HIV Is Independently Associated With Detectable Coronary Artery Calcium

Priscilla Y. Hsue, Steven G. Deeks, Amanda Schnell, Melissa Krone, Yu Xie, Theodore Lee, Karen Ordoval, Gautham Reddy, Peter Ganz, Jeffrey N. Martin, University of California, San Francisco, San Francisco General Hospital, San Francisco, CA

Background: HIV patients are at increased risk for cardiovascular disease. It remains unclear whether this is because of HIV infection itself, its treatment, or an excess of traditional risk factors. Detection of coronary artery calcium (CAC) by computerized tomography (CT scan) in HIV-uninfected persons is a strong predictor of coronary artery disease independent of traditional risk factors. We used this approach to investigate the role of HIV infection in coronary artery disease.

Methods: We measured CAC using a 16-detector Philips CT scanner in 247 HIV-infected individuals and 45 uninfected adults. None had symptoms of active coronary artery disease. CAC scoring was determined by the modified Agatston method. The independent role of HIV infection *per se*, HIV-related disease factors, and other traditional risk factors in influencing CAC was determined by multivariable regression.

Results: The median age was 49 years (IQR 43-54) for the HIV patients and 48 years (IQR 43-54) for the uninfected; 91% those with HIV and 78% of the uninfected were men. The median duration of HIV infection was 16 years, the median CD4 cell count was 471;

73% were on antiretroviral therapy (ART). Among the HIV-infected, 38% had detectable CAC versus 29% of the uninfected ($p=0.022$); 16% of the HIV-infected had a calcium score > 100 vs. 4% of controls ($p=0.039$). After adjusting for age, gender, race, smoking, hypertension, and diabetes mellitus, the HIV-infected subjects had a significantly higher prevalence of detectable CAC (OR = 2.7, 95% CI 1.06-6.7, $p=0.037$). A similar effect was observed when restricting the HIV-infected to subjects who had never used ART (OR=3.3; 95% CI 0.77-13.9; $p=0.11$). Among HIV-infected subjects, neither duration of ART or protease inhibitors, or proportion of time with a detectable HIV RNA level were associated with the presence of CAC. Among the HIV-infected, only age, gender, and race were associated with CAC.

Conclusions: HIV infection is independently associated with a higher prevalence of CAC and, thus, subclinical coronary artery disease. This effect was observed even among those who had never received antiretroviral therapy, arguing for a treatment-independent effect of HIV infection.

3:30 p.m.

3:30 p.m.

1045-261

Coronary Velocity Flow Reserve Is Affected by Coronary Calcification in Asymptomatic Patients With Mild Coronary Artery Disease

Dimitrios Tsiapras, Irene Mastorakou, Vasiliki Vartela, Olga Karapanagiotou, Stamatis Kyzopoulos, Spyridoula Katsiloulis, Vassili Voudris, Onassis Cardiac Surgery Center, Athens, Greece

Background: An estimate of total atherosclerotic burden in asymptomatic individuals, may improve coronary risk stratification. Coronary calcium score (CCS) above 300 identify high risk patients (pts). However, there is an inconsistency in SPECT myocardial perfusion and CCS. The aim of this study was to evaluate the coronary velocity flow reserve in asymptomatic pts with mild coronary artery disease and wide range of calcification.

Methods: We studied 48 asymptomatic pts who had undergone a cardiac scan with a dual source 64 slice computer tomography and left anterior descending (LAD) diameter stenosis less than 60% (range 20-60%) was detected. The CCS was calculated for all vessels (total CCS) and LAD territory separately (LAD CCS). A Vivid7 GE echocardiographic apparatus was used for distal LAD flow interrogation, from a modified 2 chamber apical view. LAD flow was recorded at baseline and after dipyridamole (0.56 mg/kg in 4 min) infusion and flow velocity (maximum and mean) was measured. Coronary flow reserve (CFR) was calculated as the ratio of peak to baseline maximum (CFRmax) and mean (CFRmean) velocities. Pts were divided in 2 groups, with low (Group L: 21 pts, CCS<300) and advanced (Group H: 27 pts, CCS>300) total CCS.

Results: Despite the different LAD CCS (L: 30 ± 33 vs H: 348 ± 198 , $p<0.001$), no significant difference was detected in LAD stenosis among groups (L: 36 ± 14 vs H: $42\pm 17\%$, $p=0.13$). Left ventricular ejection fraction was similar in both groups (L: 63 ± 7 vs H: $62\pm 6\%$, $p=ns$) while no resting regional wall motion abnormalities were detected. In Group L, a significant increase in both CFRmax (L: 2.70 ± 0.53 vs H: 1.93 ± 0.28 , $p<0.001$) and CFRmean (L: 2.71 ± 0.52 vs H: 1.91 ± 0.32 , $p<0.001$) was detected. Using linear regression analysis correlation was detected between total CCS and CFRmax or CFRmean ($r=0.58$, $p<0.05$ for both) and LAD CCS and CFRmean ($r=-0.63$, $p<0.05$). LAD stenosis (in this range of values) did not show any significant correlation with CFR (max or mean).

Conclusion: Coronary calcification seems to be more important in coronary velocity flow reserve than the absolute reduction of lumen diameter stenosis, in asymptomatic pts with mild coronary artery disease.

3:30 p.m.

1045-262

Fast Computer-Aided CT-Based Quantitation of Pericardial and Thoracic Fat and Their Association With Coronary Calcium

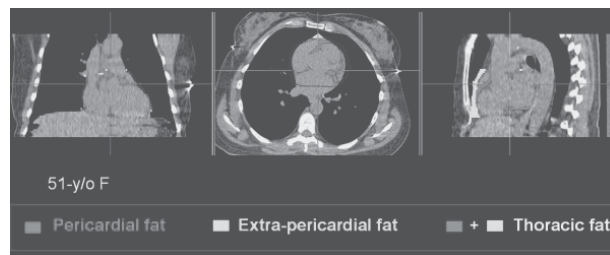
Damini Dey, Balaji Tamarappoo, Nakazato Ryo, Abhishek Shah, Amit Ramesh, Heidi Gransar, Romalisa Miranda-Peats, Ioannis Kakadiaris, Piotr J. Slomka, Nathan D. Wong, Daniel S. Berman, Cedars-Sinai Medical Center, Los Angeles, CA, University of California, Irvine, CA

Background: Pericardial fat may provide added risk information regarding coronary artery disease. We extended previously developed quantitation of thoracic fat volume (TFV) from non-contrast coronary calcium (CC) CT scans (CCS), QFAT, to quantify pericardial fat volume (PFV), and investigated the association of PFV, TFV with CC.

Methods: QFAT measures TFV automatically from user-defined range of CT slices. In addition, pericardial fat contours (PFC) are generated by spline interpolation between 5-7 user-defined control points, placed roughly on the pericardium. Contiguous fat voxels within PFC are automatically identified as pericardial fat. PFV and TFV were quantified over the entire heart extent for 177 CCS. In 105 patients, abdominal visceral fat area (VFA) was measured from an additional single-slice CT. Multiple logistic regression was used to examine association of PFV, TFV with CC (Agatston score >0).

Results: PFV and TFV showed excellent correlation with VFA ($R=0.79$, $R=0.89$, $p<0.0001$), and moderate correlation with BMI ($R=0.55$, $R=0.51$, $p<0.0001$). PFV and TFV showed higher association with CC than BMI [PFV: $p=0.007^*$, Odds Ratio (OR) 4.4; TFV: $p<0.001^*$, OR 8.7], measured waist circumference/height (W/H) [PFV: $p=0.07$, OR 3.0; TFV: $p=0.003^*$, OR 5.6], or standard risk factors [PFV: $p=0.1$, OR 2.8; TFV: $p=0.03^*$, OR 3.9] (*-significant).

Conclusion: PFV and TFV can be quantified quickly from CCS, and are associated with CC. Our results suggest that PFV and TFV are more relevant to CC than BMI or W/H.



1045-263

Relationship Between Arterial Stiffness, Assessed Using Pulse Wave Velocity and Coronary Artery Calcification Score as Assessed by 64 Multislice Computed Tomography

Delle Donne Grazia, Marchese Procolo, Di Girolamo Andrea, Fiocchi Federica, Ligabue Guido, Romagnoli Renato, Rossi Rosario, Modena Maria Grazia, University of Modena and Reggio Emilia. Institute of Cardiology, Modena, Italy, University of Modena and Reggio Emilia. Institute of Radiology, Modena, Italy

Objective. Arterial stiffness (AS), assessed using carotid-femoral pulse wave velocity (cfPWV), predicts all-cause and cardiovascular mortality. Our aim is to evaluate its association with coronary calcification score (CACs), that predicts the onset of coronary artery disease, and Framingham risk score (FRs).

Methods. We evaluate 50 consecutive non diabetic patients (mean age 55.5 ± 9.4 , 72% men) who underwent 64 multislice computed tomography (64-MSCT) for clinically suspected coronary artery disease (CAD). We evaluated the AS calculating cfPWV and Augmentation Index (AIx) before 64-MSCT. CACs was blindly calculated with volumetric scoring method. cfPWV and AIx was calculated using established methods: ECG-gated waveforms of the right carotid, right femoral and radial artery were obtained by applanation tonometry. Blood samples were obtained within the week before the procedure and Framingham risk score (FRSc) was also calculated.

Results. cfPWV was significantly correlated with volumetric CACs ($r=0.59$; $r^2=0.35$; $p<0.0001$) and FRs ($r=0.64$; $r^2=0.41$; $p<0.0001$). Multivariable logistic regression model was used to identify independent predictors of the presence of CACs. The parameters independently associated with the presence of CACs resulted: cfPWV (OR 2.8; 95% CI 1.5-5.1; $p=0.0001$), triglyceride levels (OR 1.1; 95% CI 1.00-1.05; $p=0.23$) and HDL cholesterol levels (OR 0.93; 95% CI 0.88-0.99; $p=0.03$) after adjustment for age, male sex, total cholesterol, LDL cholesterol, history of smoking, systolic blood pressure, body mass index, and use of anti-hypertensive drugs and statins. No relationship between AIx and CACs was found ($p=0.25$).

Conclusions. As gold standard of arterial stiffness measurement, cfPWV (not the AIx) is related to subclinical coronary atherosclerosis regardless of conventional risk factors. Because its strong correlation with CACs (likely because they share the same underlying pathophysiological process) and FRs, cfPWV may be used as complementary tools for the assessment of cardiovascular risk in suspected CAD.

3:30 p.m.

1045-264

Cystatin C Is Associated With Coronary Artery Calcification in the Dallas Heart Study

Parag C. Patel, Jason B. Lindsey, Colby R. Ayers, Ronald Peshock, Amit Khara, James A. de Lemos, Sachin Gupta, Pradeep PA Mammen, Mark H. Drazner, David W. Markham, University of Texas Southwestern Medical Center, Dallas, TX

Background: Cystatin C, a novel marker of renal function, has been associated with cardiovascular disease. We tested the hypothesis that cystatin C is associated with atherosclerosis as measured by coronary artery calcification (CAC).

Methods: Cystatin C was measured in 2395 subjects of the Dallas Heart Study, a multiethnic population based study involving patients 30 to 65 years of age. CAC was also assessed by CT and scored using the Agatston method. The associations of cystatin C with different cutoffs of CAC were evaluated by univariable and multivariable analyses.

Results: Cystatin C levels ranged from 0.46 to 6.55 mg/l. In univariable analysis, increasing gender-specific quartiles of cystatin C were associated with increasing levels of CAC ($p<0.001$). In multivariable analysis adjusting for traditional cardiovascular risk factors, LV mass, and body mass index, log transformed cystatin C was associated with CAC ≥ 50 ($p=0.02$) and CAC ≥ 100 ($p<0.001$) but not with CAC ≥ 10 ($p=0.1$). After the addition of various measures of renal function to the model, this association remained robust for CAC ≥ 100 but not for CAC ≥ 50 (Table).

Conclusion: Higher levels of cystatin C were associated with subclinical atherosclerosis as measured by CAC. This association was attenuated, but remained significant after adjustment for most measures of renal function. The relationship between elevated cystatin C and adverse cardiovascular outcomes may in part be due to increased atherosclerosis burden.

Association of Cystatin C With CAC ≥ 50 and CAC ≥ 100 in the Dallas Heart Study

Outcome Variable: CAC ≥ 50	P-value Log Cystatin C	OR	95% CI
Model	0.017	2.31	1.16-4.59
Model + Cr	0.159	1.84	0.79-4.30
Model + MDRD*	0.026	2.51	1.12-5.64
Model + CG*	0.125	1.84	0.85-4.01
Outcome Variable: CAC ≥ 100			
Model	< 0.001	3.48	1.65-7.33
Model + Cr	0.052	2.49	0.99-6.27
Model + MDRD*	0.005	3.68	1.50-9.04
Model + CG*	0.014	2.94	1.25-6.93

Model: adjusted for age, gender, race, diabetes, history of hypertension, systolic blood pressure, history of myocardial infarction, smoking history, high and low density lipoprotein, CRP, LV mass, and body mass index.

* MDRD = estimated GFR by the Modification of Diet in Renal Disease equation, CG = estimated GFR by the Cockcroft-Gault equation.

3:30 p.m.

1045-265

Cardiac Magnetic Resonance Imaging Is a Useful Diagnostic Adjunct in ST-Elevation Myocardial Infarction Patients Without a Culprit Coronary Artery

Madeline Stark, John R. Lesser, Scott W. Sharkey, Christopher J. Solie, Barbara T. Unger, Terrence F. Longe, David M. Larson, Timothy D. Henry, Minneapolis Heart Institute Foundation at Abbott Northwestern Hospital, Minneapolis, MN

Background: Approximately 15% of STEMI patients do not have a culprit coronary artery although many have elevated positive biomarkers. Our objective was to determine the current utilization and diagnostic value of cardiac MRI (CMR) in this subset of patients.

Methods: Data from a prospective registry of STEMI patients from the Minneapolis Heart Institute Level 1 MI program was queried. From March 2003 to July 2008, 306 (14.8%) out of 2,066 consecutive patients did not have a culprit artery; of these, 145 (47%) had elevated cardiac biomarkers. CMR was performed at the discretion of the attending cardiologist. CMR diagnosis included myocarditis (gadolinium uptake sparing endocardium and/or edema in non-coronary distribution), MI (gadolinium uptake involving endocardium in a coronary distribution), stress cardiomyopathy (no gadolinium uptake with abnormal wall motion in >1 coronary distribution), non-ischemic cardiomyopathy (cardiomyopathy without MI) and normal.

Results: CMR was performed in 81 (26%) of 306 patients without a culprit artery with increasing frequency over time. (36% in 2004, 49% in 2007). A definitive diagnosis was made by CMR in 78% of patients including 85% (53/62) with (+) enzymes and 53% (10/19) with (-) enzymes. Diagnosis by CMR and mortality is listed in the Table:

CMR Diagnosis	Positive Biomarkers N=62	Negative Biomarkers N=19	1-Year Death
Myocarditis	18 (29%)	2 (10%)	1 (0.5%)
MI	Acute 16 (26%) Old 2 (2%)	Acute 5 (26%)	1 (0.5%)
Stress Cardiomyopathy	14 (22%)	1 (5%)	0
Non-ischemic Cardiomyopathy	3 (5%)	2 (10%)	0
Normal	9 (14%)	9 (47%)	2 (1%)

Conclusions: CMR is a valuable diagnostic adjunct in patients presenting with a presumed STEMI without a clear culprit artery especially in those with positive cardiac biomarkers.

3:30 p.m.

1045-266

Preoperative Identification of Bicuspid Aortic Valves: Cardiac Magnetic Resonance Imaging Versus Two-Dimensional Echocardiography

S. Chris Malaisrie, Byron Yip, Daren S. Danielson, James Carr, Issam Mikati, Edwin C. McGee, Jr., Richard Lee, Patrick M. McCarthy, Northwestern University, Chicago, IL

Background: The prevalence of bicuspid aortic valve (BAV) in the population is 1-2 percent, but more patients with BAV require surgery for aortic valve disease than those with normal trileaflet aortic valves.

Methods: From April 2004 to December 2007, 565 patients underwent an aortic valve operation. Of these patients, 56 patients had both a preoperative two-dimensional echocardiography (ECHO) and cardiac magnetic resonance imaging (MRI) at our institution. Characteristics of the study group were age 59, male gender 77%, ejection fraction 56% and associated coronary artery disease 14%. The results of ECHO and MRI were classified as BAV, trileaflet aortic valve (TAV), or indeterminate.

Results: Of the 56 patients, 35 had BAV as assessed at the time of surgery (70%). The accuracy of ECHO for the preoperative identification of BAV was 65%. Corresponding accuracy of MRI was 94% in the same group of patients. ECHO failed to identify BAV in 3 patients and was indeterminate in 18 patients. MRI failed to identify 1 patient with BAV

and was indeterminate in 2 patients.

Conclusions: Preoperative ECHO does not accurately identify patients with BAV. Lack of diagnostic accuracy may have pertinent clinical ramifications on surgical threshold for aneurysm resection and patient selection for transcatheter heart valve therapy. More advanced imaging such as MRI may be important in identifying patients with BAV prior to aortic valve surgery.

Table. Accuracy of ECHO versus MRI in preoperative identification of BAV

	BAV	TAV
BAV ECHO	25	0
TAV ECHO	3	10
Indeterminate ECHO	10	8
BAV MRI	36	0
TAV MRI	1	17
Indeterminate MRI	1	1

3:30 p.m.

1045-267

Thrombus Aspiration During Primary Percutaneous Coronary Intervention Improves Myocardial Viability and Infarct Transmurality: A Magnetic Resonance Imaging Study

Yoshimori An, Shuichiro Kaji, Atsushi Yamamuro, Koichi Tamita, Tomoko Tani, Makoto Kinoshita, Natsuhiko Ehara, Atsushi Kobori, Takeshi Kitai, Takafumi Yamane, Kite Kim, Shunsuke Funakoshi, Noriyuki Kimura, Shigefumi Morioka, Toru Kita, Yutaka Furukawa, Kobe City Medical Center General Hospital, Kobe, Japan

Background: Improvement of coronary reperfusion and clinical outcomes by thrombus aspiration during primary percutaneous coronary intervention (PCI) has been shown in patients with acute myocardial infarction (AMI). However, the effect of thrombus aspiration on myocardial viability remains uncertain. The purpose of this study was to evaluate the influence of thrombus aspiration on infarction size and infarct transmural in patients with AMI using cardiac magnetic resonance imaging (MRI).

Methods: We performed cardiac MRI in 91 patients with AMI one month after successful primary PCI. Of these, 44 patients underwent thrombus aspiration (TA-group), whereas 47 patients underwent PCI without thrombus aspiration (non-TA group). Myocardial viability assessed by delayed contrast enhancement and left ventricular ejection fraction (LVEF) were evaluated using cardiac MRI at 1 month after AMI. The index of infarct transmural was defined as the ratio of the lesion volume with delayed contrast enhancement to transmural myocardial volume.

Results: Baseline characteristics including age, gender, time from onset to needle and the ratio of left anterior descending artery lesion were similar between the two groups. There was no significant difference in transmural volume of infarct lesion between the two groups (22.9 \pm 14.1mL versus 19.4 \pm 16.3mL; P=0.45). However, the index of infarct transmural was significantly lower in TA group than in non-TA group (49.7 \pm 10.3% versus 62.1 \pm 11.9%; P<0.0001). LVEF appeared modestly better in the TA group. (59.2 \pm 12.6% versus 55.4 \pm 10.2%; P=0.14)

Conclusions: Thrombus Aspiration during primary PCI in AMI augmented myocardial salvage by reducing infarct transmural. The augmentation of myocardial salvage might lead to improved LV systolic function.

3:30 p.m.

1045-268

Myocardial Haemorrhage Is Predictive of Persistent ST Elevation After Revascularized ST Elevation Myocardial Infarction

James C. Weaver, David D. Ramsay, Maurits Binnekamp, David Rees, Jane A. McCrohon, St George Hospital, Sydney, Australia, University Of New South Wales, Sydney, Australia

Background: Myocardial haemorrhage on T2 weighted cardiac MRI (CMR) represents severe reperfusion injury after revascularized ST elevation myocardial infarction (STEMI). This study aimed to evaluate the relationship between myocardial haemorrhage, microvascular obstruction (MVO), myocardial tissue oedema and ST segment resolution (STR).

Methods: After successful primary angioplasty serial 12 lead electrocardiograms were taken every 2 hours for 6 hours, 8 hourly for 1 day and then daily until discharge. Gadolinium enhanced CMR was performed at 4.5 \pm 1 days. Myocardial tissue oedema, representing the culprit artery area at risk (AAR), was defined as a hyperenhanced region on T2 imaging and myocardial haemorrhage as a hypoenhanced area within this region. Infarction was a hyperenhanced region on inversion recovery T1 weighted gradient echo imaging 10 minutes after gadolinium and MVO a hypoenhanced area within this infarcted segment. Salvaged myocardium was defined as AAR volume minus infarct volume expressed as percent of AAR.

Results: 30 patients, age 55 \pm 13 yrs, were included in the analysis. On CMR the AAR was 37.7 \pm 12% and infarct size 22.2 \pm 13% of LV mass. MVO was present in 77% (mean 3.9 \pm 4% of LV mass) and myocardial haemorrhage in 53% (2.9 \pm 3% LV mass) of patients. Haemorrhage had a close correlation with MVO extent (r=0.90, p<0.001) and infarct size (r=0.82, p<0.001). Those with haemorrhage, compared to those without, had less STR (67 vs 80% p=0.04) and higher residual ST segments (1.7 vs 0.6mm, p<0.01) after revascularization. This relationship was not as robust with MVO presence (p=0.11 and p=0.06 respectively). Patients with haemorrhage had more AAR (p=0.01) but less myocardium salvaged by primary angioplasty (27 vs 60% AAR, p<0.0001).

Conclusion: Myocardial haemorrhage defined on CMR after revascularized STEMI is closely associated with MVO, infarct size and inversely with the amount of salvaged myocardium. Those with myocardial haemorrhage have less STR and higher residual ST segments confirming its importance as a marker of microvascular perfusion. Whether the extent of haemorrhage has additional prognostic value over MVO alone is currently being explored.

3:30 p.m.

1045-269

Infarct Tissue Heterogeneity Assessed With Contrast-Enhanced Magnetic Resonance Imaging Predicts Spontaneous Ventricular Arrhythmia in Patients With Ischemic Cardiomyopathy and Implantable Cardioverter-Defibrillator

Stijntje D. Roes, C. Jan Willem Borleffs, Rob J. Van der Geest, Jos J.M. Westenberg, Nina Ajmone Marsan, Theodorus A.M. Kaandorp, Katja Zeppenfeld, Hildo J. Lamb, Albert de Roos, Martin J. Schalij, Jeroen J. Bax, Leiden University Medical Center, Leiden, The Netherlands

Background: The relation between infarct tissue heterogeneity on contrast-enhanced magnetic resonance imaging (MRI) and the occurrence of spontaneous ventricular arrhythmia (VA)(or sudden cardiac death (SCD)) is unknown. Therefore, the study purpose was to evaluate the predictive value of infarct tissue heterogeneity assessed with contrast-enhanced MRI on the occurrence of spontaneous VA with subsequent implantable cardioverter-defibrillator (ICD) therapy (as surrogate of SCD) in patients with previous myocardial infarction (MI).

Methods: Ninety-one patients (65±11 years) with previous MI scheduled for ICD implantation underwent cine-MRI to evaluate left ventricular (LV) function and volumes and contrast-enhanced MRI for characterization of scar tissue (infarct gray zone as measure of infarct tissue heterogeneity, infarct core and total infarct size).

Results: Appropriate ICD therapy was documented in 18 patients (20%) during a median follow-up of 8.5 months (interquartile range 2.1-20.3). Multivariable Cox proportional hazards analysis revealed that infarct gray zone was the strongest predictor of the occurrence of spontaneous VA with subsequent ICD therapy (hazard ratio 1.04, confidence interval 1.00-1.08, chi-square 4.0,p=0.04).

Conclusions: Infarct tissue heterogeneity on contrast-enhanced MRI is the strongest predictor of spontaneous VA with subsequent ICD therapy (as surrogate of SCD) among other clinical and MRI variables e.g. total infarct size, LV function and volumes, in patients with previous MI. Consequently, MRI assessment of infarct tissue heterogeneity in patients with ischemic cardiomyopathy might enable better risk stratification for SCD and consequently provide better selection criteria for ICD implantation compared to current criteria as LV function and New York Heart Association classification.

3:30 p.m.

1045-270

Correlation of Pericardial and Mediastinal Fat With Coronary Artery Disease, Metabolic Syndrome, and Cardiac Risk Factors

Onn Chenn, Ijaz Ahmad, Betty Hua, Joshua Socolow, Igor Klem, Sorin J. Brenner, Terrence Sacchi, John F. Heitner, New York Methodist Hospital, Brooklyn, NY, Duke Univ Medical Center, Durham, NC

Background: Obesity and abdominal fat have been shown to correlate with coronary artery disease (CAD) and may play a role in development of metabolic syndrome (MS). The significance of pericardial adipose tissue (PAT) and mediastinal adipose tissue (MAT) is less clearly defined.

Objective: To study the association between PAT and MAT measured by cardiac magnetic resonance with: 1) severity of CAD, 2) MS and 3) cardiac risk factors (CRF) for CAD.

Methods: We enrolled 100 consecutive patients, 63 male, who underwent CMR for cardiac evaluation and had coronary angiogram performed within 12 months. We measured PAT and MAT on 4-chamber cine view. The surface area of fat was measured by computer analysis from free-hand region of interest (ROI) curves. The presence and the extent of CAD were measured using Duke Jeopardy Score. MS was considered positive if the patient had 3 or more of the 5 criteria. The CRF included hypertension (HTN), diabetes mellitus (DM), hyperlipidemia, smoking, peripheral vascular disease (PVD) and a family history of premature CAD (FH).

Results: PAT had significant correlation with MS and HTN, but not with CAD. MAT did not have a significant correlation with either CAD or MS, but did correlate with DM, hyperlipidemia, smoking and FH. The combination of PAT and MAT correlated with MS and all the risk factors, except PVD, but did not correlate with CAD.

Conclusion: The combination of MAT and PAT correlates with MS and a number of CRF's but does not correlate with CAD.

	Pericardial Fat(cm2)	Mediastinal Fat (cm2)	Total Fat (cm2)
CAD	8.3 {p-value=0.317}	19.5 {p-value=0.16}	27.7 {p-value 0.03}
Metabolic Syndrome	9.3 {p-value=0.0003}	18.9 {p-value=0.19}	26.8 {p-value=0.02}
Cardiac Risk Factors			
HTN	9.5 {p-value=0.008}	19.6 {p-value=0.08}	29.1 {p-value=0.03}
DM	9.9 {p-value=0.08}	21.2 {p-value=0.05}	31.2 {p-value=0.03}
Hyperlipidemia	9.0 {p-value=0.56}	20.4 {p-value=0.01}	29.4 {p-value=0.02}
Smoking	9.2 {p-value=0.86}	13.1 {p-value=0.05}	22.2 {p-value=0.27}
PVD	11.9 {p-value=0.008}	19.5 {p-value=0.79}	32.2 {p-value=0.05}
FH	9.0 {p-value=0.74}	23.2 {p-value=0.02}	31.2 {p-value=0.58}

1045-271

Serial Evaluation of Circumferential Strain for Monitoring of Progressive Cardiac Dysfunction in Duchenne Muscular Dystrophy Patients

Kan N. Hor, Sean C. Hagenbuch, Robert J. Fleck, Janaka P. Wansapura, Wojciech Mazur, D. Woodrow Benson, William M. Gottliebson, Cincinnati Children's Hospital Medical Center, Cincinnati, OH, Ohio Heart and Vascular Center, Christ Hospital, Cincinnati, OH

Background: Duchenne Muscular Dystrophy (DMD), an X-linked disorder, is characterized by progressive skeletal muscle weakness and cardiac dysfunction. It has recently been shown that circumferential LV myocardial strain (ϵ_{cc}) becomes progressively more abnormal in a cross-section of DMD patients at all stages of disease, but to date no data on serial ϵ_{cc} changes in individual DMD patients have been reported. We hypothesized that serial ϵ_{cc} changes can be detected in individual DMD patients within a time frame when left ventricular ejection fraction (EF) changes are insignificant.

Methods: Review of our center's CMR database identified DMD males who underwent serial cardiac MRI (CMR) at our center at least 6 months apart. Data gathered from successive studies on the same DMD individuals included age and CMR EF. Additionally, archived tagged CMR cine images of the mid-LV from the serial CMR studies of these patients were analyzed for composite ϵ_{cc} using HARP® software (Diagnosoft Inc). ϵ_{cc} values (which were normally distributed) for each patient between time points were analyzed via paired Student's t-test, while EF values (not normally distributed) for the same patients at the same times were compared via Wilcoxon signed rank test.

Results: Data from 25 DMD males (mean age at initial study 14.56 ± 4.15 yrs, range 8.04 - 24.87 yrs) was analyzed, with a mean time between CMR studies per patient of 13.6 ± 4.0 months (range 6.2 - 25 months). ϵ_{cc} with an initial mean of -13.3 ± 2.7 %, declined in all DMD patients during the specified interval by an average of 1.61 ± 1.28 % (p<.001). EF, with an initial mean of 61.5 ± 10.4 %, declined by an insignificant average of 1.9 ± 1.75% (p= 0.30). Detailed analysis showed EF decreased in only 15 of the 25 patients, while it increased in 10 of the patients between the two time intervals.

Conclusions: In DMD patients, ϵ_{cc} abnormalities progress relatively rapidly during a time period when EF is relatively constant. As such, serial ϵ_{cc} analysis may provide a reliable and early surrogate endpoint to monitor efficacy of therapy in patients with DMD cardiac dysfunction.

3:30 p.m.

1045-272

Assessing the Severity of Valvular Aortic Stenosis by Phase-Contrast Magnetic Resonance Imaging

Hajime Abe, Nobuo Iguchi, Toru Takii, Hiroyuki Watanabe, Yasuki Hen, Haruhiko Machida, Tetsuya Tobaru, Ryuta Asano, Masatoshi Nagayama, Jun Umemura, Tetsuya Sumiyoshi, Sakakibara Heart Institute, Tokyo, Japan

Background: Assessing the aortic valvular orifice and peak flow velocity is important in evaluating the severity of aortic stenosis. Currently this assessment is mostly done using echocardiography. However, the echocardiographic approach is less reliable in patients with view-blocking calcifications. Using phase-contrast sequences of magnetic resonance imaging (MRI), high flow signal at the aortic orifice is clearly visualized and peak flow velocity can be evaluated quantitatively even in patients with severe calcification.

Methods: We studied 61 patients (male 30, mean age72±7.7 years) with moderate or severe valvular aortic stenosis using MRI (Siemens Sonata 1.5T). Transthoracic echocardiography (TTE) and transesophageal echocardiography (TEE) were also performed in all patients, and peak flow velocity (PV) and aortic valve area (AVA) were calculated. We conducted quantitative analysis of aortic blood flow using velocity-encoded cine (VEC) phase-contrast MR images with the imaging plane carefully positioned perpendicular to the aorta. Area of high flow signal was traced over the VEC images and PV was calculated from a region of interest assigned over the VEC images. We evaluated the correlation between MRI-derived data and the data derived from TTE and TEE. Statistic analysis was done by linear regression and Bland Altman plot.

Results: MRI-derived planimetry correlated well with AVA derived from TTE (R=0.78, P<0.05) and from TEE (R=0.84, P<0.05). PV derived from MRI also correlated with PV derived from TTE (R=0.81, P<0.05). In 11 cases, it was difficult to trace the orifice of aortic valve by TEE and TTE because of severe calcification. Even in these cases, VEC images were so clear that the area of high flow signal could be traced definitively.

Conclusions: Phase-contrast MRI is a reliable noninvasive method to evaluate the severity of valvular aortic stenosis.

3:30 p.m.

1045-273

Longitudinal Versus Cross-Sectional Studies of Effects of Aging on Ventricular Structure and Function Using Cardiac Magnetic Resonance Imaging

Dipti Gupta, Mark Goldman, Sunil T. Mathew, Jing Han, Katherine McGrath, Michael Passick, William Schapiro, Jie J. Cao, Nathaniel Reichke, St Francis Hospital, Roslyn, NY, Cardiology Division, Stony Brook University (SUNY), NY

Background: Cross-sectional studies of effects of aging on ventricular structure and function, including Framingham, MESA, the Dallas Heart Study and studies from our own laboratory have uniformly demonstrated lower ventricular chamber volumes in older normal subjects. We sought to assess aging effects on ventricular size and function prospectively in a carefully screened normal cohort.

Methods: Normotensive, non-diabetic, non-obese (BMI<28) volunteers (n= 57, 31 females), aged 20-89 at intake (59±13 yrs), were screened, including 2D echocardiography and CMR performed (1.5T Siemens Sonata or Avanto) at baseline and 5 years. TrueFISP cine imaging was used to obtain contiguous 8mm short axis slices of both left (LV)

and right (RV) ventricles. LV and RV volumes at end-diastole and end-systole were determined (Medis, MASS) and indexed (i) to body surface area. Ejection fraction (EF) was also calculated.

Results: Systolic blood pressure increased (120 ± 12 to 130 ± 20 mm Hg, $p < .0001$), LV and RV end diastolic volumes increased (113 ± 30 to 136 ± 37 , 114 ± 31 to 134 ± 37 ml, $p < .0001$ for both), as did end systolic volumes (45 ± 17 to 59 ± 23 , 55 ± 21 to 60 ± 22 ml, $p < .0001$ and $p = .01$ respectively). LVEF decreased (61 ± 7 to $58 \pm 7\%$, $p < .004$), while RVEF increased slightly (53 ± 6 to $56 \pm 7\%$, $p = .01$). There were no major gender differences. Subjects with intake age < 50 years and those ≥ 50 years behaved similarly. **Conclusions:** In contrast to cross-sectional studies, which demonstrate reduced LV and RV volumes in older subjects, this prospective study demonstrates that chamber volumes increase with age. This discordance may be due to generational differences which affect cross-sectional, but not longitudinal studies.

3:30 p.m.

1045-274

Quantitative Assessment of Myocardial Fibrosis by Contrast-Enhanced Magnetic Resonance Imaging in Patients With Severe Aortic Valve Disease: Validation Against Histopathology

Clerio Azevedo, Marcelo Nigri, Maria Higuchi, Flavio Tarasoutchi, Pablo Pommerantzeff, Carlos Brandao, Roney Sampaio, Jose Parga, Luiz Avila, Guilherme Spina, Max Grinberg, Carlos Rochitte, Heart Institute (InCor) University of São Paulo Medical School, São Paulo, Brazil

Background: Severe aortic valve disease (AVD) is characterized by progressive accumulation of interstitial myocardial fibrosis (MF). We sought to determine whether the amount of MF measured by delayed-enhanced magnetic resonance imaging (deMRI) demonstrated good correlation when compared with the gold-standard histological analyses. In addition, we investigated the relationship between the amount of MF and LV function before aortic valve replacement (AVR) surgery.

Methods: Fifty-four patients scheduled to undergo AVR surgery were examined by cine and deMRI in a 1.5T scanner. From the deMRI dataset, the amount of MF was automatically determined as the sum of pixels with signal intensity (SI) above a threshold value calculated as: mean SI of total myocardium + 2SD of a remote area SI + 2SD of air SI. The remote area was manually delineated in a myocardial region free of hyperenhancement. In addition, interstitial MF was quantified by histological analysis of myocardial samples obtained during AVR surgery and stained with picrosirius red. Eight subjects who died of noncardiac causes and had no previous history of cardiovascular disease served as controls for the quantitative histological analyses.

Results: The amount of MF determined by histopathology was higher in patients with AVD than in controls ($24.6 \pm 9.8\%$ versus $6.0 \pm 1.8\%$, $P < 0.0001$). The amount of MF by deMRI was $3.72 \pm 2.17\%$. Quantification of MF by deMRI showed good correlation with the measurements obtained by histopathology ($y = 3.10x + 13.0$; $r = 0.69$, $P < 0.0001$). Considering histopathology as the reference, ROC analysis revealed good accuracy of deMRI in identifying patients with increased MF (area under the curve = $0.92 [0.81$ to $1.00]$). In addition, the amount of MF by deMRI showed an inverse correlation with LV ejection fraction ($r = -0.67$) and direct correlations with LV end-diastolic volume ($r = 0.46$), LV end-systolic volume ($r = 0.62$) and LV mass ($r = 0.46$) ($p < 0.001$ for all).

Conclusions: DeMRI allows for the non-invasive quantification of MF with good accuracy when compared with histopathology in patients with severe aortic valve disease. In addition, the amount of MF by deMRI is associated with worse LV functional parameters before AVR surgery.

3:30 p.m.

1045-275

Blood Oxygen Level-Dependent Magnetic Resonance Imaging in Comparison to Fractional Flow Reserve for the Detection of Coronary Artery Stenosis

Matthias Voehringer, Jacqueline A. Flewitt, Jordin D. Green, John V. Tyberg, Matthias G. Friedrich, Libin Cardiovascular Institute, Calgary, AB, Canada

Background: Blood Oxygen Level-Dependent Cardiovascular Magnetic Resonance Imaging (BOLD-CMR) uses deoxygenated hemoglobin as a biomarker for myocardial perfusion and ischemia but has so far not been compared to the invasive gold standard fractional flow reserve (FFR).

Objective: To compare FFR and BOLD-CMR for the detection of a coronary stenosis in the canine heart.

Methods: In $n=7$ dogs a coronary stenosis was induced with an intracoronary balloon catheter in the left circumflex or left anterior descending coronary artery. FFR and BOLD-CMR signal intensity (SI) were assessed simultaneously before and during intravenous adenosine infusion ($420 \mu\text{g/kg/min}$). BOLD-CMR was performed on a 1.5T MR scanner (MAGNETOM Avanto, Siemens, Germany) using a balanced steady-state free precession sequence. Measurements were taken at baseline, at a moderate stenosis (S1, FFR between 0.8 and 0.9) and high-grade stenosis (S2, FFR between 0.6 and 0.7). The affected and remote myocardium were determined by first pass perfusion imaging during intracoronary gadolinium injection. Paired t-test was performed for BOLD-CMR SI at rest and during adenosine infusion. ROC analysis was used to explore the ability of adenosine-induced BOLD-CMR SI increase to detect a functional significant coronary stenosis as defined by FFR.

Results: The mean adenosine-induced BOLD-CMR SI increase at baseline was $12.4 \pm 3.1\%$, $p < 0.01$ for affected myocardium and $11.6 \pm 2.0\%$, $p < 0.01$ for remote myocardium. The responses to adenosine at S1 were similar ($11.2 \pm 2.5\%$, $p < 0.01$ and $15.2 \pm 2.6\%$, $p < 0.01$, respectively). The adenosine response at S2 was blunted and not significantly different from the baseline for the affected myocardium ($3.7 \pm 2.4\%$, $p = 0.18$), whereas it was unchanged for the remote myocardium ($11.9 \pm 2.2\%$, $p < 0.01$). By ROC curve analysis a BOLD-CMR SI increase of less than 6.2% was found to correctly classify a functional significant stenosis

according to FFR with 86% sensitivity and 86% specificity (AUC 0.85).

Conclusions: BOLD-CMR is in good agreement with FFR for the detection of a functional significant coronary stenosis and might be an accurate noninvasive alternative to FFR. Further clinical studies are warranted.

3:30 p.m.

1045-276

A Simple Visual Score of Delayed Enhancement Cardiac Magnetic Resonance Predicts Clinical Ventricular Arrhythmias and Sudden Death Risk in Patients With Hypertrophic Cardiomyopathy

Claudia Raineri, Sergio Leonardi, Gaetano M. De Ferrari, Stefano Ghio, Marialaura Buscemi, Laura Scelsi, Michele Pasotti, Roberto Dore, Eloisa Arbustini, Arturo Raisaro, Fondazione IRCCS Policlinico S.Matteo, Pavia, Italy

Background: Since sudden cardiac death (SCD) may be the first manifestation of hypertrophic cardiomyopathy (HCM), the identification of high risk patients is essential. Aim of this study was to assess the relationship between cardiovascular magnetic resonance (CMR) delayed enhancement (DE) and both spontaneous ventricular tachycardia (VT) and risk of SCD in HCM patients.

Methods: A total cohort of 118 consecutive HCM patients (mean age 43 years, 75% males) underwent a thorough evaluation including clinical examination, CMR, Holter ECG, treadmill test and genetic testing. According to the ACC/ESC Clinical Expert Consensus Document on HCM we considered at increased risk for SCD patients with at least one of: prior cardiac arrest (CA) or sustained VT (sVT), family history of a premature HCM related SCD, identification of a high risk mutant gene, unexplained syncope, abnormal blood pressure response during treadmill test, non sustained (ns) VT on Holter ECG, maximum left ventricular wall thickness ≥ 30 mm. Patients without any of these risk factors were considered to be at low risk. To each of the 17 segments, 0 points were attributed in the absence of DE, 1, 2 and 3 points in case of DE involvement 50% of the segment, respectively. Each segment score was then added to obtain a total DE score. End-points were either the presence of clinical ventricular arrhythmias (nsVT/sVT/CA) or risk status for SCD.

Results: Compared to patients without arrhythmias, those with nsVT/sVT/CA ($n=34$) had a higher DE score [median 11.5 (6-21) vs 8 (2.5-13) $p = .002$]; DE score was also the only independent predictor of clinical VT in multivariate analysis ($p = .001$). Moreover DE score, was significantly greater among patients at risk for SCD ($n=53$) compared to patients at low risk ($n=65$) [median 12 (6-18) vs 6.5 (2-11), $p = .001$] and was found to be an independent predictor ($p = .015$) of SCD risk together with maximum left ventricular wall thickness ($p = .001$) in the multivariable model.

Conclusions: A simple semiquantitative index of DE is a significant multivariate predictor of both clinical ventricular arrhythmias and of risk for SCD and may contribute to risk assessment in borderline or controversial cases.

3:30 p.m.

1045-277

Prognostic Value of Late Gadolinium Enhancement in Patients With Nonischemic Cardiomyopathy

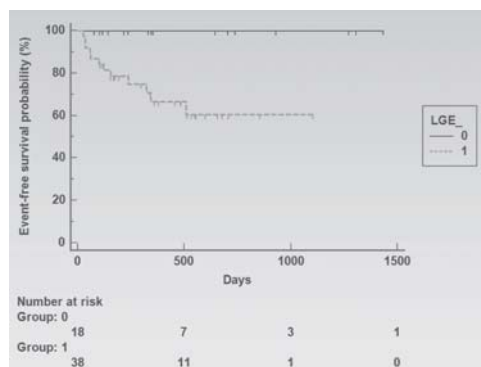
Juan Gaztanaga, Javier Sanz, Ricardo Esquitin, Susanna Prat, Gonzalo Pizarro, Sorin C. Danciu, Valentin Fuster, Mario Garcia, Mount Sinai School of Medicine, New York, NY

Background: Patients with non-ischemic cardiomyopathy are at elevated risk for cardiovascular events. The presence of late gadolinium enhancement (LGE) in cardiac magnetic resonance (CMR) may be associated with impaired prognosis but its significance is still being investigated.

Methods: We studied 56 consecutive patients with non-ischemic cardiomyopathy (left ventricular [LV] ejection fraction [LVEF] $\leq 40\%$) referred for CMR. They were analyzed for the presence of LGE and LV function parameters. Patients were followed for a composite endpoint of hospitalization for congestive heart failure (CHF) and all cause-mortality.

Results: LGE was observed in 68% ($n=38$) of the patients. There was no significant differences in age (48 ± 15 vs 52 ± 12 years, $p=0.34$), gender (76% vs 50% males, $p=0.09$), LVEF ($25 \pm 10\%$ vs $26 \pm 9\%$, $p=0.71$), LV end-systolic volume 231 ± 118 ml vs 199 ± 69 ml, $p=0.29$), and right ventricular ejection fraction ($34 \pm 14\%$ vs $40 \pm 17\%$, $p=0.19$) between LGE+ and LGE- patients, respectively. At a median follow-up of 462 days (range 78 to 1435), there were 12 events, including one death and 11 CHF hospitalizations. All events occurred in the LGE+ group. Event free survival was significantly worse ($p=0.012$) for the LGE+ patients (figure).

Conclusion: The presence of LGE in patients with non-ischemic cardiomyopathy strongly predicts the occurrence of adverse events. This may be important in risk stratification and management.



3:30 p.m.

3:30 p.m.

1045-278

Prognostic Value of Delayed Hyper-Enhancement Cardiac Magnetic Resonance Imaging in Patients With Endomyocardial Biopsy Positive Amyloidosis

Bethany A. Austin, Scott Flamm, E. Rene Rodriguez, Carmela Tan, W.H. Wilson Tang, David O. Taylor, Randall C. Starling, Milind Y. Desai, Cleveland Clinic, Cleveland, OH

Background: In patients with biopsy-proven cardiac amyloidosis (CA), delayed hyper-enhancement-cardiac magnetic resonance (DHE-CMR) has a high diagnostic accuracy. We sought to determine prognostic value of DHE-CMR in CA. **Methods:** We studied 47 consecutive patients with suspected CA (mean age 63 ± 13 years, 70 % men, 55 % with New York Heart Association class > 2) that underwent electrocardiography (ECG), echocardiography (TTE), DHE-CMR (Siemens 1.5 T scanner, Erlangen, Germany) & biopsy (38 endomyocardial, 9 extracardiac) between 1/05-7/08. Low voltage on ECG was defined as S wave in lead V1 + R wave in lead V5/V6 < 15 mm. TTE (including tissue Doppler) parameters & myocardial performance index (MPI) [(isovolumic contraction time + isovolumic relaxation time)/ejection time] were recorded. CMR was positive if there was diffuse DHE of subendocardium extending to adjacent myocardium. All-cause mortality was recorded. **Results:** At baseline, 59 % patients had low voltage on ECG, 67 % had deceleration time < 150 msec & 53 % had $E/E' > 15$ (on Doppler TTE). Mean MPI, left ventricular ejection fraction & septal thickness were 0.51 ± 0.3 , $51 \% \pm 13$ & $1.5 \text{ cm} \pm 0.5$, respectively. At 1 year after biopsy, there were 9 (19 %) deaths. Results of survival analysis are shown in Table. Presence of DHE on CMR was associated with worse 1 year survival (log rank statistic p -value = 0.03). **Conclusions:** Presence of diffuse DHE on CMR is associated with poor 1 year prognosis in CA & may represent more extensive infiltration & greater disease burden.

Table: Cox-Proportional Hazard Survival Analysis in Biopsy Proven Cardiac Amyloidosis

Variable	χ^2	p value
Age	3.8	0.05
Gender	0.15	0.69
New York Heart Association Class	3.3	0.07
Low voltage on electrocardiogram	0.67	0.41
Left atrial size $> 20 \text{ cm}^2$	0.76	0.39
Left ventricular ejection fraction	2.21	0.14
Interventricular septal thickness	1.7	0.19
$E/E' > 15$ on Doppler echocardiography	1.12	0.29
Deceleration time on Doppler echocardiography ≤ 150 msec	1.41	0.23
Myocardial performance index	2.10	0.15
Diastology grade	0.35	0.55
Delayed hyper-enhancement on cardiac magnetic resonance	4.91	0.03

3:30 p.m.

1045-279

The Right Ventricle in Systemic Sclerosis: Insights From Cardiac Magnetic Resonance Imaging

Sotiris Plastiras, Nikolaos Kelekis, Panayiotis Mitseas, Nikolaos Economopoulos, Panayiotis Vlachoyiannopoulos, Haralampos Moutsopoulos, George Tzelepis, University of Athens Medical School, Athens, Greece

Background: Cardiac magnetic resonance imaging (MRI) is a useful modality for assessing cardiac function and detecting myocardial fibrosis of the left ventricle in systemic sclerosis

Methods: Forty four consecutive patients with SSC and no history of ischemic cardiomyopathy, or risk factors for coronary artery disease were included in the study. All patients underwent standard Doppler Echocardiography with estimation of pulmonary artery systolic pressure (PASP), and delayed-enhanced cardiac MRI following IV administration of gadolinium. Clinical and laboratory data were recorded in all patients. MRI data were analyzed for indices of systolic and diastolic function, presence of hyperenhancing areas, and presence of wall motion abnormalities of RV. All patients were followed up for up to 62 months (38, range from 20 to 62 months) post-cardiac MRI.

Results: For the entire group, the average end-diastolic volume (EDV) normalized to body surface area (BSA) was $61.34 \pm 15.72 \text{ mL/m}^2$, the end-systolic volume (ESV)/BSA $59.08 \pm 28.39 \text{ mL/m}^2$ and the ejection fraction (EF) was $54.01 \pm 10.08\%$. Patients with or without $\text{PASP} > 40 \text{ mmHg}$ did not differ in EDV/BSA, ESV/BSA, or EF ($p > 0.05$ for all). When compared to published reference values, all indices of RV systolic and diastolic function were abnormal. Analysis of delayed-enhanced images showed that 4 patients had late enhancement; in 2 out of those 4 patients the appearance of RV resembled arrhythmogenic right ventricular cardiomyopathy. The majority of patients had kinematic abnormalities of the RV free wall, ranging from hypokinesias to dyskinetic areas and overt aneurysms.

Conclusions: The systolic and diastolic function indices of the right ventricle, as measured by cardiac MRI, are abnormal in systemic sclerosis patients. Myocardial fibrosis which most likely accounts for the abnormal function is detected by the currently available MRI techniques only in a small portion of patients.

REFERENCES

- Maceira AM, Prasad SK, Khan M, Pennell DJ. Reference right ventricular systolic and diastolic function normalized to age, gender and body surface area from steady-state free precession cardiovascular magnetic resonance. Eur Heart J. 2006;27:2879-88.

1045-280

A Novel Delayed Enhancement MRI-Based Method to Detect Esophageal Wall Injury Following Ablation of Atrial Fibrillation

Troy J. Badger, Yaw A. Adjjei-Poku, Nathan S. Burgon, Eric Fish, Saul Kalvaitis, Mark Fletcher, Nazem Akoum, Eugene Kholmovski, Edward V. R. DiBella, Rob S. MacLeod, Nassir F. Marrouche, Division of Cardiology, University of Utah School of Medicine, Salt Lake City, UT

Background. Atrial fibrillation (AF) ablation is known to cause thermal injury to the esophagus. We report the detection of esophageal tissue damage using delayed-enhancement MRI (DE-MRI) in both the acute and chronic stages post-AF ablation.

Methods. Patients underwent DE-MRI scans prior to, 24 hours and 3 months following catheter ablation for AF. Three-dimensional segmentations of the left atrium (LA) and esophagus were performed with application of a color look-up table to illuminate enhanced tissue. Qualitative assessment analyzed the presence of esophageal enhancement. Two patients with esophageal enhancement underwent esophagogastroduodenoscopy (EGD) for lesion confirmation.

Results. No patients (0/93) experienced enhancement prior to ablation, at 24 hours 16/46 (34.8%) had esophageal enhancement and at three months 3/68 (4.4%) experienced enhancement. All patients with esophageal enhancement (19/19) demonstrated LA enhancement in close proximity. Both patients who underwent EGD had lesions that correlated with MRI findings. The figure below illustrates a pre-ablation scan (left) with no esophageal enhancement, as well as a 24-hour post-ablation scan (middle) with enhancement (red). EGD confirms the location and injury (right).

Conclusions. Esophageal tissue damage from RF ablation can be detected by DE-MRI post-procedure. This noninvasive method may be used to assess the severity of subclinical esophageal injury post-ablation.

3:30 p.m.

1045-281

Incidence and Prognostic Value of Intra Myocardial Hemorrhage During ST Elevation Myocardial Infarction Treated by Percutaneous Coronary Intervention

Nicolas Amabile, Alexis Jacquier, Frederic Cohen, Olivier Com, Jean-Michel Bartoli, Franck Paganelli, Guy Moulin, University of Marseille School of Medicine, Marseille, France

Background: Intra myocardial hemorrhage (IMH) is a rare finding complicating evolution of STEMI that is hardly identified in clinical current practice.

Objectives: To determine the incidence and the prognosis value of IMH in STEMI treated by PCI using cardiac MRI

Methods: We consecutively screened for inclusion patients with STEMI treated within the first 12 hours of evolution by primary or rescue PCI and undergoing cardiac MRI between day 3 to day 5 after symptoms onset. We excluded patients with subendocardial necrosis from the analysis. Baseline clinical, biological and EKG characteristics were collected. IMH lesion was identified on STIR-T2 images by the presence of a hyposignal within the core of the bright myocardium. Adverse cardiac events were defined as a composite of death +stroke +acute coronary syndrome +acute heart failure occurring during the first year following STEMI.

Results: n=80 patients were finally included and n=9 patients (11%) presented IMH lesions (Age= 58.7 ± 3.8 / Male gender: 88% /Anterior location: 89%). Whereas there was no significant difference regarding risk factors and angiographic baseline characteristics, patients developing IMH presented a higher glycemia during PCI (10.2 ± 0.8 vs. $7.6 \pm 0.3 \text{ mmol/L}$, $p=0.01$). The STEMI complicated with IMH lesions were larger as showed by the significantly higher CPK peak (7523 ± 844 vs. $2316 \pm 218 \text{ IU/L}$), lower LVEF (36.9 ± 1.6 vs. $48.3 \pm 1.4 \%$) and larger end-diastolic (80 ± 6.2 vs. $67.8 \pm 1.9 \text{ mL/m}^2$) and end-systolic (46.8 ± 6.3 vs. $34.4 \pm 1.9 \text{ mL/m}^2$) LV volumes ($p < 0.05$ for all). The incidence of adverse cardiac events was higher in the IMH group than in the no IMH group during the first year following the STEMI ($p=0.01$ by log-rank analysis). Cox regression analysis revealed that IMH lesions on initial MRI were an independent predictor of poor clinical outcome (Relative Risk for adverse cardiac events: $3.5 / 95\% \text{ IC } 1.2-10 / p=0.02$).

Conclusion: IMH is a rare but severe finding in STEMI treated by PCI, associated with a larger myocardial infarction and a worse clinical outcome. Early identification of IMH using MRI after STEMI could be useful to identify subjects with high-risk profile who could benefitate from a more intense medical therapy.

3:30 p.m.

1045-282

Late Gadolinium Enhancement in Arrhythmogenic Right Ventricular Cardiomyopathy Correlates With the Severity of Heart Failure but Not the Incidence of Arrhythmia

Tadashi Wada, Teruo Noguchi, Hideo Okamura, Takashi Noda, Kazuhiro Satomi, Wataru Shimizu, Takashi Kurita, Kazuhiro Suyama, Naoaki Aihara, Hatsue Ueda, Naoaki Yamada, Shiro Kamakura, The Division of Cardiology, National Cardiovascular Center, Suita City, Japan

Background: Late gadolinium enhancement (LGE) on cardiac magnetic resonance can indicate myocardial fibrosis. However, the clinical significance of LGE in arrhythmogenic right ventricular cardiomyopathy (ARVC) remains unclear. From histological studies of explanted hearts in ARVC, two different patterns emerge: a "fatty infiltrative" pattern and a "fibrofatty" pattern. In clinical outcomes, patients with the former pattern exhibit more arrhythmic profiles, whereas patients with the latter pattern have a higher incidence of heart failure. We hypothesized that LGE in ARVC might reflect fibrofatty infiltration and correlate with the severity of heart failure.

Methods: Cardiac magnetic resonance, using a 1.5T clinical system, was performed in 20 patients (43 ± 16 years; 65% male) who fulfilled the Task Force criteria for ARVC. LGE was evaluated 10 minutes after contrast injection. Patients were divided into two groups according to the presence or absence of LGE: an LGE-positive group (n = 14) and an LGE-negative group (n = 6). We sought to correlate LGE with the incidence of arrhythmia, histological findings from endomyocardial biopsy, the severity of heart failure, plasma levels of brain natriuretic peptide (BNP), right and left ventricular end-diastolic volume index (EDVI), end-systolic volume index (ESVI), and ejection fraction.

Results: In comparison with the LGE-negative group, the LGE-positive group showed decreased RV ejection fraction (24 ± 8% versus 43 ± 10%, p<0.05), decreased left ventricular ejection fraction (40 ± 15% versus 60 ± 5%, p<0.05), increased RVEDVI (191 ± 82ml/m² versus 86 ± 13ml/m², p<0.05), increased RVESVI (153 ± 80ml/m² versus 50 ± 15ml/m², p<0.05), and elevated BNP (281 ± 285pg/ml versus 25 ± 19pg/ml, p<0.05). There was no significant difference in spontaneous and inducible ventricular tachycardia between the two groups. In 5 of the 8 LGE-positive patients, endomyocardial biopsies showed fibrofatty infiltration of the myocardium, whereas none of the LGE-negative patients showed this type of histology.

Conclusions: In ARVC, LGE may be a useful modality for predicting histological characteristics and severity of heart failure, but not the incidence of arrhythmia.

3:30 p.m.

1045-283

Detection of Cardiac Amyloidosis by Contrast Magnetic Resonance Imaging Using an Inversion Recovery T1 Scout Sequence

Sorin C. Danciu, Juan Gaztanaga, Javier Sanz, Susanna Prat, Gonzalo Pizarro, Valentín Fuster, Mario García, Mount Sinai School of Medicine, New York, NY, Advocate Illinois Masonic Medical Center, Chicago, IL

Background: Cardiac amyloidosis (CA) is difficult to differentiate non-invasively from other types of restrictive cardiomyopathy (RCM). Amyloid deposition has been shown to alter the kinetics of gadolinium in the myocardium and blood. We used a cardiac magnetic resonance (CMR) inversion time (TI) scout sequence to compare patients with RCM who had endomyocardial biopsy (EMB).

Methods: We included 14 consecutive male patients (age 72±11 years, LV ejection fraction 47±11%) with RCM and clinically suspected CA who underwent both CMR and EMB. A single breath-hold, steady state free precession, TI scout sequence (TR=42.6 ms) was performed 5-10 min after the administration of 0.2 mmol/kg of gadolinium. TI to nulling of blood (mid LV cavity), myocardium (areas with increased wall thickness) and skeletal muscle (trapezius) were measured.

Results: CA was detected by EMB in 8 (57%) patients. The TI nulling time of the myocardium was significantly shorter in EMB (+) patients (Table). The difference between the TI nulling times of skeletal muscle and myocardium was the best parameter to differentiate between EMB (+) and (-) patients. A difference value >75 ms detected CA with 100% sensitivity (8/8), 80% specificity (5/6), 90% positive predictive value (8/9) and 100% negative predictive value (5/5).

Conclusions: The difference in TI nulling times of skeletal muscle and myocardium is easily obtainable by contrast enhanced-CMR. Differences >75 ms are useful to identify amyloid deposition in patients with RCM.

Table

	EMB (+) (N=8)	EMB (-) (N=6)	P value
TI to nulling Skeletal muscle (ms)	232±47	264±31	0.15
TI to nulling Myocardium (ms)	156±37	207±40	0.03
TI to nulling Blood (ms)	168±36	158±48	0.7

3:30 p.m.

1045-284

Influence Of Midwall Fibrosis On Diastolic Dysfunction In Nonischemic Cardiomyopathy: A Cardiac Magnetic Resonance Study

Antonella Moreo, Giuseppe Ambrosio, Benedetta De Chiara, Min Pu, Tam Tran, Francesco Mauri, Subha V. Raman, Ohio State University, Columbus, OH, Niguarda Hospital, Milan, Italy

Background: Accumulating evidence indicates that myocardial fibrosis contributes substantially to the diastolic impairment seen in patients with cardiomyopathy, which in turn may contribute to reduced left ventricle (LV) function and poorer prognosis. Different fibrosis patterns such as patchy, transmural, and midwall can be reliably identified by cardiac magnetic resonance studies with late post-gadolinium myocardial enhancement imaging (LGE-CMR). Moreover, recent data indicates that in patients with nonischemic cardiomyopathy (NICM) presence of midwall myocardial fibrosis predicts adverse cardiac outcomes. Accordingly, we sought to investigate the influence of myocardial midwall fibrosis on severity of diastolic dysfunction in NICM patients.

Methods and Results: 58 consecutive patients (49±15 years) with NICM undergoing LGE-CMR and echocardiography were investigated. Patients were excluded if LGE showed pattern of fibrosis indicative of infarct scar. Diastolic function was assessed by pulsed-Doppler analysis and tissue Doppler imaging (TDI). The mean LV ejection fraction was 29±15%. Visible midwall fibrosis was present in 59% among the overall population; however, prevalence of this pattern significantly increased in patients having elevated LV filling pressures estimated by TDI-derived E/E' (68% in patients with E/E'>10 vs 32% with E/E' ≤10; p=0.02). In univariate linear regression analysis E/E' was significantly correlated with age, ejection fraction, end-diastolic volume index, and presence of midwall fibrosis (p<0.05, all). At multivariate analysis, end-diastolic volume index (p=0.018, beta=0.034) and presence of midwall fibrosis (p=0.027, beta=2.55) remained significantly and

independently correlated with the degree of diastolic dysfunction.

Conclusions: In patients with NICM, presence of midwall myocardial fibrosis by LGE significantly correlates with the degree of diastolic dysfunction. These findings provide insights into the pathophysiology of midwall fibrosis-mediated cardiac impairment in this specific subgroup of patients.

3:30 p.m.

1045-285

Magnetic Resonance Imaging and Response to Cardiac Resynchronization Therapy: Relative Merits of Left Ventricular Dyssynchrony and Scar Tissue

Nina Ajmone Marsan, Jos J. Westenberg, Claudia Ypenburg, Rutger J. van Bommel, Stijntje D. Roes, Laurens F. Tops, Rob J. van der Geest, Eric Boersma, Ernst E. van der Wall, Martin J. Schalij, Jeroen J. Bax, Leiden University Medical Center, Leiden, The Netherlands

Background: cardiac magnetic resonance imaging (MRI) may be important for selection of candidates for cardiac resynchronization therapy (CRT), being particularly suited for assessment of scar tissue and providing measures of left ventricular (LV) dyssynchrony. The aim of this study was to assess the relative value of a novel measure of LV dyssynchrony derived from MRI and the extent of scar tissue for prediction of response to CRT.

Methods: A total of 35 consecutive heart failure patients scheduled for CRT were included. CMR was performed before CRT to assess LV dyssynchrony, defined as the standard deviation of 16 segment time-to-maximum radial wall thickness (SDT-16) obtained from a cine-set of short-axis slices. Delayed-enhanced MRI was applied to evaluate the extent/location of scar tissue. Standard echocardiography was performed before and 6 months after implantation to determine response to CRT, defined as a reduction ≥15% in LV end-systolic volume. Twenty healthy subjects were included as normal controls.

Results: At 6 months follow-up, 21 patients (60%) were classified as responders. LV dyssynchrony (SDT-16) was significantly higher in patients [88 ms (67-99)] as compared to controls [26 ms (22-31), p<0.001] and in responders as compared to non-responders [97 ms (90-106) vs. 60 ms (47-71), p<0.001]. Furthermore, SDT-16 was strongly associated with response to CRT (OR=3.8, p=0.031). ROC curve analysis revealed that a cut-off value of SDT-16 ≥78 ms yielded a sensitivity of 82% and a specificity of 80% to predict response to CRT (AUC 0.9).

The total amount of scar (TOTscar) was significantly greater in non-responders as compared to responders [35% (12-48) vs. 3% (0-8), p<0.001], while no difference was found between the 2 groups for the scar location. The TOTscar was significantly associated with response to CRT (OR=0.87, p=0.047) and ROC curve analysis revealed that a cut-off value of 13% yielded a sensitivity of 85% and a specificity of 79% to predict response to CRT (AUC 0.85).

Conclusion: MRI offers the unique opportunity to assess LV dyssynchrony and scar extent in a single setting. Both these parameters are important independent predictors of echocardiographic response to CRT.

3:30 p.m.

1045-286

Impact of Myocardial Salvage on Cardiac Autonomic Function in Patients Undergoing Mechanical Reperfusion Therapy for Acute Myocardial Infarction

Axel Bauer, Julinda Mehilli, Petra Barthel, Alexander Müller, Adnan Kastrati, Georg Schmidt, Deutsches Herzzentrum und Technische Universität München, Munich, Germany

Background: Cardiac autonomic dysfunction after myocardial infarction (MI) is associated with increased risk for death. Salvage of jeopardized myocardium is the main mechanism by which patients benefit from reperfusion therapy. The impact of myocardial salvage on autonomic function is unknown. Aim of the present study was therefore to analyze the impact of myocardial salvage on autonomic function as assessed by heart rate deceleration capacity (DC) and heart rate turbulence slope (TS).

Methods: 854 consecutive patients undergoing mechanical reperfusion therapy for first MI were enrolled. Paired ^{99m}Tc-sestamibi scintigraphy studies (acute and 7-14 days after reperfusion) were used to calculate myocardial salvage index. DC and TS were assessed from Holter recordings 7-14 days after reperfusion. Patients were categorized into three groups by salvage index: <30% (n=244), 30-60% (n=257), ≥60% (n=353).

Results: In the three groups, DC was 5.2(IQR 3.5-7.1)ms, 5.7(4.1-7.3)ms, and 6.4(5.0-8.0)ms, whilst TS was 5.3(2.6-8.4)ms/RR, 6.9(3.2-11.7)ms/RR, and 7.8(4.1-13.2)ms/RR, respectively (p<0.0001 for both). After adjustment for left ventricular ejection fraction, initial perfusion defect, creatine kinase, age, diabetes, sex and medical therapy, patients with salvage index <30% had a 2.6-fold risk (95% CI 1.8-3.9, p<0.001) of having abnormal DC (≤4.5ms) or TS (≤2.5ms/RR). However, patients who developed autonomic dysfunction defined by abnormal DC and TS had a poor prognosis independent of whether or not the salvage index was <30% (5-year mortality rates of 16.5% and 17.3%, respectively).

Conclusions: In patients undergoing mechanical reperfusion therapy for MI, salvage index is an independent predictor of cardiac autonomic dysfunction but does not affect its prognostic value.

ACC.ORAL CONTRIBUTIONS

908

Nuclear Cardiology/ Cardiac Positron Emission Tomography

Monday, March 30, 2009, 2:00 p.m.-3:30 p.m.

Orange County Convention Center, Room W308C

2:00 p.m.

0908-3

Patients Presenting for Diagnostic Non-Invasive Cardiac Testing in the Study of Myocardial Perfusion and Coronary Anatomy Imaging Roles in CAD (SPARC): Differences in Referral Patterns to SPECT, PET, AND 64-Coronary CT Angiography

Marcelo F. Di Carli, James R. Johnson, Barbara A. Johnson, Mariya Gaber, Jonathan Hainer, Rory Hachamovitch, SPARC Investigators, Brigham and Women's Hospital, Boston, MA

Background: The Study of Myocardial Perfusion and Coronary Anatomy Imaging Roles in CAD (SPARC) is a prospective, multicenter (40 geographically diverse academic and practice sites), registry assessing outcomes after stress SPECT, PET, and 64 slice CCTA in patients (pts) with suspected/known CAD. **Methods:** Of 3,019 pts enrolled in SPARC, this analysis focused on 1,703 pts (56%) with intermediate-high CAD likelihood (LK) and no prior CAD. Each site recorded pt demographics, history, and imaging results using standardized methods.

Results: Overall, 90% of pts were symptomatic and the calculated LK was 0.42. Of 565 (33%) SPECT, 548 (32%) PET, and 590 (35%) CCTA, 40% of pts had abnormal studies with infrequent high risk findings (<5%; defined as severe ischemia, 3VD, and/or LM CAD). CCTA pts were younger, more frequently had angina, but less often diabetes (Table 1). PET pts were more likely diabetic, female, older, and dyspneic, with greater LK and BMI, but angina uncommon. SPECT pts more often had normal test results, but were between PET and CCTA in other characteristics.

Conclusions: SPARC provides a unique opportunity to assess intermediate LK pts undergoing non-invasive cardiac testing in the US. Our findings suggest distinct referral patterns to these three imaging modalities.

Baseline Characteristic	SPECT N=565 [n (%)]	PET N=548 [n (%)]	CCTA N=590 [n (%)]
Mean (\pm SD) age (yr)	59.8 (11)*	62.7 (11)	58.4 (11)
Male gender	279 (49%)*	225 (41%)	308 (52%)*
Mean (\pm SD) BMI (kg/m ²)	30.2 (7.0)*	34.1 (9.6)	29.3 (6%)*
Diabetes	173 (31%)*	225 (41%)	94 (16%)*, **
Anginal symptoms	449 (80%)*	370 (66%)	504 (85%)*, **
Dyspnea	136 (24%)*	239 (44%)	134 (23%)*
CAD Likelihood	0.38 \pm 0.29*	0.45 \pm 0.33	0.41 \pm 0.39
Normal study	441 (78%)*	341 (62%)	237 (40%)*, **
Non-obstructive CAD	441 (78%)*	341 (62%)	404 (68%)*
Abnormal - significant ischemia (SDS \geq 8)	9 (1.6%)	43 (7.8%)	NA
Abnormal - non obstructive	NA	NA	167 (28.3%)
Abnormal - 1 VD	NA	NA	102 (17.3%)
Abnormal - 2 VD	NA	NA	55 (9.0%)
Abnormal - 3 VD	NA	NA	21 (4.0%)
Abnormal - Left Main	NA	NA	8 (1.0%)

*p<0.05 vs PET, **p<0.05 vs SPECT

2:15 p.m.

0908-4

The Prognosis of Normal Stress-Only SPECT Myocardial Perfusion Imaging Studies

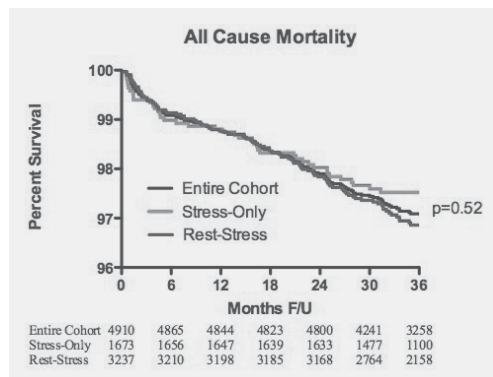
William Duvall, Melanie Wijetunga, Thomas Klein, Rittu Hingorani, Milena Henzlova, Mount Sinai Medical Center, New York, NY

Background: Stress-only myocardial perfusion imaging (MPI) saves time and radiation exposure but a benign prognosis of a normal stress-only study has not been validated.

Methods: Patients at lower pre-test risk for coronary artery disease (CAD) presenting for a Tc-99m SPECT MPI over a 2 year period underwent a stress-only protocol. If the stress images were normal (with or without attenuation correction), rest imaging was not done. Outcomes of the stress-only group were compared to a two-part rest-stress protocol group. Only patients with normal perfusion and left ventricular function, no known CAD, and no pre-organ transplantation were included. All-cause mortality was determined using the Social Security Death Index; survival was analyzed by Kaplan-Meier statistics.

Results: Out of 10,609 patients who had stress MPI during the time period, 1,673 had a normal stress-only study and 3,237 had a normal rest-stress study with a mean follow-up of 40 \pm 9 months. The 1 year all-cause mortality was 1.3% in the stress-only group and 1.2% in the rest-stress group (p=0.52). While there was a greater proportion of low pre-test risk score patients in the stress-only group (90% vs 74%), there was no significant difference in mortality between groups based on stressor (exercise vs pharmacologic), patient location (inpatient vs outpatient), or pre-test risk score (low, intermediate, or high).

Conclusions: A normal stress-only MPI has an excellent 1 year prognosis comparable to that of a normal two-part rest-stress MPI.



2:30 p.m.

0908-5

Prevalence of False Positive Exercise Electrocardiograms in Women? Results From the What is the Optimal Method for Ischemia Evaluation in Women (WOMEN) Trial

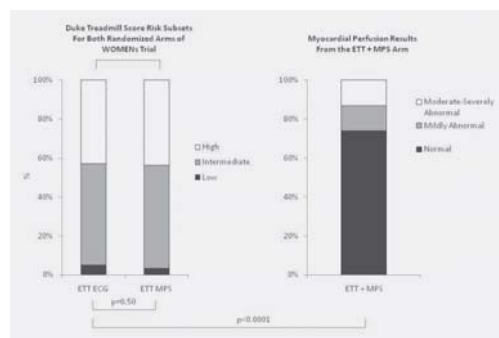
Robert C. Hendel, Jennifer H. Mieres, Gary V. Heller, C. Noel Bairey-Merz, William E. Boden, Leslee J. Shaw, WOMEN Investigators, Emory University, Atlanta, GA, Midwest Heart Specialists, Winfield, IL

Background: The accuracy of the exercise (ETT) electrocardiogram (ECG) is less in women than men; yet clinical guidelines recommend its initial use for those capable of maximal ETT. Our study aim was to compare the prevalence of ECG and myocardial perfusion SPECT (MPS) abnormalities in women.

Methods: WOMEN is a North American, randomized trial (RCT) of ETT ECG vs. ETT+MPS in 825 symptomatic women at intermediate-high pretest risk of coronary disease. A quality control core laboratory evaluated >95% of ECG and MPS acceptable. The Duke treadmill score (DTS) (Time - (5x ST Δ) - (4x chest pain [1:non-limiting, 2:limiting])) was scored low (>5) to high (<11) risk. Rest/stress MPS were interpreted by 17-segment model (segments scored 0:normal to 4:absent uptake). Summed stress scores <4 to >8 were normal to moderate-severely abnormal.

Results: Women (average age 63 years) exercised to 8.5 metabolic equivalents on the Bruce protocol; 94% achieved target heart rate. Low (4%), intermediate (53%), and high (43%) risk DTS were similar for ETT ECG and ETT+MPS (p=0.49). Despite frequent intermediate-high risk DTS, MPS were more often normal (74%, p<0.0001, Figure). Of women randomized to ETT+MPS, MPS was normal in 87% with an intermediate-high risk DTS; suggesting a high false positive rate.

Conclusions: This is the first diagnostic RCT in symptomatic women revealing highly prevalent false positive ECGs. An initial diagnostic strategy involving MPS may help to resolve the dilemma of indeterminate-abnormal ECG findings.



2:45 p.m.

0908-6

Attenuation Corrected SPECT Myocardial Perfusion Imaging Provides Highly Effective Risk Stratification for Future Cardiac Events

Ahmet L. Guler, Peter Chien, Alan Ahlberg, Osman Faheem, Deborah Katten, Gary V. Heller, University of Connecticut/Hartford Hospital, Hartford, CT

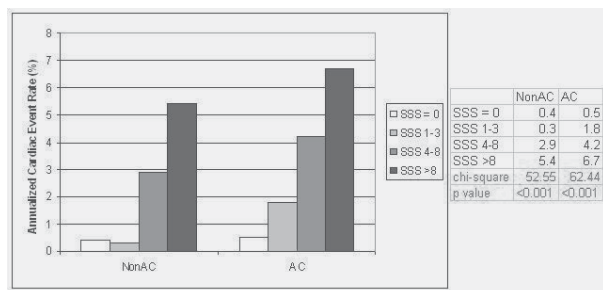
Background: Although attenuation correction (AC) in SPECT MPI studies improves diagnostic accuracy, its role in risk stratification for future cardiac events is unknown.

Methods: Consecutive patients who underwent Tc-99m rest-stress SPECT MPI studies with AC at Hartford Hospital were identified. Myocardial perfusion was analyzed through calculation of AC and non-AC summed stress scores (SSS) using a standard 17-segment model.

Results: Of 1,711 patients, follow-up was complete in 91% over 1.8 \pm 1.1 years. Of these 1,562 patients, the proportion of SSS = 0 was significantly higher with AC (77%) than non-AC (41%, p < 0.001). Patients with an AC-SSS = 0 had a low incidence (< 1%) of early revascularization. Moreover, only 33 of 1,491 patients (2%) without early revascularization

had adverse cardiac events. The AC-SSS in patients with adverse cardiac events (7.4 ± 8.3) was significantly higher than in those without events (1.3 ± 3.6 , $p < 0.001$). Effective risk stratification was achieved using either non-AC or AC SSS data (both $p < 0.001$, Figure 1). However, an AC-SSS 1-3 was associated with a significantly higher annualized event rate than a non AC-SSS 1-3.

Conclusion: SPECT imaging with AC provides highly effective and incremental risk stratification for future cardiac events.



3:00 p.m.

0908-7

Value of Transient Ischemic Dilatation for Risk Stratification of Patients Undergoing Gated Rubidium-82 Positron Emission Tomography Imaging

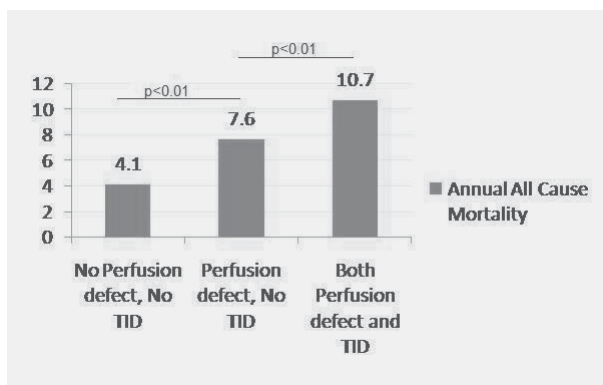
Arun Padala, Anuj R. Shah, Alan Ahlberg, Aravind R. Kokkila, Deborah Katten, Gary V. Heller, Hartford Hospital, University of Connecticut, Hartford, CT

Background: The role of Transient ischemic dilation (TID) is not well established for risk stratification for patients undergoing Rubidium-82 Positron Emission Tomography myocardial perfusion imaging (Rb-82 PET MPI).

Methods: We assessed 615 patients who underwent Rb-82 PET MPI in our nuclear laboratory, excluding those who had early revascularization ≤ 60 days of the stress test. All studies were interpreted in a blinded fashion using the ASNC/ACC 17 segment model. Patients were followed for annual all cause mortality rates using the Social Security Death Index. Patients were risk stratified by presence or absence of TID in addition to using perfusion variables, summed stress scores [SSS]. Accordingly, a SSS ≥ 4 , presence of TID were considered abnormal. The incremental role of TID over perfusion variables was assessed by regression analysis.

Results: The mean age was 64 years, 52.5% were women, 28% had a history of MI and 22% had a history of revascularization. In follow-up, 83 (13.7%) patients had deceased. Patients with SSS 0-3, 4-8, ≥ 8 the annual all cause mortality rates were 3.8%, 7.1% and 10.1% respectively ($p < 0.01$). TID had incremental prognostic role compared to SSS alone ($p < 0.01$ across all the groups) on regression analysis (fig). In patients with a SSS ≥ 8 , the group with TID had a trend for higher events 11.2 v/s 9.6 ($p=0.07$).

Conclusions: In patients undergoing gated Rb-82 PET MPI, the presence of TID in those with abnormal perfusion is associated with a higher mortality rate.



914

ACC.ORAL CONTRIBUTIONS

Coronary Calcium and Coronary CT Angiography

Tuesday, March 31, 2009, 8:00 a.m.-9:30 a.m.
Orange County Convention Center, Room W308C

8:00 a.m.

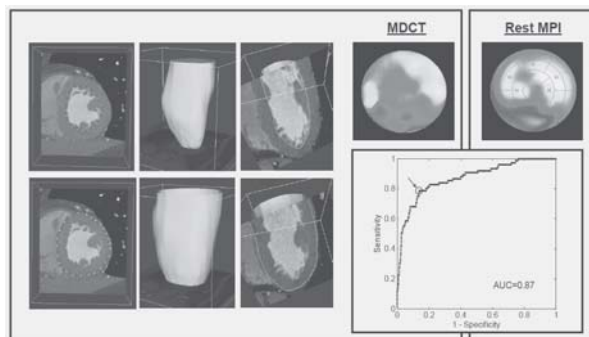
0914-3

Volumetric Quantification of Myocardial Perfusion Using Analysis of Multidetector Computed Tomography Three-Dimensional Datasets: Comparison With Nuclear Perfusion Imaging

Nadja Kachenoura, Federico Veronesi, Joseph A. Lodato, Cristiana Corsi, Rupa Mehta, Barbara Newby, Roberto M. Lang, Victor Mor-Avi, University of Chicago, Chicago, IL

Background. Detection of perfusion abnormalities from MDCT images is based on visual interpretation of 2D slices. We developed a technique for quantitative 3D analysis of myocardial perfusion and tested it against SPECT myocardial perfusion imaging (MPI).

Methods. We studied 44 patients undergoing CT coronary angiography (CTCA): 15 controls and 29 patients including 15 post myocardial infarction. MDCT datasets acquired for CTCA were analyzed using custom software to generate bull's eye display of myocardial perfusion, and calculate an index of extent and severity of perfusion abnormality Q_h for 16 segments. Visual interpretation of MDCT derived bull's eyes was compared with resting MPI scores on a coronary artery and patient basis. Quantitative MDCT perfusion data were used for objective detection of perfusion defects. **Results.** MDCT derived bull's eyes reflected perfusion defects in agreement with MPI (kappa 0.70 by territory; 0.79 by patient). Quantitative data also agreed with MPI: 1) correlation between summed Q_h and MPI scores: 0.87 (territory), 0.84 (patient); 2) area under ROC curve 0.87; sensitivity 0.79-0.92, specificity 0.83-0.91, accuracy 0.83-0.89 for objective detection of abnormalities. **Conclusions.** Our 3D technique for MDCT analysis allows accurate objective detection of fixed perfusion defects. This perfusion information can be obtained without additional radiation or contrast load, and, when combined with stress, may aid in elucidating the significance of coronary lesions.



8:15 a.m.

0914-4

The Coronary Calcium Score by Electron Beam Computed Tomography Provides Incremental Long-Term Prognostic Information Over Myocardial Perfusion Imaging With Single-Photon Emission Computed Tomography

Su Min Chang, Faisal Nabi, Leif E. Peterson, John J. Mahmarian, Methodist DeBakey Heart & Vascular Center, Houston, TX

Background: It is unclear whether the coronary artery calcium score (CACS) adds incremental value to the long-term prognostic power of stress tomographic myocardial perfusion imaging (SPECT).

Methods: We prospectively followed 1035 generally asymptomatic subjects without prior cardiovascular disease (age 57.8 ± 9.8 years, 73% male, 10% diabetics) who underwent CACS and stress SPECT within a close time period (median 23 days). CACS was calculated using the Agatston method and categorized as normal or minimal (0-10), mild (11-100), moderate (101-400), and severe (>400). Stress SPECT was categorized as normal and abnormal. Median follow-up was 6.9 years. End points analyzed were 1) cardiac events (cardiac death, nonfatal myocardial infarction [MI] and coronary revascularization) and 2) all-cause death and MI.

Results: The prevalence of an abnormal SPECT increased with increasing CACS: 1% with a normal or minimal (0-10), 1.5% with mild (11-100), 8% with moderate (101-400), and 29% with severe (>400) CACS ($p < 0.001$). Event rates significantly increased with increasing CACS and abnormal vs normal SPECT ($p < 0.001$). Among patients with a normal SPECT, the annualized event rate in patients with CACS >400 was significantly higher than in those with CACS <10 (2.97% vs 0.67% for cardiac events; 2.14 vs 0.56% for death/MI, all $p < 0.001$). By multivariate analysis CACS added incremental value for predicting events over clinical and SPECT information. Time point analysis in subjects with normal SPECT showed that CACS added significant prognostic value 4 and 5 years after initial testing for predicting cardiac events ($p=0.03$) and death/MI ($p=0.01$).

Conclusions: CACS and SPECT results are independent and complementary predictors

of short-term risk for cardiac events. However, a severe (>400) CACS identifies subjects at higher long-term risk for cardiac events despite a normal SPECT. Our results support the role of CACS testing in subjects with normal SPECT to clarify long-term risk and thereby selectively target individuals for aggressive risk factor modification and therapeutic interventions.

8:30 a.m.

0914-5

Coronary CT Angiography Is a Better Predictor for Both Early and Late Cardiac Events Than Conventional Risk Scores and Calcium Scoring in Patients With Suspected Coronary Artery Disease

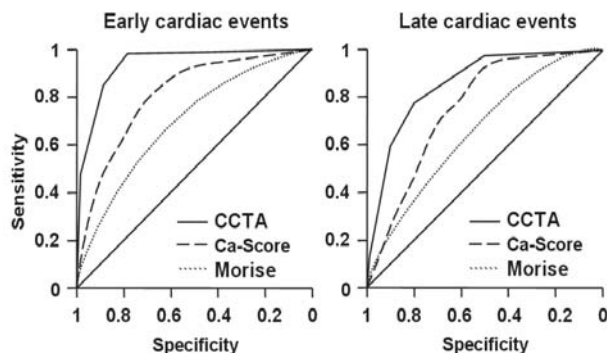
Martin Hadamitzky, Tanja Meyer, Franziska Hein, Stefan Martinoff, Albert Schömig, Jörg Hausleiter, Deutsches Herzzentrum München, Munich, Germany

Background: Several studies have demonstrated a high accuracy of coronary CT angiography (CCTA) for detection of obstructive coronary artery disease (CAD), some studies also showed a good prediction of subsequent cardiac events. But it is not yet proven, that CCTA is more predictive than conventional risk scores or calcium scoring (CACS).

Methods: We analyzed 1376 patients with suspected CAD undergoing both CCTA and CACS in our institution between December 2003 and October 2006. The maximum stenosis of all coronary segments >1.5mm was assessed semiquantitatively (<25%, 25-49%, 50-74%, ≥75%). Endpoint was the occurrence of cardiac events (cardiac death, nonfatal myocardial infarction and coronary revascularization) either within 90 days of CCTA (early events) or later (late events).

Results: During a median follow-up of 21 months (total range 10 to 51 months) there were 159 early and 33 late events. CCTA demonstrated the strongest association both with early and late events (hazard ratio 134 and 11.0 respectively, $p<0.001$). In a receiver operator curve analysis the area under the curve of 0.92 for early and 0.84 for late event was significantly higher than the curve of CASC (0.80 and 0.75 respectively) and the Morise score as the best clinical predictor (0.73 and 0.68 respectively) (all $p<0.01$).

Conclusion: The current data suggest, that compared with conventional methods, CCTA carries additional prognostic information not only for the identification of obstructive CAD, but also for the long term follow up.



8:45 a.m.

0914-6

Increased All-Cause Mortality Is Conferred by Nonobstructive Plaque as Detected by 64-Slice Cardiac Computed Tomographic Angiography

James K. Min, Fay Y. Lin, Sunil Mirchandani, Daniel S. Berman, Leslee J. Shaw, Tracy Q. Callister, Cornell University Medical Center, New York, NY, Tennessee Heart and Vascular Institute, Hendersonville, TN

Background: Cardiac computed tomographic angiography (CCTA) can diagnose nonobstructive, as well as obstructive coronary artery disease. The clinical import of nonobstructive plaque by CCTA is unclear.

Methods: We studied all-cause mortality of a large cohort of patients with nonobstructive plaque by CCTA from a single community-based practice. Methods: Consecutive patients were eligible if they had clinically indicated CCTAs at two US outpatient cardiology practices between 2006-2008. Patients were excluded if they had obstructive coronary artery disease or prior revascularization with either PCI or CABG.

Results: 2815 patients were observed over a median followup of 1.22 years, during which 39 patients (1.4%) died. 1567 (55.7%) had nonobstructive coronary artery disease while the remainder had no plaque visualized by CCTA. There was a statistically significant difference in all-cause mortality between patients with no plaque and nonobstructive plaque by CCTA (log-rank $p<0.001$, figure 1). In multivariate Cox proportional hazards regression, nonobstructive plaque by CCTA (HR 2.75) was independently predictive of all-cause mortality, in addition to age, current tobacco use and sex, while taking a cholesterol-lowering drug was protective ($p<0.05$ for all). The mortality of patients with no coronary artery plaque was 0.4% over the period of observation.

Conclusions: Increased risk by nonobstructive plaque, as detected by CCTA. Patients with no evident coronary artery plaque have an excellent intermediate-term prognosis. CCTA may be useful to risk reclassify patients not only with obstructive but also with nonobstructive disease for the purpose of aggressive risk factor modification.

0914-7

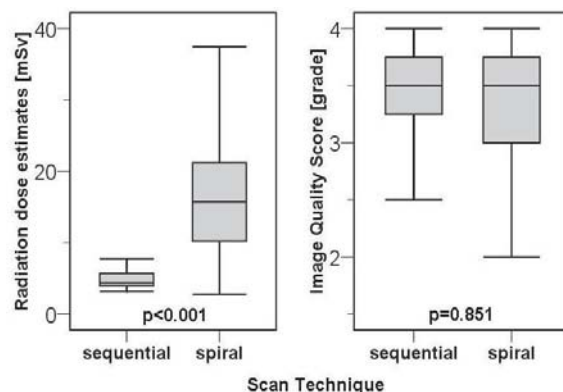
Impact of a Prospective ECG-Triggered Sequential Scanning Technique on Image Quality and Radiation Dose: A Subgroup Analysis of the PROTECTION I Study

Jörg Hausleiter, Franziska Hein, Bernhard Bischoff, Tanja Meyer, Martin Hadamitzky, Albert Schömig, Stefan Martinoff, Deutsches Herzzentrum München, Munich, Germany

Background: A considerable radiation exposure is associated with coronary CT angiography (CCTA). The international multivendor PROspective Multicenter Study On Radiation Dose Estimates Of Cardiac CT AngiOgraphy IN Daily Practice (PROTECTION I) - study investigated the radiation exposure of CCTA. Recently, a prospective ECG-triggered sequential CCTA scan technique has been developed to reduce exposure to ionizing radiation. The purpose of this analysis was to determine the effect of a sequential scan technique on image quality (IQ) and radiation dose.

Methods: This analysis comprises 1546 64-slice CCTA studies of 47 international study sites. IQ was assessed using a 4-point score (1: nondiagnostic - 4: excellent IQ). IQ was analyzed in all patients studied with sequential scan technique ($n=99$; 100%) and randomly selected patients studied with spiral scan technique ($n=424$; 29%). Radiation dose was estimated from the dose-length-product.

Results: The sequential scan mode was used in 99 (6%) of all studies. Heart rate was significantly lower in patients studied with the sequential scan mode (56 vs. 63 min⁻¹; $p<0.001$). While sequential scan mode significantly reduced radiation dose estimates by 69%, IQ was comparable in both groups (see Figure).



Conclusions: The PROTECTION I study suggests, that the sequential CCTA scan technique significantly reduces radiation dose without impairing image quality when compared to the standard retrospective spiral data acquisition.

ACC.POSTER CONTRIBUTIONS

1054

Nuclear Cardiology/PET; Exercise Physiology and Testing

Tuesday, March 31, 2009, 9:30 a.m.-12:30 p.m.
Orange County Convention Center, West Hall D

9:30 a.m.

1054-233

Confronting the Epidemic of Cardiovascular Disease in Developing Countries: Utilization of Nuclear Cardiology Worldwide

Joao V. Vitola, Leslee J. Shaw, Adel Allam, Pilar Orellana, Amalia Peix, Annare Ellmann, Kevin Allman, BN Lee, Chanika Siritara, Felix Keng, Gianmario Sambucetti, Marla Kiess, Raffaele Giubbini, Salaheddine Bouyoucef, Zuo-Xiang He, Gregory Thomas, Fernando Mut, Maurizio Dondi, International Atomic Energy Agency Work Group on Nuclear Cardiology, Vienna, Austria

Background: In 2005, 80% of cardiovascular disease deaths occurred in developing countries. If continued, this will overburden health care systems and hamper social development. Strategies to promote dissemination of effective diagnostic and prognostic testing algorithms can help. One of the objectives of the International Atomic Energy Agency is to enhance capabilities of countries to address needs related to health conditions through the application of nuclear techniques.

Methods: In 2008, countries were queried as to annual utilization of nuclear cardiology (UNC) procedures. Estimated UNC was calculated dividing the number of procedures per year by the population and divided into groups of high, moderate-high, moderate, low to moderate and low UNC.

Results: Worldwide UNC can be seen in the figure below. United States and Canada had high UNC. Most western European countries, Australia, and Japan had moderate-high UNC. South America had a mix of low and moderate UNC. Eastern Europe, Russia and Asia had low UNC. A large part of Africa had limited information/non-existent UNC. Generally, UNC mirrored gross domestic product (GDP).

Conclusions: Worldwide UNC varied greatly among countries, influenced by GDP,

physician access to training/education programs and governmental policies. Information, guidelines of appropriate utilization and training, can foster growth and aid developing countries to confront the epidemics of cardiovascular diseases in a cost effective way.



9:30 a.m.

1054-234

Evaluation of Image Registration in a Solid State Cardiac SPECT System With an Ultra-Low Dose X-ray-Based Attenuation Correction

Richard Conwell, Hetal Babla, Chuanyong Bai, Joel Kindem, Jamshid Maddahi, Digirad Corporation, Poway, CA, UCLA - David Geffen School of Medicine, Los Angeles, CA

Background: CT-based attenuation correction (AC) is becoming the standard on hybrid SPECT/CT systems because the x-ray based CT rapidly produces a virtually noise free attenuation map. However, when applied to cardiac SPECT studies, misregistration of the emission-to-transmission images has been reported in as high as 42% of the studies. Misregistration can occur: 1) during patient translation from one modality to the other and 2) because the degree of respiratory motion within the scans is inconsistent due to the much shorter CT scan time used to minimize patient dose. In this work with a dedicated cardiac SPECT camera, an ultra-low dose x-ray transmission source is employed for transmission scans. This configuration enables high quality attenuation maps to be obtained over a period of time that includes multiple respiratory cycles ensuring the same degree of respiratory motion in the emission and transmission scans, but with an inconsequential added patient exposure. In addition, because the same solid-state detectors are used for both the emission and transmission scans, the patient is not translated between scans, further reducing the misregistration.

Methods: A triple head, upright solid-state camera was used for both emission and transmission scans of 34 patients for both rest and stress cardiac SPECT studies. For transmission scans, via x-ray fluorescence, a mono-energetic, collimated line source was formed which allowed transmission scans to be finished in one minute with a patient dose of about 5 μ Sv.

Results: No patient studies showed misregistration introduced by respiratory motion. Overall, patient studies showed translational misregistration of 1 pixel (6.5mm) in 9% of the studies, 2 pixels in 6% and a rotational misregistration in 3% of the studies.

Conclusions: We developed a new x-ray-based transmission approach for AC in cardiac SPECT cameras with negligible (5 μ Sv) patient dose. This enables high-quality transmission scans with the same degree of respiratory motion as the emission scans, thus eliminating misregistration due to respiratory motion. Patient studies show significantly reduced misregistration as compared to what has been reported for hybrid SPECT/CT systems.

9:30 a.m.

1054-235

Vascular Dysfunction Measured by Fingertip Thermal Monitoring Is Associated With Abnormal Myocardial Perfusion

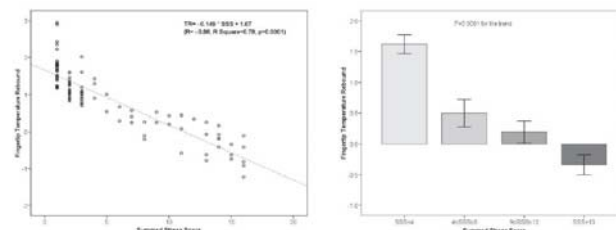
Naser Ahmadi, Anila Saeed, Sumithra Tirunagaram, Fereshteh Hajsadeghi, Wasy Ahmad, Manzoor Bevinall, Khurram Nasir, Harvey Hecht, Morteza Naghavi, Matthew Budoff, Los Angeles Biomedical Research Institute at Harbor UCLA Medical Center, Torrance, CA

Background: Previous studies have shown that vascular dysfunction measured by Digital Thermal Monitoring (DTM) correlates with the burden of atherosclerosis risk factors measured by Framingham Risk Score (FRS) as well as with coronary calcium score in asymptomatic patients. This study investigated the correlation between DTM and extent of myocardial ischemia measured by myocardial perfusion imaging (MPI) in symptomatic patients.

Methods: 116 consecutive patients with chest discomfort, age 57 ± 10 years, underwent MPI and DTM. Fingertip temperature rebound (TR), the DTM index of vascular reactivity, was assessed after 2 minutes of arm-cuff induced reactive hyperemia. The extent of myocardial perfusion defect was measured by the summed stress score (SSS).

Results: TR progressively decreased from 1.61 ± 0.15 in $SSS < 4$ (, to 0.5 ± 0.22 in $SSS 4-8$, to 0.26 ± 0.15 in $SSS 9-13$ and to 0.37 ± 0.19 in $SSS > 13$ ($p = 0.0001$). After adjusting for cardiac risk factors, the odds ratio of the lowest vs. 2 upper tertiles of TR was 3.93 for $SSS \geq 4$ and 9.65 for $SSS \geq 8$ compared to $SSS < 4$. TR correlated well with SSS ($r = -0.88$, $p = 0.0001$). The addition of FRS to TR increased the area under the ROC curve for prediction of abnormal MPI ($SSS \geq 4$) from 0.65 to 0.84 ($p < 0.05$).

Conclusion: Vascular dysfunction measured by DTM is associated with myocardial perfusion defect, independent of age, gender and cardiac risk factors. Further studies are needed to corroborate our findings and define the clinical utility of DTM for cardiovascular risk assessment.



9:30 a.m.

1054-236

Prognostic Value of Stress Myocardial Perfusion SPECT and the Impact of Body Mass Index on Cardiac Mortality

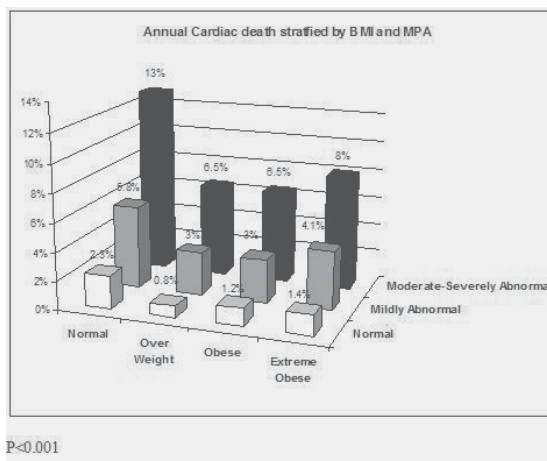
Abdul Hakeem, Sabha Bhatti, Jeffrey R. Cook, Zainab Samad, Su Min Chang, University of Cincinnati College of Medicine, Cincinnati, OH, Methodist DeBakey Heart and Vascular Institute, Houston, TX

Background: Obesity has been identified as a risk factor for coronary artery disease. Recently, however, the "obesity paradox" of better short-term outcome in obese has been observed. We evaluated the prognostic value of MPS in risk stratifying patients across the entire spectrum of BMI.

Method: 1718 patients (age 65 ± 10 y/o) underwent MPS (95 % gated). Pts were classified into 4 BMI groups: normal (18-24.9 kg/m² n=257), overweight (25 to 29.9 n=585), obese (30 to 34.9 n=470), and severely obese (≥ 35 n=406). The extent and severity of MPS were determined using Sum Stress Score. Pts were followed up for 2.15 ± 0.8 years for cardiac death (CD) and non fatal events (MI, late revascularization > 90 days)

Result: The prevalence of abnormal MPS was not significant different across weight groups. (Normal 46 %, overweight 41 %, obese 43% and severely obese 43% $p = 0.5$) The annual CD rate was significantly higher in pts with abnormal scan across all BMI groups and rose as a function of MPS abnormalities. The CD rate was 2 fold higher in pts with normal BMI compared to overweight and obese groups for all levels of perfusion defects $p < 0.001$. (Table) Across all BMI groups the combined events increased with perfusion abnormalities. (Normal 11.6% vs 3.1%, overweight 8.2 % vs 3.3%, obese 8 % vs 3.5% and severely obese 10% vs 3.5%, all $p < 0.05$)

Conclusion: MPS provides effective risk stratification across all weight categories. Overweight and obese pts appear to be at lower risk of CD in the short term compared to normal weight pts.



9:30 a.m.

1054-237

Clinical Variables Related To Abnormal Myocardial Flow Reserve Quantified With Positron Emission Tomography Myocardial Perfusion Imaging

Maria C. Ziadi, Robert A. deKemp, Benjamin Chow, Terrence Ruddy, Renee Hessian, Ross A. Davies, Ann Guo, Kathryn Williams, Judy Etele, Linda Garrard, Rob SB Beanlands, University Of Ottawa Heart Institute, Ottawa, Canada

Background: Quantification of myocardial flow reserve (MFR) with positron emission tomography (PET) may help overcome the current limitations of relative perfusion in the evaluation of coronary artery disease. Our objective was to characterize patients with

preserved MFR versus patients with impaired MFR in patients with normal or abnormal summed stress scores (SSS).

Methods: We evaluated 147 consecutive patients who underwent a pharmacological Rubidium-82 or Ammonia-13 PET perfusion study. We identified 4 groups: I-a) normal SSS (<4) and normal MFR (≥2.5); I-b) normal SSS and abnormal MFR (<2.5); II-a) abnormal SSS (≥4) and normal MFR and II-b) abnormal SSS and abnormal MFR.

Results: Clinical parameters, electrocardiogram (ECG) response and ancillary findings were compared. Patients with abnormal MFR were older than those with preserved MFR. Patients in group II-b were more likely to have diabetes, an ischemic ECG response and transient ischemic dilatation (TID). In this group, ECG response and TID were highly specific of impaired MFR.

Conclusions: Individuals with abnormal MFR are older. Patients with SSS ≥ 4 with abnormal MFR are characterized of having more diabetes, more TID and more ischemic ECG responses suggesting more diffuse coronary artery disease. Such patients may be at increased risk. Though, this requires further study with larger prospective outcome evaluation.

Table

Patient Characteristics	Group I SSS <4 (N= 85)		Group II SSS ≥4 (N=62)	
	I-a MFR ≥ 2.5 (n=47)	I-b MFR <2.5 (n=38)	II-a MFR ≥ 2.5 (n=16)	II-b MFR <2.5 (n=46)
Age (#)	58±11	66±12(*)	51±11	66±12(*)
Diabetes Mellitus (#)	9 (19%)	13 (34%)	4 (25%)	26 (57%)(**)
Ischemic ECG response (#)	0 (0%)	2 (5%)	1 (6%)	17 (37%)(***)
TID (#)	0 (0%)	1 (3%)	0 (0%)	16 (35%)(***)

(#) p= <0.05 ANOVA; (*) p= < 0.05 Versus MFR ≥ 2.5; (**) p= < 0.05 versus groups I-a and II-a; (***) p= < 0.05 versus all groups

9:30 a.m.

1054-238

Ultrafast Cardiac Camera in Myocardial Perfusion SPECT: Initial Multicenter Comparison With Standard Dual Detector Cameras

FP Esteves, P. Raggi, R. Folks, Z. Keidar, JW Askew, S. Rispler, MK O'Connor, L. Verdes, EV Garcia, Emory University School of Medicine, Atlanta, GA, Rambam Medical Center, Haifa, Israel

Objective: To compare myocardial perfusion SPECT using a novel ultrafast dedicated cardiac camera (UFC), (GE Healthcare), with standard dual detector cameras (S-SPECT) in patients with known or suspected coronary artery disease (CAD).

Methods: 126 patients (77 men, mean age 63 ± 13 years) had 1-day Tc-99m tetrofosmin rest/stress SPECT. UFC images were acquired on list mode prior to S-SPECT images. The UFC is equipped with CZT solid state detectors and has no moving parts. Rest and stress acquisition times were 4 and 2 min for UFC and 14 and 12 min for S-SPECT. Two blinded readers independently scored all scans using a 5-point scale on a patient level and on a vascular territory level. A third blinded reader scored the discordant cases. Image quality was scored on a 3-point scale and automated left ventricular ejection fractions (LVEF) were correlated.

Results: For UFC, image quality was considered excellent in 85%, adequate in 13% and suboptimal in 2%. For S-SPECT, image quality was considered excellent in 67%, adequate in 32%, and suboptimal in 1%. There was a high correlation between UFC and S-SPECT for rest and stress automated LVEF (r=.93, p<0.001 for both). Table shows % agreement rates between UFC and S-SPECT based on the presence or absence of CAD using S-SPECT as gold standard.

% agreement	CAD	LAD	LCX	RCA
Abnormal	86 (25/29)	75 (12/16)	92 (11/12)	93 (14/15)
Normal	85 (82/97)	98 (108/110)	93 (106/114)	87 (97/111)

Conclusions: Preliminary data suggest that UFC provides diagnostic performance comparable to S-SPECT. Acquisitions can be done in a much shorter time with high image quality because of its improved count sensitivity over S-SPECT cameras.

9:30 a.m.

1054-239

Risk Stratification of Diabetic Patients With Single Photon Emission Computed Tomography Myocardial Perfusion Imaging (SPECT-MPI): Does Duration of Disease and Type of Therapy Matter?

Dimitrios Barmopoulos, Gerasimos Stavens, Alan Ahlberg, David M. O'Sullivan, Deborah M. Katten, Gary V. Heller, Hartford Hospital, Hartford, CT

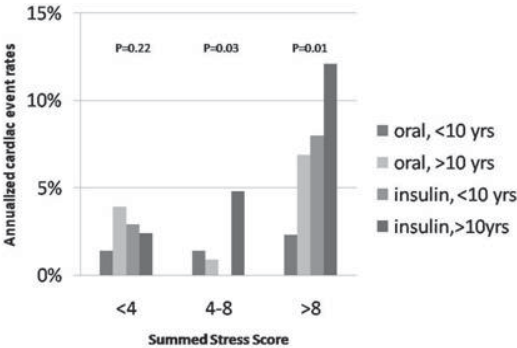
ECG-gated SPECT MPI is highly effective in risk stratification for adverse cardiac events. Diabetes is predisposing to an aggressive form of vascular disease, but the impact of its duration and type of therapy on risk stratification is unknown.

From the Hartford Hospital nuclear cardiology clinical database, 995 diabetic patients who underwent exercise or pharmacologic SPECT with complete follow-up were identified. Patients with early revascularization (≤60 days) were excluded. Images were interpreted using the ACC/ASNC standard 17-segment scoring model.

Of the 886 patients receiving medications for diabetes, 98 suffered cardiac death or nonfatal MI during follow-up. A Receiver Operator characteristics curve demonstrated

that diabetes of 10 years duration provided the maximum sensitivity and specificity for prediction of adverse outcome. Multivariate analysis identified the following as independent predictors of adverse outcome: Post-stress ejection fraction (EF) <40% (p< 0.001), Age (p=0.003), Insulin therapy (p=0.031), Diabetes duration>10 yrs (p= 0.038), Summed Stress Score (SSS)>8 (p= 0.046). For patients with a SSS 4-8 or ≥8, diabetes duration and type of therapy significantly enhanced risk stratification. Similar findings emerged for patients with a post-stress EF<40%.

For diabetic patients undergoing ECG-gated SPECT MPI, disease duration and type of therapy have independent prognostic value. Integration of these variables with ECG-gated SPECT enhances risk stratification.



9:30 a.m.

1054-240

Fluorodeoxyglucose Positron Emission Tomography May Prevent Cardiovascular Events in Patients With Ischemic Cardiomyopathy at an Experienced Center With Ready Access to FDG: A PARR-2 Sub-study

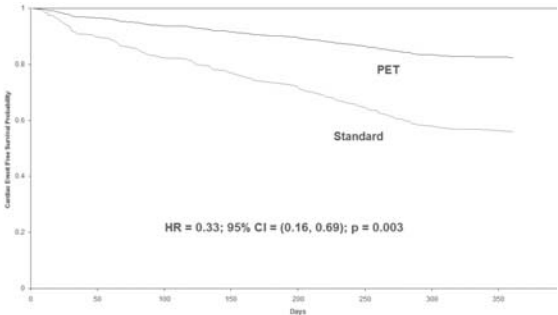
Arun Abraham, Graham Nicholl, Rob deKemp, Linda Garrard, Kathryn Williams, Ann Guo, Terrance D. Ruddy, Benjamin JW Chow, Ross A. Davies, Lloyd Duschesne, H. Haddad, Lyall Higginson, P. Hendry, R. Masters, Thierry Messana, Jan DeSilva, Rob S. Beanlands, University of Ottawa Heart Institute, Ottawa, ON, Canada, University of Washington, Seattle, WA

Introduction PARR-2 trial showed that FDG PET imaging guided revascularization had a trend for event-free survival benefit. We undertook a post-hoc sub-group analysis of PARR-2 looking at the benefit of FDG PET in an experienced center with ready access to FDG.

Methods Inclusion criteria for the PARR-2 trial were an EF <35%, suspected CAD, no MI within 4 weeks. Patients were randomized to FDG PET assisted therapy versus standard care. The primary outcome was the composite endpoint of cardiac death, MI, or re-hospitalization for cardiac cause. When PET identified viable myocardium, revascularization was recommended. Alternate imaging in the control arm was performed at the MD's discretion.

Results Included were 111 patients (56 PET; 55 standard care). There were no significant differences between groups in age, gender, ejection fraction, creatinine, diabetes, prior CABG and symptoms. At 1 year, there were 11 (21%) composite outcome events in the PET arm compared to 24 (44%) standard care arm. Adjusted survival curves (Fig 1) showed a benefit for PET guided strategy (hazard ratio = 0.33; 95% CI 0.16-0.69; p=0.003). Compared to the other patients in PARR2 (n=319), this subgroup was older (64±10 vs 62±10, p=.08), had lower EF (25±7 vs 27±8, p=.04) and had less previous CABG (13% vs 21%, p=.07) (p<0.05).

Conclusion Despite an older population with lower EF, in an experienced center with ready access to FDG, FDG PET guided revascularization improves clinical outcomes.



9:30 a.m.

9:30 a.m.

1054-241

Inflammation and Coronary Microvascular Dysfunction Assessed by Positron Emission Tomography in Patients With Cardiac Syndrome X

Alejandro Recio-Mayoral, Ernesto Trallero, Ornella Rimoldi, Paul B Bhamra-Ariza, Paolo G. Camici, Juan C. Kaski, Cardiac and Vascular Sciences, St George's Hospital, London, United Kingdom, MRC Clinical Sciences Centre, Imperial College, Hammersmith Hospital, London, United Kingdom

Background: Coronary microvascular dysfunction (CMD) plays a role in the pathogenesis of cardiac syndrome X (CSX) (angina with angiographically normal coronary arteries). Previous studies have shown that increased C-reactive protein (CRP) levels correlate with symptoms and severity of myocardial ischemia in these patients. We sought to assess whether CMD in CSX patients correlates with the degree of systemic inflammation, as assessed by high sensitivity CRP levels.

Methods: We studied 18 patients (mean age 50±11; 15 women) who fulfilled strict criteria for CSX, and 18 age and gender matched controls. By using positron emission tomography (oxygen-15 labeled water) myocardial blood flow (MBF, ml/min/g) was measured both at rest and during adenosine (140 µg/kg/min) in all patients and controls. Patients were -a priori- subdivided into 2 groups according to CRP levels at study entry: ≤3 mg/L (n=7) and >3 mg/L (n=11).

Results: Global resting MBF and adenosine MBF were similar in patients and controls (1.20±0.23 versus 1.11±0.17; p=0.19 and 3.16±1.01 versus 3.68±0.93; p=0.12, respectively). Coronary flow reserve (CFR; adenosine/rest MBF) was significantly reduced in CSX patients compared with controls (2.66±0.73 versus 3.46±0.79, p=0.004). After correction of resting flow for heart rate-systolic blood pressure product (index of myocardial oxygen consumption) the resulting values for corrected CFR (adenosine/rest corrected MBF) were similar in patients and controls (2.26±0.55 versus 2.63±0.60, p=0.06). Of importance however, patients with CRP > 3mg/L had more severe angina and ST-segment depression during adenosine testing and a more severe reduction in CFR (2.12±0.35) compared with CSX patients with CRP ≤ 3mg/L (3.00±0.71; p=0.003). Moreover, a significant negative correlation was found between CRP levels and CFR (r=-0.59, p=0.01) in CSX patients.

Conclusions: CSX patients with increased CRP levels (>3 mg/L) have reduced CFR suggestive of CMD, compared with healthy controls and those CSX patients with lower CRP levels (≤3 mg/L). Our findings also suggest that inflammation may modulate both microvascular function and the occurrence of symptoms and ST-segment changes in these patients.

9:30 a.m.

1054-242

Stress Testing and Prediction of Adverse Cardiac Events in Asymptomatic Diabetics: Meta-Analysis of Nine Studies

Gurusher S. Panjra, Raffay Khan, Carolina Valdiviezo, Nagesh Jadhav, Diwakar Jain, Johns Hopkins Hospital, Baltimore, MD, Drexel University College of Medicine, Philadelphia, PA

Background: Coronary artery disease is the leading cause of death in diabetes. Role of screening in asymptomatic diabetes is still under discussion. There exists a need to identify an appropriate test which can provide prognostic information beyond detection of coronary artery disease. We compared SPECT myocardial perfusion imaging (SPECT) and Stress Echocardiography (ECHO) for prediction of adverse cardiac events in diabetics with asymptomatic or unknown CAD.

Method: PUBMED was searched using various combinations of terms "coronary artery disease", "diabetes", "SPECT", "Imaging", "Echocardiogram" "stress testing" and "Nuclear." Individual study references were hand searched. Studies with less than 50 patients, symptomatic or known CAD, mean follow up < 1 year or not reporting incidence of hard events were excluded. Hard events were defined as myocardial infarction or death. Random effects model was used to compare studies due to significant heterogeneity.

Results: Search resulted in 35 studies. Out of these 9 studies met our criteria. A total of 3135 patients were included (Males 2593; Females 1422). Mean age was 60 ± 4yrs. Mean follow up was 3.3 ± 1.7 years. 2647 patients underwent SPECT compared to 488 in ECHO group. 1850 (59 %) patients had an abnormal study (SPECT = 1408; ECHO = 135). A total of 113 adverse events (3.6%) occurred over 3 years: 77 (4.1 %) in those with positive study compared to 36 (2.8 %) in those with negative study group. Patients with abnormal SPECT had a higher odds ratio of hard events compared to those with an abnormal ECHO (OR 3.13, CI 1.91-5.12 vs 2.36, CI 1.04-5.36, respectively). Average annual event rate in patients with abnormal study compared to those with normal study were: SPECT (9.3 % vs 0.8%) and ECHO (1.6 % vs 1.5%)

Conclusion: Asymptomatic diabetics with an abnormal stress test have a higher adverse cardiac event rate compared to those with those with a normal study. Patients with a positive SPECT study have a higher risk of having an adverse event compared to those with a positive ECHO. Beyond detection of CAD in asymptomatic diabetics, SPECT compared to ECHO is more effective in identification of patients at higher risk for adverse cardiac events.

1054-243

Attenuated Pulse Pressure Response to Exercise Identifies Patients With Normal Myocardial Perfusion Imaging at Risk for Future Events

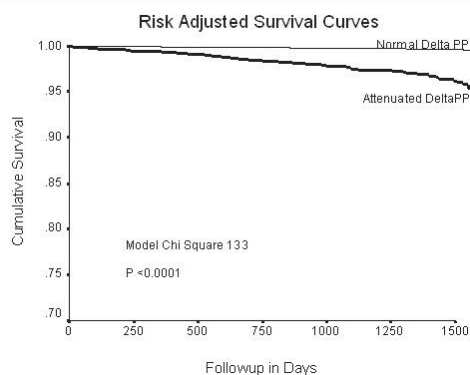
Deepak Thomas, Mouaz Al-Mallah, Daniel E. Forman, Marcelo F. Di Carli, Sharmila Dorbala, Brigham & Women's Hospital, Boston, MA

Increased pulse pressure (PP) relates to vascular stiffness; attenuated rise in PP during exercise may be a marker of endothelial dysfunction and early atherosclerosis. We sought to determine the incremental value of PP during exercise relative to known risk markers to predict future all cause death/myocardial infarction (ACD/MI) in patients (pts) with normal myocardial perfusion imaging (MPI).

Methods: We studied 3133 consecutive pts without prior coronary artery disease and a normal exercise Technetium-99m MPI, excluding pts with left bundle branch block/paced rhythm and hemodialysis. Rest PP, peak stress PP and the difference (ΔPP) were computed. Attenuated ΔPP was defined as ≤70 mmHg. Over a mean follow-up of 2 years, 111 ACD/MI occurred. Cox proportional hazards analysis was performed adjusting for age, gender, hypertension, diabetes, smoking, medications, workload, fall in peak systolic blood pressure >10 mm Hg, rest PP, Duke treadmill score, heart rate recovery, ejection fraction and ΔPP.

Results: The cohort (mean age 58±12 yrs) included 56% females, 53% hypertensives, 15% diabetics and 14% who smoked. Pts with ACD/MI were older, more often male, had higher rest PP, lower heart rate recovery, ejection fraction and lower ΔPP. Attenuated ΔPP (not rest PP) was an independent and incremental (to known risk markers) predictor of ACD/MI (model χ^2 139, p<0.0001) (Figure).

Conclusions: Attenuated PP response to exercise is a simple marker to identify pts with normal MPI at increased risk of ACD/MI.



9:30 a.m.

1054-244

The Diagnostic Accuracy of Clinical Interpretation Versus Blinded Interpretation in SPECT

Mitra Sahebzamani, Salman Haq, Lesan Banko, Igor Klem, Joshua A. Socolow, Sorin J. Brener, Terrence Sacchi, John F. Heitner, New York Methodist Hospital, Brooklyn, NY, Duke University Medical Center, Durham, NC

Background: Clinical interpretation of single photon emission computed tomography (SPECT) incorporates a number of clinical information (i.e. patient demographics, ECG changes, symptoms and hemodynamic responses) in the final assessment. There is scant data available on the utility of this added clinical information to the myocardial perfusion interpretation.

Objective: To assess the added benefit of clinical information to the overall myocardial perfusion interpretations of a SPECT study.

Methods: This retrospective study encompassed 182 patients who were referred for cardiac catheterization after a SPECT stress test (69 exercise, 24 Dobutamine, and 89 Dipyridamole). Mean age was 56 ± 10 yrs and 55% female. The stress test was initially interpreted incorporating all clinical data such as demographics, ECG, Symptoms, and hemodynamic response. The same physician blinded to all clinical information later interpreted the SPECT study based on myocardial perfusion only. A positive study was defined as any segment on a 17-segment model that was defined as ischemic or infarct. Cardiac catheterization was interpreted blindly and a significant stenosis >70% was considered positive for coronary artery disease.

Results: There was no significant difference in sensitivity of the diagnostic interpretation when clinical data was included compared to the blinded interpretation (80% (48/60) vs. 72% (46/64), respectively p=0.29). There was no significant difference in between the two groups for negative predictive value (77% (40/52) vs 81% (78/96), respectively, p=0.53). However, there was a significant reduction in specificity when the clinical information was added (33% (40/122) vs 66% (78/118) p<0.001). Similarly, there was a statistically significant difference between incorporation of clinical data and blinded interpretation for positive predictive value in SPECT interpretation (37% (48/130) vs 54% (46/86), respectively p=0.02).

Conclusions: Clinical information to SPECT interpretation adds an insignificant improvement in sensitivity with a marked reduction in specificity and positive predictive value.

9:30 a.m.

9:30 a.m.

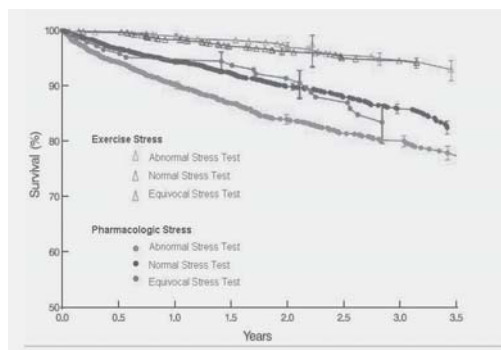
1054-245

Predictors of Mortality in 5944 Patients > Age 65 Undergoing Exercise Versus Pharmacologic MPI Stress Tests

Deborah H. Kwon, Venu Menon, Penny L. Houghtaling, Elizabeth Lieber, Richard C. Brunken, Manuel D. Cerqueira, Wael A. Jaber, Cleveland Clinic Foundation, Cleveland

Background: Elderly patients are under-represented in clinical trials and registries. The prognostic value of quantitative myocardial perfusion imaging (MPI) in this population is unclear. We analyzed the prognostic value of the pharmacologic and exercise MPI test impression in a large diverse elderly population.

Methods: We identified 5944 consecutive patients, age > 65 (75.3 ± 6.1 , 60% male) who underwent exercise (1664 patients, mean age 72.4 ± 5.1 , 74% male) or adenosine (4610 patients, mean age 75.3 ± 6.1 , 54% male) MPI between January 2004-January 2008. The overall physician's impression of the test (normal, equivocal, abnormal) was prospectively recorded. The primary end-point was all-cause mortality. Overall and stratified nonparametric survival estimates were obtained by Kaplan and Meier method. **Results:** During a median follow-up time of 2.4 years there were 745 deaths. There were more abnormal stress tests in the adenosine vs. exercise group (33% vs. 29%, $p < 0.001$). The mortality rate was significantly higher in the adenosine vs. exercise group (15% vs. 4%, $p < 0.001$). There was no difference in mortality amongst patients who exercised regardless of test impression. In contrast, an abnormal stress test predicted mortality in the adenosine group. (see Figure) **Conclusion:** The ability to exercise during MPI seems to neutralize the impact of the test result in elderly patients. However, in patients undergoing pharmacologic MPI, the results of the test provide incremental risk stratification.



9:30 a.m.

1054-246

Increased Survival in Walking Adenosine Stress Patients With Normal SPECT

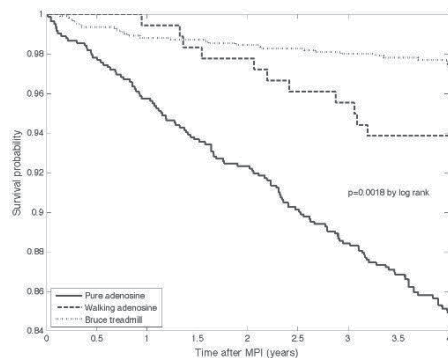
Daniel R. Schimmel, Jr., Sean P. Dyer, Scott M. Leonard, Nils P. Johnson, Thomas A. Holly, Northwestern University Feinberg School of Medicine, Chicago, IL

Background: Even with normal a SPECT study, patients selected for adenosine stress have a worse survival than exercise stress patients. In patients who are able, low-level treadmill exercise is commonly performed during adenosine infusion (a "walking" adenosine). The prognosis of patients undergoing walking adenosine is unknown.

Methods: Our cohort included patients undergoing adenosine or treadmill stress with SPECT imaging during 2003 and 2004. Adenosine studies were classified as walking or "pure" (no low-level exercise). Summed stress score (SSS) was determined using a 20-segment model with each segment rated from 0 (normal) to 4 (absent activity). Patients with a $SSS \geq 4$ (likely abnormal) or missing demographic information were excluded. All-cause mortality was determined using the Social Security Administration death index through mid July 2008.

Results: A total of 2,098 patients were included, of which 821 (39.1%) were pure adenosine, 179 (8.5%) were walking adenosine, and 1,098 (52.3%) were treadmill exercise. Over an average of 3.9 ± 0.7 years of follow-up, 164 (7.8%) died. See Figure.

Conclusions: Patients with a normal SPECT scan who are able to undergo a walking adenosine protocol have a better prognosis than those who cannot perform low-level exercise. Both adenosine groups have a worse survival than patients who can perform a treadmill protocol. As perfusion abnormalities cannot explain the differential survival, likely this effect is mediated by comorbidities and functional capacity.



1054-247

Myocardial Ischemia Threshold by SPECT for Revascularization Survival Benefit

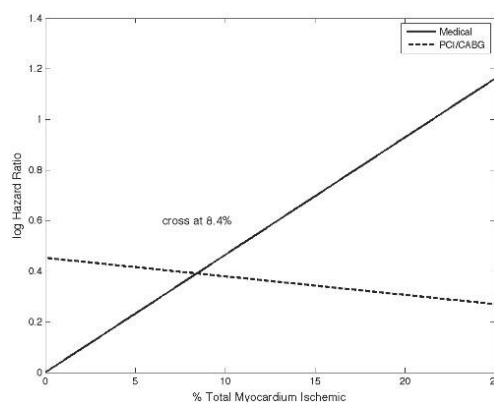
Daniel R. Schimmel, Jr., Nils P. Johnson, Thomas A. Holly, Northwestern University Feinberg School of Medicine, Chicago, IL

Background: Prior work has suggested a survival benefit for PCI/CABG versus medical therapy (MT) in patients who demonstrate a certain level of myocardial ischemia. The level of ischemia at which the survival benefit for PCI/CABG exceeded MT was approximately 10% by SPECT. However, this threshold has not been independently verified.

Methods: We included patients between 1/1995 and 2/2005 who were referred for rest/stress SPECT imaging. Patients were excluded if they had a known history of CAD or a gated $LVEF < 35\%$. Summed difference score (SDS) was graded using a 20-segment model scored from 0 (normal) to 4 (absent activity). The % myocardium ischemic was calculated as the $SDS/80$. We identified patients who underwent PCI/CABG within 60 days of their SPECT scan. All-cause mortality was determined using the Social Security Administration death index through the end of 4/2008.

Results: A total of 11,062 patients met inclusion criteria. 242 (2.2%) underwent an initial strategy of PCI/CABG. 1,617 (14.6%) patients died during 6.6 ± 2.6 years of follow-up. Significant covariates, a propensity score, SDS, treatment arm, and an interaction term were included in a Cox proportional hazards model (see figure).

Conclusions: The survival benefit from PCI/CABG exceeded that for MT when over 8.4% of the myocardium demonstrated a reversible defect by SPECT. These results confirm prior work suggesting a threshold of myocardial ischemia which must be present for an initial strategy of PCI/CABG to confer a benefit over MT alone.



1054-248

The Clinical Significance of an Abnormal ECG During Dipyridamole SPECT With a Normal Perfusion Study

Mitra Sahebzamani, Joshua A. Socolow, Igor Klem, Sorin J. Brenner, Terrence Sacchi, John F. Heitner, New York Methodist Hospital, Brooklyn, NY, University Medical Center, Durham, NC

Background: The significance of ST-segment changes during stress testing in the setting of normal myocardial perfusion study on single photon emission computed tomography (SPECT) is controversial and appears to be dependent on the type of stress. Prior studies have shown that a normal perfusion study with an abnormal electrocardiogram (ECG) during exercise or dobutamine portends a good prognosis, however, with dipyridamole, this is less clear.

Objectives: To assess the prognostic value of the presence of ischemic ECG changes during dipyridamole SPECT and its relation to major cardiovascular events

Methods: We followed 313 patients who underwent a SPECT study for the evaluation of coronary artery disease. The abnormal EKG was defined as a ST-segment depression ≥ 1 mm, 0.8 mm from the J point in 3 consecutive beats. Myocardial perfusion was considered abnormal if either ischemia or infarct was present in any segment on a 17-segment model. The patients were followed up by phone interview for the occurrence of major events (death, myocardial infarction, or revascularization) with a mean follow up of 25 ± 5 months. We divided patients into 3 groups: Group A- Dipyridamole stress with abnormal ECG and normal perfusion (22 pts); Group B- Dipyridamole stress with a normal ECG and an abnormal perfusion (221); Group C- Exercise or Dobutamine stress with an abnormal ECG and normal myocardial perfusion study (70); and compared Group A to Group B and C.

Results: The mean age was 56 years, 75% female. Group A had 8 events (36%) on mean follow up. In comparison, Group B had 87 events (39%) on follow up, which was not significantly different to Group A, $p = 0.78$. Group C, however, had a statistically significant lower event rate than Group A, with 11 events (16%) on follow up, $p = 0.04$.

Conclusions: An abnormal ECG with a normal myocardial perfusion study on SPECT during Dipyridamole portends a worse prognosis than patients who have an abnormal ECG and normal perfusion during Exercise or Dobutamine, and a similar prognosis as patients who have an abnormal perfusion with a normal ECG during Dipyridamole.

9:30 a.m.

1054-249

Diagnostic Certainty of the Myocardial Perfusion Scan Interpretation and Long-Term Outcomes in Patients Undergoing Exercise and Vasodilator Stress Myocardial Perfusion SPECT

Aiden Abidov, Sean W. Hayes, John D. Friedman, Louise Thomson, Xingping Kang, Ishac Cohen, Piotr Slomka, Guido Germano, Daniel S. Berman, Cedars-Sinai Medical Center, Los Angeles, CA, William Beaumont Hospital, Royal Oak, MI

Background: Previously published prognostic data regarding myocardial perfusion SPECT (MPS) is based mostly on the analyses of perfusion scores or simple dichotomous approach (normal vs. abnormal scans). In the real-world practice, however, substantial number of MPS studies is interpreted as borderline scans. We sought to evaluate a prognostic significance of the levels of diagnostic certainty in pts undergoing exercise (ETT) or vasodilator stress MPS.

Methods: Study population consisted of 20,249 pts (41% women, age 65 ± 13 yrs), who underwent exercise (62%) or vasodilator stress MPS and then were followed up for 3.4 ± 2.4 yr. Analysis of the diagnostic and prognostic data was performed separately in the exercise (ETT) and vasodilator stress MPS groups, distributed by the results of the expert clinical reading of the scans into the following categories: normal; probably normal; equivocal; probably abnormal, and definitely abnormal MPS. Cox proportional hazards analysis was deployed to assess the value of clinical/MPS variables in predicting cardiac death (CD). Risk adjustment took in consideration age, gender, historical and clinical variables, symptoms and severity and extent of the perfusion defects.

Results: During the follow-up there were 756 CD events: 195 (1.7%) in ETT and 551 (7.3%, $p < 0.001$) in vasodilator MPS. In both stressor groups, observed and risk-adjusted CD rates in pts with definitely and probably normal MPS were low ($< 1\%$ /yr). It remained low in pts with equivocal ETT MPS, whereas pts with equivocal vasodilator MPS demonstrated significantly higher mortality (HR=7.3 for unadjusted and 2.9 for risk-adjusted CD rate compared to equivocal ETT MPS, both $p < 0.001$). Further significant increase in observed and predicted CD rate was noted in pts with probably and definitely abnormal MPS regardless of stressor.

Conclusions: Levels of diagnostic certainty effectively risk-stratify pts with ETT and vasodilator stress MPS. Definitely or probably normal MPS is associated with excellent long-term prognosis regardless of the stressor type. Borderline scans in vasodilator MPS are associated with a significantly higher long-term cardiac mortality compared to that in pts with ETT MPS.

9:30 a.m.

1054-250

Assessment of the Effects of Age and Exercise Training on the Cardiac Sympathetic Nervous System by PET Imaging

Gwen M. Bernacki, James H. Caldwell, Jeanne M. Link, John R. Stratton, University of Washington, Seattle, WA

Background: Cardiovascular function declines with age. Using Positron Emission Tomography (PET) imaging, the purpose of this study was to determine whether normal aging or exercise training cause changes in the cardiac sympathetic nervous system function in healthy volunteers.

Methods: Sedentary subjects were rigorously screened and underwent PET studies before and after 6 months of supervised exercise training. Pre-synaptic norepinephrine transporter-1 function was measured using PET imaging of [^{11}C]-meta-hydroxyephedrine, a norepinephrine analog, and expressed as a permeability-surface area product (PS_{nt} in mL/min/mL tissue). Post-synaptic function was measured as β -adrenergic receptor density (β'_{max} in pmol/mL tissue) by imaging the β receptor antagonist [^{11}C]-CGP12177. Myocardial blood flow (MBF in mL/min/mL tissue) was measured by imaging [^{15}O]-water.

Results: Baseline studies were done in 22 young and 31 old, and post-training studies were done in 14 young and 22 old. At baseline, there were no significant differences in β'_{max} density (15.1 ± 1.3 young, 13.1 ± 0.9 old where $p = 0.17$) or MBF (0.76 ± 0.03 vs. 0.82 ± 0.03 where $p = 0.73$) but there was a trend for reduced PS_{nt} with aging (1.12 ± 0.11 vs. 0.85 ± 0.06 where $p = 0.06$). Training increased VO_2 max by 13% ($p < 0.0001$). There were no changes with training in β'_{max} density or PS_{nt} ($p > 0.05$ for both). The trend for a reduction in PS_{nt} with aging persisted after training (1.18 ± 0.17 vs. 0.82 ± 0.08 where $p = 0.07$).

Conclusion: Little difference in cardiac sympathetic nervous system function was found with aging or as a result of endurance training, suggesting that such changes do not occur or that current PET imaging methods may be inadequate to measure small serial differences in a highly reproducible manner.

9:30 a.m.

1054-251

Prognostic Value of PET Myocardial Perfusion Imaging in Patients With Suspect or Known Coronary Artery Disease

Niti B. Aggarwal, Imran S. Syed, J. Wells Askew, David O. Hodge, Todd D. Miller, Panithaya Chareonthaitawee, Mayo Clinic, Rochester, MN

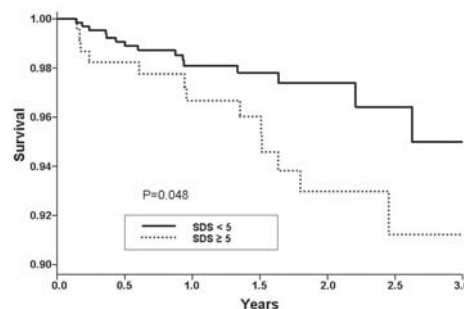
Background: There are limited data on the prognostic value of stress positron emission tomography (PET) myocardial perfusion imaging (MPI) in patients (pts) with known/suspected coronary artery disease (CAD). The objective of the study was to evaluate the prognostic value of contemporary PET-MPI at a tertiary center.

Methods: Mortality was obtained by the Social Security Death Index in 878 consecutive pts who underwent stress PET-MPI (N-13 ammonia=239; rubidium-82=639). Each of 17 standard myocardial segments was scored by two blinded observers using a 5-point system (0=normal to 4=absent tracer uptake). Summed scores at stress (SSS), rest

(SRS) and difference (SDS=SSS-SRS) were calculated (0=normal). Mean follow-up was 1.6 ± 1.0 years.

Results: Mean age was 60 ± 11 years, 54% were males. The average BMI was 37.0 ± 8.9 and 41% were diabetic. Abnormal PET-MPI was present in 51% (median: SSS=7, SDS=5). The number of pts in each summed score category was: SSS=0, 427; SSS=1-8, 246; SSS ≥ 9 , 205; SDS<5, 651; and SDS ≥ 5 , n=227. In a multivariate model, SDS was independently associated with mortality (HR = 1.06, $p = 0.05$). The Kaplan-Meier survival curve was significantly better for SDS<5 than for SDS ≥ 5 (Fig 1).

Conclusion: PET-MPI has significant prognostic value in pts with known/suspected CAD. With severe and extensive ischemia, mortality approached 3% per year.



9:30 a.m.

1054-252

Influence of End-Stage Renal Disease for Cardiac Risk in Diabetic Patients Assessed by Stress Myocardial Perfusion SPECT Images

Hiroshi Fukuda, Hiroki Hase, Tatsuhiko Furuhashi, Ryo Nakazato, Taeko Kunimasa, Yuri Tanaka, Hiroyasu Ishikawa, Nobuhiko Joki, Kaoru Sugi, Masao Moroi, Toho University Ohashi Medical Center, Division of Cardiovascular Medicine, Tokyo, Japan

Background: It is unclear whether diabetic patients with end stage renal disease (ESRD) have a risk of cardiac events equivalent to diabetic patients with coronary artery disease (CAD). The purpose of this study was to investigate whether ESRD should be considered a cardiac event risk equivalent in diabetic patients without prior myocardial infarction.

Methods: We enrolled 340 consecutive diabetic patients (64 ± 10 years, male=212) without known prior myocardial infarction who underwent stress myocardial perfusion SPECT images. Patients with estimated glomerular filtration rate (GFR) of 15 to 60 mL/min/1.73m² were excluded. CAD was defined as a presence of abnormal image. We categorized participants based on level of kidney function and SPECT results; 1) GFR>60mL/min/1.73m², no CAD (n=185) as a reference group, 2) ESRD (GFR<15mL/min/1.73m² or receiving hemodialysis), no CAD (n=61), 3) GFR>60mL/min/1.73m², CAD (n=69), and 4) ESRD, CAD (n=25). Cox hazards analysis was used to calculate relative risks of cardiac events.

Results: The results are shown in Table. There were 4 cardiac deaths, 22 acute coronary syndromes, and 12 congestive heart failures during 28 ± 18 months.

Conclusions: ESRD confers cardiac event risk that is higher and not equivalent to a CAD in diabetic patients without known prior myocardial infarction. Diabetic patients with ESRD are at a much greater risk for cardiac events than those without and should be needed careful follow up, particularly, in the presence of abnormal image.

Relative risks of cardiac events by multivariate cox hazards analysis

	GFR>60/ No CAD	ESRD/ No CAD	GFR>60/ CAD	ESRD/ CAD
Relative risk	1.0	5.5	3.6	16.7
95%CI	-	2.141-14.350	1.347-9.763	6.236-44.574
p value	-	0.0004	0.0108	<0.0001

9:30 a.m.

1054-253

Short-Term Impact of Noninvasive Cardiac Imaging on Medical Management: Results From the Study of Myocardial Perfusion and Coronary Anatomy Imaging Roles in CAD (SPARC) Trial 90-Day Follow-up

Marcelo F. Di Carli, James R. Johnson, Barbara A. Johnson, Mariya Gaber, Jonathan Hainer, Rory Hachamovitch, SPARC Investigators, Brigham and Women's Hospital, Boston, MA

Background: Post-cardiac imaging prognosis is often examined, but its impact on short-term medical management is unclear.

Methods: Baseline and 90-day cardiac medication (MED) use was collected in all pts recruited into SPARC (Study of Myocardial Perfusion and Coronary Anatomy Imaging Roles in CAD) a prospective, 40 site registry assessing outcomes after stress SPECT, PET, or 64 slice CCTA in 3,019 patients (pts) with suspected/known CAD. We assessed 90-day post-test MED changes (Δ ; defined as change in dose and/or add/remove ≥ 1 MED) in 1,703 pts (56%) with intermediate-high CAD likelihood and no prior CAD.

Results: Table 1 shows baseline MED in 565 (33%) SPECT, 548 (32%) PET, and 590 (35%) CCTA pts. Most often, MED change was the addition of aspirin, lipid lowering

agents, and an anti-hypertensive. MED Δ was more common after abnormal (ABNL) than normal (NL) test result [SPECT (25% vs 40%) than PET (32% vs 51%) and CCTA (30% vs 51%), all $p<0.002$], but less frequent after SPECT than PET or CCTA across test results ($p<0.015$). MED Δ occurred, at most, in half of ABNL test patients.

Conclusions: Although significant changes in cardiac MED occur after cardiac imaging, they occur in less than one third of patients with normal results and at most half of patients with abnormal results.

	SPECT	PET	CCTA
MED	N=565 [n (%)]	N=548 [n (%)]	N=590 [n (%)]
Aspirin	44.9%	46.7%	47.1%
Lipid Lowering Agent	48.9%	52.6%	50.0%
ACE	27.4%	35.2%	19.7%*
Beta-Blockers	32.5%	38.5%	28.8%*
Other Anti-Hypertensives	5.1%	5.1%	3.6%
Calcium Blockers	15.1%	18.1%	11.2%**
Nitrates	5.0%	4.4%	5.3%
Coumadin	4.6%	7.8%	2.4%*
Plavix	2.7%	3.3%	3.2%
Anti-Arrhythmics	1.0%	0.9%	0.8%
Ranexa	1.9%	2.2%	2.2%

* $p<0.001$ across groups; ** $p<0.005$ across groups

9:30 a.m.

1054-254 Low Prevalence of Significant Inducible Ischemia in Stable Symptomatic Diabetic Patients

Jamieson M. Bourque, Chetan A. Patel, Denny D. Watson, George A. Beller, University of Virginia Health System, Charlottesville, VA

Introduction: Individuals with diabetes are at high risk for coronary artery disease and cardiac events. Accordingly, there is a high level of referral for symptoms in this population. We sought to identify the clinical characteristics, stress and imaging findings, and prevalence of significant myocardial ischemia in a cohort of outpatient, stable, symptomatic patients with diabetes.

Methods: The study cohort included 465 consecutive outpatients with diabetes and symptoms suspected of ischemia who had pharmacologic or exercise stress, gated-SPECT myocardial perfusion imaging over a one-year period. Clinical, stress, and imaging variables were prospectively collected and analyzed. Three observers performed visual and quantitative assessment of the extent and severity of ischemia using a 17-segment model.

Results: Of the 3,114 patients imaged over one-year, 774 had diabetes (24.9%), and 60.1% of these (465) had symptoms. The mean age of the symptomatic diabetic cohort was 60.5 ± 11.0 years with 49.3% males. One-half were referred by non-Cardiologists. These patients had high levels of cardiac risk factors: 85.2% had hypertension; 75.1% hyperlipidemia; 52.5% obesity; and 31% tobacco use; 22.4% had prior myocardial infarction, and 11.0% had reduced left-ventricular (LV) ejection fraction $<45\%$. Medical therapy included anti-platelets in 58.7%, ACE-inhibitors or ARBs in 41.5%, and beta-blockers in 50.3%. ST-depression was found in 5.6%, and 18.3% had an elevated end-systolic volume index $\geq 25\text{cc}/\text{m}^2$. In this cohort 90% had no or $<5\%$ of the left-ventricle ischemic. High-risk ischemia of $\geq 20\%$ of the LV was seen in only 1.3%; only 3.5% had $\geq 10\%$ LV ischemia, the threshold relevant for revascularization.

Conclusions: In this group of stable, symptomatic diabetics, the risk of significant ischemia was surprisingly quite low, comparable to that seen in the asymptomatic cohort in the DIAD study. Given the high prevalence in ACS, the risk of ischemia clearly varies according to the population studied. Symptoms are likely difficult to correctly identify in this group. Moreover, the intensive medical therapy in this population may have lowered the amount of provokable myocardial ischemia prior to testing.

9:30 a.m.

1054-255 Resting SPECT Defects Add Prognostic Information to Ejection Fraction

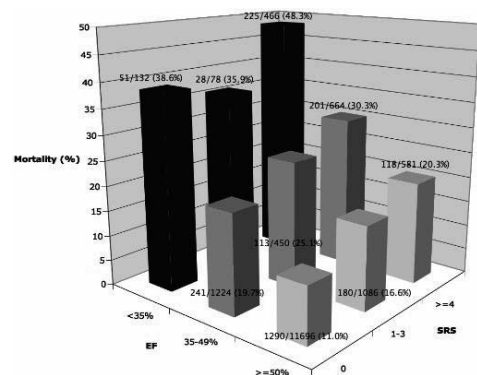
Nils P. Johnson, Thomas A. Holly, Robert O. Bonow, Edwin Wu, Northwestern University Feinberg School of Medicine, Chicago, IL

Background: Left ventricular ejection fraction (EF) has long been identified as a significant prognostic marker. The presence and extent of myocardial hibernation and fibrosis may carry additional prognostic information. We explored the hypothesis that resting perfusion defects independently predict all-cause mortality after accounting for EF.

Methods: We studied patients with rest/stress SPECT between 5/1996 and 7/2006. Only patients with an EF determined by gated SPECT were included. Gated EFs above 80% ($N=472$) were analyzed as 80%, and those below 10% ($N=4$) were excluded. Resting SPECT tracer uptake was scored from 0 (normal) to 4 (absent) using a 20 segment model to compute the summed rest score (SRS). All-cause mortality was identified from the Social Security Administration death index through the end of 7/2008.

Results: Of the 16,377 patients, 2,447 (14.9%) died over the mean follow-up period of 5.4 ± 2.6 years. Using a Cox proportional hazards model, SRS alone (hazard ratio [HR]=1.047, $\text{chi}^2=222.1$), EF alone (HR=0.968, $\text{chi}^2=416.8$), and EF with SRS (adjusted SRS HR=1.019, EF HR=0.973, $\text{chi}^2=445.8$) significantly ($p<0.001$) predicted all-cause mortality.

Conclusion: The severity of resting perfusion defects on SPECT imaging adds prognostic information to left ventricular EF. All-cause mortality increases with decreasing EF and increasing SRS. Our data could form the basis for a prognostic EF-SRS scoring system after a SPECT study.



9:30 a.m.

1054-256 Prognostic Impact of Blunted Heart Rate Response to Adenosine in Patients With End-Stage Renal Disease

Rajesh Venkataraman, Fadi G. Hage, Todd A. Dorfman, Jaekyeong Heo, Raed A. Aql, Angelo M. de Mattos, Ami E. Iskandrian, University of Alabama at Birmingham, Birmingham, AL

Background: The HR increase during adenosine infusion is due to direct sympathetic stimulation. We hypothesized that a blunted HR response, which is probably due to sympathetic denervation, would be associated with a worse outcome in patients with ESRD.

Methods: A total of 139 patients being evaluated for renal transplantation (RT) and who had adenosine stress MPI and coronary angiography within 6 months of the MPI were included in this study. A control group of 54 patients (normal renal function and non diabetic) were included for comparison of HR response. Baseline clinical, laboratory, angiographic and mortality data were collected prospectively. All cause mortality was defined as the outcome measure. Percentage change in HR ($\%\Delta\text{HR}$) was calculated as $[(\text{peak HR} - \text{baseline HR})/\text{baseline HR}] \times 100$.

Results: The mean age was 54 ± 9 years; 30% were women, 68% were diabetic and 30% had left ventricular ejection fraction (LVEF) $\leq 40\%$. The mean $\%\Delta\text{HR}$ was 19.2 ± 18 , while the $\%\Delta\text{HR}$ in the control group was 33 ± 25 ($P<0.0001$). The mean number of diseased vessels by coronary angiography was 1.7 ± 1.2 and 46% underwent coronary revascularization. At a mean follow-up of 3.4 ± 1.5 years, 50 deaths occurred (36%). Those who died were more likely to have a lower LVEF, larger mean perfusion defect size and more diseased vessels by angiography (all $P<0.05$). The $\%\Delta\text{HR}$ was lower in non-survivors than survivors (12.6 ± 14 vs. $23 \pm 19\%$, $P=0.0017$). Patients with a $\%\Delta\text{HR}$ below the median value were more likely to have a lower left ventricular ejection fraction and a larger end-diastolic volume ($p<0.05$, each). In a multivariate logistic regression model comprising total perfusion defect size, LVEF, number of diseased vessels by angiography, diabetes, age and $\%\Delta\text{HR}$, $\%\Delta\text{HR}$ alone was an independent predictor of all-cause mortality (adjusted OR=5.5, CI 2.3-12.9, $p=0.0001$).

Conclusions: Patients with ESRD have a blunted HR response to adenosine and the degree of blunting is a strong independent predictor of all-cause mortality.

9:30 a.m.

1054-257 Blunting of the Heart Rate Response to Adenosine and Regadenoson in Relation to Hyperglycemia and the Metabolic Syndrome in the ADVANCE MPI Trials

Fadi G. Hage, Billy Franks, Jaekyeong Heo, Luiz Belardinelli, Brent Blackburn, Whedy Wang, Ami E. Iskandrian, University of Alabama at Birmingham, Birmingham, AL, Astellas USA, Deerfield, IL

Background: Adenosine and regadenoson cause a rapid increase in heart rate (HR) when used as stress agents during myocardial perfusion imaging (MPI). We have previously demonstrated that patients with diabetes mellitus (DM) have a blunted HR response due to cardiac autonomic dysfunction. We test the hypothesis that the HR response to adenosine and regadenoson is related to hyperglycemia and the presence of the metabolic syndrome (MS).

Methods: We studied the HR changes in 2,000 patients (643 DM patients) in the ADENOSCAN Versus Regadenoson Comparative Evaluation for Myocardial Perfusion Imaging 1 and 2 trials in relation to their blood sugar level on the day of the MPI and the presence of the MS.

Results: Increasing blood sugar levels resulted in blunting of the HR response even after controlling for DM (HR response decreases by 1.63% per 1mmol/L increase in blood sugar, $P<0.0001$). In fact, non-DM patients sustained a greater decrease in their HR response with hyperglycemia (1.21% lower in non-DM compared to DM per 1mmol/L increase in blood sugar, interaction P value 0.008). Using multiple regression, blood sugar levels independently accounted for a decrease in the HR response after adjusting for DM, beta-blocker intake, baseline HR, age, gender, renal function, systolic blood pressure, and left ventricular systolic function ($P<0.05$). This model was able to explain ~ 30% of the variability in the HR response. Patients with MS had a blunted HR response compared to those without it (32.42 ± 0.52 vs. $36.15 \pm 0.71\%$, $P<0.0001$). Furthermore, an increase in the number of features of MS is associated with a linear decrease in the HR response (-0.92% decrease for every additional criterion met, $P<0.05$), and this effect is additive to the presence of DM. Importantly, blood sugar levels continued to be a determinant of the

HR response in patients with MS even after adjusting for the presence of DM.

Conclusions: The HR response to adenosine and regadenoson is blunted in patients with hyperglycemia and in those with the MS. These results suggest that factors that precede the development of DM may be associated with cardiac autonomic neuropathy and may help explain the contribution of hyperglycemia and the MS to cardiovascular risk.

9:30 a.m.

9:30 a.m.

1054-258

Quarter-Time Wide Beam Reconstruction: Evaluation of SPECT Myocardial Perfusion and Function

E. Gordon DePuey, Srinivas Bommireddipalli, John Clark, Anna Leykekhman, Linda Thompson, Marvin I. Friedman, Haim Kermay, St. Luke's-Roosevelt Hospital/Columbia University, New York, NY, UltraSPECT, Ltd., Haifa, Israel

Background: Previously we reported that compared to iterative reconstruction with OSEM, wide beam reconstruction (WBR), which incorporates resolution recovery and models noise during reconstruction without applying a post-processing filter, allows half-time SPECT acquisition with preserved diagnostic quality. We now postulate that with further Poisson noise modeling quarter-time acquisition is possible.

Methods: The half-time WBR algorithm was optimized for quarter-time acquisition based upon anthropomorphic cardiac phantom data and a pilot group of 48 patients (pts). Then using the modified algorithm, 208 pts (91 men, 117 women, mean chest circumference = 41 in) were imaged at rest (R) and stress (S) (9/32 mCi ^{99m}Tc-sestamibi) full-time with OSEM, and again quarter-time with the modified WBR algorithm. 180-degree, 64-stop, full-time single-day rest (R) (25 second-per-stop (sps)) and 8-frame per cardiac cycle post-stress (S) (20sps) gated SPECT, and then quarter-time R (6sps) and post-S (4 sps) gated SPECT were acquired. Blinded observers graded scan quality (1=poor to 5=excellent) based on myocardial uniformity, endocardial/epicardial edge definition, and background noise. Perfusion defects were scored using a 17-segment model. Using Myometrix® software, EDV, ESV, and LVEF were calculated.

Results: For the 208 prospective pts mean image quality for R full-time OSEM and quarter-time WBR were similar (3.6 vs. 3.5, p NS). For S, quarter-time WBR quality (4.3) was superior to full-time OSEM (3.9) (p= 1.8E-17). Of 48 pts with abnormal scans (SSSs >2 by OSEM) mean SSSs, SRSSs, and SDSs were not significantly different with quarter-time WBR vs. full-time OSEM (11.2 vs 10.9), (9.2 vs. 9.0), (2.0 vs. 1.9) (p's NS). There was a good correlation of LVEF, EDV, and ESV determined by WBR vs. OSEM (r's = 0.92, 0.97, and 0.98). ESVs were higher with WBR (52cc vs. 46cc, p=2.6E-23) primarily due to better delineation of the valve plane at end-systole, whereas EDVs were similar (94cc vs. 96cc, p NS). Thus EFs were lower with WBR (49.1 vs 57.6, p=1.6E-48).

Conclusions: For perfusion SPECT quarter-time WBR affords image quality, defect characterization, and functional assessment equivalent to full-time OSEM.

9:30 a.m.

1054-259

Comparison of Phase Analysis of Gated Myocardial Perfusion SPECT to Tissue Doppler Imaging for Assessment of Left Ventricular Dyssynchrony and Prediction of Response to Cardiac Resynchronization Therapy

Mark M. Boogers, Serge D. van Kriekinge, Guido Germano, Petra Dibbitts-Schneider, Marcel P. Stokkel, Daniel S. Berman, Jeroen J. Bax, Leiden University Medical Center, Leiden, The Netherlands, Cedars-Sinai Medical Center, Los Angeles, CA

Background: Several clinical trials using echocardiography have demonstrated the significance of left ventricular (LV) dyssynchrony for prediction of response to cardiac resynchronization therapy (CRT). Recently, a novel toolbox for phase analysis on gated myocardial perfusion single-photon emission computed tomography (GMPS) has emerged to assess LV dyssynchrony. Aim was to compare the specified algorithm for phase analysis on GMPS to tissue Doppler imaging for the assessment of LV dyssynchrony. In addition, it aims to demonstrate whether GMPS may predict response to CRT.

Methods: In 40 consecutive severe heart failure patients (New York Heart Association (NYHA) functional class III or IV), LV ejection fraction ≤35% and prolonged QRS interval (≥120ms), GMPS and 2-dimensional echocardiography with tissue Doppler imaging were performed. Clinical status was evaluated with NYHA class, 6-min walk test and quality-of-life score. After 6 months of CRT, clinical evaluation and 2-dimensional echocardiography were rehearsed and patients who improved ≥1 grade in NYHA class were considered responders to CRT. Histogram bandwidth (HBW) and phase standard deviation (SD), indicators of LV dyssynchrony derived from GMPS, were correlated to septal-to-lateral delay on TDI. Next, HBW and phase SD were compared between responders and non-responders.

Results: After 6 months of CRT, 24 (60%) patients were considered as responders to CRT. HBW (r=0.69, P<0.0001) and phase SD (r=0.65, P<0.0001) agreed well with tissue Doppler imaging for assessment of LV dyssynchrony. Furthermore, responders showed significant higher levels of HBW (94±23° vs. 68±21°, P<0.0001) and phase SD (26±6° vs. 18±5°, P<0.01) compared to non-responders. For HBW and phase SD, optimal point for prediction of response to CRT was defined at 72.5° and 19.6°, respectively. Good area under the curve was observed for HBW (0.83) and phase SD (0.85), yielding similar sensitivity of 83% and specificity of 81%.

Conclusions: LV dyssynchrony assessed with the novel algorithm for phase analysis on GMPS was well-correlated to LV dyssynchrony from tissue Doppler imaging. In addition, phase analysis on GMPS may be useful for prediction of response to CRT.

1054-260

Outcomes Analysis of Stress Only Gated Myocardial Perfusion Imaging With Attenuation Correction in Patients With Suspected Coronary Artery Disease

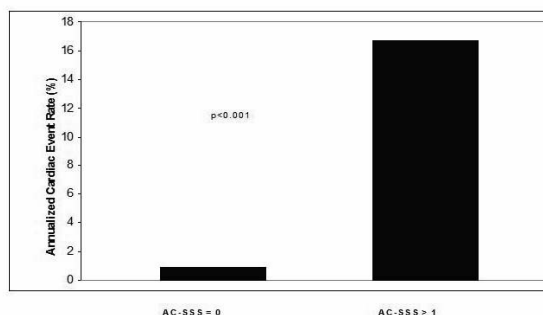
Arshad Yekta, Richard Ruffin, Alan Ahlberg, Deborah Katten, Gary Heller, Hartford Hospital, Hartford, CT

Background: Stress-only myocardial perfusion imaging (MPI) with attenuation correction (AC) excludes the acquisition of rest images, potentially leading to a more rapid study completion and improving laboratory efficiency. However, the prognostic value of a stress-only strategy, particularly in relation to MPI results, has not been adequately evaluated.

Methods: Consecutive patients referred for chest pain without a prior history of myocardial infarction (MI) were scheduled for stress-only Technetium-99m MPI. After application of AC, a summed stress score (SSS) was calculated using the standard 17-segment scoring model. Patients were followed for the occurrence of coronary revascularization, non-fatal MI or cardiac death and censored at the first event.

Results: Of 721 patients, follow-up was complete in 93% over 1.4 ± 0.7 years. Of these 672 patients, 96% had a SSS of 0. The AC-SSS in patients having either undergone coronary revascularization or suffered an adverse cardiac event (4.8 ± 7.1) was higher than in those who did not (0.1 ± 1.0, P <0.001). Cumulative cardiac event-free survival in patients with a SSS of 0 (98.8%) was significantly higher than in those with a SSS >0 (72.5%, P <0.001). Similar findings were observed in relation to the annualized cardiac event rate (figure).

Conclusion: Stress-only myocardial perfusion imaging with AC effectively stratifies patient risk for subsequent cardiac events. Patients with completely normal results carry a very low risk for cardiac events.



9:30 a.m.

1054-261

Evidence of Coronary Calcium in Patients With Normal Positron Emission Tomography Myocardial Perfusion Imaging Scans Likely to Influence Physicians to Initiate Statins or Recommend Optimal Medical Therapy

John H. Lee, Ryan Longmore, Richard Markiewicz, A. I. McGhie, James H. O'Keefe, Bai-Ling Hsu, Kevin Kennedy, Randall C. Thompson, Timothy M. Bateman, Kevin A. Bybee, Mid America Heart Institute, Kansas City, MO, University of Missouri-Kansas City, Kansas City, MO

Background: Perfusion imaging is limited in its inability to detect non-obstructive coronary artery disease (CAD) and potentially misclassifying patients as normal who in fact have substantive plaque burden. Positron emission tomography (PET) with computed tomography (CT) myocardial perfusion imaging (MPI) has the advantage of same-setting measurement of coronary artery calcium score (CACS) which can be used as an index of plaque burden. Although there is an abundance of data suggesting the important prognostic information gained from CACS, little is known about the therapeutic changes if any that may result from normal PET perfusion with CAC.

Methods: Consecutive patients in a single academic medical center in Kansas City with no history of CAD and normal perfusion on their stress rubidium-82 PET/CT MPI scan between March 2007 and May 2008 were identified and enrolled. A retrospective review of patient electronic medical records was performed to identify therapeutic changes made after identifying CAC as a part of the PET/CT MPI protocol. Categorical variables were analyzed with χ^2 while quantitative variables with the Student's t-test.

Results: Of the 760 patients without known CAD and normal perfusion on PET MPI, 487 (64.1%) had subclinical CAD based on an abnormal CACS. Increasing age, male gender, hypertension, and hyperlipidemia were all univariately associated with the presence of CAC (p<0.05). Patients with CAC were more likely to be at intermediate Framingham risk versus low risk in those without CAC (p=0.003). Following the PET/CT MPI, patients with CAC were also more likely to be initiated on statin therapy (20.4% vs 11%; p=0.002) or recommended to initiate more optimal medical therapy (17.9% vs 3.3%; p<0.001). Those with greater amounts of CAC were more likely to undergo optimization of medical therapy for CAD: at CACS = 0, 34.3%; at >0 but <400, 49.9%; and >400, 65.4% (p<0.001).

Conclusion: Subclinical CAD detected by the presence of CAC in patients with normal perfusion on PET MPI influences physicians to optimize medical therapies for CAD particularly through initiation of statin therapy.

9:30 a.m.

9:30 a.m.

1054-262

Diabetics With Positive SPECT Myocardial Perfusion Imaging Referred for Catheterization: Gender Bias?

Osman Faheem, Yaqoob Mohyuddin, A. F. Iqidar, A. L. Guller, Dhruva Chawla, Alan Ahlberg, Gary Heller, Hartford Hospital, Hartford, CT

Background: Female patients with diabetes are known to be at high risk for cardiovascular events. How this affects decision making after non-invasive testing has not been examined. We evaluated the impact of gender on referral for cardiac catheterization after stress SPECT myocardial imaging.

Methods: Patients with diabetes and suspected CAD referred for stress gated SPECT MPI were identified in our database from January 1996 to December 2005. Patients with known CAD, prior SPECT MPI, and prior cardiomyopathy were excluded. Studies were interpreted using the 17-segment ACC/ASNC model. A summed difference score SDS < 2 was considered no ischemia, SDS 2-7, mild to moderate ischemia and SDS ≥ 8, severe ischemia. Cardiac catheterization referral rate was examined in relation to the SDS for patients sent to catheterization lab within 60 days after SPECT MPI.

Results: 2834 diabetic patients with no known CAD underwent SPECT MPI (1221 [43.1%] men, 1613 [56.9%] women). Referral to catheterization was similar in diabetic men and women for patients with no ischemia or mild to moderate ischemia on SPECT. In diabetic patients with severe ischemia, the percentage referred for cardiac catheterization was higher in men than in women, although the difference was not statistically significant.

Sum Difference Score (SDS)	Males N = 1,221 n (%)	Men referred to cath N = 165 n (%)	Females N = 1,613 n (%)	Women referred to cath N = 136 n (%)	p-value
SDS ≥ 8	91 (7.4)	67 (73.6)	74 (4.6)	45 (60.8)	NS (<0.10)
SDS ≥ 2-7	198 (16.2)	64 (32.3)	233 (14.4)	56 (24.0)	NS (<0.10)
SDS < 2	932 (76.3)	34 (3.6)	1306 (81.0)	35 (2.6)	NS (<0.25)

Conclusion: In diabetic patients without prior CAD, there is no gender bias in referral for cardiac catheterization after positive SPECT MPI. The degree of ischemia determines the referral to cardiac catheterization, not gender.

9:30 a.m.

1054-263

Phase 1 Human Safety, Dosimetry, Biodistribution, and Rest/Stress Myocardial Imaging Characteristics of F-18 Labeled BMS747158

Jamshid Maddahi, Henry Huang, Johannes Czernin, Heinrich Schelbert, Frank Bengel, Christiaan Schiepers, Anna Wijatkyk, Joel Lazewatsky, Qi Zhu, James Case, Richard Sparks, Michael Phelps, David Geffen School of Medicine at UCLA, Los Angeles, CA, Lantheus Medical Imaging, Billerica, MA

Background: F-18 labeled BMS747158 is a novel myocardial perfusion imaging tracer that targets mitochondrial complex 1. In this Phase 1 study, human safety, dosimetry, biodistribution, and myocardial imaging characteristics of this tracer were evaluated at rest and stress in normal subjects.

Methods: 13 normal subjects received 222 MBq intravenously at rest and 4 more subjects received 101 MBq at rest and, on a second day, 157 MBq at peak pharmacologic stress with adenosine infusion (Adeno). Dynamic PET was obtained over the heart for 10 minutes followed by sequential cardiac and whole body imaging. Physical exam, blood chemistry, vital signs, ECG, and EEG were monitored prior to and after injection. Residence times were determined from multi-exponential regression of organ ROI data in 13 rest and 4 Adeno subjects, normalized by injected dose. Radiation dose estimates were calculated using the MIRD schema with OLINDA/EXM. Myocardial, liver, blood pool and lung Standardized Uptake Values (SUV) were determined at different time intervals. **Results:** There were no adverse events related to the tracer. The top four highest-dose organs and their respective mean dose estimates (in mSv/MBq) at rest were kidneys (0.065), myocardium (0.047), stomach (0.040) and liver (0.039) and with Adeno were myocardium (0.10), salivary glands (0.083), kidneys (0.060) and liver (0.048). Mean effective dose (ED) was 0.017 mSv/MBq at rest and 0.019 mSv/MBq with Adeno. ED was very similar to that of commonly used F-18 labeled FDG, but the dose to the critical organ was lower than that of FDG by a factor of 2.5 (rest) and 1.7 (Adeno). Myocardial SUVs at 10, 30, 60 and 149 minutes were respectively 3.9±0.9, 4.2±1.1, 4.5±1.2, and 4.1±1.4 and significantly ($p<0.01$) increased with Adeno, at respective time intervals, to 10.5±1.5, 10.8±2.1, 10.3±2.1, and 8.4±2.1. Myocardial to background ratio rapidly improved with time.

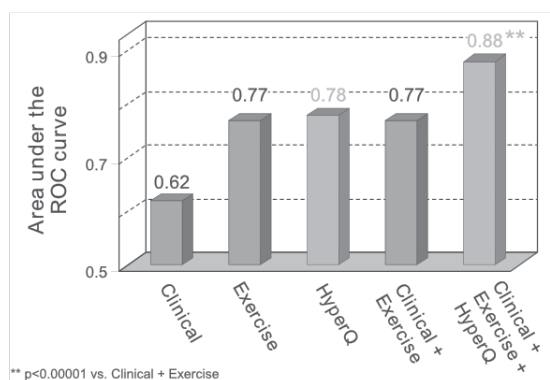
Conclusions: These preliminary data suggest that F-18 labeled BMS747158 is clinically safe, has acceptable dosimetry, and has a high myocardial uptake at rest, that significantly increases with adenosine stress. F-18 labeled BMS747158 offers a unique potential for rest-stress myocardial perfusion PET imaging.

1054-264

Detection of Stress-Induced Myocardial Ischemia Using Analysis of Depolarization Abnormalities

Tali Sharir, Konstantine Merzon, Iren Kruchin, Andrzej Bojko, Haim Silber, Pierre Chouraqui, Procordia - Maccabi Healthcare Services, Tel-Aviv, Israel, Chaim Sheba Medical Center, Tel Hashomer, Israel

Detection of stress-induced myocardial ischemia typically focuses on changes in the repolarization phase of the ECG, manifested in the ST segment. However, ischemia also induces changes in the depolarization phase, which can be quantified by analysis of high-frequency mid-QRS components. We aimed to determine incremental diagnostic value of this technique over standard ECG exercise testing. **Methods:** Exercise SPECT myocardial perfusion imaging (MPI) was performed in 941 consecutive pts (630 men) referred for evaluation of CAD at 2 medical centers and used as gold standard of ischemia. Conventional exercise ECG was combined with high resolution ECG acquisition, which was digitized and analyzed using the HyperQ™ System (BSP, Israel). A 50% decrease in the intensity of high frequency QRS components (HyperQ) during exercise was used as an index of ischemia. Logistic regression was used to assess incremental diagnostic value of HyperQ data over conventional ST analysis. **Results:** Moderate/severe MPI ischemia was found in 52 pts. HyperQ index was more sensitive than ST segment analysis (69% vs 48%, $p=0.03$) with similar specificity (84%). HyperQ index offered significant incremental diagnostic value over clinical and exercise test data (fig) and correlated to ischemia severity ($R^2=0.8$, $p<0.001$). **Conclusions:** HyperQ analysis provides a significant improvement over conventional ST segment analysis in detecting ischemia, and may thus aid in enhancing the non-invasive diagnosis of ischemic heart disease.



9:30 a.m.

1054-265

Exercise Capacity in Women Versus Men: The Impact of Ventricular-Arterial Stiffening

Carolyn S. Lam, Barry A. Borlaug, Steve R. Ommen, Jasmine Grewal, Robert B. McCully, Patricia A. Pellikka, Mayo Clinic, Rochester, MN

Background: The mechanisms underlying sex differences in exercise capacity are unclear. Left ventricular (LV)-vascular stiffening increases with aging, affects women more than men, and may contribute to exercise intolerance.

Methods: Consecutive patients with LV ejection fraction ≥50% and no ischemia (n=393) underwent treadmill exercise echo within 90 days (median 1 day) of resting Doppler echocardiography. Effective arterial elastance (Ea) = 0.9*SBP/stroke volume, LV end-systolic elastance (Ees) = 0.9*SBP/end-systolic volume and LV diastolic elastance (Ed) = end-diastolic pressure/ end-diastolic volume, where LV end-diastolic pressure was derived from E/e', were determined as measures of arterial and ventricular stiffness. Exercise capacity was measured in metabolic equivalents (METs).

Results: (Table) At baseline women had smaller BSA, LV volume and stroke volume but higher heart rate and similar cardiac index compared to men. LV-vascular stiffening was greater in women than men, even after adjusting for age and BSA. Peak METs were lower in women than men despite similar peak blood pressure, heart rate, double product and LV diastolic pressure. Adjusting for age and BSA, Ea, Ees and Ed each correlated with METs ($r = -0.26$, -0.17 and -0.30 , respectively; all $p<0.001$).

Conclusions: Ventricular-vascular stiffening is greater in women than in men and is associated with reduced exercise capacity. Agents targeting LV-vascular stiffening may improve exercise performance particularly in women.

Parameter	Men	Women
N	219	174
Age, y	61±14	59±14
Body surface area (BSA), m ²	2.10±0.20	1.78±0.21*
% Hypertension	55	49
% Beta blockers	39	35
Baseline (Rest)		
Systolic blood pressure (SBP), mmHg	123±16	122±18
Diastolic blood pressure, mmHg	71±12	71±11
Heart rate, bpm	65±13	69±14*
Ejection fraction, %	60±10	64±7*Φ
LV end-diastolic volume/BSA, ml/m ²	59.4±16.0	55.7±13.9*Φ
Left atrial volume/BSA, ml/m ²	33.5±10.8	31.0±10.9*Φ
Stroke volume/BSA, ml/m ²	47.8±9.1	45.3±12.4*Φ
Cardiac index, L/min/m ²	2.99±0.64	3.05±0.83
Ea, mmHg/ml	1.15±0.25	1.45±0.41*Φ
Ees, mmHg/ml	2.93±1.57	3.94±1.80*Φ
Ea/Ees	0.48±0.28	0.42±0.20*
Mitral E, cm/s	0.72±0.21	0.76±0.21
Septal e', cm/s	0.074±0.027	0.079±0.085
E/e'	10.9±4.7	11.1±4.8
LV end-diastolic pressure, mmHg	18±3	19±3
Ed, mmHg/ml	0.16±0.04	0.20±0.06*Φ
Exercise		
METs	9.9±2.9	8.3±2.5*Φ
Peak systolic blood pressure, mmHg	162±25	160±26
Peak diastolic blood pressure, mmHg	77±13	75±14
Peak heart rate, bpm	142±24	145±26
Double product	23066±5661	23156±5590
Ejection fraction, %	66±12	68±8
Mitral E, cm/s	0.94±0.27	0.97±0.26
Septal e', cm/s	0.095±0.033	0.102±0.033
E/e'	11.0±5.8	10.3±4.1
LV end-diastolic pressure, mmHg	19±3	18±2

*p<0.05 vs men in unadjusted comparison (by t-test)
Φp<0.05 vs men in comparisons adjusted for age and body surface area where appropriate (by linear least-squares regression)

9:30 a.m.

1054-266

Evaluation of Origin of Plasma Norepinephrine at Peak Exercise in Patients With Heart Failure Using Systemic 123I-MIBG Imaging

Takaya Tsuchida, Nagaharu Fukuma, Keiko Oikawa, Hiroko Hayashi, Akiko Ushijima, Kazuyo Kato, Yuko Kato, Noriko Aisu, Hiroshi Takahashi, Hiroshi Kishida, Kyoichi Mizuno, Nippon Medical School, Tokyo, Japan

Background: Past studies suggested that plasma norepinephrine during exercise originates in sympathetic nerve endings and that the main origin differs among pathophysiological conditions. **AIMS:** This study investigated the most important site of sympathetic terminals as an origin of plasma norepinephrine during exercise in patients with heart failure using (123I)-metaiodobenzylguanidine (MIBG) scintigraphy.

Methods: Twenty patients with organic heart disease underwent exercise testing and (123I)-MIBG scintigraphy. Systemic (123I)-MIBG uptake was measured 4 hours after (123I)-MIBG injection, and the heart-to-brain (H/B) and lower limb-to-brain ratios (L/B) were calculated. Plasma norepinephrine concentration was measured at rest and at peak exercise. Subjects were divided into two groups: those with preserved left ventricular ejection fraction (LVEF> or =45%, n=8) and those with reduced LVEF (<45%, n=12).

Results: Plasma norepinephrine at rest did not correlate with H/B or L/B. In the preserved LVEF group, plasma norepinephrine at peak exercise was correlated with H/B (r=0.722), but not with L/B. In the reduced LVEF group, the norepinephrine response to peak exercise correlated with L/B (r=0.642), but not with H/B.

Conclusions: The present findings suggest that norepinephrine concentration is regulated by sympathetic terminal function of working muscles in patients with impaired LVEF and by that of the heart in patients with preserved LVEF.

9:30 a.m.

1054-267

Detection of Coronary Artery Disease in Hypertensive Patients With ST-Segment Changes During Exercise Testing

Charalampos Liakos, Andreas Michaelides, Leonidas Raftopoulos, Charalampos Antoniadis, Gregory Vysoulis, George Andrikopoulos, Nikolaos Ioakeimides, Konstantinos Tsioufis, Dimitrios Soulis, Christodoulos Stefanadis, 1st University Department of Cardiology, Athens Medical School, Hippokraton Hospital, Athens, Greece

Background: Patients with arterial hypertension frequently present ischaemic electrocardiographic (ECG) changes during exercise testing (ET) without actually suffering from coronary artery disease (CAD). The purpose of this study was to establish possible ECG criteria during ET for detecting CAD in hypertensives with ischaemic ST-segment response.

Methods: We recruited 382 hypertensives (224 males, 58 ± 8 years) with ischaemic ECG changes during ET. All underwent a treadmill test (Bruce protocol). The actual presence of CAD was ascertained by a coronary angiography.

Results: From 382 hypertensives undergoing angiography, only 76 (20%) had CAD, while 306 (80%) had normal arteries. During exercise, 287 patients (75%) (group A) presented ST-segment depression in II-III-aVF-V6, 271 (94%) of which had normal arteries. The

rest 95 (25%) of the studied patients (group B) presented ST-segment depression in II-III-aVF and/or V4-V6, 60 (63%) of which had CAD. Furthermore, 251 patients of group A presented ST-segment depression during 4th-6th min of the recovery period in V4-V6, 247 (98%) of which had normal arteries. Another 28 patients of group B presented ST-segment depression during 4th-8th min of the recovery period in V4-V6, 22 (79%) of which had CAD (Table1).

Conclusions: Hypertensive patients who present ST-segment depression during exercise in leads II-III-aVF and/or V4-V6 and the duration of this depression at the recovery phase is prolonged (4th-8th min) are more likely to have CAD.

Table1 Exercise ST-segment changes in correlation with angiographic data

ST-segment Depression	CAD (n=76)	No-CAD (n=306)	p-value
Exercise: II-III-aVF (mm)	1.7±0.3	1.8±0.5	NS
Exercise: V4-V5 (mm)	1.6±0.2	0.4±0.1	<0.05
Exercise: V6 (mm)	0.8±0.3	2.0±0.5	<0.05
Recovery (4th-6th min): V4-V6 (mm)	0.2±0.2	1.2±0.2	<0.01
Recovery (4th-8th min): V4-V6 (mm)	1.3±0.3	0.2±0.1	<0.01
• II-III-aVF-V6 during exercise	16/76 (21%)	271/306 (89%)	<0.01
• • PLUS V4-V6 4th-6th min of recovery	4/76 (5%)	247/306 (81%)	<0.01
• II-III-aVF±V4-V6 during exercise	60/76 (79%)	35/306 (11%)	<0.01
• • PLUS V4-V6 4th-8th min of recovery	22/76 (29%)	6/306 (2%)	<0.01

9:30 a.m.

1054-268

When Is Exercise Training Possible After Elective Coronary Stenting?

Yoshimitsu Soga, Hiroyoshi Yokoi, Masashi Iwabuchi, Hideyuki Nosaka, Masakiyo Nobuyoshi, Kokura Memorial Hospital, Kitakyushu, Japan

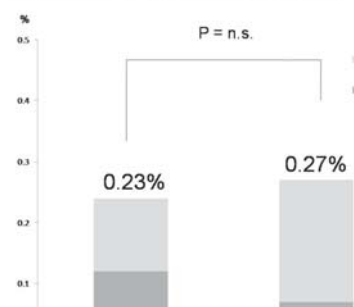
Background: It has been believed that exercise training immediately after coronary stenting induce stent thrombosis. However a little is reported about safety of exercise training immediately after coronary stenting.

Aim: To investigate the safety and efficacy of exercise training after elective coronary stenting.

Method: We enrolled 2351 patients who underwent elective coronary stenting. Groups of patients (exercise group 865 patients and control group 1486 patients) were compared. We performed exercise training below anaerobic threshold (AT) level from the next day after coronary stenting. We evaluate the incidence of stent thrombosis and major adverse event (MAE: death, myocardial infarction and stroke).

Result: At 30 days, clinical follow-up information was obtained in 2327 (99%) patients. No cardiac events occurred during exercise on the next day after stenting. There was no significant difference in the frequency of MAE (0.35% vs. 0.34%, p=0.51) or stent thrombosis (0.23% vs. 0.27%, p=0.65) within 30 days, and there were no exercise-related events. The exercise continuation rate was significantly higher (74% vs. 26%, p<0.0001) and unscheduled hospital visiting was lower (8% vs. 13%, p=0.0005) in the exercise therapy group at 30 days. **Conclusion:** Based on these findings, the safety of exercise training below AT level after elective coronary stenting within thirty days was favorable. And the starting of exercise therapy from the next day was effective for exercise continuation within 30 days.

Incidence of Stent thrombosis at



9:30 a.m.

1054-269

Excellent Functional Capacity in Patients With Ischemic Exercise Electrocardiography Predicts a Negative Stress Imaging Test and Very Low Late Mortality

Patricia P. Dang, Amogh Bhat, Ezra A. Amsterdam, University of California - Davis, Medical Center, Sacramento, CA

Background: Patients (pts) with positive treadmill exercise electrocardiography (ExECG) commonly undergo secondary evaluation by noninvasive stress imaging (ExEcho) or myocardial perfusion scintigraphy (MPS). Functional capacity is a strong predictor of prognosis and, indirectly, of the presence of coronary artery disease. We hypothesized that high functional capacity with positive (ischemic) ExECG (≥1.0 mm ST deviation) would predict 1) negative results on subsequent ExEcho

or MPS and 2) low late mortality.

Methods: We analyzed data in consecutive patients with positive ExECG associated with a functional capacity of ≥ 10 METS who were referred for subsequent ExEcho or MPS. All-cause mortality during follow-up was determined from the Social Security Death Index.

Results: The study group comprised 575 pts (age 51 ± 9 yrs; 228 women; 347 men) of whom 448 were referred for ExEcho and 127 were referred for MPS. ExEcho was negative in 93% (415/448) of pts and MPS was negative in 91% (115/127). During a mean follow-up interval of 5.9 ± 3.3 yrs (range 0.9-12.4 yrs), there were 6 deaths (all-cause mortality 1%, average annual mortality 0.17%).

Conclusions: Excellent functional capacity with positive ExECG is associated with a high rate of negative stress imaging tests and very low late all-cause mortality. These findings suggest that selected patients with positive ExECG and high functional capacity may not require additional cardiac testing.

9:30 a.m.

1054-270

Respiratory Stress Response: A Novel Diagnostic Method to Detect Coronary Artery Disease From Finger Pulse Wave Analysis

Amos Katz, Yosi Blaer, Ian Orlov, Jamal Jafari, Barzilai Medical Center, Ashkelon, Israel

Background: Respiratory maneuvers have been shown to reveal manifestations of myocardial ischemia. Some Pulse Wave characteristics are associated with significant coronary artery disease (S-CAD). Incorporating and developing those elements produced a novel non invasive test to detect S-CAD employing the Respiratory Stress Response (RSR) test.

We evaluated this noninvasive simple test (RSR) as an indicator of S- CAD

Methods: RSR accuracy was assessed in 193 consecutive patients referred for coronary angiography (CA). Phase I - feasibility and phase II - confirmation . RSR (%) was calculated by proprietary software; analyzing the relative spectral power of the respiratory peak area at 0.1Hz derived the finger pulse wave oscillations measured by photoplethysmography during 70-sec of deep, paced breathing at a rate of 6 breaths per minute (0.1Hz).

The CA were analyzed visually (Phase I) and by QCA (phase II) .S-CAD was defined as luminal stenosis>70% of at least one coronary artery diameter ≥ 2 mm, or LM stenosis>50%.

Results: Patient's characteristics and the test results are presented in the table. In both phases S-CAD pts had significantly lower RSR compared to pts without S-CAD $p<0.001$. Multivariate logistic regression analysis, adjusted to CAD risk factors found RSR to be an independent indicator of S-CAD in phase I (OR=59, 8.7-399.6, 95% CI, $p<0.001$) and II (OR=15.4, 4.4-53.5, 95% CI, $P<0.001$)

Conclusion: The novel RSR test is a simple accurate non-invasive bedside tool for detection of S-CAD.

	Age (Y)	Male %	% S-CAD	Sensitivity	Specificity	PPV	NPV
Phase I N=98	64.6 \pm 11.3	68.4	66.3	0.80	0.82	0.9	0.68
Phase II N=95	62.4 \pm 13.3	74	49	0.87	0.63	0.7	0.83

9:30 a.m.

1054-271

Prognostic Significance of Exercise-Induced Left Bundle Branch Block

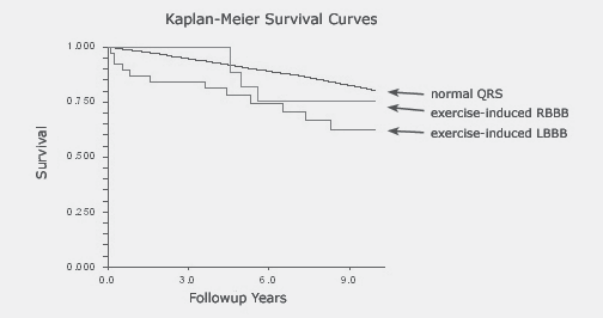
Michael Y. Ho, Kusum Lata, Joshua Abella, Jonathan Myers, Victor F. Froelicher, Stanford University School of Medicine, Stanford, CA, Palo Alto Veterans Affairs Medical Center, Palo Alto, CA

Background: Exercise-induced left bundle branch block (LBBB) is an uncommon phenomenon that has been reported to occur in approximately 0.5% of all patients undergoing exercise testing. The only previous study used matched controls and had a short follow up period.

Methods: 9,939 patients who underwent clinical exercise treadmill testing from 1987 to 2006 at two Veteran Affairs Medical Centers were evaluated. Patients were followed for 10 years and all-cause mortality was the primary endpoint. Kaplan-Meier with log-rank test and Cox regression analysis was performed. Exercise-induced bundle branch blocks were recorded using continuous ECG monitoring during and for 5 minutes post exercise. Patients with underlying interventricular conduction delays at baseline were excluded.

Results: Thirty-eight cases of exercise-induced were identified (0.4%). Over 10 years, there was a 3.4% annual death rate in the exercise-induced LBBB patients and 2.6% in those with exercise-induced right bundle branch block, compared to 1.9% in those without interventricular conduction delay. (Log-rank chi-squared=8.7; $P=0.01$) Patients with exercise-induced LBBB had a Cox proportional hazard ratio of 2 (95% CI: 1 to 4).

Conclusion: Our study confirms the low prevalence of exercise-induced LBBB in a population referred for clinical exercise testing as well as its associated risk.



9:30 a.m.

1054-272

Defining the Optimal Prognostic Window for Cardiopulmonary Exercise Testing in Patients With Heart Failure

Ross Arena, Marco Guazzi, Jonathan Myers, Mary Ann Peberdy, Daniel Bensimhon, Paul Chase, Peter Brubaker, Brian Moore, Dalane Kitzman, Virginia Commonwealth University, Richmond, VA

Background: Ventilatory efficiency (VE/VO₂ slope) and peak oxygen consumption (VO₂) provide robust prognostic information in patients with heart failure (HF) undergoing cardiopulmonary exercise testing (CPX). The purpose of the present study is to assess the prognostic characteristics of CPX at different time intervals.

Methods: Six hundred and twelve subjects (74% male, mean age: 60.1 ± 13.2 years, ejection fraction: $34.6 \pm 13.8\%$, ischemic etiology: 47%) underwent CPX and were tracked for major cardiac events over a three year period at six month intervals. All event-free subjects were tracked for the entire three-years.

Results: Mean VE/VO₂ slope and peak VO₂ were 35.3 ± 9.5 and 15.5 ± 6.0 mL O₂·kg⁻¹·min⁻¹, respectively. There were a total of 196 major cardiac events (145 deaths/40 transplants/11 left ventricular assist device implantations). Both the VE/VO₂ slope and peak VO₂ were prognostically significant during the initial two year tracking period. The VE/VO₂ slope remained prognostically significant from 24-30 months while peak VO₂ was not predictive during the third year of follow-up (Table 1).

Table 1

	Chi-square	Hazard Ratio (95% CI)	p-value
VE/VO ₂ slope			
0-6 months (59 events)	87.2	1.07 (1.06-1.09)	<0.001
6-12 months (45 events)	23.7	1.06 (1.04-1.09)	<0.001
12-18 months (34 events)	22.2	1.07 (1.04-1.10)	<0.001
18-24 months (31 events)	26.1	1.09 (1.06-1.13)	<0.001
24-30 months (16 events)	16.2	1.10 (1.05-1.16)	<0.001
30-36 months (11 events)	3.8	NS*	0.05
Peak VO ₂			
0-6 months (59 events)	34.1	0.82 (0.77-0.87)	<0.001
6-12 months (45 events)	12.9	0.89 (0.83-0.95)	<0.001
12-18 months (34 events)	6.6	0.91 (0.85-0.98)	0.01
18-24 months (31 events)	13.3	0.86 (0.79-0.93)	<0.001
24-30 months (16 events)	2.1	NS*	0.15
30-36 months (11 events)	0.77	NS*	0.38

*NS: Not significant

Conclusion: These results indicate that commonly assessed CPX variables retain prognostic value for at least two years. The VE/VO₂ slope is the superior predictor of adverse events throughout follow-up, although peak VO₂ provides additional predictive value particularly during the first year of follow-up.

9:30 a.m.

1054-273

Impaired Heart Rate Recovery Is Associated With New-Onset Atrial Fibrillation

Thomas Maddox, Colleen Ross, P. Michael Ho, David Magid, John S. Rumsfeld, Denver VAMC, Denver, CO, University of Colorado Denver, Denver, CO

Background: Autonomic dysfunction appears to play a significant role in the development of incident atrial fibrillation (AF), and impaired heart rate recovery (HRR) during exercise treadmill testing (ETT) is a known marker for autonomic dysfunction. However, whether impaired HRR is associated with incident AF is unknown. Accordingly, we studied the association of HRR with the development of incident AF.

Methods: In a large HMO, we studied patients referred for ETT between 2001 and 2004 without a prior history of AF. Patients were categorized by normal or impaired HRR (HR decrease ≥ 12 BPM one minute after peak exercise) on ETT. The primary outcome was the incidence of AF. Cox proportional hazards modeling was used to control for age, sex, HTN, CHF, CAD, mitral valve disease, obesity, and DM. Secondary analyses explored the relationship between impaired HRR, modeled as a continuous variable, and AF, and explored interactions between cardiac medication use, HRR, and AF.

Results: 8236 patients met study inclusion criteria, and 2425 (29.4%) had impaired HRR on ETT. In general, patients with impaired HRR were older, female, and had more co-morbidities and cardiac medications. During a median follow-up period of 3.1 years, 99 (4.1%) of patients with impaired HRR and 93 (1.6%) of patients with normal HRR developed AF. After multi-variable adjustment, patients with impaired HRR were more

likely to develop AF than patients with normal HRR (HR 1.43, 95% CI 1.06, 1.93). In addition, there was a linear trend between impaired HRR and AF (HR 1.05 per one beat decrease in HRR, 95% CI 0.99, 1.11). No interactions between cardiac medications, HRR, and AF were noted.

Conclusions: After controlling for demographic and clinical factors, patients with impaired HRR on ETT were significantly more likely to develop new-onset AF, as compared to patients with normal HRR. These findings support the hypothesis that autonomic dysfunction contributes to the development of AF. Future studies are needed to test whether interventions known to improve HRR, such as exercise training, may delay or prevent AF.

9:30 a.m.

1054-274

Sudden Death Risk Associated With United States Triathlon Competition

Kevin M. Harris, Jason T. Henry, Eric Rohman, Tammy S. Haas, James Hodges, William O. Roberts, Barry J. Maron, Minneapolis Heart Institute Foundation at Abbott Northwestern Hospital, Minneapolis, MN

Background: The sudden death (SD) risk associated with the marathon is about 0.8/100,000 participants. While the triathlon (swim, bike, and run) has become increasingly popular with hundreds of thousands of competitors each year, the risks associated with this sport are unknown.

Methods: We assembled the fatal events occurring in 2846 USA Triathlon sanctioned events between January 2006 and September 2008 using a variety of sources including: Lexis-Nexis database, internet search engines, Minneapolis Heart Institute Sudden Death in Young Athletes Registry and USA Triathlon records. The total number of triathlon participants was identified using on-line tabulations of race results. Triathlons were characterized based on length of the swimming segment: short (<750m); medium (751-1500m); long (>1500m).

Results: Over the 33-month period, 14 SDs occurred in sanctioned races, including 13 during the swimming segment and one during the bike. Ages were 28 to 55 years; 11 were male. Of the 14 deaths, 6 occurred in short, 4 in medium and 4 in long races. The total number of participants was 922,810 with 40% female. Therefore, the overall SD risk associated with the triathlon was 1.5/100,000 participants, higher in males than in females (2.0 vs. 0.8, respectively; $p=0.13$; 95% CI: 0.11-1.43). SD rate in relation to event length was: 1.7/100,000 participants for short, 0.8 for medium and 2.9 for long events ($p=0.40$). Triathlon SD events were more common in 2008 (2.4/100,000) compared to 2007 (1.2) and 2006 (0.7) ($p=.23$). The SD risk for the triathlon is higher than for the marathon (1.5/100,000 vs. 0.8/100,000 participants; $p=.058$; rate ratio 1.92; CI 1.0-3.7 $p=.058$).

Conclusions: SD risk associated with the triathlon is not inconsequential and is greater than that of the marathon. Deaths during triathlons are virtually confined to the swimming portion.

9:30 a.m.

1054-275

Heart Failure Patients in the Intermediate Range of Peak VO_2 : Additive Value of Heart Rate Recovery and the VE/VCO_2 Slope in Predicting Mortality

Luiz Eduardo F. Ritt, Ricardo B. Oliveira, Sandra Mandic, Ross Arena, Mary Ann Peberdy, Daniel Bensimhon, Paul Chase, Peter Brubaker, Brian Moore, Dalane Kitzman, Marco Guazzi, Jonathan Myers, Veterans Affairs Hospital, Stanford University, Palo Alto, CA, Virginia Commonwealth University Medical Center, Richmond, VA

Background: cardiopulmonary exercise test (CPX) is used to predict outcomes in heart failure (HF). Patients with peak VO_2 values $\geq 14 \text{ mL}\cdot\text{kg}^{-1}\cdot\text{min}^{-1}$ and $< 10 \text{ mL}\cdot\text{kg}^{-1}\cdot\text{min}^{-1}$ have been considered to be at lower and high risk, respectively. Management of patients who fall within the "intermediate range" of peak VO_2 (10 to $14 \text{ mL}\cdot\text{kg}^{-1}\cdot\text{min}^{-1}$) remains a challenge. We tested the hypothesis that heart rate recovery (heart rate 1-minute post exercise, HRR_1) and the VE/VCO_2 slope complement peak VO_2 in predicting cardiac mortality among HF patients in the intermediate range.

Methods: multicenter analysis, 1167 HF patients followed for cardiac mortality (mean of 21 ± 13 months) were divided into 3 groups: group A, peak $\text{VO}_2 \geq 14 \text{ mL}\cdot\text{kg}^{-1}\cdot\text{min}^{-1}$, $n=671$; group B, peak $\text{VO}_2 > 10$ to $< 14 \text{ mL}\cdot\text{kg}^{-1}\cdot\text{min}^{-1}$, $n=330$, and group C, $\text{VO}_2 \leq 10 \text{ mL}\cdot\text{kg}^{-1}\cdot\text{min}^{-1}$, $n=166$. Univariate and multivariate proportional hazards analyses were performed using CPX responses and other clinical variables to determine predictors of survival. Optimal cutpoints were determined using ROC analysis.

Results: cardiac mortality was 13%, 22% and 26% in groups A, B, and C, respectively ($p < 0.05$; A vs. B and A vs. C, no differences in B vs. C). The optimal cutpoints for HRR_1 and the VE/VCO_2 slope were $< 16 \text{ beats}\cdot\text{min}^{-1}$ and > 34 , respectively. Overall, peak VO_2 , HRR_1 , the VE/VCO_2 slope and ejection fraction (EF) were significant univariate predictors of cardiac mortality. Multivariately, the hazard ratios (HR) for the VE/VCO_2 slope, HRR_1 , and peak VO_2 were 2.36 (95% CI 1.64-3.40; $p < 0.001$), 1.70 (95% CI 1.14-2.51; $p = 0.008$) and 1.62 (95% CI 1.15-2.29; $p = 0.006$), respectively, while EF was removed from the regression. Compared to group A, patients in the intermediate range, with either an abnormal VE/VCO_2 slope or HRR_1 had almost 2-fold higher risk of cardiac mortality, whereas those with both responses normal had the same mortality. Those with both HRR_1 and VE/VCO_2 slope abnormal responses had a higher mortality risk than those with peak $\text{VO}_2 \leq 10 \text{ mL}\cdot\text{kg}^{-1}\cdot\text{min}^{-1}$ (HR 3.51 95% CI 2.33-5.29, $p < 0.001$ and HR 3.11 95% CI 2.07-4.68, $p < 0.001$, respectively). **Conclusion:** HRR_1 and the VE/VCO_2 slope powerfully stratify cardiac mortality in HF patients who fall into the intermediate range for peak VO_2 .

1054-276

Peripheral Endothelial Function Is a Primary Clinical Target for Enhanced External Counterpulsation in Patients With Refractory Angina

Randy W. Braith, Darren P. Casey, Darren T. Beck, Wilmer W. Nichols, Calvin Y. Choi, Mathean A. Khuddus, C. Richard Conti, Department of Applied Physiology and Kinesiology, University of Florida, Gainesville, FL, Department of Cardiovascular Medicine, University of Florida, Gainesville, FL

Background: Enhanced external counterpulsation (EECP) is a noninvasive therapy for treatment of coronary artery disease (CAD). EECP provides angina relief and improves long-term prognosis but mechanism(s) underlying the clinical benefits remain unknown. This was the first randomized, sham-controlled study to investigate the extra-cardiac effects of EECP on arterial function.

Methods: We randomized (2:1 ratio) 30 symptomatic patients with CAD to 35 1-hr sessions of EECP ($n=20$) or 35 1-hr sessions of sham-EECP ($n=10$). Flow-mediated dilation of the brachial (BFMD) and femoral (FFMD) arteries was performed using ultrasound. Forearm (FBF) and calf (CBF) blood flow were measured with plethysmography. Radial artery pressure waveforms were recorded by applanation tonometry and aortic pressure waveforms were generated using a mathematical transfer function. Augmentation index (Ala), timing of the reflected pressure wave (ΔTp), and LV wasted energy were calculated from the generated aortic pressure waveform. Carotid to femoral pulse wave velocity (CF-PWV) was determined by tonometry. Plasma nitric oxide (NOx), asymmetric dimethylarginine (ADMA), exercise duration, angina threshold, and oxygen consumption (VO_2) were measured pre and post.

Variable	EECP (n = 20)		Sham (n = 10)	
	Baseline	35 Sessions	Baseline	35 Sessions
BFMD (%)	3.7 \pm 0.2	5.8 \pm 0.4*	4.2 \pm 0.7	4.3 \pm 0.6
FFMD (%)	2.6 \pm 0.2	3.5 \pm 0.3*	2.8 \pm 0.4	2.8 \pm 0.3
FBF (ml/min/100ml)	19.3 \pm 1.3	23.5 \pm 1.4*	19.0 \pm 1.6	18.9 \pm 1.5
CBF (ml/min/100ml)	15.2 \pm 1.4	18.8 \pm 1.0*	17.1 \pm 1.6	16.9 \pm 1.5
Ala (%)	24 \pm 3	16 \pm 4*	23 \pm 2	22 \pm 4
ΔTp (ms)	134 \pm 3	144 \pm 2*	135 \pm 4	131 \pm 4
LVWE (msec-mmHg ⁻²)	54 \pm 9	33 \pm 6*	49 \pm 8	48 \pm 7
CF-PWV (m/sec)	12.1 \pm 0.5	10.2 \pm 0.4*	11.5 \pm 0.7	11.6 \pm 0.5
NOx ($\mu\text{mol/L}$)	21.5 \pm 2.5	32.8 \pm 3.4*	24.8 \pm 5.2	25.3 \pm 6.4
ADMA ($\mu\text{mol/L}$)	0.66 \pm 0.04	0.44 \pm 0.03*	0.75 \pm 0.07	0.74 \pm 0.09
Exercise Time (sec)	582 \pm 40	771 \pm 56*	550 \pm 71	566 \pm 68
Time to Angina (sec)	392 \pm 45	602 \pm 44*	366 \pm 43	374 \pm 31
VO_2 Peak (ml/kg/min)	17 \pm 1.0	21 \pm 1.3*	16 \pm 1.5	17 \pm 1.3

* $p < 0.05$

Results:

Conclusion: EECP therapy improves peripheral endothelial function and reduces arterial stiffness. These vascular adaptations decrease LV afterload and myocardial oxygen demand, and increase anginal threshold in patients with refractory angina.

9:30 a.m.

1054-277

Exercise Training in Chagas Cardiomyopathy: Effects on Functional Performance, Quality of Life, and BNP Serum Levels

Marcia Lima, Manoel Otávio Rocha, Maria do Carmo Nunes, Lidiane Sousa, Francilú Belotti, Maria Clara Alencar, Henrique Costa, Marcos Campos, Leonardo Baptista, Érika Baião, Raquel Brito, Felipe Barbosa, Antônio Ribeiro, Federal University of Minas Gerais (UFMG), Belo Horizonte, Brazil, Federal University of Jequitinhonha and Mucuri Valleys (UFVJM), Diamantina, Brazil

Background: The effects of the exercise training (ET) have not yet been evaluated in Chagas cardiomyopathy (CC), whose peculiarities set it apart from others causes of heart failure. Our objective was to determine the effects of ET on the functional capacity, quality of life, and serum BNP levels, of patients with CC.

Methods: This was a randomized, controlled, single-blind trial that recruited 37 patients with CC (age range 31-63, 59% men), sinus rhythm and no regular physical activity. Patients with pacemakers, *diabetes mellitus*, or other comorbidities were not considered eligible. Patients were randomly assigned either to experimental group (EG), $n=18$, or to a control group (CG), $n=19$. Patients in the EG were allocated to 36 sessions of ET, three times a week with 60 minutes of duration. Both groups were assessed by exercise stress test, serum BNP, six minute walk test (6MWT), Goldman Functional Classification (GFC), and Quality of life (QoL) questionnaire SF-36 at baseline and at the end. A significance level of $p \leq 0.05$ was established.

Results: At baseline there was no difference between the groups. In the EG, significant increases in peak VO_2 (9.95 ± 5.29 vs. $2.56 \pm 6.54 \text{ mL/Kg/min}$, $p=0.001$), exercise time (3.03 ± 1.56 vs. $0.84 \pm 1.98 \text{ min}$, $p<0.001$), 6MWT distance (67.83 ± 54.69 vs. $8.44 \pm 49.13 \text{ m}$, $p=0.001$), and GFC (8 vs. 1 patient, $p=0.008$) were attained when compared to the CG. There was an improvement in every QoL domain, being significant in three: vitality (8.61 ± 10.40 vs. 0.00 ± 9.24 , $p=0.013$), role-emotional (18.52 ± 50.13 vs. -20.37 ± 39.84 , $p=0.012$), and mental health (15.78 ± 19.18 vs. 3.11 ± 14.10 , $p=0.031$). The reduction on BNP levels was not significant (-6.77 ± 81.58 vs. $25.98 \pm 118.69 \text{ pg/ml}$, $p=0.952$).

Conclusion: Improvements in functional capacity and exercise tolerance, with positive reflexes on quality of life suggest benefits of ET in patients with Chagas cardiomyopathy.

Financial Support: CNPq

9:30 a.m.

1054-278 **A Multivariable Model From HF-ACTION Predicting Peak VO2 in a Heart Failure Population**

William E. Kraus, Stephen J. Ellis, Jerry L. Fleg, Steven J. Keteyian, Ileana L. Piña, Daniel R. Bensimhon, Eric S. Leifer, Dalane W. Kittzman, Christopher M. O'Connor, David J. Whellan, for the HF-ACTION Investigators, Duke University, Durham, NC, NHLBI, Washington, DC

Background. HF-ACTION was a randomized controlled clinical trial of exercise training in 2331 individuals with systolic heart failure (HF). Enrollees were physically inactive and receiving optimal HF therapy, including 95% on beta-blockers. **Methods.** Symptom-limited cardiopulmonary exercise testing measured peak oxygen consumption (pVO₂). Multivariable linear regression with backward variable selection was used to identify predictors of baseline pVO₂. Of 35 initial variables those with the highest p-values were eliminated sequentially until all those remaining had p<0.05. Among the remaining 19, all with partial R-square <0.01 were eliminated at once with the 11 variables remaining shown with p-values and partial R²s. **Results.** The total R² for the model was 0.388. For individual variables, an approximate 8-year older age or a 6-unit increase in BMI corresponded to a 1-unit (1 mL/kg/min) decrease in pVO₂. Men had a mean adjusted pVO₂ that was ~2 units greater than women. Blacks had lower pVO₂ than non-blacks. NYHA class II subjects had a higher pVO₂ (2 units) than class III or IV subjects. Diabetes, peripheral arterial disease (PVD), lower left ventricular ejection fraction (LVEF), abnormal ventricular conduction, living in the US Northeast, and testing by cycle ergometry each predicted lower pVO₂. **Conclusion.** Multiple demographic and clinical variables predict pVO₂ in those with stable systolic HF, with age explaining the largest amount and over 60% of the variation in pVO₂ remaining unexplained.

Variable	Coefficient	95% CI	P-value	Partial R-square
Age	-0.13	(-0.14, -0.11)	<0.0001	0.12
BMI	-0.16	(-0.18, -0.13)	<0.0001	0.07
Sex	-2.1	(-2.5, -1.7)	<0.0001	0.06
Race			<0.0001	0.06
NYHA Class (II/IV vs. II)	-2.0	(-2.4, -1.7)	<0.0001	0.06
Vent. cond.	5-component		<0.0001	0.028
Geographic Region	6-component		<0.0001	0.027
CPX mode (bike vs. TM)	-2.5	(-3.2, -1.9)	<0.0001	0.025
Diabetes	-1.2	(-1.5, -0.83)	<0.0001	0.021
LVEF	0.07	(0.05, 0.09)	<0.0001	0.021
PVD	-2.0	(-2.6, -1.4)	<0.0001	0.017

9:30 a.m.

1054-279 **Which Equation for Percent Predicted Peak Oxygen Consumption Provides the Best Prognostic Assessment in Patients With Heart Failure?**

Ross Arena, Marco Guazzi, Jonathan Myers, Mary Ann Peberdy, Daniel Bensimhon, Paul Chase, Peter Brubaker, Brian Moore, Dalane Kittzman, Virginia Commonwealth University, Richmond, VA

Background: Peak oxygen consumption (VO₂) is commonly assessed in patients with heart failure (HF) undergoing cardiopulmonary exercise testing (CPX). The purpose of the present investigation is to assess the prognostic ability of several well-established peak VO₂ prediction equations in a large HF cohort. **Methods:** One thousand and eighty-two subjects (70% male, mean age: 57.4 ±13.7 years, ischemic etiology: 43%) diagnosed with HF underwent CPX to determine peak VO₂. Percent-predicted peak VO₂ was calculated according to normative values proposed by Wasserman et al (equation), Jones et al (equation), the Copper Clinic (below low fitness threshold), a veteran's administration male referral data set (equation) and the St. James Take Heart Project for women (equation). The prognostic significance of percent-predicted VO₂ values derived from the two latter, sex specific, equations were assessed collectively (VA/St. James). **Results:** There were 165 major cardiac events (114 deaths, 41 transplants and 10 left ventricular assist device implantations) during the two year tracking period. Receiver operating characteristic (ROC) curve and univariate Cox regression analyses are listed in Table 1.

	Mean Actual Value and Percent Predicted	ROC curve area (95% CI)	Optimal Threshold	Hazard Ratio (95% CI)	p-value
Peak VO2	15.3 ±5.6 mlO ₂ •kg ⁻¹ •min ⁻¹	0.71 (0.67-0.75)	<13 mlO ₂ •kg ⁻¹ •min ⁻¹	3.1 (2.2-4.2)	<0.001
Wasserman et al	59.9 ±22.7%	0.74 (0.70-0.78)	<50%	4.2 (3.0-5.7)	<0.001
Jones et al	67.8 ±39.6%	0.72 (0.68-0.76)	<50%	3.9 (2.9-5.4)	<0.001
VA/St. James	51.8 ±18.1%	0.71 (0.68-0.75)	<44%	3.4 (2.5-4.7)	<0.001
Copper Clinic	55.5 ±18.9%	0.72 (0.68-0.76)	<48%	3.4 (2.5-4.6)	<0.001

Conclusion: Actual peak VO₂ and the percent-predicted models included in this analysis all were significant predictors of major cardiac events. It appears that the percent-predicted VO₂ value derived from the equations proposed by Wasserman et al may slightly outperform other expressions of this CPX variable.

9:30 a.m.

1054-280 **Attenuated Heart Rate Recovery Is a Strong Predictor of Mortality in Patients With Left Ventricular Systolic Dysfunction**

Pedro L. Carmo, Antonio Ferreira, Carlos Aguiar, Renata Gomes, João Brito, Sónia Lima, Pedro Sousa, Sandra Feliciano, Miguel Mendes, Aniceto Silva, Hospital de Santa Cruz, Carnaxide, Portugal

Background:An attenuated heart rate recovery (HRR) following exercise test (ET) portends a higher mortality risk in asymptomatic subjects as in patients (pts) with coronary heart disease. Its prognostic value in heart failure pts has yet to be confirmed. The aim of this study was to determine the prognostic implications of attenuated HRR relative to well established prognostic factors - peak oxygen uptake (pVO₂) and VE/VCO₂ slope - in heart failure. **Methods:**We evaluated 171 pts (age 55±10 years, 45 female) with an ejection fraction <40% who underwent a treadmill-based cardiopulmonary exercise test (CPET) for risk stratification. The difference between maximal heart frequency and the frequency at the end of the first minute of recovery was defined as HRR. ROC curve analyses were used to identify the HRR value that more accurately predicted death. **Results:**Therapy at the time of CPET included a beta-blocker in 149 pts (77%) and an ACE inhibitor or ARB in 177 pts (91%). During follow-up (920 ± 449 days) 12 pts died. HRR was significantly lower in pts who died (7.7± 6.0 bpm vs 15.8 ± 13.7 bpm; P= 0.042). HRR ≤10 bpm (present in 70 pts) was associated with higher mortality, even after adjustment for the effects of age, gender, body mass index, coronary heart disease aetiology, diabetes, smoking, left bundle branch block, mean blood pressure, heart rate, pVO₂, and VE/VCO₂ slope (adjusted HR= 5.2, 95% CI, 1.0-26.1). In this multivariable analysis, VE/CO₂ slope remained an independent prognostic factor (HR=1.04 per unit increase, 95% CI, 1.0-1.1), but not pVO₂. **Conclusions:**In pts with left ventricular systolic dysfunction, a HRR ≤10 bpm at the first minute after a cardiopulmonary exercise test is an independent predictor of mortality, and adds prognostic information to the VE/VCO₂ slope. HRR should be considered when estimating the outcome of heart failure pts with low ejection fraction.

9:30 a.m.

1054-281 **Exaggerated Exercise Blood Pressure Response Is Related to a State of Inflammatory Activation, Impaired Thrombosis/Fibrinolysis System and Arterial Stiffening in Essential Hypertension**

Kyriakos Dimitriadis, Costas Tsioufis, Dimitris Syrseloudis, Eirini Andrikou, Panayiotis Agelopoulos, Giorgos Metallinos, Ioannis Kallikazaros, Christodoulos Stefanadis, First Cardiology Clinic, University of Athens, Hippokraton Hospital, Athens, Greece

Background: There are conflicting data regarding the cardiovascular prognostic value of a hypertensive response to exercise (HRE), while low-grade inflammation, arterial stiffness and impaired fibrinolysis are associated with atherosclerosis progression. In this study we examined the correlations between HRE, high-sensitivity C-reactive protein (hs-CRP), plasminogen-activator inhibitor type 1 (PAI-1) and arterial stiffening, in essential hypertensives. **Methods:** 84 newly diagnosed untreated non-diabetic subjects with stage I to II essential hypertension [58 men, mean age=52 years, office blood pressure (BP)=145/93 mmHg] with a negative treadmill exercise test (Bruce protocol) were divided into those with HRE (n=24) (peak systolic BP >210mmHg in men and >190 in women) and to those without HRE (n=60). Moreover, in all subjects venous blood samples were drawn for estimation of hs-CRP and PAI-1 levels, whereas arterial stiffness was evaluated on the basis of carotid to femoral pulse wave velocity (PWV), by means of a computerized method (Complior SP). **Results:** Patients with HRE compared to those without HRE were older (56±9 vs 50±9 years, p<0.05) and had greater 24-h systolic BP (138±14 vs 131±12 mmHg, p<0.05). Although groups did not differ regarding metabolic profile and left ventricular mass index (p=NS for all), patients with HRE as compared to those without HRE exhibited higher levels of PWV (8.7±1.6 vs 7.7±1.3 m/sec, p<0.005), hs-CRP (5.1±1.2 vs 2.1±0.8 mg/l, p<0.0001) and PAI-1 (38.6±8.5 vs 18.9±2.6 ng/ml, p<0.05). In the total population, peak systolic BP was related to 24-h systolic BP (r=0.238, p<0.05), PWV (r=0.288, p<0.005) and hs-CRP (r=0.439, p<0.0001), whereas there was no association with PAI-1 levels (p=NS). By analysis of covariance it was revealed that PWV, hs-CRP and PAI-1 values remained significantly different between groups after adjustment for confounders (p<0.05). **Conclusion:** Hypertensives with a HRE exhibit augmented hs-CRP, PAI-1 and PWV values. These findings suggest that impaired thrombosis/fibrinolysis system, arterial stiffening and microinflammation may be mechanisms that contribute to exercise hypertension and increase risk in this setting.

9:30 a.m.

1054-282

Real-Time Cine and Myocardial Perfusion With Treadmill Stress Cardiac Magnetic Resonance in Patients Referred for Stress SPECT

Subha V. Raman, Mihaela Jekic, Jennifer A. Dickerson, Eric L. Foster, Orlando P. Simonetti, The Ohio State University, Columbus, OH

Background: To date, stress cardiac magnetic resonance (CMR) has relied on pharmacologic stress due to lack of MR-compatible treadmills. We tested a new system for exercise stress CMR in patients with suspected myocardial ischemia.

Methods: A treadmill was modified for safe placement in the MRI room by replacing all ferromagnetic components except the motor with non-magnetic equivalents. Thirteen patients age 58±7 years referred for stress SPECT, 9 with known coronary disease, were prospectively enrolled. After rest Tc99m SPECT imaging, patients underwent resting real-time cine CMR. The patient table was then moved just outside the magnet for supine ECG recording followed by treadmill stress. 12-lead ECG monitoring was performed throughout stress. At peak stress, Tc99m was injected and patients rapidly returned to their prior position in the magnet for post-exercise real-time cine followed immediately by first-pass myocardial perfusion imaging. The patient table was pulled out of the magnet for 5-10 min of recovery monitoring with 12-lead ECG. The patient was sent back into the magnet for recovery cine and resting perfusion followed by delayed post-gadolinium imaging. Post-CMR, patients went to the adjacent SPECT lab to complete stress nuclear imaging. Each modality's images were reviewed blinded to other results.

Results: All patients (body mass index 28±4) completed the single exercise, combined SPECT-MRI imaging protocol, averaging 9.6±2.6 min of the Bruce protocol. Mean time to completion of cine MRI post-exercise was 71±6 sec, and to completion of perfusion imaging 90±6 sec. Accuracy in five patients who underwent coronary angiography was 5/5 for CMR and 3/5 for SPECT. Follow-up at 60 days indicated freedom from cardiovascular events in 13/13 CMR-negative and 12/13 SPECT-negative patients.

Conclusions: Exercise stress CMR including wall motion and perfusion is feasible in patients with suspected ischemic heart disease. Further modifications to this system are needed to reliably complete post-stress CMR imaging within 1 minute, and allow further testing of accuracy and prognostic value of this new stress imaging system compared to stress SPECT.

9:30 a.m.

1054-283

Enhanced Sympathetic Excitation at Peak Exercise as a Possible Cause of Prolongation of Heart Rate Recovery in Patients With Myocardial Infarction

Akiko Ushijima, Nagaharu Fukuma, Hiroko Hayashi, Kazuo Kato, Yuko Kimura, Noriko Aisu, Takaya Tsuchida, Hiroshi Takahashi, Hiroshi Kishida, Kyoichi Mizuno, Nippon Medical School, Tokyo, Japan

Background: Heart rate recovery (HRR) after exercise is known as a predictor of cardiac death in patients with heart disease. The mechanism is not fully understood, although a parasympathetic mechanism has been reported. To elucidate the factors that influence HRR, we evaluated the relationship of HRR with exercise performance and plasma norepinephrine (NE), lactic acid and B-type natriuretic peptide (BNP) responses to exercise testing.

Methods: The study population consisted of 52 male patients (age 58±10 years) who had experienced myocardial infarction without residual ischemia, uncompensated heart failure or atrial fibrillation. All subjects underwent a symptom-limited cardiopulmonary exercise test without a cool-down period and echocardiography. NE, lactic acid and BNP were measured at rest and at peak exercise.

Results: HRR did not correlate with the left ventricular ejection fraction, peak VO_2 , lactic acid and BNP. HRR significantly correlated with the increment in heart rate (HR) from rest to peak exercise (ΔHR) ($r=0.30$, $p<0.05$). ΔHR was divided into two phases at the anaerobic threshold (AT) level, HRR significantly correlated with HR (peak-AT) ($r=0.409$, $p<0.01$), but not with HR (AT-rest). There was a significant negative correlation between HRR and NE both at rest and at peak exercise ($r=-0.286$, $p<0.05$, $r=-0.310$, $p<0.05$). HRR was also correlated significantly with $\Delta\text{HR}/\log\Delta\text{NE}$ as an index of sensitivity to NE ($r=0.42$, $p<0.01$). Based on multiple regression analysis, ΔHR and $\log\Delta\text{NE}$ predicted HRR ($R^2=0.467$, $p=0.0027$).

Conclusions: Sympathetic excitation during exercise leads to an extended HRR in patients with myocardial infarction. These findings suggest that enhanced sympathetic excitation at maximum exercise suppresses parasympathetic reactivation and results in prolongation of HRR.

9:30 a.m.

1054-284

Changes in P Wave Duration Due to Ischemia During Exercise Testing

Jonathan C. Maganis, Myrvin H. Ellestad, Ronald Selvester, Bikash Gupta, Memorial Heart and Vascular Institute, Long Beach, CA, Long Beach Memorial Medical Center, Long Beach, CA

Background: ST segment depression, initiated by ischemia, has been the standard measure during exercise testing. It is well recognized that these ECG changes are due to subendocardial ischemia secondary to an increase in left ventricular end diastolic pressure (LVEDP). The increase in LVEDP is also associated with an increased left atrial pressure, resulting in distension of the left atrial wall that contributes to increasing P wave duration (PDUR). We report on a study to measure PDUR during maximum exercise testing to diagnose myocardial ischemia.

Methods: Three hundred twelve patients ($n=312$) with suspected coronary disease had maximum exercise testing with nuclear scintigrams. PDUR was measured at rest and

within one minute after exercise after ECG complexes were magnified four times (100 mm/sec, 40 mm/mV). The changes in PDUR were compared with nuclear scintigrams. An increase of PDUR greater than 15 milliseconds (ms) correlated with ischemia on the nuclear images.

Results: PDUR had a sensitivity of 78% and a specificity of 84%. ST segment depression had a sensitivity of 37% and a specificity of 84%. In patients with upslowing ST segment changes PDUR sensitivity was 78% and specificity was 76%. Sensitivity and specificity were also stratified by men and women (Table).

Conclusions: PDUR change with exercise is more sensitive than ST segment depression. From our data, we conclude that PDUR increase with exercise makes a significant contribution to the detection of ischemia during exercise testing.

		Sensitivity %	Specificity %
P Duration > 15 ms			
Total Patients	n=312	78	84
Men	n=178	78	85
Women	n=134	79	82
ST Depression			
Total Patients	n=312	37	84
Men	n=178	39	83
Women	n=134	32	84
Upsloping ST Changes & P Duration > 15 ms			
Total Patients	n=47	78	76
Men	n=26	83	80
Women	n=21	66	72

9:30 a.m.

1054-285

Failing Myocardium in Non-Heart Failure Hypertensive Patients

Felix M. Valencia-Serrano, Fernando Cabrera-Bueno, Juan Jose Gomez-Doblas, Eduardo de Teresa Galvan, Hospital Virgen de la Victoria, Malaga, Spain

Background: We sought to analyse the effects of exercise on myocardial shortening and its determinants in hypertensive patients with both normal ejection fraction and myocardial shortening at rest. Subtle alterations in myocardial function predict adverse outcomes in hypertensive patients with preserved ejection fraction.

Methods: A total of 52 subjects, 32 hypertensive patients with normal systolic function (ejection fraction $\geq 60\%$, stress corrected midwall fractional shortening (sc-MWS) $\geq 78\%$ and without left ventricular hypertrophy) and 20 matched healthy controls, underwent exercise echocardiography. Hemodynamic, M-mode and Doppler echocardiography parameters were compared at rest and during exercise among groups.

Results: Midwall shortening and sc-MWS were significantly depressed in hypertensive patients during exercise ($p=0.037$ and 0.036 respectively). Whereas in control subjects circumferential and meridional end-systolic stress decreased during exercise no significant afterload changes were noted in hypertensive patients. In normal subjects, but not in hypertensive, end-diastolic volume increased significantly during exercise. Left ventricular mass was comparable in both groups although hypertensive patients showed higher relative wall thickness ($p=0.003$). Finally, in multiple regression analysis, relative wall thickness ($p=0.020$) and changes in end diastolic volume ($p=0.002$), but not circumferential ($p=0.307$) or meridional end-systolic stress ($p=0.182$) modifications, were independently related with the change in myocardial shortening during exercise in hypertensive patients.

Conclusions: exercise unmasks a failing myocardium in hypertensive patients without clinical heart failure, left ventricular hypertrophy or evidence of depressed myocardial shortening at rest and this abnormal response is independently related with concentric remodeling and inadequate increase in end-diastolic volume during exercise.

9:30 a.m.

1054-286

High Intensity Interval Training in CHD Patients: Optimization of Time Spent Near $\text{VO}_{2\text{max}}$

Anil Nigam, Thibaut Guiraud, Mathieu Gayda, Philippe Meyer, Martin Juneau, Laurent Bosquet, Montreal Heart Institute, Montreal, QC, Canada

Background: Data suggests that high intensity interval training (HIT) versus moderate intensity continuous is more effective at improving $\text{VO}_{2\text{max}}$ in CHD patients. HIT consists in alternating short periods of high intensity exercise with short periods of low intensity exercise. We sought to compare several HIT protocols in order to identify the optimal one for achieving the longest time near $\text{VO}_{2\text{max}}$.

Method: Fifteen CHD patients without ST segment depression (mean age 64 years, mean $\text{VO}_{2\text{max}}=40.5$ ml/min/kg) performed a continuous incremental exercise test on cycle ergometer to assess peak VO_2 and maximal aerobic power (MAP). Then, they performed 4 HIT sessions in random fashion, which varied in duration (15 or 60 s) and type of recovery (0% or 50% of MAP), but had similar exercise intensity (100% of MAP). At each session, subjects were requested to carry out the maximum number of repetitions. VO_2 was measured during each session to determine the time spent above 95% and 80% of $\text{VO}_{2\text{max}}$.

Results:

	Mode A	Mode B	Mode C	Mode D
Phases duration	(15/15s)	(15/15s)	(1/1min)	(1/1min)
Type of recovery	Passive (0%)	Active (50%)	Passive (0%)	Active (50%)
Performance (s)	1767 ± 434 §	717 ± 526 *	1539 ± 560	837 ± 573 *
Time above 95% VO2max (s)	220 ± 332	277 ± 183	208 ± 208	251 ± 200
Time above 80% VO2max (s)	714 ± 589	608 ± 420	561 ± 327	626 ± 348

§ different from all others (p<0,005)

* different from mode A and C (p<0,05)

Conclusion: Irrespective of protocol duration, a passive recovery phase allowed patients to perform more repetitions than an active recovery phase. Importantly, longer duration was not concomitant with a longer time spent near VO₂max. However, when considering perceived exertion, patient comfort and the slight although not significantly higher time spent above 80% of VO2max, Mode A appears to be the optimal HIT protocol for these coronary patients.

ACC.ORAL CONTRIBUTIONS

922

Cardiac MRI: Applications

Tuesday, March 31, 2009, 2:00 p.m.-3:30 p.m.
Orange County Convention Center, Room W308C

2:00 p.m.

0922-3

An Edematous Change and Scar Tissue Detected by Magnetic Resonance Imaging After Radiofrequency Ablation of Isthmus-Dependent Atrial Flutter

Miki Yokokawa, Hiroshi Tada, Keiko Koyama, Shigeto Naito, Shigeru Oshima, Koichi Taniguchi, Gunma Prefectural Cardiovascular Center, Maebashi, Japan

Background: Transient inflammatory changes following thermal injury from radiofrequency ablation and development of scar tissue would allow a direct comparison of electrophysiologic results and permit correlation with clinical outcomes. **Methods:** Fifty-seven patients underwent radiofrequency ablation of the cavo-tricuspid isthmus (CTI) for isthmus-dependent atrial flutter (AFL; 14 females, 60 ± 10 years). Contrast-enhanced magnetic resonance imaging (MRI) was performed before CTI ablation, and the length, wall thickness and morphology of the CTI were determined. During CTI ablation, bipolar electrograms were recorded along the ablation line during proximal coronary sinus pacing, and an interval of double potential (DP) was measured to determine complete isthmus block. Contrast-enhanced MRI was also performed 1 day after and 1 month after CTI ablation, and the change of CTI wall thickness and the prevalence of delayed enhancement at the CTI after ablation were analyzed. **Results:** The mean CTI length was 44 ± 10 mm. The 31 patients (54%) showed concave characteristics, and pouch-like recesses were seen in 16 patients (28%). Complete isthmus block was obtained in all 57 patients, and the mean DP intervals were 102 ± 20 ms. One day after the CTI ablation, the contrast-enhanced MRI revealed delayed enhancement at the CTI in 47 patients (82%), and relative to baseline CTI wall thickness was significantly increased (1.6 ± 0.1 mm vs. 2.3 ± 0.2 mm, p < 0.0001). In contrast, one month after ablation, those edematous changes had disappeared, and the CTI thickness was not significantly different from baseline. The delayed enhancement at the CTI was clearly found in 49 patients (86%). No correlation was observed between the prevalence of scar tissue after CTI ablation and the CTI morphology. **Conclusions:** MRI is useful to assess the creation of endocardial edema and scar tissue resulting from CTI ablation. These results may correlate with anatomical isthmus block after CTI ablation in a large portion of patients with isthmus-dependent AFL.

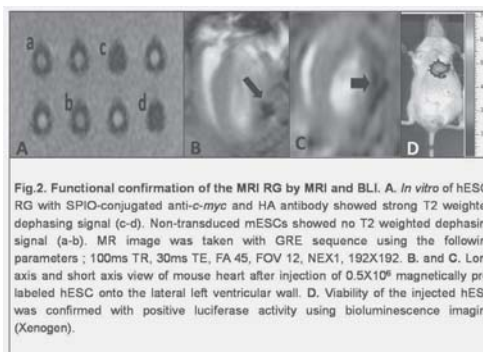
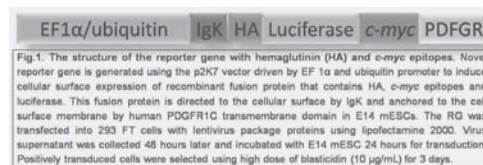
2:15 p.m.

0922-4

A Novel MRI Reporter Gene to Determine Stem Cell Viability

Jaehoon Chung, Kehkooli Kee, Renee R. Pera, Phillip C. Yang, Stanford University, Stanford

Background: MRI is ideal to evaluate myocardial cell therapy. Superparamagnetic iron oxide nanoparticle (SPIO) has been widely used for this purpose. However, this technique does not provide information of cell viability. A novel reporter gene (RG) is designed (Fig1). Employing SPIO-conjugated antibodies, MRI signal specific to cell viability can be generated. **Methods:** H9 human embryonic stem cell (hESC) line was transduced with this RG followed by imaging with 3T MRI. **Results:** hESC-RG was confirmed by bioluminescence and FACS. MRI showed significant signal generated from viable hESC-RG (Fig2A). Magnetically pre-labeled hESC were injected into LV and the dephasing signal was noted (Fig2B,C). **Conclusions:** The novel MRI RG enabled viable embryonic stem cells to generate significant molecular MRI signal.



0922-5

Diagnostic Value of Standard and Extended ECG Leads for the Detection of Acute and Chronic Myocardial Infarction After Reperfusion Therapy: Comparison to Size, Localization and Transmurality of Infarction as Assessed by Contrast-Enhanced Magnetic Resonance Imaging

Nikolaus Sarafoff, Ruth Vochem, Stephanie Fichtner, Stefan Martinoff, Markus Schwaiger, Albert Schömig, Tareq Ibrahim, Deutsches Herzzentrum München, Klinik für Herz- und Kreislauferkrankungen, Munich, Germany

Background: The electrocardiogram (ECG) is a fast and easy method to detect acute and chronic myocardial infarction (MI). In clinical studies acute MI is currently diagnosed based on standard ECG (12-lead) using TIMI or ESC/ACCF/AHA/WHF definitions. In addition to ST elevation the latter do also incorporate ST depression and T wave changes. Extended lateral (V7-V9) or right ventricular (rV3-rV6) leads are proposed to generally increase sensitivity of infarct detection, particularly for the right ventricular involvement.

Methods: We enrolled 220 Patients with acute MI who underwent primary PCI on the day of admission and contrast-enhanced magnetic resonance imaging (cMRI) 7 days after the acute event. Standard ECGs were recorded on admission, after reperfusion, at discharge and at 6 months. ECGs were analyzed according to the joint ESC/ACCF/AHA/WHF criteria and TIMI criteria, respectively. Additional ECG leads V7-9 were further recorded in 189 patients and rV3-rV6 in 183 patients on the day of admission. ECG findings were compared to infarct size, localisation, transmural and right ventricular infarction (RVI) as assessed by cMRI.

Results: Delayed contrast enhancement by cMRI was present in 218/220 (99%) patients and 30% showed RV involvement. ESC/ACCF/AHA/WHF criteria were more sensitive than TIMI criteria for the overall detection of acute MI (71% vs. 57%; p=0.002), because they allowed a more sensitive detection of lateral MI (p=0.001) and small MI (p=0.017). Recording of additional leads V7-9 did not increase overall sensitivity with either definition, and rV3-rV6 leads allowed detection of RVI with a sensitivity of 26%. Sensitivity for Q-waves within standard leads for the detection of chronic MI after 6 months was 55%. While cMRI infarct size was significantly larger in Q-wave-MI compared to Non-Q-wave-MI (p=0.0001), the presence of Q-waves was not associated with transmural extent of infarction.

Conclusion: ESC/ACCF/AHA/WHF criteria are superior to TIMI ECG criteria in diagnosing acute MI because it allows a more sensitive detection of lateral and small MI. Extended leads V7-9 do not increase overall sensitivity, and rV3-rV6 provide low sensitivity for the detection of RVI.

2:45 p.m.

0922-6

Pacemaker and Implantable Cardioverter Defibrillator Safety for Patients Undergoing Magnetic Resonance Imaging (The MagnaSafe Registry)

Jennifer Cohen, Heather Costa, Robert Russo, Scripps Clinic, La Jolla, CA

Background: The purposes of the MagnaSafe Registry pilot study are to determine the safety of magnetic resonance imaging (MRI) for patients with permanent pacemakers (PM) and implantable cardioverter-defibrillators (ICD), and to evaluate a pre and post MRI scan device programming protocol.

Methods: Informed consent was obtained by a cardiologist; non-invasive monitoring and ACLS equipment were available; and device interrogation was performed pre and post MRI. Prior to imaging, all ICD therapies were programmed to monitor only. Patients with symptomatic bradycardia or PM dependence were programmed to an asynchronous pacing mode. All patients were programmed pre-scan to disable the magnet response.

Pacing thresholds, lead impedance, P/R wave amplitude, and battery voltage were recorded pre and post MRI. Data was obtained by retrospective chart review.

Results: Between January 2006 to October 2008, 89 patients underwent 113 clinically-indicated MRI scans at Scripps Clinic. A repeat MRI on a separate day was performed in 10 patients. Mean age was 75 ± 12 years. MRI duration was 46.9 ± 19.4 min and was performed an average of 2.5 ± 2.1 years after device implant. A total of 90 generators (61 PM and 29 ICD), and 177 leads were scanned. Pacer dependence was noted in 23% (16/71). A decrease in battery voltage of at least 0.01 V occurred in 16% (10/61), with a mean decrease of 0.03 ± 0.02 V. The mean change in lead impedance (atrial, RV, and LV) was $17.8 \pm 22.2 \Omega$. The average change in P wave amplitude was -0.02 ± 0.45 mV and R wave was -0.06 ± 0.82 mV. The average lead threshold change pre- and post- MRI was 0.03 ± 0.15 V. No patient had more than one lead with a threshold increase and none of the LV leads were affected. One device with a 0.75 V threshold rise required temporary reprogramming. Pacing threshold returned to baseline at 72 hour post-scan device interrogation.

Conclusions: A very low incidence of either lead impedance or pacing threshold change was noted after clinically-indicated MRI in patients with permanent pacemakers and implantable cardioverter-defibrillators, and no major complications were noted. This pilot study validates a device programming protocol for the prospective, multicenter MagnaSafe Registry.

3:00 p.m.

0922-7

Magnetic Resonance Imaging With Targeted Iron-Oxide Labeling Detects Differential Cardiac Cell Survival After Doxorubicin and Myocardial Infarction in Culture and In Vivo

Rajesh Dash, Trevor Chan, Mayumi Yamada, Marietta Paningbatan, Bat-Erdene Myagmar, Philip M. Swigart, Phillip C. Yang, Paul C. Simpson, Jr., San Francisco VA Medical Center, San Francisco, CA, Stanford University, Stanford, CA

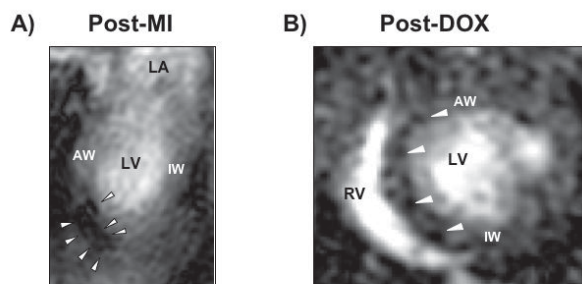
Background: Heart failure from myocardial infarction (MI) or doxorubicin (DOX), used in cancer therapy, is preceded by significant cell apoptosis. Real-time, non-invasive detection of early cardiac apoptosis might impact patient treatment and outcomes. Early apoptosis is detected by Annexin V protein (ANX) binding to externalized membrane phosphatidylserine. To this end, we previously conjugated ANX to superparamagnetic iron oxide (ANX-SPIO). This conjugate specifically binds to early apoptotic cardiac cells in culture and is detectable by in vitro magnetic resonance imaging (MRI).

Hypothesis: We tested whether ANX-SPIO could detect cardiac apoptosis, *in vivo*, via MRI (3 Tesla, GE Excite, WI) after ischemic or oxidative injury.

Methods: Mice underwent LAD ligation or intraperitoneal, cardiotoxic DOX (25mg/kg) injection. After 24-48 hours, ANX-SPIO was given by tail vein, and mice were imaged by T2-weighted cardiac MRI (3 Tesla, GE Excite).

Results: After MI and DOX, myocardial T2 MRI signal was detectable within 30 minutes of ANX-SPIO delivery, exhibiting either a focal (MI) or diffuse (DOX) signal distribution (see Figure). Peak signal was evident 24 hours after ANX-SPIO delivery, and decreased over the next 2 weeks.

Conclusion: Cardiac MRI using ANX-SPIO can accurately detect myocardial apoptosis *in vivo*. Distinct MRI signal distributions were noted following ischemic (MI) versus oxidative (DOX) injury. This molecular imaging strategy may help identify 'at risk' cardiac cell populations.



ECG- and respiratory-gated T2-weighted cardiac MRI of mice post-MI (A, 2-chamber view) and post-DOX (B, short axis view), 30 minutes after tail vein injection of 100 μ l ANX-SPIO. Note *focal* T2 signal void (white arrows) of ANX-SPIO in antero-apex of post-MI heart, and *diffuse* septal, anterior and inferior T2 signal void in post-DOX heart. (LA, left atrium; LV, left ventricle; RV, right ventricle; AW, anterior wall; IW, inferior wall)